# THE ROLE OF RAP1 IN *DROSOPHILA* MORPHOGENESIS

Nathan J. Harris

A dissertation submitted to the faculty of the University of North Carolina at Chapel Hill in partial fulfillment of the requirements for the degree of Doctor of Philosophy in the Department of Biology.

Chapel Hill
2012

Approved by:

Dr. Mark Peifer

Dr. Victoria Bautch

Dr. Stephen Rogers

Dr. Bob Duronio

Dr. Adrienne Cox

**ABSTRACT**

NATHAN J. HARRIS: The Role of Rap1 in *Drosophila* Morphogenesis
(Under the Direction of Mark Peifer)

Without proper apicobasal polarity, epithelial cells cannot properly assemble into various tissues or change cell shape in a coordinated fashion to allow for proper development. Loss of polarity in *Drosophila* embryonic development leads to defects in cell-cell adhesion as adhesion complexes are no longer proper localized, disrupting coordination of the actin cytoskeletons between the cells that make up a tissue. As a result, tissues quickly become disorganized, appearing multilayered. Here, we show that loss of the small GTPase Rap1 causes defects in apical constriction during Drosophila gastrulation, leading to a failure to properly invaginate the mesoderm. This suggested that Rap1 modulates connection of adherens junctions to the actin cytoskeleton. As a result, we broadened our initial studies to learn the role of Rap1 in regulating the actin cytoskeleton and polarity during morphogenesis. In embryos lacking maternal and zygotic Rap1, we observed early defects in the localization of the apical polarity proteins, Baz and aPKC. Additionally, Rap1 mutants exhibit defects in apical tension as the sizes of cell apices in mutants wildly vary from cell to cell. Further exploration of these initial results suggests that Rap1 performs a critical role in the regulation of the establishment and elaboration of apical polarity during early *Drosophila* embryogenesis.

# ACKNOWLEDGEMENTS

# TABLE OF CONTENTS

# LIST OF TABLES

Tables

# LIST OF FIGURES

# ABBREVIATIONS

αcat        α-catenin

Abl         Ableson kinase

AF-6        afadin

AJ          Adherens junction

AP          anterior-posterior

aPKC        atypical protein kinase C

Arm         Armadillo/β-catenin

Baz         Bazooka

Cno         Canoe

Cta         Concertina

Crb         Crumbs

DEcad       DE-cadherin

Dlg         Discs large

DV          dorsal-ventral

Dzy         Dizzy/PDZ-GEF/Gef26

Ena         Enabled

Eve         Even-skipped

Fog         Folded gastrulation

GBE         germband extension

GEF         guanine nucleotide exchange factor

GFP         green fluorescent protein

Lgl         Lethal giant larvae

| | |
|---|---|
| M | maternal |
| MT | microtubule |
| MyoII | Myosin II |
| MZ | maternal and zygotic |
| Nrt | Neurotactin |
| Pyd | Polychaetoid/ZO-1 |
| R | Roughened |
| RA | Ras association domain |
| Rok | Rho kinase |
| Scrib | Scribble |
| Sdt | Stardust |
| SEM | scanning electron microscopy |
| Sna | Snail |
| Sqh | Spaghetti squash |
| Stg | String/cdc25 |
| Twi | Twist |
| WT | wild-type |
| ZA | zonula adherens |

**CHAPTER 1**

COOPERATION TO BECOME SOMETHING MORE: DEVELOPMENT'S
STRUGGLE

Starting out as a ball of naïve cells, the cells of an embryo need to effectively

communicate with one another to become a more elaborate system.  This early

communication, cells understanding their place within this ball, is a fact that we, enjoying

the benefits of effective cellular communication, take for granted.  Without the ability to

dictate and understand one's place in space, the ability to move into or form other spaces

becomes impossible, and this becomes obvious when we looks at situations where defects

run rampant during multi-cellular development exhibiting hiccups in the regulation of

cell polarity or cell adhesion. Since both proper cell-cell adhesion and underlying cell

polarity are primary systems that underlie and maintain communication between cells

within in the context of a tissue, it is vital that we understand both the main players that

establish both systems as well as players that link or modulate the two.

Working in the Peifer Lab, our tools allow us to uniquely ask questions in regard

to both cell-cell adhesion and cell polarity, due the plethora of genetic mutants that exist

for components of these two systems within our model, *Drosophila melanogaster*. More

importantly, examining combinations of these mutants allows us to answer questions

regarding the interaction of both systems so that ultimately we can understand how they

interface to allow effective and efficient morphogenesis during development.

Examination of embryonic development in *Drosophila* also allows for other advantages

providing unique insight into these systems since we can examine multiple, dynamic

morphogenetic processes.  Previous work has made us appreciate that these dynamic

processes often use the same core machinery in novel ways, allowing events that often

look radically different from one another to occur. Additionally, before the first

morphogenetic processes even begin, we can make observations on cellular behavior as

polarity and adhesion are first established within a naïve monolayer of cells.  Lastly,

events during *Drosophila* embryogenesis are often replicated in the multi-cellular

development of a variety of animals highlighting the importance of these mechanisms to

build the people we are today.

My work in the Peifer Lab has focused on a small signaling protein, the GTPase

Rap1, and its role in early development of *Drosophila* embryogenesis. This work has

straddled a number of developmental processes as we worked backwards from more

gross defects in the morphogenetic processes of mesoderm invagination and germband

extension to understanding how Rap1 works on a cellular level via early control of

polarity. In examining Rap1's effects on establishing epithelial polarity, my work

expanded into understanding how the polarity cues, Bazooka (Baz) and atypical protein

kinase C (aPKC) altered localization of Rap1's downstream effector, the scaffolding

protein, Canoe (Cno).  Lastly, this work also highlights potential interactions between

Rap1 and Rho signaling pathways in regard to regulating cell shape.

**Cell Shape Regulation: Rho1 and Cdc42 Battle It Out**

Proper regulation of cell shape is essential for efficient morphogenesis during

*Drosophila* development (Harris et al., 2009). Loss or alteration of this control has severe

consequences for a variety of tissues. During development of the *Drosophila* embryo,

changes in the apical shape of epithelial cells are vital to internalizing various tissues and elongation of the anterior-posterior axis. Without these changes, tissues often remain frozen in the wrong areas of the embryo, causing additional dysfunction in development. Modulation of cell shape requires cooperation between a number of cellular systems, specifically cell adhesion complexes, polarity cues, signaling pathways, and the cytoskeleton to allow communication within and between cells within a tissue. Signaling pathways centered around the small GTPases Rho and Cdc42, have known roles in controlling both polarity and cell adhesion (Sawyer et al., 2009a).

Rho has been shown throughout *Drosophila* development to be important in the remodeling and maintenance of cell adhesion (Magie et al., 2002). Simultaneous reductions in Rho and the transmembrane adhesion protein DE-cadherin (DE-cad) lead to additional defects in *Drosophila* embryonic development suggesting that the two work with one another to properly maintain contiguous layers of epithelia (Fox et al., 2005). The developing *Drosophila* eye provides an outstanding model for examining Rho function. Loss of Rho here leads to fragmentation of cell junctions and enlarged cell apical area, linking the Rho signaling pathway with cell adhesion and cell shape regulation (Warner and Longmore, 2009b). This indicates that *Rho* mutant cells lack contractile activity required to maintain cell shape.

The small GTPase Cdc42 has been shown to counter the activity of Rho in development, setting the stage for a balance of power that is essential for proper cell shape regulation, and hence, morphogenesis. Reducing Cdc42 in the face of lost Rho activity causes cell shape to revert back to wild-type apical cell area, indicating that cdc42 and Rho are actively working against one another to control cell shape (Warner

3

and Longmore, 2009a). However, while loss of Cdc42 alone causes a reduction in apical cell area, it does not alter cell junctions in a noticeable way (Warner and Longmore, 2009a). This suggests that while Cdc42 is not responsible in modulating cell junctions like Rho, it does counter Rho's effect on cell shape area. This reduction of apical cell area suggests that loss of cdc42 causes hyperactivity of Rho1, and data also shows that Rho1 signaling is working downstream of cdc42 signaling. How does Cdc42 dampen Rho signaling, therefore regulating cell shape? Evidence suggests that this occurs via the recruitment of the polarity cues, Par-6 and aPKC, as recruitment of ectopic aPKC to the membrane rescues Rho loss of function, unlike overexpression of Cdc42 (Warner and Longmore, 2009a). This antagonism between Rho and Cdc42 in the developing eye sets the stage for how modulation of polarity and signaling pathways regulate cell shape to allow for proper cell shape change during the morphogenetic events that are important for development.

**Mesoderm Invagination: Actomyosin Contractility Drives Apical Constriction**

Specification and invagination of the future mesoderm is the first step of *Drosophila* gastrulation. The mesoderm consists of a stripe of cells along the ventral midline about 18 cells wide and 60 cells long that are specified via upregulation of the transcription factors, Snail (Sna) and Twist (Twi) (Harris et al., 2009; Thisse et al., 1987). These transcription factors have a number of downstream targets that then cause this swath of cells to constrict apically, creating a bend in the epithelial monolayer, eventually forming an internalized tube of tissue. Once inside, this tissue then delaminates and migrates through the embryo, forming a layer of mesoderm underneath the ectoderm (Dawes-Hoang et al., 2005). Expression of Twi drives transcription of the extracellular

signaling ligand, Folded gastulation (Fog) (Costa et al., 1994). Once secreted, Fog interacts with a G-protein coupled receptor to create an apical activation of Rho signaling within the presumptive mesoderm using the G-protein α subunit 12/13 Concertina (Cta), and the Rho activator, RhoGEF2 (Barrett et al., 1997; Rogers et al., 2004; Sweeton et al., 1991).  Active Rho signaling then works to cause flattening and constriction of the apical cell surface (Dawes-Hoang et al., 2005). This apical constriction depends on downstream targets of Rho that regulate proper localization and organization of the actin cytoskeleton as well as proper localization and activation of the actin motor, non-muscle Myosin II (MyoII) (Dawes-Hoang et al., 2005).

Additional players, like the non-receptor tyrosin kinase, Ableson kinase (Abl), work independently, but cooperate with Rho signaling in the apical recruitment and organization of the actin cytoskeleton.  Blocking Rho signaling via loss of Cta and disrupting Abl function almost completely abolishes the ability of mesodermal cells to apically constrict (Fox and Peifer, 2007).  Since Abl functions by downregulating activity of the actin anti-capping protein, Enabled (Ena), it was suggested that excessive Ena activity leads to a disorganized actin cytoskeleton that is crippled in its ability to effectively cause cell constriction (Grevengoed et al., 2003). Indeed, Fox and Peifer (2007), observed increased apical localization of Ena in the mesoderm in *Abl* mutants. Besides Abl/Ena's regulation of an apical network of actin, the transmembrane protein T48 also works independent of the Fog/Cta pathway to regulate Rho activity, specifically modulating the localization of active Rho signal (Kolsch et al., 2007).  Loss of T48 causes a reduction in the ability of mesodermal cells to localize RhoGEF2 apically, creating a break in the ability of Fog and Cta to activate Rho, and subsequently, MyoII

5

(Kolsch et al., 2007). However, Kolsch et al. (2007) observed that mesoderm lacking both Cta and T48 exhibited increased inability to apically recruit RhoGEF2, indicating that Cta has some ability to regulate RhoGEF2's localization. Therefore, like Abl/Ena mentioned before, T48 acts as a modulator of the contractile machinery, allowing more effective apical constriction, and as a result, successful mesoderm invagination.

In addition to Abl/Ena and T48, it has become clear that other unidentified targets of Sna and Twi may also regulate efficacy of apical constriction as loss of either factor leads to novel effects not explained by known players, specifically a role in maintaining cell shape change and temporal control of cell constriction. Mesoderm cells with reduced or no Twi fail to retain their cell shape change during successive waves of myosin activation and cell constriction (Martin et al., 2009). In contrast, cells with reduced or no Sna can retain their cell shape change, but fail to constrict effectively due to uncoordinated MyoII activity (Martin et al., 2009). This work highlighted a novel aspect of how apical constriction works: via periodic pulses of MyoII activity that constrict the apical cell area, and a "ratchet" that maintains this reduction in apical cell area. This change in how we look at apical constriction, and as a result, mesoderm invagination emphasizes the need to identify further modulators of apical constriction and to determine whether this regulation of apical contractility occurs in other developmental processes.

**Germband Extension: Actomyosin Contractility Driving Cell Intercalation**

As mentioned before, cells often use the same core machinery in novel ways to undergo very different morphogenetic events. Along with other mechanisms, the Rho signaling pathway described above also controls another cellular movement during the stages of gastrulation in Drosophila embyogenesis, germband extension. Starting with an

event also involving apical constriction known as posterior midgut invagination, germband extension effectively lengthens the anterior/posterior axis of the ectoderm while shortening the dorsal/ventral axis of the developing embryo (Harris et al., 2009; Sawyer et al., 2010). This process requires coordination between two important biological processes: directional cellular division and cell shape change.

Directional cellular division appears to be most significant during the latter part of the fast phase of germband extension (da Silva and Vincent, 2007). This phase is characterized by rapid headward extension of the posterior tip of the germband to about 40% egg length within the first twenty-five minutes. Another phase, the slow phase, finishes germband extension within another seventy minutes ending with the posterior tip reaching about 70% egg length. Observation of cell division on the posterior germband demonstrates a significant bais toward the anterior/posterior axis during the last ten minutes of the fast phase, which is not present during the following slow phase (da Silva and Vincent, 2007). Blocking cell division by loss of the cell cycle regulator Cdc25/String (Stg) leads to reduced overall extension by the end of the fast phase, while not altering the rate of extension during the slow phase further suggesting that directed cell division participates in effective germband extension (da Silva and Vincent, 2007). However, da Silva and Vincent (2007) also observed that disruption of segmental patterning through loss of the transcription factor Even skipped (Eve) causes reduced germband extension during both phases. So while loss of Eve causing randomization of cell division in the posterior germband may explain its effect on the fast phase of germband extension, its effect on the slow phase demonstrates the existence of other mechanisms controlling germband extension.

Besides directed cell division, much of germband extension is controlled by changes in cell shape within the lateral ectoderm. Measuring changes between dorsal/ventral and anterior/posterior cell boundaries during germband extension demonstrated the potential effect simple changes in cell dimensions can have on lengthening of the tissue (Sawyer et al., 2011). However, alongside these basic changes in cell dimensions, cells are more actively moving within the tissue to allow for germband extension via cell intercalation (Harris et al., 2009; Zallen, 2007). Cells undergo intercalation in multiple ways, but it is dependent on the proper planar polarization of polarity cues and actomyosin components along dorsal/ventral and anterior/posterior cell boundaries respectively (Bertet et al., 2004; Blankenship et al., 2006). Once this planar polarity is established, the enrichment of actomyosin components along the anterior/posterior cell boundaries causes uneven cortical tension, resulting in exchanges between anterior/posterior and dorsal/ventral cell partners, and therefore, axis elongation (Harris et al., 2009). Planar polarity along both axes appears to work by feedback between the proteins involved. For example, disrupting the latter stages of Rho signaling by loss of the Rho effector, Rho kinase (Rok), disrupts planar polarity due to its role in phosphorylating both the regulatory light chain of MyoII, Spaghetti squash (Sqh), and Baz causing very different outcomes (Simoes Sde et al., 2010). Rok's phosphorylation of Baz appears to block its binding to phospholipids of the cell membrane resulting in a reduced presence of Baz in areas of Rok activity. In contrast, Rok's phosphorylation of Sqh activates the motor activity of MyoII allowing for contractile activity of the actin cytoskeleton (Dawes-Hoang et al., 2005; Simoes Sde et al., 2010; Winter et al., 2001). While this feedback may reinforce or elaborate planar

8

polarity, it is not clear that it has a role in establishing this polarity. Interestingly, loss of Eve disrupts planar polarity along both the anterior/posterior and dorsal/ventral axes, highlighting a currently unknown pathway between Eve's transcriptional control of patterning and the cell mechanics that lead to planar polarity (Zallen and Wieschaus, 2004).

**Epithelial Polarity: Bazooka Brings Everyone Together**

Ultimately, to allow proper execution of the previously described morphogenetic movements above, there are a number of cell behaviors that are required to allow cells to properly coordinate with one another. Of note, is the establishment of polarity within and between cells allowing them to correctly determine which direction is which, resulting in the overall body axes. Study of polarity within *Drosophila* allows for a unique look at how polarity is primarily established, as instead of starting as a ball of cells like many other animals, like mice or humans, the blastoderm of *Drosophila* embryos consists of a polarized epithelial monolayer formed during a process called cellularization. During cellularization, about six thousand syncytial nuclei simultaneously surround themselves with cell membranes (Harris et al., 2009). These are established by rapid inward progression of membrane materials over the course of an hour. The front of membrane ingression, the cellularization front, is defined by contractile rings enriched for MyoII and other modulators of the actin cytoskeleton, like RhoGEF2 and the actin formin, Dia (Grosshans et al., 2005; Padash Barmchi et al., 2005). Following behind this front are adhesive complexes known as basal cell junctions that are identified by enriched localization of the adhesion proteins, E-cad and Arm (Muller and Wieschaus, 1996). Loss of components within the either these basal junctions or the cellularization front disrupts

9

the formation of the contractile rings and effective membrane ingression (Grosshans et al., 2005; Hunter and Wieschaus, 2000). While polarity along the forming cell membranes isn't firmly established during early and mid stages of cellularization, polarity exists within the cytoskeletons surrounding the syncytial nuclei to help aid effective membrane ingression, similar to cytokinesis during general cell division. A key hallmark of this cytoskeleton polarity is defined by an array of microtubules resembling an inverted basket with centrosomes located above each nucleus (Warn and Warn, 1986). By the end of cellularization, the newly formed epithelial monolayer quickly establishes polarity along its cell membranes before gastrulation begins.

Initial polarity in Drosophila is identified by the enrichment of multiple polarity cues on the apical lateral membranes of cells within the blastoderm. Atop the hierarchy of protein interactions that establishes this polarity is the polarity cue, Baz (Harris and Peifer, 2004, 2005). Besides global disruption of either the actin or microtubule cytoskeletons in embryos, loss of Baz is the first event that disrupts apical accumulation of other polarity cues during this stage, suggesting the importance of understanding how Baz itself is apically localized (Harris and Peifer, 2005). Harris and Peifer (2004, 2005) were able to clearly show the importance of Baz localization in apical recruitment of other polarity cues and adherens junctions (AJs) through examination of other polarity mutants. They found that while loss of aPKC or AJ components led to gross defects in early gastrulation movements, their loss didn't cause defects in apical accumulation of Baz. Since neither loss of aPKC or AJs caused Baz to become mislocalized, it became important to understand how Baz localization was controlled. Further analysis showed that proper localization of Baz required both formation of an apical actin scaffold and

microtubule transport via dynein, a minus-end directed microtubule motor (Harris and Peifer, 2005). Additionally, mislocalization of Baz could be caused by overexpression of Baz suggesting that the levels of Baz need to be properly regulated (Harris and Peifer, 2005). Baz mislocalized in this matter also co-localized with other polarity cues and AJs, indicating that Baz is likely to recruit these proteins apically once properly put in place. However, while Baz is important for bringing everyone together in a tight apical accumulation at the end of cellularization, its role quickly changes as gastrulation proceeds, and polarity begins to mature, as the various polarity cues it was responsible for recruiting begin to separate into three main polarity zones.

**Polarity Maturation: aPKC Altering Polarity into Unique Zones**

During the morphogenetic movements of gastrulation the polarity of the *Drosophila* ectoderm begins to mature. The first sign of this change in polarity is demonstrated by apical movement of enrichments of Baz, aPKC, and AJs as the ectodermal cells apices begin to flatten, similar to what is observed in the presumptive mesoderm as it undergoes apical constriction and subsequent invagination (Tepass, 2002). Once moved apically, Baz and AJs separate away from aPKC and its partner the polarity cue Par6, due to phosphorylation of Baz by aPKC (Harris and Peifer, 2005; Morais-de-Sa et al., 2010). Blocking this phosphorylation of Baz, and hence proper separation of aPKC/Par6 from Baz/AJs, leads to breakdown of the epithelia, demonstrating the importance of modulating polarity (Morais-de-Sa et al., 2010). Once separated from Baz, aPKC and Par6 are allowed to form a complex with two other polarity cues, Crumbs (Crb) and Stardust (Sdt), to define the upmost polarity zone known as the superapical space (Krahn et al., 2010). Baz and AJs localize just underneath this

11

newly established zone, forming a zone of their own, the zonula adherens (ZA). Along the same lines, the basolateral cues, Discs large (Dlg), Lethal giant larvae (Lgl), and Scribble (Scrib) also form their own zone basally to the ZA (Johnson and Wodarz, 2003). Unlike the two other zones, this basal zone is considerably larger, covering about two-thirds of the cell body. Its apical-most boundary is defined by relative enrichments of its components (Harris and Peifer, 2004). Towards the very end of embryogenesis, this basolateral complex of proteins will form an adhesive complex called the septate junction that functions similarly to the tight junctions that exist in mammals like mice and humans (Furuse and Tsukita, 2006; Tepass and Hartenstein, 1994).

In addition to these polarity cues separating themselves into distinct zones along the lateral cell membrane, changes also occur in the planar localization of these polarity cues, as described above during our look at the morphogenetic movement of germband extension. Baz and AJs also exhibit other changes in their localization. When polarity is first established, both Baz and AJs are localized as distinct apical puncta called spot AJs (Tepass and Hartenstein, 1994). As germband extension begins, these spots transform into belt-like structures, making a solid pattern of localization along a cell-cell boundary that is called belt AJs (Tepass and Hartenstein, 1994). While this transition from spot AJs and belt AJs is easily observable, what regulates this transition is poorly understood. Loss of aPKC provides some insight as these mutants exhibit a collapse of Baz and AJs into a large single puncta on dorsal/ventral cell boundaries within the lateral ectoderm (Harris and Peifer, 2007). Further examination by disrupting the actin and microtubule cytoskeletons through drug treatment suggest that proper balance between the forces of these two networks are probably responsible for proper belt junction formation (Harris

and Peifer, 2007). Additional evidence indicates that the AJ component α-catenin (αcat) may help translate actomyosin forces to regulate E-cad localization, and therefore, cell-cell adhesion during germband extension (Rauzi et al., 2010). While promising, these few pieces of evidence emphasize another potential class of polarity regulators that needs to be identified or better understood.

**Developmental Tweaks: Rap1 Signaling Potentially Helps Everyone Cooperate**

Within the last decade, it has been suggested that the small GTPase Rap1 plays roles in morphogenesis, potentially regulating cell-cell adhesion, polarity, and migration (Bos, 2005). Rap1 is a member of the Ras superfamily, sharing high sequence identity with the canonical Ras proteins. However, it exhibits a key difference from Ras proteins with the replacement of residue 61 in Rap1 with a Threonine instead of the Glutamine conserved in various Ras proteins' switch 2 effector domains (Fig. 1A). In mammals, there are two genes that produce closely related forms of Rap1 – Rap1a and Rap1b. Rap1 also has a more distantly related relative in mammals, Rap2. Looking specifically at Rap1a sequences throughout multiple species, we see striking conservation of the protein, with over 85% identity between Drosophila and human Rap1 (Fig. 1B). Originally characterized as a Ras antagonist, due to evidence suggesting Rap1 traps the Ras effector Raf (Bos et al., 2001), more recent work suggests the situation is not this simple, as both GTPases use these effectors at either different times or in different places of the cell (Gloerich and Bos, 2011).

Rap1, as a signaling molecule, has a wide range of effectors and regulators in mammals (Bos, 2005). Many of them are important for regulating Rap signaling in regards to cell adhesion. However, only a subset have conserved homologs in Drosophila

13

and they are beginning to be characterized. PDZ-GEF/Gef26/Dizzy (dzy), a Rap1

activator, is required for proper anchoring of stem cells in their niche in the *Drosophila*

testis (Wang et al., 2006). Dzy also has roles both in remodeling cell adhesion during

mesoderm invagination and hemocyte migration during *Drosophila* embryogenesis

(Huelsmann et al., 2006; Spahn et al., 2012). In mammalian cell culture, C3G, another

Rap1 activator, is required for the proper maturation of AJs (Hogan et al., 2004). Of

special interest to the Peifer lab is the Rap1 effector, afadin (AF-6)/Canoe (Cno), which

has roles in AJ regulation. The large, multidomain Cno localizes to AJs, and is very

similar to its mammalian counterpart AF-6, carrying two Ras association domains (RA)

at the N-terminus, a FHA domain, a DIL domain, a PDZ domain, and a well-conserved

C-terminus consisting of proline-rich domains and an actin binding site (Boettner et al.,

2003; Bos, 2005; Hoshino et al., 2005; Sawyer et al., 2009b). Cno's RA domains

preferentially bind active Rap1 over the *Drosophila* homolog of H-Ras, Ras1, while the

homolog of R-Ras, Ras2 is not bound by Cno at all (Boettner et al., 2003).

Rap1 works to regulate AJs in both flies and mammals, often in partnership with

AF-6/Cno. The first indication that Rap1 might regulate AJs came from studies in

*Drosophila* in Rap1 mutant cells; loss of Rap1 disrupted E-cadherin and Cno localization

(Knox and Brown, 2002). Closer examination revealed that localization of AJ proteins

was collapsing to a point between two or more mutant cells, most likely where daughter

cells met post-mitosis (Knox and Brown, 2002). In mammals, evidence in cultured cells

suggests that Rap1 regulates AF-6 to modulate cadherin levels. Rap1 is activated during

the initial formation of cell-cell contacts through its interaction with the Rap1 activator,

C3G (Hogan et al., 2004). When either Rap1's binding domain is ablated from AF-6 or

active Rap1 binds to full-length AF-6, E-cad endocytosis is significantly lowered, causing stabilization of E-cad at cell membranes (Hoshino et al., 2005).  Likewise, AF-6 may be important in preserving or sequestering active Rap1 since loss of AF-6 through RNAi knockdown caused a decrease in the levels of active Rap1 (Zhang et al., 2005). This reduction in active Rap1 translated into a reduction in adhesion strength, suggesting that Rap1 either functions in initially setting up or maintaining cell-cell adhesion.

As Rap1's protein sequence is highly conserved, it seems plausible that Rap1 functions very similarly in many different animals.  *Drosophila* provides a great model system for analysis of Rap1's functions in vivo.  In this model system, Rap1 is encoded by one gene instead of two, eliminating the potential for redundancy seen in mammalian systems.  Rap1 was first discovered as the gene *Roughened* (*R*); the original allele showed defects in eye development causing disorganized or ruptured facets in the multi-faceted *Drosophila* eye (Asha et al., 1999; Hariharan et al., 1991).  The original $R^1$ allele was actually a gain of function form of Rap1.  Using reversion of its dominant phenotype, numerous null alleles were created.  Examination of Rap1 loss of function revealed to a variety of defects during development including complete degeneration of the egg chamber during oogenesis and abnormal behavior of mesoderm during embryogenesis (Asha et al., 1999).

While there are multiple morphogenetic events in which to study the relationship between cell adhesion and cytoskeletal regulation during *Drosophila* development, dorsal closure has been particularly useful.  Dorsal closure consists of two processes occurring together in a coordinated manner, apical constriction of a dorsal group of cells known as the amnioserosa and movement of the neighboring lateral ectoderm over the dorsal side

of the embryo, resulting in an embryo completely covered in epidermis (Harris et al.,

2009).  At the leading edge of the lateral ectoderm, a contractile actomyosin cable is

formed between cells through AJs.  When levels of the Rap1 effector, Cno, are reduced,

actin and MyoII accumulate at the leading edge normally, but the aminoserosa separates

from the lateral ectoderm as dorsal closure proceeds, suggesting effects on cell-cell

adhesion (Boettner et al., 2003; Choi et al., 2011).  However, while localization of AJs

proteins are not noticeably affected, additional evidence suggests that there indeed

alterations in actin dynamics since localization of Ena is altered in mutants with reduced

Cno or lacking the Cno binding partner, ZO-1/Polychaetoid (pyd) (Choi et al., 2011).

Further, when levels of Pyd or Cno are reduced in *ena* zygotic mutants, an increased loss

of epithelial integrity was observed (Choi et al., 2011).  These results suggest that Cno

and Pyd potentially work in complex to regulate Ena localization during dorsal closure.

During dorsal closure as well as throughout *Drosophila* development, active Rap1

binds to Cno as previously mentioned above.  Both Rap1 and Cno localize to AJs during

*Drosophila* embryogenesis and throughout larval development consistent with them

being partners (Boettner et al., 2003; Knox and Brown, 2002; Sawyer et al., 2009b).

Previous genetic evidence suggests they work together.  When levels of Rap1 are reduced

in *cno* zygotic mutants, there is notably enhancement of *cno* phenotypes, as significantly

more embryos display a lack of dorsal epidermis (Boettner et al., 2003).  However,

neither expression of a constitutively active form of Rap1 (Rap1$^{CA}$) nor of Cno lacking

Rap1 binding domains (cno$^{\Delta N}$) completely rescue *cno* zygotic phenotypes suggesting that

Rap1 has functions that are both dependent and independent of Cno in regulating

morphogenesis and cell adhesion in *Drosophila* (Boettner et al., 2003).

**Circle of Life: Answers Beget Additional Questions**

While work in Drosophila has yielded excellent results so far in understanding how cells cooperate with one another, it has also highlighted a multitude of additional questions that are begging to be answered. Continued work in Drosophila, especially as more tools continue to be developed, will allow us to answer these questions, and discover additional ones, continuing an exciting of cycle in understanding the world around us, starting with the cells that came together to build us into the people we are today.

## References

Asha, H., de Ruiter, N.D., Wang, M.G., Hariharan, I.K., 1999. The Rap1 GTPase functions as a regulator of morphogenesis in vivo. Embo J 18, 605-615.

Barrett, K., Leptin, M., Settleman, J., 1997. The Rho GTPase and a putative RhoGEF mediate a signaling pathway for the cell shape changes in Drosophila gastrulation. Cell 91, 905-915.

Bertet, C., Sulak, L., Lecuit, T., 2004. Myosin-dependent junction remodelling controls planar cell intercalation and axis elongation. Nature 429, 667-671.

Blankenship, J.T., Backovic, S.T., Sanny, J.S., Weitz, O., Zallen, J.A., 2006. Multicellular rosette formation links planar cell polarity to tissue morphogenesis. Developmental cell 11, 459-470.

Boettner, B., Harjes, P., Ishimaru, S., Heke, M., Fan, H.Q., Qin, Y., Van Aelst, L., Gaul, U., 2003. The AF-6 homolog canoe acts as a Rap1 effector during dorsal closure of the Drosophila embryo. Genetics 165, 159-169.

Bos, J.L., 2005. Linking Rap to cell adhesion. Current opinion in cell biology 17, 123-128.

Bos, J.L., de Rooij, J., Reedquist, K.A., 2001. Rap1 signalling: adhering to new models. Nat Rev Mol Cell Biol 2, 369-377.

Choi, W., Jung, K.C., Nelson, K.S., Bhat, M.A., Beitel, G.J., Peifer, M., Fanning, A.S., 2011. The single Drosophila ZO-1 protein Polychaetoid regulates embryonic morphogenesis in coordination with Canoe/afadin and Enabled. Molecular biology of the cell 22, 2010-2030.

Costa, M., Wilson, E.T., Wieschaus, E., 1994. A putative cell signal encoded by the folded gastrulation gene coordinates cell shape changes during Drosophila gastrulation. Cell 76, 1075-1089.

da Silva, S.M., Vincent, J.P., 2007. Oriented cell divisions in the extending germband of Drosophila. Development 134, 3049-3054.

Dawes-Hoang, R.E., Parmar, K.M., Christiansen, A.E., Phelps, C.B., Brand, A.H., Wieschaus, E.F., 2005. folded gastrulation, cell shape change and the control of myosin localization. Development 132, 4165-4178.

Fox, D.T., Homem, C.C., Myster, S.H., Wang, F., Bain, E.E., Peifer, M., 2005. Rho1 regulates Drosophila adherens junctions independently of p120ctn. Development 132, 4819-4831.

Fox, D.T., Peifer, M., 2007. Abelson kinase (Abl) and RhoGEF2 regulate actin organization during cell constriction in Drosophila. Development 134, 567-578.

Furuse, M., Tsukita, S., 2006. Claudins in occluding junctions of humans and flies. Trends in cell biology 16, 181-188.

Gloerich, M., Bos, J.L., 2011. Regulating Rap small G-proteins in time and space. Trends in cell biology 21, 615-623.

Grevengoed, E.E., Fox, D.T., Gates, J., Peifer, M., 2003. Balancing different types of actin polymerization at distinct sites: roles for Abelson kinase and Enabled. The Journal of cell biology 163, 1267-1279.

Grosshans, J., Wenzl, C., Herz, H.M., Bartoszewski, S., Schnorrer, F., Vogt, N., Schwarz, H., Muller, H.A., 2005. RhoGEF2 and the formin Dia control the formation of the furrow canal by directed actin assembly during Drosophila cellularisation. Development 132, 1009-1020.

Hariharan, I.K., Carthew, R.W., Rubin, G.M., 1991. The Drosophila roughened mutation: activation of a rap homolog disrupts eye development and interferes with cell determination. Cell 67, 717-722.

Harris, T.J., Peifer, M., 2004. Adherens junction-dependent and -independent steps in the establishment of epithelial cell polarity in Drosophila. The Journal of cell biology 167, 135-147.

Harris, T.J., Peifer, M., 2005. The positioning and segregation of apical cues during epithelial polarity establishment in Drosophila. The Journal of cell biology 170, 813-823.

Harris, T.J., Peifer, M., 2007. aPKC controls microtubule organization to balance adherens junction symmetry and planar polarity during development. Developmental cell 12, 727-738.

Harris, T.J., Sawyer, J.K., Peifer, M., 2009. How the cytoskeleton helps build the embryonic body plan: models of morphogenesis from Drosophila. Curr Top Dev Biol 89, 55-85.

Hogan, C., Serpente, N., Cogram, P., Hosking, C.R., Bialucha, C.U., Feller, S.M., Braga, V.M., Birchmeier, W., Fujita, Y., 2004. Rap1 regulates the formation of E-cadherin-based cell-cell contacts. Mol Cell Biol 24, 6690-6700.

Hoshino, T., Sakisaka, T., Baba, T., Yamada, T., Kimura, T., Takai, Y., 2005. Regulation of E-cadherin endocytosis by nectin through afadin, Rap1, and p120ctn. The Journal of biological chemistry 280, 24095-24103.

Huelsmann, S., Hepper, C., Marchese, D., Knoll, C., Reuter, R., 2006. The PDZ-GEF dizzy regulates cell shape of migrating macrophages via Rap1 and integrins in the Drosophila embryo. Development 133, 2915-2924.

Hunter, C., Wieschaus, E., 2000. Regulated expression of nullo is required for the formation of distinct apical and basal adherens junctions in the Drosophila blastoderm. The Journal of cell biology 150, 391-401.

Johnson, K., Wodarz, A., 2003. A genetic hierarchy controlling cell polarity. Nature cell biology 5, 12-14.

Knox, A.L., Brown, N.H., 2002. Rap1 GTPase regulation of adherens junction positioning and cell adhesion. Science 295, 1285-1288.

Kolsch, V., Seher, T., Fernandez-Ballester, G.J., Serrano, L., Leptin, M., 2007. Control of Drosophila gastrulation by apical localization of adherens junctions and RhoGEF2. Science 315, 384-386.

Krahn, M.P., Buckers, J., Kastrup, L., Wodarz, A., 2010. Formation of a Bazooka-Stardust complex is essential for plasma membrane polarity in epithelia. The Journal of cell biology 190, 751-760.

Magie, C.R., Pinto-Santini, D., Parkhurst, S.M., 2002. Rho1 interacts with p120ctn and alpha-catenin, and regulates cadherin-based adherens junction components in Drosophila. Development 129, 3771-3782.

Martin, A.C., Kaschube, M., Wieschaus, E.F., 2009. Pulsed contractions of an actin-myosin network drive apical constriction. Nature 457, 495-499.

Morais-de-Sa, E., Mirouse, V., St Johnston, D., 2010. aPKC phosphorylation of Bazooka defines the apical/lateral border in Drosophila epithelial cells. Cell 141, 509-523.

Muller, H.A., Wieschaus, E., 1996. armadillo, bazooka, and stardust are critical for early stages in formation of the zonula adherens and maintenance of the polarized blastoderm epithelium in Drosophila. The Journal of cell biology 134, 149-163.

Padash Barmchi, M., Rogers, S., Hacker, U., 2005. DRhoGEF2 regulates actin organization and contractility in the Drosophila blastoderm embryo. The Journal of cell biology 168, 575-585.

Rauzi, M., Lenne, P.F., Lecuit, T., 2010. Planar polarized actomyosin contractile flows control epithelial junction remodelling. Nature 468, 1110-1114.

Rogers, S.L., Wiedemann, U., Hacker, U., Turck, C., Vale, R.D., 2004. Drosophila RhoGEF2 associates with microtubule plus ends in an EB1-dependent manner. Current biology : CB 14, 1827-1833.

Sawyer, J.K., Choi, W., Jung, K.C., He, L., Harris, N.J., Peifer, M., 2011. A contractile actomyosin network linked to adherens junctions by Canoe/afadin helps drive convergent extension. Molecular biology of the cell 22, 2491-2508.

Sawyer, J.K., Harris, N.J., Peifer, M., 2009a. Morphogenesis: multitalented GTPases seeking new jobs. Current biology : CB 19, R985-987.

Sawyer, J.K., Harris, N.J., Slep, K.C., Gaul, U., Peifer, M., 2009b. The Drosophila afadin homologue Canoe regulates linkage of the actin cytoskeleton to adherens junctions during apical constriction. The Journal of cell biology 186, 57-73.

Sawyer, J.M., Harrell, J.R., Shemer, G., Sullivan-Brown, J., Roh-Johnson, M., Goldstein, B., 2010. Apical constriction: a cell shape change that can drive morphogenesis. Developmental biology 341, 5-19.

Simoes Sde, M., Blankenship, J.T., Weitz, O., Farrell, D.L., Tamada, M., Fernandez-Gonzalez, R., Zallen, J.A., 2010. Rho-kinase directs Bazooka/Par-3 planar polarity during Drosophila axis elongation. Developmental cell 19, 377-388.

Spahn, P., Ott, A., Reuter, R., 2012. The PDZ-GEF Dizzy regulates the establishment of adherens junctions required for ventral furrow formation in Drosophila. Journal of cell science.

Sweeton, D., Parks, S., Costa, M., Wieschaus, E., 1991. Gastrulation in Drosophila: the formation of the ventral furrow and posterior midgut invaginations. Development 112, 775-789.

Tepass, U., 2002. Adherens junctions: new insight into assembly, modulation and function. BioEssays : news and reviews in molecular, cellular and developmental biology 24, 690-695.

Tepass, U., Hartenstein, V., 1994. The development of cellular junctions in the Drosophila embryo. Developmental biology 161, 563-596.

Thisse, B., el Messal, M., Perrin-Schmitt, F., 1987. The twist gene: isolation of a Drosophila zygotic gene necessary for the establishment of dorsoventral pattern. Nucleic Acids Res 15, 3439-3453.

Wang, H., Singh, S.R., Zheng, Z., Oh, S.W., Chen, X., Edwards, K., Hou, S.X., 2006. Rap-GEF signaling controls stem cell anchoring to their niche through regulating DE-cadherin-mediated cell adhesion in the Drosophila testis. Developmental cell 10, 117-126.

Warn, R.M., Warn, A., 1986. Microtubule arrays present during the syncytial and cellular blastoderm stages of the early Drosophila embryo. Exp Cell Res 163, 201-210.

Warner, S.J., Longmore, G.D., 2009a. Cdc42 antagonizes Rho1 activity at adherens junctions to limit epithelial cell apical tension. The Journal of cell biology 187, 119-133.

Warner, S.J., Longmore, G.D., 2009b. Distinct functions for Rho1 in maintaining adherens junctions and apical tension in remodeling epithelia. The Journal of cell biology 185, 1111-1125.

Winter, C.G., Wang, B., Ballew, A., Royou, A., Karess, R., Axelrod, J.D., Luo, L., 2001. Drosophila Rho-associated kinase (Drok) links Frizzled-mediated planar cell polarity signaling to the actin cytoskeleton. Cell 105, 81-91.

Zallen, J.A., 2007. Planar polarity and tissue morphogenesis. Cell 129, 1051-1063.

Zallen, J.A., Wieschaus, E., 2004. Patterned gene expression directs bipolar planar polarity in Drosophila. Developmental cell 6, 343-355.

Zhang, Z., Rehmann, H., Price, L.S., Riedl, J., Bos, J.L., 2005. AF6 negatively regulates Rap1-induced cell adhesion. The Journal of biological chemistry 280, 33200-33205.

**A.**

```
      23                          45   60*                76
H-Ras  LIQNHFVDEYDPTIEDSYRKQVV /// GQEEYSAMRDQYMRTGE
Rap1a  FVQGIFVEKYDPTIEDSYRKQVE /// GTEQFTAMRDLYMKNGQ
Rap2   FVTGTFIEKYDPTIEDFYRKEIE /// GTEQFASMRDLYIKNGQ
R-Ras  FIQSYFVSDYDPTIEDSYTKICS /// GQEEFGAMREQYMRAGH


             Switch 1                 Switch 2
```

**B.**

```
hRap1     MREYKLVVLGSGGVGKSALTVQFVQGIFVEKYDPTIEDSYRKQVEVDCQQCMLEILDTAG 60
dRap1     MREYKIVVLGSGGVGKSALTVQFVQCIFVEKYDPTIEDSYRKQVEVDGQQCMLEILDTAG 60
          *****:******************* ********************* ************


hRap1     TEQFTAMRDLYMKNGQGFALVYSITAQSTFNDLQDLREQILRVKDTEDVPMILVGNKCDL 120
dRap1     TEQFTAMRDLYMKNGQGFVLVYSITAQSTFNDLQDLREQILRVKDTDDVPMVLVGNKCDL 120
          ******************.*************************:****:********


hRap1     EDERVVGKEQGQNLARQWCNCAFLESSAKSKINVNEIFYDLVRQINRKTPVEK-KKPKKK 179
dRap1     EEERVVGKELGKNLATQFN-CAFMETSAKAKVNVNDIFYDLVRQINKKSPEKKQKKPKKS 179
          *:******* *:*** *:   ***:*:***:*:***:**********:*:* :* *****.


hRap1     SCLLL 184
dRap1     LCVLL 184
          *:**
```

**Figure 1.1. Rap1 is in the Ras superfamily. (A)** Rap1 shows high identity with canonical Ras proteins. The asterisk marks residue 61, which in Rap proteins is Threonine (T) instead of Glutamine (Q). **(B)** Human and Drosophila Rap1 show 85% sequence identity suggesting highly similar functionality during development.

# CHAPTER 2

## THE DROSOPHILA AFADIN HOMOLOG CANOE REGULATES LINKAGE OF THE ACTIN CYTOSKELETON TO ADHERENS JUNCTIONS DURING APICAL CONSTRICTION

Jessica K. Sawyer[1], Nathan J. Harris[1], Kevin C. Slep[1], Ulrike Gaul[3], and Mark Peifer[1,2]

[1]Department of Biology, University of North Carolina at Chapel Hill, Chapel Hill, NC 27599, USA; [2]Lineberger Comprehensive Cancer Center, University of North Carolina at Chapel Hill, NC 27599, USA; [3]Laboratory of Developmental Neurogenetics, Rockefeller University, New York, NY 10065, USA

**Preface**

The following paper characterized the role of Cno in the process of apical constriction during the mesoderm invagination. Initially, we found that loss of Cno causes epithelial breakdown, but not to the same extent as mutants of core components of cell adhesion, indicating that Cno regulates, but not essential for cell adhesion. Next, we observed that *cno* mutants displayed an inability to properly internalize their mesoderm similar to mutants affecting Rho signaling and cell adhesion further suggesting that Cno regulates cell adhesion or potentially actomyosin activity. In examining Cno's role in both of these processes, we examined the localization of actin, myosin, and components of AJs (E-cad and Arm). Although, we did not observe noticeable defects in apical localization of AJs, we did observe actin and myosin "balls" centered in the apices of the cell undergoing apical constriction suggesting an inability of the apical actomyosin

network to alter the cell membrane potentially due to improper tethering of this network to cell junctions as these "balls" also exist in arm mutants. Furthermore, closer examination uncovered minor localization of AJ components to these "balls", suggesting the tearing away of AJs from the cell cortex. We were able to reinforce the idea that Cno acts as a scaffold linking AJs to a contractile actomyosin network in three ways: Cno co-localizes to AJs, has a C-terminal actin binding domain, and has a PDZ domain that binds E-cad. In addition, we found that loss of Arm or Cno's binding partner Echinoid (Ed) did not alter Cno localization suggesting that the mechanisms for regulating its localization have yet to be uncovered. However, global disruption of the actin cytoskeleton did alter Cno localization indicating that the newly discovered actin binding domain of Cno is important for cortical association.

My part in this work was characterizing the role of the Cno's binding partner Rap1, a small GTPase. Rap1 was previously shown to interact with Cno during dorsal closure, a later morphogenetic event in Drosophila embryogenesis (Boettner et al., 2003). Previous work also suggested that Rap1 may have defects in mesoderm invagination (Asha et al., 1999). As a result, I examined *Rap1* mutants to compare to the defects we observed in *cno* mutants. I found that loss of Rap1 lead to epithelial breakdown, indicating a similar role in regulating cell adhesion. Also, Rap1 mutants fail to complete mesoderm invagination, with mutants displaying the same actin and myosin rich "balls" found in Cno mutants. However, I observed additional issues in gastrulation that resulted in a twisted ventral midline, unlike *cno* mutants, suggesting Cno-independent roles for Rap1 in gastrulation. Lastly, I found that Cno localization was altered in *Rap1* mutants leading to reduced Cno localized at the cell cortex, supporting a pathway where Rap1

regulates Cno localization, and ultimately, its ability to strengthen the attachment between the apical actomyosin network and the cell cortex via its interaction with AJs.

**Abstract**

Cadherin-based adherens junctions (AJs) mediate cell adhesion and regulate cell shape change. The nectin-afadin complex also localizes to AJs and links to the cytoskeleton. Mammalian afadin has been suggested to be essential for adhesion and polarity establishment, but its mechanism of action is unclear. In contrast, *Drosophila's* afadin homolog Canoe (Cno) has suggested roles in signal transduction during morphogenesis. We completely removed Cno from embryos, testing these hypotheses. Surprisingly, Cno is not essential for AJ assembly, or for AJ maintenance in many tissues. However, morphogenesis is impaired from the start. Apical constriction of mesodermal cells initiates but is not completed. The actomyosin cytoskeleton disconnects from AJs, uncoupling actomyosin constriction and cell shape change. Cno has multiple direct interactions with AJ proteins, but is not a core part of the cadherin-catenin complex. Instead Cno localizes to AJs by a Rap1 and actin-dependent mechanism. These data suggest Cno regulates linkage between AJs and the actin cytoskeleton during morphogenesis.

**Introduction**

Embryonic cells self-assemble tissues and organs. This morphogenesis process requires dynamic regulation of cell adhesion and cell shape change (Halbleib and Nelson, 2006), which are coordinated by cell-cell adherens junctions (AJs). AJs link neighboring cells to each other and to the apical actin cytoskeleton. Central to AJs are cadherins, transmembrane homophilic adhesion proteins. Their cytoplasmic tails bind βcatenin (fly

26

Armadillo (Arm)), which binds αcatenin (αcat). αcat can directly bind actin filaments.

Each of these proteins is essential for cell adhesion and epithelial integrity, with loss

leading to very early defects in embryogenesis (Cox et al., 1996; Kofron et al., 1997;

Larue et al., 1994; Müller and Wieschaus, 1996; Torres et al., 1997). It was assumed AJs

directly link to actin via the catenins. However, things are more complex. While E-

cadherin (Ecad) binds both catenins, and αcat binds actin, these interactions are mutually

exclusive, and thus cadherin-catenin complexes cannot bind actin (Drees et al., 2005;

Yamada et al., 2005). However, many morphogenetic events require intimate

interactions between AJs and the cytoskeleton, prompting us to explore other proteins

that may regulate adhesion and linkage to actin.

One interesting candidate is the nectin-afadin complex. Nectins are

transmembrane immunoglobulin domain proteins co-localizing with Ecad at AJs

(Takahashi et al., 1999) and mediating homophilic and heterophilic adhesion (Sakisaka et

al., 2007). The four mouse nectins complicate loss-of-function analysis, but expression

of soluble nectin extracellular domain diminishes cell adhesion in culture (Honda et al.,

2003). These and other data (e.g. Tachibana et al., 2000; Fukuhara et al., 2002) led the

authors to suggest nectins are "necessary and sufficient for the recruitment of Ecadherin

to the nectin-based cell-cell adhesion sites and [are] involved in the formation of

Ecadherin-based cell-cell AJs".

Nectins are thought to associate with actin via the Factin binding protein afadin

(=AF6), which binds via its PDZ domain to nectin C-termini and localizes to AJs

(Mandai et al., 1997). Afadin's structure suggests a scaffolding role (Fig. 1A). It has two

Ras association (RA) domains, Forkhead-associated (FHA) and Dilute (DIL) domains,

and a C-terminal actin-binding domain. Rap1 is thought to be the preferred binding

partner for the RA domains (Linnemann et al., 1999), and afadin and Rap1 are

functionally linked (Kooistra et al., 2006). Afadin provides a potential direct link

between nectins and actin, and afadin also associates with other actin binding proteins,

including αcat (Pokutta et al., 2002; Tachibana et al., 2000).

This raised the possibility afadin plays an important role in adhesion. Afadin

knockdown in MDCK cells reduced Ecad at AJs after $Ca^{2+}$ shift, though, surprisingly,

total cell surface Ecad and catenin association were unchanged (Sato et al., 2006). *afadin*

null embryoid bodies have many AJ and tight junction proteins mislocalized (Komura et

al., 2008), suggesting afadin is important in establishing polarity and cell adhesion.

Afadin knockout in mice resulted in embryonic lethality, with defects during and after

gastrulation. These workers concluded afadin is "a key molecule essential for structural

organization of cell–cell junctions of polarized epithelia during embryogenesis (Ikeda et

al., 1999)", or that loss of afadin "disrupts epithelial cell–cell junctions and cell polarity

during mouse development" (Zhadanov et al., 1999). However, *afadin's* phenotype is

much milder than those caused by loss of Ecad (Larue et al., 1994) or α-E-catenin (Torres

et al., 1997), which disrupt the trophectoderm epithelium and block implantation.

*Drosophila* has one afadin homolog, Canoe (Cno; Miyamoto et al., 1995), and at

least one nectin, Echinoid (Ed), to which Cno binds (Wei et al., 2005). Cno also

genetically interacts with and binds Rap1 (Boettner et al., 2003) and Polychaetoid

(Pyd=fly Zona Occludens-1; ZO-1; Takahashi et al., 1998). Surprisingly, studies of Cno

suggested a different model in which it is a scaffold for signal transduction proteins. *cno*

genetically interacts with Receptor tyrosine kinase/Ras, JNK, Notch, and Wnt pathways

28

(Matsuo et al., 1999; Takahashi et al., 1998; Miyamoto et al., 1995; Carmena et al., 2006), but mechanisms by which Cno influences signaling remain unclear. As in mice, Cno regulates morphogenesis. Zygotic mutants have defects in cell shape change during dorsal closure (Boettner et al., 2003; Jürgens et al., 1984; Takahashi et al., 1998), and in asymmetric divisions and cell fate choice in the nervous system and mesoderm (Carmena et al., 2006; Speicher et al., 2008). However, these studies left intact maternally contributed wildtype Cno.

These data provide several alternate hypotheses for Cno/afadin function: at one extreme, it may be essential in cell adhesion while at the other it may transduce signals regulating cell shape change. *Drosophila* provides powerful tools to distinguish between these mechanistic hypotheses. Here we examine the consequences of completely eliminating Cno function from the onset of embryogenesis. Our data suggest Cno regulates links between AJs and actin during apical constriction, providing one possible solution to the dilemma posed by Weis and Nelson (Drees et al., 2005; Yamada et al., 2005).

**Results**

***Complete loss of Cno leads to severe morphogenesis defects***

Cno plays important roles in dorsal closure, mesoderm, and neural development (see Introduction), but these studies only examined zygotic mutants. We hypothesized maternal Cno masked earlier roles. To eliminate maternal and zygotic Cno ($cno^{MZ}$ mutants), we screened for new *cno* alleles on a Flippase-recombination target (FRT) chromosome (*cno* is very close to the FRT site), allowing us to remove Cno from the germline (Chou et al., 1993). $cno^{R2}$ has an early stop codon (K211Stop) after the first RA

binding domain (Fig. 1A), suggesting it is null. Maternal and zygotic $cno^{R2}$ mutants lost

Cno immunoreactivity with a C-terminal antibody (Fig. 1B vs. C; imaged on the same

slide), confirming that there is not stop codon readthrough or re-initiation. While it is

possible the remaining short protein fragment is produced, we think this is unlikely.

First, nonsense mediated mRNA decay usually efficiently degrades mRNAs with such

early stop codons (Gatfield et al., 2003; Muhlemann et al., 2008). Second, we could not

detect a stable product of $cno^2$, with a much later stop codon (Q1310Stop; data not

shown). Finally, a second independent early truncation has a similar phenotype (see next

paragraph).

To assess how complete Cno loss affects morphogenesis, we examined cuticles

secreted by epidermal cells (Fig. 1D). Zygotic *cno* mutant embryos die; 88% have

defects in head involution but close dorsally (Fig. 1E), while 11% have defects in head

involution and dorsal closure (Fig. 1F). Loss of maternal Cno is not fully rescued by

zygotic wildtype Cno; ~30% of paternally rescued mutants die, with defects in head

involution (data not shown). $cno^{MZ}$ mutants (Fig. 1G) are much more severe than zygotic

mutants, consistent with strong maternal contribution. Most $cno^{MZ}$ embryos (83%)

entirely lack ventral cuticle, secreted by ventral neurogenic epidermis, but retain dorsal

cuticle, secreted by non-neurogenic dorsal epidermis (Fig. 1G). $cno^{R10}$ MZ mutants (a

second putative null; Q140STOP) had similar phenotypes (data not shown). The $cno^{MZ}$

phenotype is not as severe as that of mutants completely lacking core AJ proteins

*DEcadherin (DEcad*; Tepass et al., 1996) or *armadillo (arm=ßcatenin,* Cox et al., 1996;

Müller and Wieschaus, 1996), in which only cuticle scraps are secreted (Fig. 1H). This

suggests Cno is not essential for epithelial integrity. However, $cno^{MZ}$ mutants mimic

*shotgun* zygotic mutants—these mutants retain maternal DEcad but lack zygotic DEcad (Tepass et al., 1996; Fig. 1I), and thus lose AJ function as maternal DEcad is depleted. This is consistent with Cno modulating adhesion during later morphogenesis.

***Cno is not essential for AJ assembly and is only required for AJ maintenance in some tissues***

To further test Cno's roles in AJs, we assessed AJ protein localization in $cno^{MZ}$ mutants. We first examined AJ assembly. During cellularization, DEcad first localizes to basal junctions near the invaginating actomyosin front and then relocalizes to apical spot AJs; as the germband extends these smooth out into belt AJs (Harris and Peifer, 2004; Tepass and Hartenstein, 1994). Initial AJ assembly in $cno^{MZ}$ was indistinguishable from wildtype (Fig. 2A vs B, C vs D; Arm and αcat also assembled correctly; Suppl. Fig. 1A-F; data not shown), and AJ proteins became apically enriched (Fig. 2F). Apical actin also appeared normal, co-localizing with DEcad (Fig. 2A' vs B', C vs. D). This is in striking contrast to the loss of junctional DEcad and polarized Factin in *arm* mutants (Fig. 2E,E'; Cox et al., 1996). Maturation of spot AJs to belt AJs (Suppl. Fig 1A-F) also proceeded normally. Finally, AJ protein levels were normal at these stages (Fig. 3, 0-4h; DEcad 102%, Arm 111%, αcat 90% of wildtype; mean of 3 experiments). Two Cno binding proteins, Pyd and Ed, localize to AJs from the start, and both localize normally in $cno^{MZ}$ mutants (Suppl Fig. 1G-J). These data suggest Cno is not essential for AJ assembly or initial maturation.

In many embryonic cells, Cno is also not essential for AJ maintenance. In $cno^{MZ}$ AJs and cell shapes remain normal in amnioserosa (Fig. 2I, arrows) and dorsal epidermal cells (Fig. 2I arrowheads, J vs. K) through germband retraction. However, in a subset of

31

ectoderm AJs are not maintained normally. As the germband extends, ectodermal cells initiate mitosis; as they divide they round up and apical AJ protein accumulation is reduced (Fig. 2L,N, arrows). As they exit mitosis, AJs reassemble and cells become columnar again. In *cno^MZ*, while dorsal ectodermal cells retain columnar shape and normal AJs (Fig. 2J), many ventral neurogenic ectodermal cells have reduced DEcad. It appears that after division they do not regain columnar shape with small apical ends (Fig. 2M,O brackets). To ensure cells properly exited mitosis, we labeled embryos with the mitotic marker anti-phosphoHistoneH3; large regions of ventral epidermis exited mitosis without properly reassembling AJs or regaining columnar shape (Fig. 2P,Q - arrows). AJ fragmentation occurred prior to loss of cortical actin (Fig. 2R, arrows). Arm and DEcad levels are also somewhat reduced at this stage (Fig. 3, 4-8h; DEcad 87%, Arm 83%, ☐cat 102% of wildtype; mean of 3 experiments). Morphogenesis is compromised: the epidermis separates from the amnioserosa (Fig. 2S, arrow) and segmental grooves never retract (Fig. 2S arrowheads). Ultimately, ventral cells are lost (Fig. 2T, brackets), likely explaining the retention of dorsal but not ventral cuticle (Fig. 1G). Thus Cno is dispensable for AJ assembly and maintenance in many tissues, but regulates AJ maintenance in some morphogenetically active cells.

## *Cno loss disrupts mesoderm invagination*

While AJs are established normally in Cno's absence, morphogenesis is affected from the start. Gastrulation initiates after cellularization. The ventralmost cells form mesoderm and undergo coordinated apical constriction triggered by a pathway involving the ligand Fog, the G protein Concertina (Cta), RhoGEF2 and Rho (Pilot and Lecuit, 2005). In response, mesodermal cells accumulate apical actin and myosin, apically

constrict (Fig. 4A,B), and internalize as a tube (Fig. 4C). If AJs are disrupted, mesoderm

invagination is compromised (Dawes-Hoang et al., 2005), and thus coordinating AJs and

actin is critical to couple actomyosin constriction to cell shape change.

$cno^{MZ}$ morphogenetic defects begin at gastrulation. Wildtype mesoderm, marked

by the transcription factor Twist, is completely internalized during gastrulation (Fig.

4D,E). In contrast, $cno^{MZ}$ mutants do not completely internalize mesoderm; many cells

remain on the embryo surface and begin to divide in this aberrant location (Fig.4G,H).

The degree of defect in mesoderm invagination varied from complete failure to defects

only at the anterior and posterior ends (data not shown).

We next examined mechanisms by which this occurs. Cno, unlike Arm, is not

essential for AJ assembly (Fig. 2A-E'), even in invaginating mesoderm (Fig. 2G vs H).

Second, Cno is not required for mesoderm specification, as $cno^{MZ}$ mesoderm expresses

Twist, the transcription factor conferring mesodermal fate (Fig. 4G,H). A third

hypothesis is that in Cno's absence, mesodermal cells fail to initiate apical constriction,

as do *RhoGEF2* mutants (Barrett et al., 1997), or fail to constrict in a coordinated way, as

do *fog* or *cta* mutants (Sweeton et al., 1991). However, $cno^{MZ}$ mutant cells initiate

constriction and do so fairly synchronously (Fig.4F vs. I; occasional cells in both

wildtype and mutant constrict more slowly than their neighbors). However, $cno^{MZ}$ cells

arrest partway through apical constriction. Live analysis using Moesin-GFP (MoeGFP)

to highlight Factin confirmed this. Wildtype mesodermal cells constrict rapidly and

fairly synchronously (Fig. 5A; Suppl. Video 1). To quantify this we measured change in

cell cross-sectional area of eight randomly chosen cells, confirming rapid, synchronous

constriction in wildtype, with occasional cells lagging behind (Fig. 5D). $cno^{MZ}$ mutants

(distinguished from paternally rescued embryos using a marked Balancer chromosome) initiated apical constriction in a timely manner, but then had a variable phenotype (like the variability in mesoderm invagination). In less severe mutants constriction went at the same rate as in wildtype (Fig. 5B,E, Suppl. Video 2), but halted prematurely—thus as mesodermal cells initiated division (Fig. 5B, 32m15s arrow), they re-emerged from the furrow. In more severe embryos (Fig. 5C,F, Suppl. Video 3), constriction was slower than in wildtype and more cells lagged behind; this delay allowed mesodermal cells to divide before being internalized. These data suggest Cno acts by a novel mechanism to ensure completion of apical constriction.

To identify this mechanism, we looked in detail at cytoskeletal rearrangements. The first step is apical recruitment of actin and myosin (Fig. 6B,H, arrows), where they assemble into a contractile network (Fig, 6A,A" data not shown); actin is also enriched in a ring at AJs (Fox and Peifer, 2007). In $cno^{MZ}$ actin and myosin are recruited to the apical cortex (Fig. 4L, arrowheads, 6D, arrow). Wildtype constricting cells elongate along the apical-basal axis, and this occurs normally in $cno^{MZ}$ mutants (Fig. 4L).

In wildtype, actomyosin constriction begins as soon as myosin arrives apically and is coupled to cell shape change, with AJs moving inward as constriction proceeds (Fig. 6A-A"). One hypothesis is that Cno regulates the extent of actomyosin constriction, so it does not go to completion in $cno^{MZ}$ mutants. However, this is not the case—instead actomyosin constriction initiated correctly (Fig. 4I) but became uncoupled from cell shape change. In wildtype actomyosin contraction is coupled to reduction in diameter of the cell's apical end (Fig.6A-A",B-B",E,H). In $cno^{MZ}$, myosin (Fig. 6C,C",D,F) and actin (Fig. 6I) both coalesced into "balls" at the cell apex, which were not contiguous

with AJs (Fig. 6E vs. F). To explore dynamic cytoskeletal rearrangements, we used

MoeGFP to visualize Factin (Suppl. Video 4 shows wild-type MoeGFP) and Zipper-GFP

(myosin heavy chain) to visualize myosin (Suppl. Video 6 shows wild-type Zipper-GFP).

In $cno^{MZ}$, balls of both Factin (Fig. 6J; Suppl. Fig. 2A vs B; (Suppl. Video 5) and myosin

(Fig. 6G; Suppl. Fig. 2C vs D; (Suppl. Video 7) coalesced as invagination proceeded.

These data support a model (Fig. 6L) in which $cno^{MZ}$ cells apically constrict without fully

effective linkage between AJs and the actomyosin network, the contractile network

detaches from AJs before full cell constriction, and mesodermal cells are not efficiently

internalized.

In contrast, other gastrulation events are more normal. Posterior midgut cells also

apically constrict (Sweeton et al., 1991), leading to internalization (Suppl. Fig. 1K).

$cno^{MZ}$ mutants successfully internalize the gut (Suppl. Fig. 1L), although the midgut

epithelium may be less organized (Suppl. Fig. 1M). Lateral ectodermal cells intercalate

during germband elongation, narrowing the ectoderm in the dorsal/ventral axis and

elongating it in the anterior-posterior axis. $cno^{MZ}$ mutants extend their germbands and

intercalation proceeds normally (Suppl. Fig. 1N,O; some $cno^{MZ}$ mutants do not extend as

far as wildtype, but this may be a secondary consequence of ventral furrow failure).

Intercalation is thought to be driven by opposing planar polarization of myosin and AJ

proteins (Suppl Fig. 1P-P"; Bertet et al., 2004; Blankenship et al., 2006; Zallen and

Wieschaus, 2004). Ectodermal cells in $cno^{MZ}$ mutants planar polarize myosin and AJ

proteins (Suppl. Fig. 1Q-Q"); in fact planar polarization is even more pronounced than in

wildtype (Suppl. Fig. 1P-P" vs Q-Q"), and mutants retain accentuated planar polarity

through the end of germband extension (Suppl. Fig. 1R vs S).

*αcat localizes to actomyosin balls in cno^MZ*

We next looked in detail at the apparent separation of AJs and the apical

actomyosin web, examining whether AJ proteins accumulated in actomyosin balls in

*cno^MZ* mutants. We first examined DEcad, a transmembrane protein. The actomyosin

"balls" were apical to AJs (Fig. 7C-C" and D-D" are sections of the same embryo at AJs

(C) or more apical (D); we visualized actomyosin balls with anti-phosphotyorosine

(PTyr), as DEcad and phalloidin are not well preserved by the same fixation). DEcad

was largely retained in AJs after detachment (Fig. 7A-A", arrows), and only weakly

localized in actomyosin balls (Fig. 7A-A", B-B" arrowheads). We sometimes noted

"strands" of DEcad joining balls to AJs (Fig. 7B-B", arrows)—these were reminiscent of

less dramatic deformations of the lateral membrane observed during normal apical

constriction (Martin et al., 2009) and may represent points of remaining attachment

between AJs and the balls. Ed also did not strongly accumulate in actomyosin balls (data

not shown). In contrast, αcat accumulated at easily detected levels in actomyosin balls

(Fig. 7C-E", arrows), as well as remaining in AJs (Fig. 7C-C", arrowheads). This is

consistent with existence of two pools of αcat, one in AJs and one bound to actin (Drees

et al., 2005).

*Canoe is enriched at tricellular AJs along with a subset of actin*

Cno localizes to AJs in embryos and imaginal discs (Takahashi et al., 1998).

However, apical junctions are already complex at their assembly. Bazooka (Baz—fly

PAR-3) and DEcad localize apically from cellularization onset (Harris and Peifer, 2004),

while aPKC, Par6 and Crumbs are recruited to an even more apical position during

gastrulation (Harris and Peifer, 2005; Hutterer et al., 2004; Tepass, 1996). AJs initially

assemble as spot AJs that do not precisely co-localize with actin, and smooth out to form belt AJs during gastrulation.

To place Cno in the apical junctional protein network, we examined its localization and explored how it localizes apically. Cno has similarities and differences in localization with AJ proteins. Apical junctions assemble as cells form from the syncytium. As actomyosin furrows ingress, DEcad localizes to basal junctions just behind invaginating actomyosin (Hunter and Wieschaus, 2000; Thomas and Williams, 1999) and also begin to localize to apical junctions, while Baz is apical throughout (Harris and Peifer, 2004). Cno also remains apical, co-localizing with DEcad at apical junctions (Fig. 8H-H", arrow), but not basal junctions (Fig. 8H-H", arrowhead). In fact, like AJ proteins and Baz (Harris and Peifer, 2004; McCartney et al., 2001), Cno is already cortical before cellularization, localizing at apical ends of syncytial furrows (Fig. 8G, arrow). As embryos gastrulate, DEcad and Baz localize more tightly to apical AJs (Harris and Peifer, 2004), as does Cno (Fig. 8I-I"). Thus Cno is part of the apical junctional complex from the start.

To get a detailed view of Cno localization, we looked at cells en face. AJs initially form as spot AJs around the apical cortex (Tepass and Hartenstein, 1994). Cno co-localizes at spot AJs apically, with some enrichment at tricellular junctions (Fig. 8A-A" arrowheads); however, when we imaged 2μm more basally, Cno, unlike AJ proteins, is strikingly enriched at tricellular junctions (Fig. 8B-B", arrowheads). Intriguingly, a subset of actin is also enriched at tricellular junctions (Fig. 8E-E" arrowheads; visualized with anti-actin Ab; this is also apparent using MoeGFP; Fig. 8E" inset). As gastrulation begins, spot AJs mature into less punctate belt AJs (Harris and Peifer, 2004). Like AJ

37

proteins and Baz, Cno also becomes more evenly distributed, but remains enriched at tricellular junctions, as does actin (Fig. 8C-D",F-F" arrowheads; actin visualized with phalloidin). Thus Cno is in apical junctions from the start, but does not strictly co-localize with AJ proteins and localizes more closely with a subset of cortical actin.

***Cno can bind DEcad but is not a core AJ component***

Cno/Afadin has known direct interactions with AJ proteins, including Nectins/Ed (Takahashi et al., 1999; Wei et al., 2005), αcat (Tachibana et al., 2000; Pokutta et al. 2002), and the tight/AJ protein ZO-1/Pyd (Takahashi et al., 1998; Yokoyama et al., 2001). This suggests Cno may have multiple, partially redundant interactions with AJs. Cno/afadin interacts with nectins via its PDZ domain (Takahashi et al., 1999; Wei et al., 2005). Ed (ending in the sequence EIIV) and Nectin1 (ending EWYV) have class II PDZ binding sites. Interestingly, DEcad also has a putative C-terminal type II PDZ binding site (it ends with the sequence GWRI; matching the consensus XøXø, where ø is any hydrophobic amino acid; Hung and Sheng, 2002) that is strongly conserved in all Diptera, which diverged ~250 million years ago (Zdobnov et al., 2002). We thus tested whether Cno's PDZ domain can bind the DEcad tail. Purified Cno PDZ domain does not bind GST alone, but does bind GST fused at its C-terminus to the last 7 amino acids of DEcad (Fig. 9A). These data are consistent with DEcad as a Cno binding partner. Given this and Cno's localization to AJs we explored whether Cno is a core component of the cadherin-catenin complex. DEcad, Arm and αcat co-IP as a stable complex from embryonic extracts (Fig. 9B). In contrast, Cno is not detected in these IPs (Fig. 9B), suggesting it is not in the core complex.

***Cno apical recruitment requires Factin but not AJs or Echinoid***

This raises questions about mechanisms by which Cno is recruited to and maintained at AJs. We first considered the hypothesis that cadherin-catenin complexes recruit Cno, since Cno/afadin can bind both αcat (Pokutta et al., 2002) and DEcad (Fig. 9A). To test this we made *arm^MZ* mutants, in which both DEcad and αcat are lost from the cortex (Fig. 9D-D"; Cox et al., 1996; Dawes-Hoang et al., 2005), disrupting AJs. Surprisingly, Cno localizes normally in *arm^MZ* mutants (Fig. 9C' vs. D'). This suggests Cno has other means of reaching the cortex.

We next tested the hypothesis that Cno is recruited by Ed. Cno is mislocalized in *ed* mutant wing disc cells, suggesting Ed helps localize Cno to AJs (Wei et al., 2005). Ed localizes to spot AJs, and transitions to belt AJs (Fig. 8A,C,D,I insets). Cno localized normally in *ed^MZ* mutants (Fig. 9E' vs. F'), consistent with the observation that *ed^MZ* mutants do not have morphogenetic defects until dorsal closure (Laplante and Nilson, 2006; Lin et al., 2007). Thus, while Cno binds Ed, Cno has other ways to localize to AJs in embryos.

Baz, which also localizes to apical junctions independently of AJs, is positioned apically by cytoskeletal cues, including binding an apical actin-based scaffold (Harris and Peifer, 2004, 2005). Afadin is a Factin binding protein (Mandai et al., 1997). We thus examined whether Cno could directly bind Factin, like afadin. We fused GST to the C-terminal 491aa of Cno, which shares sequence conservation with afadin's Factin binding site, and performed actin sedimentation assays to determine if Cno directly associates with Factin. GST alone was a negative control and GST-αcat (671-906) a positive control (Pokutta et al., 2002). Little GST pelleted with Factin; most remains in the

supernatant (Fig. 10A; 11% pelleted; mean of 6 experiments). GST-αcat pelleted with

Factin (Fig. 10A; 84% pelleted; mean of 3 experiments). GSTCno (1560-2051) also

pelleted with Factin (Fig. 10A; 41% pelleted; mean of 4 experiments), to a degree similar

to afadin (Lorger and Moelling, 2006), suggesting Cno can directly bind Factin.

Cno's ability to bind actin and its co-localization with a subpool of actin at

tricellular junctions suggested the hypothesis that Cno is recruited apically by an actin-

based scaffold. To test this, we examined Cno localization after depolymerizing actin

with cytochalasin. When actin is depolymerized at the end of cellularization, DEcad

remains cortical but distributes all along the apical-basal axis (Harris and Peifer, 2005;

Fig 10B" vs. C"). Strikingly, Cno is lost from the cortex and accumulates in the

cytoplasm or nucleus (Fig. 10C-C",E-E"; residual cortical Cno was present in cells where

some cortical actin remained; arrow). We saw similar effects in extended germband

embryos (Suppl. Fig. 3). These data suggest Cno is recruited/retained at the cortex, at

least in part, by interacting with the cortical actin cytoskeleton.

### Rap1 is essential for mesoderm invagination and Cno cortical recruitment

Both afadin and Cno bind the small GTPase Rap1, and this is thought to activate

Cno during dorsal closure (Boettner et al., 2000; 2003). We thus examined whether Rap1

also works with Cno during mesoderm invagination, by generating $Rap1^{MZ}$ mutants using

the null allele $Rap1^{CD3}$ (deleting the entire coding region; Asha et al., 1999). Previous

work suggested Rap1 plays a role in gastrulation, as midline cells, which meet at the

ventral midline after gastrulation, did not do so in $Rap1^{MZ}$ (Asha et al., 1999). We

extended this analysis. Loss of maternal and zygotic Rap1 disrupts ventral cuticle (Fig.

1J), and Twist positive mesoderm remained on the surface after gastrulation (Fig. 4J), as

in *cno^{MZ}*. In some *Rap1^{MZ}* mutants the germband became twisted during gastrulation (Fig. 4K), as is seen in mutants like *fog* that disrupt invagination of both mesoderm and the posterior midgut (Sweeton et al., 1991).

To further examine parallels between *Rap1^{MZ}* and *cno^{MZ}* mutants, we examined localization of AJ and cytoskeletal proteins. Initial AJ assembly was normal in *Rap1^{MZ}* (Suppl. Fig. 4A vs B), as in *cno^{MZ}* (Fig. 2A-D'). However, as in *cno^{MZ}*, coupling between actomyosin constriction and cell shape change was disrupted in *Rap1^{MZ}*. Balls of actin (Fig. 6O) and myosin (Fig. 6M,N) appeared at the apical surface of mesodermal cells, and cell constriction halted prematurely, with myosin balls not contiguous with AJs (Fig. 6N). These data are consistent with Cno and Rap1 acting together in this process.

Cno binds Rap1, and epistasis analysis suggests Rap1 acts upstream of Cno in dorsal closure (Boettner et al., 2003). We thus explored whether Rap1 regulates Cno recruitment to AJs. We examined Cno localization during cellularization and early gastrulation in *Rap1^{MZ}* mutants. Cno recruitment to the cortex was substantially reduced at cellularization and early gastrulation (Fig. 9G-J'). This suggests Rap1 binding plays an important role in Cno cortical recruitment.

We also explored Rap1 localization, using GFP-Rap1 driven by its endogenous promotor (Knox and Brown, 2002), to see if its localization was consistent with a role in recruiting Cno to AJs. During cellularization, GFP-Rap1 accumulated in the cytoplasm, in a large structure just above nuclei (Suppl. Fig. 4C, arrowheads), and all along the lateral cell cortex, from apical junctions (Suppl. Fig. 4C, arrows) to the basal end (Suppl. Fig. 4C, inset). GFP-Rap1 remained cortically enriched during gastrulation (Suppl. Fig. 4E, H). Interestingly, in apically constricting cells of the posterior midgut, while GFP-

41

Rap1 is found all along lateral membranes (Suppl. Fig. 4G-G', arrow), it accumulates at elevated levels in a region overlapping the AJs (Suppl. Fig. 4G, arrowhead). We next examined whether Cno is required for GFP-Rap1 cortical localization. We saw no differences in GFP-Rap1 localization in wildtype or $cno^{MZ}$ (Suppl. Fig. 4D,F,H-I'), consistent with Rap1 acting upstream of Cno in the pathway.

**Discussion**

AJs mediate cell adhesion and anchor and regulate the underlying actin cytoskeleton. We have a working model for how cadherin-catenin complexes regulate these events, but less is known about the parallel system of nectins and the linker afadin/Cno. Studies in mammalian cells and embryos largely focus on a model in which the nectin-afadin complex is critical for cell adhesion, working in parallel with cadherin-catenins (see Introduction). In contrast, studies of *Drosophila* Cno suggest it is a scaffold for signal transduction (see Introduction). We completely removed maternal and zygotic Cno, allowing us to assess the consequences of complete loss of function from the onset of embryogenesis, and explore Cno's mechanism of action.

*Cno is not essential for AJ assembly or maturation*

Work in cultured mammalian cells using nectin misexpression or dominant negative approaches led to the model that nectin-afadin complexes play a key role in cell adhesion, recruiting cadherins to nascent AJs (Honda et al., 2003; Tachibana et al., 2000). However, multiple nectins made genetic tests of this hypothesis problematic. Afadin knockout in mice resulted in defects at and after gastrulation and subsequent lethality (Ikeda et al., 1999; Zhadanov et al., 1999). However, defects occurred much later than those caused by loss of core AJ proteins (Larue et al., 1994; Torres et al., 1997). Thus

the mouse data suggested loss of zygotic afadin does not disrupt adhesion to the same degree as loss of cadherin-catenin; however, as these embryos retained maternal afadin, an essential role for afadin in adhesion and epithelial integrity remained possible.

We tested whether Cno is essential for AJ assembly or maintenance by completely removing maternal and zygotic Cno from the onset of fly embryogenesis. The results were striking. Initial assembly of cadherin-catenin based AJs, establishment of epithelial cell polarity, and organization of apical actin were all normal in Cno deficient embryos. Further, the first step in AJ maturation, coalescence of spot AJs into belt AJs underlain by actin, was completed on schedule, unlike what was observed in afadin knockdown MDCK cells (Sato et al., 2006). These results are in strong contrast to loss of Arm, which disrupts all these events (Cox et al., 1996; Müller and Wieschaus, 1996). Thus Cno is not essential for AJ assembly or initial maturation. Further, many tissues maintained normal AJs and architecture through late embryogenesis, suggesting that Cno is not essential for AJ maintenance per se, or essential to maintain actin-AJ connections in non-morphogenetically active tissues, as these are essential for AJ integrity (e.g, Quinlan and Hyatt, 1999). Differences between our work and that in cultured mammalian cells could reflect differences in assembly and regulation of AJs in insects and mammals. However, they suggest further exploration of whether afadin is essential for AJ assembly in mammals is warranted; e.g., generating afadin null epithelial cells or maternally mutant mice.

Loss of Cno does affect maintenance of tissue architecture in a subset of cells. Many cells in the neurogenic ectoderm lost columnar shape, and membrane DEcad was reduced. This coincided with two morphogenetic events: a series of cell divisions, and

43

invagination of a subset of cells to form the CNS. Both involve significant AJ remodeling, and thus the ventral epidermis is particularly susceptible to reducing DEcad levels (Tepass et al., 1996; Uemura et al., 1996). The neuroepithelium is also the tissue most susceptible to afadin loss in mice (Ikeda et al., 1999; Zhadanov et al., 1999), perhaps because of similarly dynamic cell behavior. It will be interesting to explore Cno's role in this morphogenetically active tissue in more detail, using genetic approaches to block cell division or neuroblast invagination; the latter alleviates effects of reducing DEcad (Tepass et al., 1996). It will also be interesting to explore mechanisms by which Cno acts—e.g. it may regulate cadherin trafficking, as suggested in mammalian cells (Hoshino et al., 2005), or it may help cells reassume a columnar shape by regulating connections between cadherin-catenin and actin.

### A role for Cno in regulating AJ:actin linkage

Crosstalk between AJs and actin is critical in many contexts, from maintaining stable adhesion to mediating morphogenesis (Gates and Peifer, 2005). The classic view of AJs postulated direct connection between cadherin-catenin complexes and actin, mediated by αcat. However, recent work undermined this idea (Drees et al., 2005; Yamada et al., 2005), raising the question of how actin is connected to AJs, and causing some to question whether such a connection even occurs. One morphogenetic event that compellingly suggests AJs are connected to actin is apical constriction, during which constriction of the apical actomyosin web is coupled to shape change (Suppl, Fig. 5A, top). Disrupting AJs uncouples these events (Dawes-Hoang et al., 2005), supporting the need for a connection, but the nature of the link was unclear.

The phenotype of cno mutants is consistent with Cno playing a critical role in this

44

connection. In its absence, AJs assemble normally, actin and myosin accumulate apically, and apical constriction initiates. However, cell constriction halts before completion, while cytoskeletal constriction continues, uncoupling these events (Suppl. Fig. 5A, bottom).

Our data are consistent with several models for Cno in this process. The first step in all is Cno recruitment to the cortex. To our surprise, this is not dependent on either the cadherin-catenin complex or the nectin Ed, though we cannot rule out a redundant role for them. Instead, the GTPase Rap1 is critical. One speculative possibility is that Rap1 binding the RA domains opens up a closed conformation, as is seen, for example, in formins (Suppl. Fig. 5B-D). Thus Rap1 recruitment of Cno to the cortex could also activate it, allowing it to interact with other partners. At least one partner is Factin. Consistent with this, Cno, like afadin, can bind Factin, and the actin cytoskeleton plays a critical role in cortical Cno localization.

Once Cno is recruited apically by Rap1 and actin, it then could help stabilize links between actomyosin and AJs in several ways. It might be a direct link, binding actin and interacting by multiple redundant and low-affinity interactions with several AJ proteins (Suppl. Fig. 5E). Cno/afadin has well documented direct interactions with Nectins, αcat, and ZO-1, and we documented a direct interaction of its PDZ domain with DEcad. Alternately, Cno may regulate interactions more indirectly. It is intriguing that αcat acts later during germband elongation in linking a stable population of Factin at spot AJs with the larger cortical actin network (Cavey et al., 2008). Our observation that αcat is strongly enriched in actin "balls" that detach from AJs in Cno's absence, while also remaining at AJs, is consistent with αcat acting on both sides of the linkage. Cno may

regulate interactions between junctional and actin-bound pools of αcat, either directly or acting as a scaffold to recruit another regulator (Suppl. Fig. 5F). It will be important to test these models—the new *Drosophila* αcat mutants (U. Tepass, pers. comm.) will help, as will two-color simultaneous imaging of Factin and AJs. It will also be important to further analyze Cno's actin binding domain by site-directed mutagenesis. Other models for Cno function remain possible. *Dictyostelium* Rap1 regulates myosin disassembly during cell motility (Jeon et al., 2007), and activated myosin can activate Rap1 (Arora et al., 2008). Cno/Rap1 might regulate actomyosin contractility, for example, and in its absence apical actomyosin might become hypercontractile. We did not observe any acceleration of cell constriction, as might be expected from the simplest versions of this model. However, Cno/Rap1 regulation of myosin remains an open possibility.

Regardless of the mechanism, Cno's enrichment at tricellular junctions along with a sub-population of actin suggests the possibility that these structures might have a special role in AJ-actin connections. Intriguing, mouse Tricellulin plays a special role at tricellular junctions in maintaining tight junctions (Ikenouchi et al., 2005). However, our analysis and that of Martin et al., (2009), suggest that all spot AJs maintain connection to the apical actin web, during normal constriction and during disconnection in cno mutants.

It will be interesting to explore how forces are generated in the apical cortex, how contractility is regulated, and how and where the contractile network is coupled to AJs. Constriction in the *Drosophila* ventral furrow is rhythmic, suggesting a racheting mechanism (Martin et al., 2009). This resembles what is seen in the one cell *C. elegans* embryo (e.g., Munro et al. 2004). One other striking thing about the ventral furrow is that cells do not constrict isometrically, but instead constrict more quickly in the

dorsal/ventral dimension than in the anterior/posterior dimension (Fig. 4F, Fig. 5A). This bias seems less pronounced in $cno^{MZ}$ mutants (Fig. 4I, 5C), perhaps suggesting a requirement for cortex-AJ connections to maintain asymmetric cell constriction.

Mammalian afadin plays a role in epithelial wound healing—in its absence, cells migrate into wounds more rapidly (Lorger and Moelling, 2006). While afadin knockdown did not affect stable AJs, it reduced AJ association with the cytoskeleton after wounding, reducing adhesion and increasing directionality of cell migration. This function required afadin's actin binding domain, providing a second context in which Cno/afadin may help link AJs and actin.

Cno is not, however, critical for all actin-AJ connections. Cadherin-based adhesion itself, which does not require Cno, involves actin-AJ interactions (Quinlan and Hyatt, 1999). Likewise, conversion of spot AJs to belt AJs, which involves connections to actin (e.g., Cavey et al., 2008; Maddugoda et al., 2007), does not require Cno. Loss of Cno also did not halt germband extension, which involves reciprocal planar polarization of myosin and AJs. However, Cno may play a restraining role in this process, as planar polarity is enhanced in $cno^{MZ}$ mutants. This is interesting, as actin depolymerization also enhanced AJ planar polarity here (Harris and Peifer, 2007), suggesting that AJ-actin connections restrain planar polarity. Perhaps in Cno's absence subtle uncoupling of AJs from actin occurs.

We thus hypothesize that Cno is one aspect of regulation of AJ-actin linkage. However, this linkage will be complex, with different proteins mediating interactions in different circumstances. The mammal-specific protein EPLIN regulates maturation/remodeling of AJ-actin connections during AJ assembly (Abe and Takeichi,

47

2008).  Likewise, αcat regulates lateral mobility of AJ complexes (Cavey et al., 2008),

and Myosin VI acting with vinculin, and Cno/afadin binding partners in the ZO-1 family

also regulate maturation of belt junctions (Ikenouchi et al., 2007; Maddugoda et al.,

2007).  Perhaps different proteins evolved to respond to distinct forces exerted on AJs,

differing either in magnitude and acceleration. Our challenge is to identify all proteins

regulating AJ-actin connections and to determine their mechanisms of action.

**Acknowledgements**

**Materials and Methods**

*Fly Stocks*

Mutations are described at flybase.bio.indiana.edu.  Wild type was *yellow white*

or *Histone-GFP*.  All experiments were done at 25°C unless noted. $cno^{R2}$ was generated

by EMS on an isogenic FRT82B line.  $cno^{R2}$ was sequenced by PCR amplifying

fragments of the *cno* coding sequence and sequencing them at the UNC-CH Genome

Analysis Facility. Cuticle preparations were made as in Wieschaus and Nüsslein-Volhard (1986). Unless noted, fly stocks were from the Bloomington Drosophila Stock Center (Bloomington, IN). Sources of other stocks are in Suppl. Table 1. *cno* germline clones were made by heat shocking 48-72h old *hsFLP[1]*; FRT82B*cno[R2]*/FRT82B*ovo[D1-18]* larvae 3hrs at 37°C. *arm[043A01]* and *ed[F72]* germline clones were generated similarly.

### *Immunofluorescence and image aquisition*

The following fixations were used: myosin/Arm/Cno/Ed, heat-methanol (Müller and Wieschaus, 1996); phalloidin/Dcad2, 10min, 10% formaldehyde; phalloidin, 5min, 37% formaldehyde. All others were fixed as in Grevengoed et al. (2001). Embryos were methanol-devitillinized, or hand-devitillinized for phalloidin. Embryo cross-sections were performed as in (Dawes-Hoang et al., 2005). For drug treatments, dechorinated embryos were washed twice with 0.9% NaCl and incubated for 30min in 1:1 octane/0.9% NaCl with 10μg/mL cytochalasin D (Sigma, St. Loius MO; dissolved in DMSO). Control embryos were treated with DMSO carrier alone. Embryos were fixed immediately after drug treatment (Harris and Peifer, 2005). All embryos were blocked/stained in PBS/1% goat serum/0.1% Triton X-100 and mounted in Aqua-Polymount (Polysciences, Warrington PA). Suppl. Table 1 lists antibodies and probes used. All images and movies were acquired at room temperature. Fixed samples were imaged with LSM510 or Pascal confocal microscopes, using a Zeiss 40X NA 1.3 Plan-Neofluar oil immersion objective, and LSM software. Live imaging was performed using the Perkin-Elmer Ultra VIEW spinning disc confocal, ORCA-ER digital camera, a Nikon 40X NA 1.3 Plan-Fluor oil immersion objective, and Metamorph software. Adobe

Photoshop CS2 was used to adjust input levels so the main range of signals spanned the entire output grayscale and to adjust brightness and contrast.

***Vector construction, Protein Expression and Protein Purification***

GST-α-catenin (671-906) was from Sabine Pokutta and Bill Weis (Stanford University, Stanford CA; Pokutta et al., 2002). The Cno-Cterminus (aa1560-2051) fragment was amplified by PCR and cloned into pGEX (GE Healthcare, Piscataway, NJ). The Cno-PDZ (aa833-929) fragment was amplified by PCR and closed into pET28 (Novagen, Gibbstown NJ). GST-Ecad (GST-DDQGWRI) was amplified by PCR and cloned into pET28. GST fusion constructs in the pGEX vector were expressed in *E.coli* BL21-Gold (DE3) cells (Stratagene, Cedar Creek TX). Bacteria were grown in LB+ media with 100μg/mL ampicillin at 37°C to $OD_{600}$ between 0.8-1.0, induced with 1mM isopropyl-g-D-thiogalactopyranoside and grown 3 hours at 37°C. Pelleted cells were resuspended in 20mM Tris pH 8.0, 200mM NaCl, 1mM EGTA, 1% Triton-X, 0.1mM PMSF + a protease inhibitor cocktail (Roche, Indianapolis IN), and lysed using a microfluidizer. The lysate was cleared by centrifugation and incubated with glutathione-agarose (GE-Healthcare) O/N at 4ºC. GST fusion proteins were purified over 20mL Bio-rad columns and where either kept on beads for subsequent manipulations or eluted with 20mM Tris pH 8.0, 200mM NaCl, 10mM Glutathione (Sigma, St. Louis MO). Constructs in the pET-28 vector ($H_6$-CnoPDZ and $H_6$-GST-Ecad) were expressed in *E.coli* BL21-Gold (DE3) cells (Stratagene, Cedar Creek TX). Bacteria were grown in LB+ media with 20μg/mL kanamycin at 37°C to $OD_{600}$ between 0.8-1.0, induced with 1mM isopropyl-g-D-thiogalactopyranoside and grown 3 hours at 37°C. Pelleted cells were resuspended in 25mM Tris pH 8.0, 300mM NaCl, 10mM imidazole, 1% □-

mercaptoethanol, 0.1mM PMSF and lysed using a microfluidizer.  The lysate was cleared

by centrifugation and incubated with $Ni^{2+}$-NTA agarose (Qiagen, Gaithersburg, MD) 3

hours at 4ºC.  The columns were washed with 20 column volumes of lysis buffer and

bound protein step eluted using 3 column volumes of lysis buffer supplemented with 285

mM imidazole.

### *Actin Sedimentation Assay*

Rabbit skeletal muscle actin (Cytoskeleton, Inc., Denver CO) was stored in 5mM

Tris, pH 8.0, 0.2mM $CaCl_2$, 0.5 mM DTT, and 0.2 mM ATP at 0.4 mg/ml.  Either 1µM

or 5µM actin was used.  Aliquots of 156.25µL were polymerized with 3.2µL 50X

polymerization buffer (2.5M KCl, 100mM $MgCl_2$, 50mM ATP, protease inhibitor

cocktail (Roche, Indianapolis IN) for 1hr at RT.  GST fusion proteins were precleared by

centrifugation for 7min at 436,000 x g at 4ºC (TLA-100 rotor, Beckman 100 tubes).

Precleared GST fusion protein (final concentrations of 5µM or 2 µM) was added to

polymerized F-actin and incubated 30min at RT.  Proteins bound to F-actin were

separated from unbound protein by centrifugation 7min at 436,000 x g at 4ºC.  Sample

buffer was added to supernatant and pellet fractions, boiled, and loaded on a 10%

polyacrylamide gel.  Gels were stained with Coomassie Brilliant Blue.

### *GST pull downs*

50µl of Glutathione beads were saturated with GST or GST-Ecad then washed

using wash buffer (25 mM Tris pH 8.0, 300 mM NaCl, 0.1% β-mercaptoethanol).  GST

and GST-Ecad-bound beads were incubated in batch with 1 ml of purified CnoPDZ,

nutating at 4ºC for 30 minutes.  Resin was pelleted and supernatant containing non-bound

CnoPDZ was removed.  Beads were washed twice in batch using 1 ml wash buffer.

Proteins were eluted from the beads using 100μl of wash buffer supplemented with 50mM Glutathione. 10μl of the eluate was loaded on a 20% polyacrylamide gel as was 10μl of the CnoPDZ load. Gels were stained with Coomassie Brilliant Blue.

*Protein Preparation and Immunoprecipitations*

Protein samples were prepared by grinding dechorionated embryos on ice in Laemmli buffer with a plastic pestle and then boiled for 5min. Immunoprecipitations were performed as described in Harris and Peifer, 2005. Samples were separated by 6% SDS-Page and immunoblotted (see Suppl. Table 1 for antibody concentrations). Signal was detected using ECL Plus (GE Healthcare, Piscataway, NJ).

*Online Supplemental Material*

Supplemental Table 1 includes genetic and antibody reagents used in this paper. Fig. S1 Cno is not required for the transition from spot to belt adherens junctions, posterior midgut invagination, and is not essential for intercalation but restrains planar polarity during germband extension. Fig. S2 The actomyosin cystoskeleton becomes uncoupled from cell shape change in $cno^{MZ}$ mutants. Fig. S3 Actin is required to retain Cno at the cortex after gastrulation. Fig. S4 GFP-Rap1 localization overlaps AJs and does not require Cno function. Fig. S5 Models for Cno function. Video 1 shows WT ventral furrow formation, MoeGFP. Video 2 shows a mild $cno^{MZ}$ mutant ventral furrow phenotype, MoeGFP. Video 3 shows a severe $cno^{MZ}$ mutant ventral furrow phenotype, MoeGFP. Video 4 shows WT ventral furrow formation, MoeGFP. Video 5 shows a $cno^{MZ}$ mutant ventral furrow phenotype highlighting the actin balls, MoeGFP. Video 6 shows WT ventral furrow formation, ZipperGFP. Video 7 shows a $cno^{MZ}$ mutant ventral furrow phenotype highlighting the myosin balls, ZipperGFP.

# References

Abe, K., and M. Takeichi. 2008. EPLIN mediates linkage of the cadherin catenin complex to Factin and stabilizes the circumferential actin belt. *Proc Natl Acad Sci USA*. 105:13-9.

Arora, P.D., M.A. Conti, S. Ravid, D.B. Sacks, A. Kapus, R.S. Adelstein, A.R. Bresnick, and C.A. McCulloch. 2008. Rap1 activation in collagen phagocytosis is dependent on nonmuscle myosin II-A. *Mol Biol Cell*. 19:5032-46.

Asha, H., N.D. de Ruiter, M.G. Wang, and I.K. Hariharan. 1999. The Rap1 GTPase functions as a regulator of morphogenesis in vivo. *Embo J*. 18:605-15.

Barrett, K., M. Leptin, and J. Settleman. 1997. The Rho GTPase and a putative RhoGEF mediate a signaling pathway for the cell shape changes in Drosophila gastrulation. *Cell*. 91:905-15.

Bertet, C., L. Sulak, and T. Lecuit. 2004. Myosin-dependent junction remodelling controls planar cell intercalation and axis elongation. *Nature*. 429:667-71.

Blankenship, J.T., S.T. Backovic, J.S. Sanny, O. Weitz, and J.A. Zallen. 2006. Multicellular rosette formation links planar cell polarity to tissue morphogenesis. *Dev Cell*. 11:459-70.

Boettner, B., E.E. Govek, J. Cross, and L. Van Aelst. 2000. The junctional multidomain protein AF-6 is a binding partner of the Rap1A GTPase and associates with the actin cytoskeletal regulator profilin. *Proc Natl Acad Sci USA*. 97:9064-9.

Boettner, B., P. Harjes, S. Ishimaru, M. Heke, H.Q. Fan, Y. Qin, L. Van Aelst, and U. Gaul. 2003. The AF-6 homolog canoe acts as a Rap1 effector during dorsal closure of the Drosophila embryo. *Genetics*. 165:159-69.

Buszczak, M., S. Paterno, D. Lighthouse, J. Bachman, J. Planck, S. Owen, A.D. Skora, T.G. Nystul, B. Ohlstein, A. Allen, J.E. Wilhelm, T.D. Murphy, R.W. Levis, E. Matunis, N. Srivali, R.A. Hoskins, and A.C. Spradling. 2007. The carnegie protein trap library: a versatile tool for Drosophila developmental studies. *Genetics*. 175:1505-31.

Carmena, A., S. Speicher, and M. Baylies. 2006. The PDZ protein Canoe/AF-6 links Ras-MAPK, Notch and Wingless/Wnt signaling pathways by directly interacting with Ras, Notch and Dishevelled. *PLoS ONE*. 1:e66.

Cavey, M., M. Rauzi, P.F. Lenne, and T. Lecuit. 2008. A two-tiered mechanism for stabilization and immobilization of E-cadherin. *Nature*. 453:751-6.

Chou, T.B., E. Noll, and N. Perrimon. 1993. Autosomal P[ovoD1] dominant female-

sterile insertions in Drosophila and their use in generating germ-line chimeras. *Development*. 119:1359-69.

Cox, R.T., C. Kirkpatrick, and M. Peifer. 1996. Armadillo is required for adherens junction assembly, cell polarity, and morphogenesis during Drosophila embryogenesis. *J Cell Biol*. 134:133-48.

Dawes-Hoang, R.E., K.M. Parmar, A.E. Christiansen, C.B. Phelps, A.H. Brand, and E.F. Wieschaus. 2005. folded gastrulation, cell shape change and the control of myosin localization. *Development*. 132:4165-78.

Drees, F., S. Pokutta, S. Yamada, W.J. Nelson, and W.I. Weis. 2005. Alpha-catenin is a molecular switch that binds E-cadherin-beta-catenin and regulates actin-filament assembly. *Cell*. 123:903-15.

Fox, D.T., and M. Peifer. 2007. Abelson kinase (Abl) and RhoGEF2 regulate actin organization during cell constriction in Drosophila. *Development*. 134:567-78.

Fukuhara, A., K. Irie, A. Yamada, T. Katata, T. Honda, K. Shimizu, H. Nakanishi, and Y. Takai. 2002. Role of nectin in organization of tight junctions in epithelial cells. *Genes Cells*. 7:1059-72.

Gates, J., and M. Peifer. 2005. Can 1000 reviews be wrong? Actin, alpha-Catenin, and adherens junctions. *Cell*. 123:769-72.

Gatfield, D., L. Unterholzner, F.D. Ciccarelli, P. Bork, and E. Izaurralde. 2003. Nonsense-mediated mRNA decay in Drosophila: at the intersection of the yeast and mammalian pathways. *Embo J*. 22:3960-70.

Grevengoed, E.E., J.J. Loureiro, T.L. Jesse, and M. Peifer. 2001. Abelson kinase regulates epithelial morphogenesis in Drosophila. *J Cell Biol*. 155:1185-98.

Halbleib, J.M., and W.J. Nelson. 2006. Cadherins in development: cell adhesion, sorting, and tissue morphogenesis. *Genes Dev*. 20:3199-214.

Harris, T.J., and M. Peifer. 2004. Adherens junction-dependent and -independent steps in the establishment of epithelial cell polarity in Drosophila. *J Cell Biol*. 167:135-47.

Harris, T.J., and M. Peifer. 2005. The positioning and segregation of apical cues during epithelial polarity establishment in Drosophila. *J Cell Biol*. 170:813-23.

Harris, T.J., and M. Peifer. 2007. aPKC controls microtubule organization to balance adherens junction symmetry and planar polarity during development. *Dev Cell*. 12:727-38.

Honda, T., K. Shimizu, T. Kawakatsu, M. Yasumi, T. Shingai, A. Fukuhara, K. Ozaki-

Kuroda, K. Irie, H. Nakanishi, and Y. Takai. 2003. Antagonistic and agonistic effects of an extracellular fragment of nectin on formation of E-cadherin-based cell-cell adhesion. *Genes Cells*. 8:51-63.

Hoshino, T., T. Sakisaka, T. Baba, T. Yamada, T. Kimura, and Y. Takai. 2005. Regulation of E-cadherin endocytosis by nectin through afadin, Rap1, and p120ctn. *J Biol Chem*. 280:24095-103.

Hung, A.Y., and M. Sheng. 2002. PDZ domains: structural modules for protein complex assembly. *J Biol Chem*. 277:5699-702.

Hunter, C., and E. Wieschaus. 2000. Regulated expression of nullo is required for the formation of distinct apical and basal adherens junctions in the Drosophila blastoderm. *J Cell Biol*. 150:391-401.

Hutterer, A., J. Betschinger, M. Petronczki, and J.A. Knoblich. 2004. Sequential roles of Cdc42, Par-6, aPKC, and Lgl in the establishment of epithelial polarity during Drosophila embryogenesis. *Dev Cell*. 6:845-54.

Ikeda, W., H. Nakanishi, J. Miyoshi, K. Mandai, H. Ishizaki, M. Tanaka, A. Togawa, K. Takahashi, H. Nishioka, H. Yoshida, A. Mizoguchi, S. Nishikawa, and Y. Takai. 1999. Afadin: A key molecule essential for structural organization of cell-cell junctions of polarized epithelia during embryogenesis. *J Cell Biol*. 146:1117-32.

Ikenouchi, J., M. Furuse, K. Furuse, H. Sasaki, S. Tsukita, and S. Tsukita. 2005. Tricellulin constitutes a novel barrier at tricellular contacts of epithelial cells. *J Cell Biol*. 171:939-45.

Ikenouchi, J., K. Umeda, S. Tsukita, M. Furuse, and S. Tsukita. 2007. Requirement of ZO-1 for the formation of belt-like adherens junctions during epithelial cell polarization. *J Cell Biol*. 176:779-86.

Jeon, T.J., D.J. Lee, S. Merlot, G. Weeks, and R.A. Firtel. 2007. Rap1 controls cell adhesion and cell motility through the regulation of myosin II. *J Cell Biol*. 176:1021-33.

Jürgens, G., E. Wieschaus, and C. Nüsslein-Volhard. 1984. Mutations affecting the pattern of the larval cuticle in Drosophila melanogaster. II. Zygotic loci on the third chromosome. . *Roux's Arch. Dev. Biol.* 193:283-295.

Knox, A.L., and N.H. Brown. 2002. Rap1 GTPase regulation of adherens junction positioning and cell adhesion. *Science*. 295:1285-8.

Kofron, M., A. Spagnuolo, M. Klymkowsky, C. Wylie, and J. Heasman. 1997. The roles of maternal alpha-catenin and plakoglobin in the early Xenopus embryo. *Development*. 124:1553-60.

Komura, H., H. Ogita, W. Ikeda, A. Mizoguchi, J. Miyoshi, and Y. Takai. 2008. Establishment of cell polarity by afadin during the formation of embryoid bodies. *Genes Cells*. 13:79-90.

Kooistra, M.R., N. Dube, and J.L. Bos. 2007. Rap1: a key regulator in cell-cell junction formation. *J Cell Sci*. 120:17-22.

Laplante, C., and L.A. Nilson. 2006. Differential expression of the adhesion molecule Echinoid drives epithelial morphogenesis in Drosophila. *Development*. 133:3255-64.

Larue, L., M. Ohsugi, J. Hirchenhain, and R. Kemler. 1994. E-cadherin null mutant embryos fail to form a trophectoderm epithelium. *Proc Natl Acad Sci USA*. 91:8263-7.

Lin, H.P., H.M. Chen, S.Y. Wei, L.Y. Chen, L.H. Chang, Y.J. Sun, S.Y. Huang, and J.C. Hsu. 2007. Cell adhesion molecule Echinoid associates with unconventional myosin VI/Jaguar motor to regulate cell morphology during dorsal closure in Drosophila. *Dev Biol*. 311:423-33.

Linnemann, T., M. Geyer, B.K. Jaitner, C. Block, H.R. Kalbitzer, A. Wittinghofer, and C. Herrmann. 1999. Thermodynamic and kinetic characterization of the interaction between the Ras binding domain of AF6 and members of the Ras subfamily. *J Biol Chem*. 274:13556-62.

Lorger, M., and K. Moelling. 2006. Regulation of epithelial wound closure and intercellular adhesion by interaction of AF6 with actin cytoskeleton. *J Cell Sci*. 119:3385-98.

Maddugoda, M.P., M.S. Crampton, A.M. Shewan, and A.S. Yap. 2007. Myosin VI and vinculin cooperate during the morphogenesis of cadherin cell cell contacts in mammalian epithelial cells. *J Cell Biol*. 178:529-40.

Mandai, K., H. Nakanishi, A. Satoh, H. Obaishi, M. Wada, H. Nishioka, M. Itoh, A. Mizoguchi, T. Aoki, T. Fujimoto, Y. Matsuda, S. Tsukita, and Y. Takai. 1997. Afadin: A novel actin filament-binding protein with one PDZ domain localized at cadherin-based cell-to-cell adherens junction. *J Cell Biol*. 139:517-28.

Martin, A.C., M. Kaschube, and E.F. Wieschaus. 2009. Pulsed contractions of an actin-myosin network drive apical constriction. *Nature*. 457:495-9.

Matsuo, T., K. Takahashi, E. Suzuki, and D. Yamamoto. 1999. The Canoe protein is necessary in adherens junctions for development of ommatidial architecture in the Drosophila compound eye. *Cell Tissue Res*. 298:397-404.

McCartney, B.M., D.G. McEwen, E. Grevengoed, P. Maddox, A. Bejsovec, and M. Peifer. 2001. *Drosophila* APC2 and Armadillo participate in tethering mitotic spindles to cortical actin. *Nat Cell Biol*. 3:933-938.

Miyamoto, H., I. Nihonmatsu, S. Kondo, R. Ueda, S. Togashi, K. Hirata, Y. Ikegami, and D. Yamamoto. 1995. canoe encodes a novel protein containing a GLGF/DHR motif and functions with Notch and scabrous in common developmental pathways in Drosophila. *Genes Dev*. 9:612-25.

Muhlemann, O., A.B. Eberle, L. Stalder, and R. Zamudio Orozco. 2008. Recognition and elimination of nonsense mRNA. *Biochim Biophys Acta*. 1779:538-49.

Müller, H.-A.J., and E. Wieschaus. 1996. *armadillo*, *bazooka*, and *stardust* are critical for formation of the zonula adherens and maintenance of the polarized blastoderm epithelium in *Drosophila*. *J Cell Biol*. 134:149-165.

Munro, E., Nance, J., and J.R. Priess JR. 2004. Cortical flows powered by asymmetrical contraction transport PAR proteins to establish and maintain anterior-posterior polarity in the early C. elegans embryo. *Dev Cell* 7:413-24.

Pilot F, and T. Lecui. (2005). Compartmentalized morphogenesis in epithelia: from cell to tissue shape. Dev Dyn. 232:685-94.

Pokutta, S., F. Drees, Y. Takai, W.J. Nelson, and W.I. Weis. 2002. Biochemical and structural definition of the l-afadin- and actin-binding sites of alpha-catenin. *J Biol Chem*. 277:18868-74.

Quinlan, M.P., and J.L. Hyatt. 1999. Establishment of the circumferential actin filament network is a prerequisite for localization of the cadherin-catenin complex in epithelial cells. *Cell Growth Differ.* 10:839-54.

Sakisaka, T., W. Ikeda, H. Ogita, N. Fujita, and Y. Takai. 2007. The roles of nectins in cell adhesions: cooperation with other cell adhesion molecules and growth factor receptors. *Curr Opin Cell Biol*. 19:593-602.

Sato, T., N. Fujita, A. Yamada, T. Ooshio, R. Okamoto, K. Irie, and Y. Takai. 2006. Regulation of the assembly and adhesion activity of E-cadherin by nectin and afadin for the formation of adherens junctions in Madin-Darby canine kidney cells. *J Biol Chem*. 281:5288-99.

Speicher, S., A. Fischer, J. Knoblich, and A. Carmena. 2008. The PDZ protein Canoe regulates the asymmetric division of Drosophila neuroblasts and muscle progenitors. *Curr Biol*. 18:831-7.

Sweeton, D., S. Parks, M. Costa, and E. Wieschaus. 1991. Gastrulation in Drosophila: the formation of the ventral furrow and posterior midgut invaginations. *Development*.

112:775-89.

Tachibana, K., H. Nakanishi, K. Mandai, K. Ozaki, W. Ikeda, Y. Yamamoto, A. Nagafuchi, S. Tsukita, and Y. Takai. 2000. Two cell adhesion molecules, nectin and cadherin, interact through their cytoplasmic domain-associated proteins. *J Cell Biol*. 150:1161-76.

Takahashi, K., T. Matsuo, T. Katsube, R. Ueda, and D. Yamamoto. 1998. Direct binding between two PDZ domain proteins Canoe and ZO-1 and their roles in regulation of the jun N-terminal kinase pathway in Drosophila morphogenesis. *Mech Dev*. 78:97-111.

Takahashi, K., H. Nakanishi, M. Miyahara, K. Mandai, K. Satoh, A. Satoh, H. Nishioka, J. Aoki, A. Nomoto, A. Mizoguchi, and Y. Takai. 1999. Nectin/PRR: an immunoglobulin-like cell adhesion molecule recruited to cadherin-based adherens junctions through interaction with Afadin, a PDZ domain-containing protein. *J Cell Biol*. 145:539-49.

Tepass, U. 1996. Crumbs, a component of the apical membrane, is required for zonula adherens formation in primary epithelia of *Drosophila*. *Dev Biol* 177:217-225.

Tepass, U., E. Gruszynski-DeFeo, T.A. Haag, L. Omatyar, T. Torok, and V. Hartenstein. 1996. shotgun encodes Drosophila E-cadherin and is preferentially required during cell rearrangement in the neurectoderm and other morphogenetically active epithelia. *Genes Dev*. 10:672-85.

Tepass, U., and V. Hartenstein. 1994. The development of cellular junctions in the Drosophila embryo. *Dev Biol*. 161:563-96.

Thomas, G.H., and J.A. Williams. 1999. Dynamic rearrangement of the spectrin membrane skeleton during the generation of epithelial polarity in Drosophila. *Journal of Cell Science*. 112:2843-52.

Torres, M., A. Stoykova, O. Huber, K. Chowdhury, P. Bonaldo, A. Mansouri, S. Butz, R. Kemler, and P. Gruss. 1997. An alpha-E-catenin gene trap mutation defines its function in preimplantation development. *Proc Natl Acad Sci U S A*. 94:901-6.

Uemura, T., H. Oda, R. Kraut, S. Hayashi, Y. Kotaoka, and M. Takeichi. 1996. Zygotic Drosophila E-cadherin expression is required for processes of dynamic epithelial cell rearrangement in the Drosophila embryo. *Genes Dev*. 10:659-71.

Wei, S.Y., L.M. Escudero, F. Yu, L.H. Chang, L.Y. Chen, Y.H. Ho, C.M. Lin, C.S. Chou, W. Chia, J. Modolell, and J.C. Hsu. 2005. Echinoid is a component of adherens junctions that cooperates with DEcadherin to mediate cell adhesion. *Dev Cell*. 8:493-504.

Wieschaus, E., and C. Nüsslein-Volhard. 1986. Looking at embryos. *In Drosophila*, A Practical Approach. D.B. Roberts, editor. IRL Press, Oxford, England. 199-228.

Yamada, S., S. Pokutta, F. Drees, W.I. Weis, and W.J. Nelson. 2005. Deconstructing the cadherin-catenin-actin complex. *Cell*. 123:889-901.

Yokoyama, S., K. Tachibana, H. Nakanishi, Y. Yamamoto, K. Irie, K. Mandai, A. Nagafuchi, M. Monden, and Y. Takai. 2001. alpha-catenin-independent recruitment of ZO-1 to nectin-based cell-cell adhesion sites through afadin. *Mol Biol Cell.* 12:1595-609.

Zallen, J.A., and E. Wieschaus. 2004. Patterned gene expression directs bipolar planar polarity in Drosophila. *Dev Cell*. 6:343-55.

Zdobnov, E.M., C. von Mering, I. Letunic, D. Torrents, M. Suyama, R.R. Copley, G.K. Christophides, D. Thomasova, R.A. Holt, G.M. Subramanian, H.M. Mueller, G. Dimopoulos, J.H. Law, M.A. Wells, E. Birney, R. Charlab, A.L. Halpern, E. Kokoza, C.L. Kraft, Z. Lai, S. Lewis, C. Louis, C. Barillas-Mury, D. Nusskern, G.M. Rubin, S.L. Salzberg, G.G. Sutton, P. Topalis, R. Wides, P. Wincker, M. Yandell, F.H. Collins, J. Ribeiro, W.M. Gelbart, F.C. Kafatos, and P. Bork. 2002. Comparative genome and proteome analysis of Anopheles gambiae and Drosophila melanogaster. *Science*. 298:149-59.

Zhadanov, A.B., D.W. Provance, Jr., C.A. Speer, J.D. Coffin, D. Goss, J.A. Blixt, C.M. Reichert, and J.A. Mercer. 1999. Absence of the tight junctional protein AF-6 disrupts epithelial cell-cell junctions and cell polarity during mouse development. *Curr Biol*. 9:880-8.
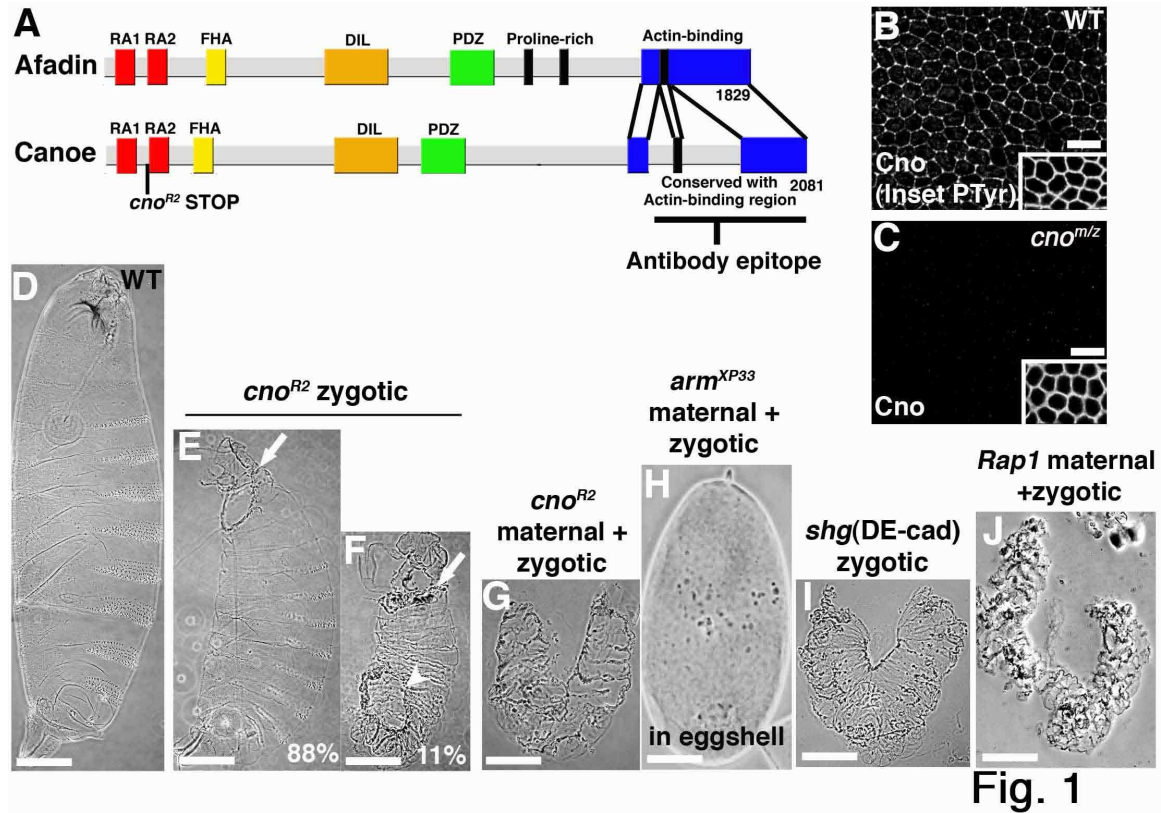
**Figure 2.1. *cno* mutants have defects in morphogenesis.** (A) Domain structures and *cno* mutant. (B,C) Stage 7 wildtype or *cno*[R2] MZ embryos, stained for Cno and for anti-phosphotyrosine (PTyr, insets) to show cell borders, and imaged on same slide. (D-J) Cuticles, anterior up. Genotypes indicated. (E,F) *cno*[R2] zygotic mutants. Head involution defects (arrows). Dorsal closure defects (arrowhead). (G) *cno*[R2] MZ. Only dorsal cuticle remains. (H) *arm*[XP33] MZ mutant (in eggshell); cuticle fragmented. (I) *shg*[R69] zygotic mutant retains only dorsal cuticle. (J) *Rap1* MZ mutant retains only dorsal cuticle (Rap1 data at end of Results). Bar = 10µm (B,C), 100µm (D-J).

60
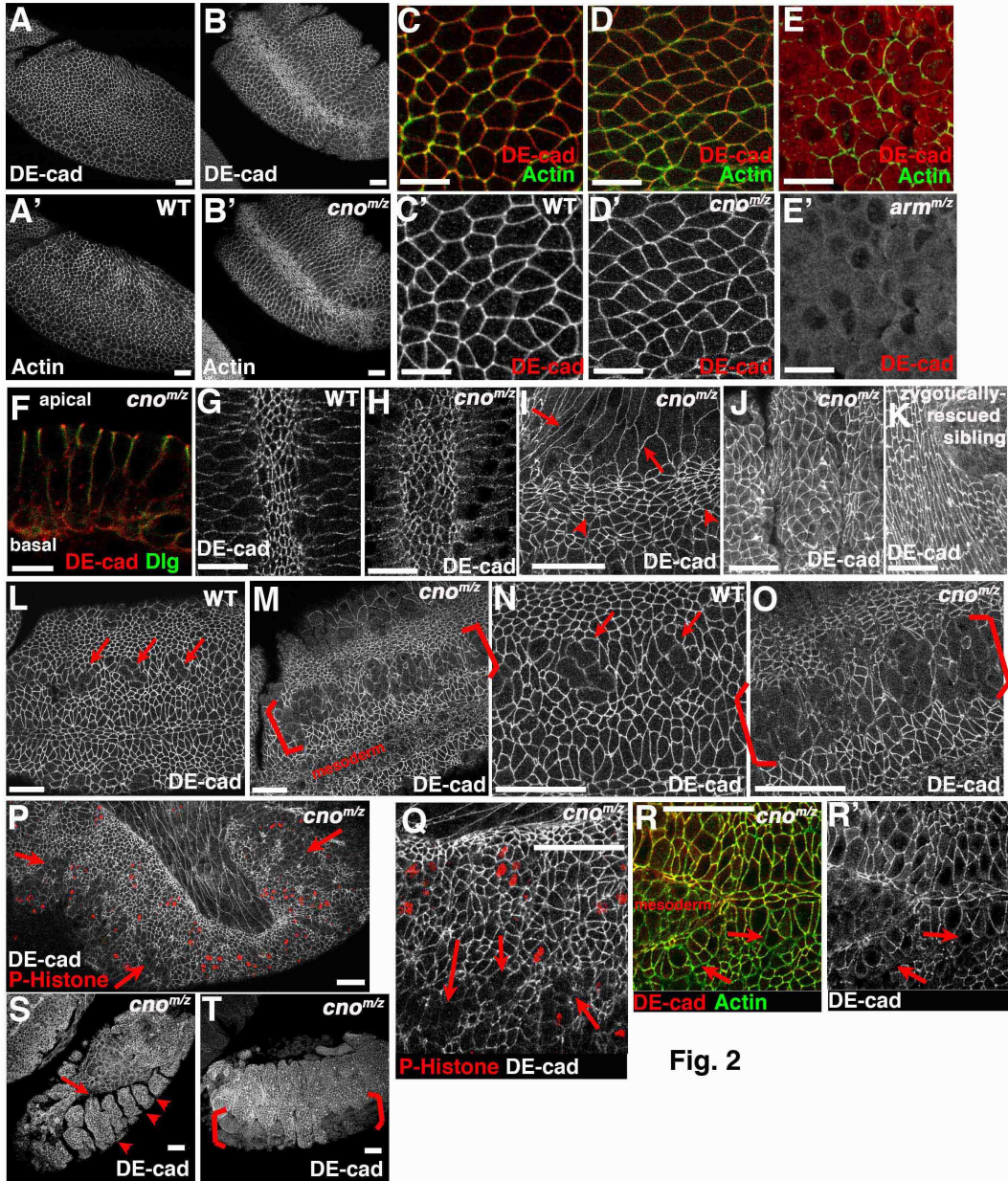
**Figure 2.2**. **Cno is not essential for AJ assembly.** Embryos, antigens and genotypes indicated. (A-F) Stage 8. (A-B') Ventrolateral views, anterior top left. (C-C') Closeup of A-A'. WT. (D-D') Closeup of B-B'. $cno^{MZ}$. (E) $arm^{MZ}$. Cortical DEcad lost. (F) Cross section, $cno^{MZ}$. DEcad remains apical. (G) Wildtype ventral furrow (H) $cno^{MZ}$. DEcad maintained. (I) Stage 11, $cno^{MZ}$. AJ normal in amnioserosa (arrows) and dorsal epidermis (arrowheads). (J,K) Dorsal epidermis, stage 13-14. (J) $cno^{MZ}$. AJs intact. (K) Paternally rescued sibling. (L-O) Lateral view, stage 9-10. (L,N = closeup) Wildtype mitotic domains (arrows). (M,O = Closeup)) $cno^{MZ}$. Some cells have reduced DEcad (brackets). (P,Q) Stage 12, $cno^{MZ}$. Arrows, fragmented AJs. (R) Ventral midline, stage 11 $cno^{MZ}$. AJ fragmentation precedes loss of cortical actin (arrows). (S,T) Stage 13/14 $cno^{MZ}$. Amnioserosa detaches from epidermis (arrow), segmental groves never retract (arrowheads), and parts of ventral epidermis are missing (bracket). Bar = 30µm (A-B, K-T), 10µm (C-J).
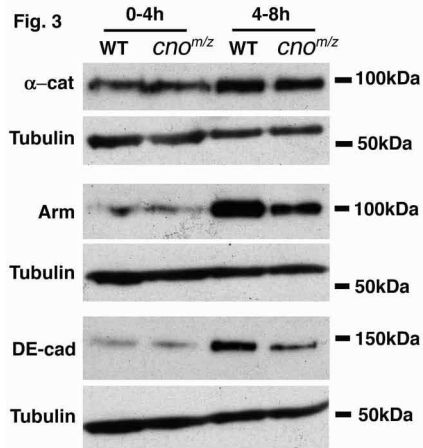
**Figure 2.3. AJ protein levels in *cno^{MZ}*.** Immunoblots, embryo extracts, antigens indicated. 0-4h through mesoderm invagination and early germband extension. 4-8 hours Extended germband, stages 8-11. Tubulin = loading control.
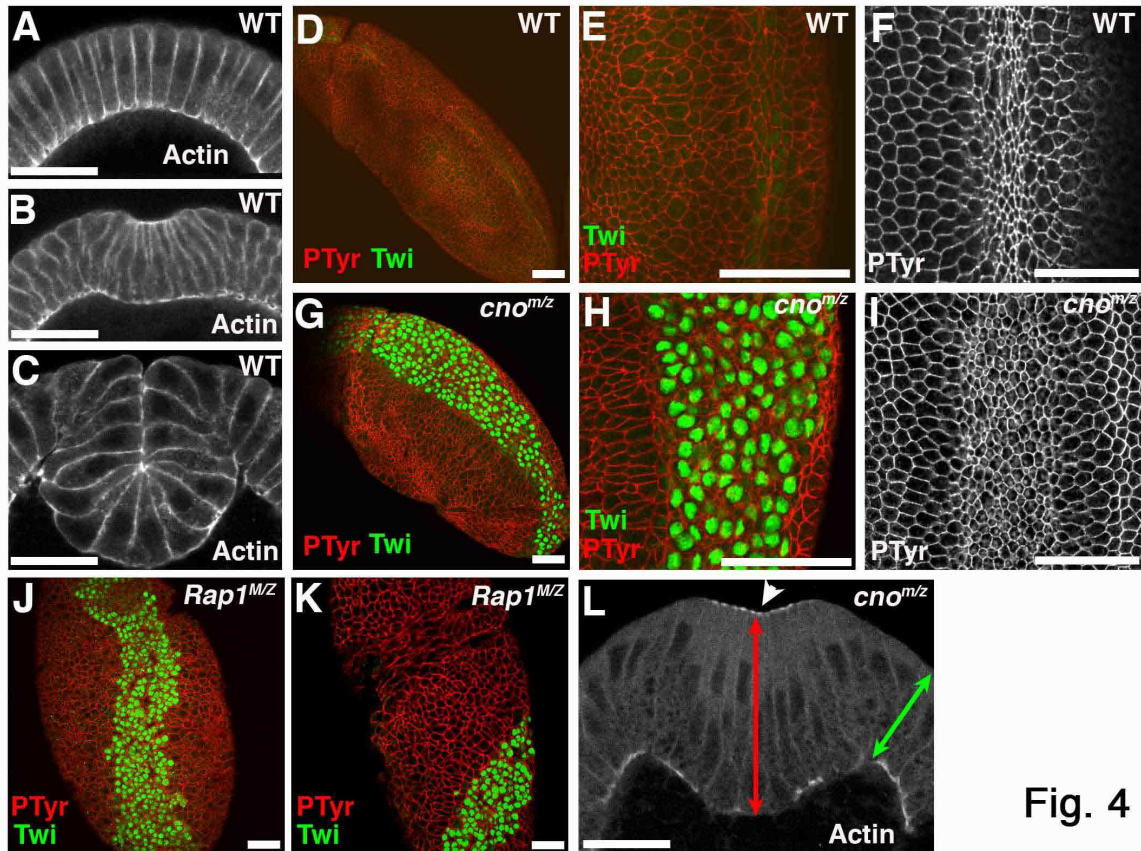
**Figure 2.4. Cno is essential for mesoderm invagination.** Embryos, antigens and genotypes indicated. (A-C) Cross sections, wildtype ventral furrow. (A) Late cellularization. (B) Initial furrowing. (C) Mesoderm internalized. (D-K) Ventral views, anterior up. (D,E) Wildtype, mesoderm completely internalized. (F) Wildtype during constriction. (G,H) $cno^{MZ}$, Twist positive cells not completely internalized. (I) $cno^{MZ}$ mesoderm initiates constriction. (J,K) $Rap1^{MZ}$ phenocopies $cno^{MZ}$, but some exhibit twisted gastrulation (K). (L) $cno^{MZ}$ mesodermal cells elongate along apical-basal axis (red arrow) relative to ectodermal neighbors (green arrow). Bar = 30µm.
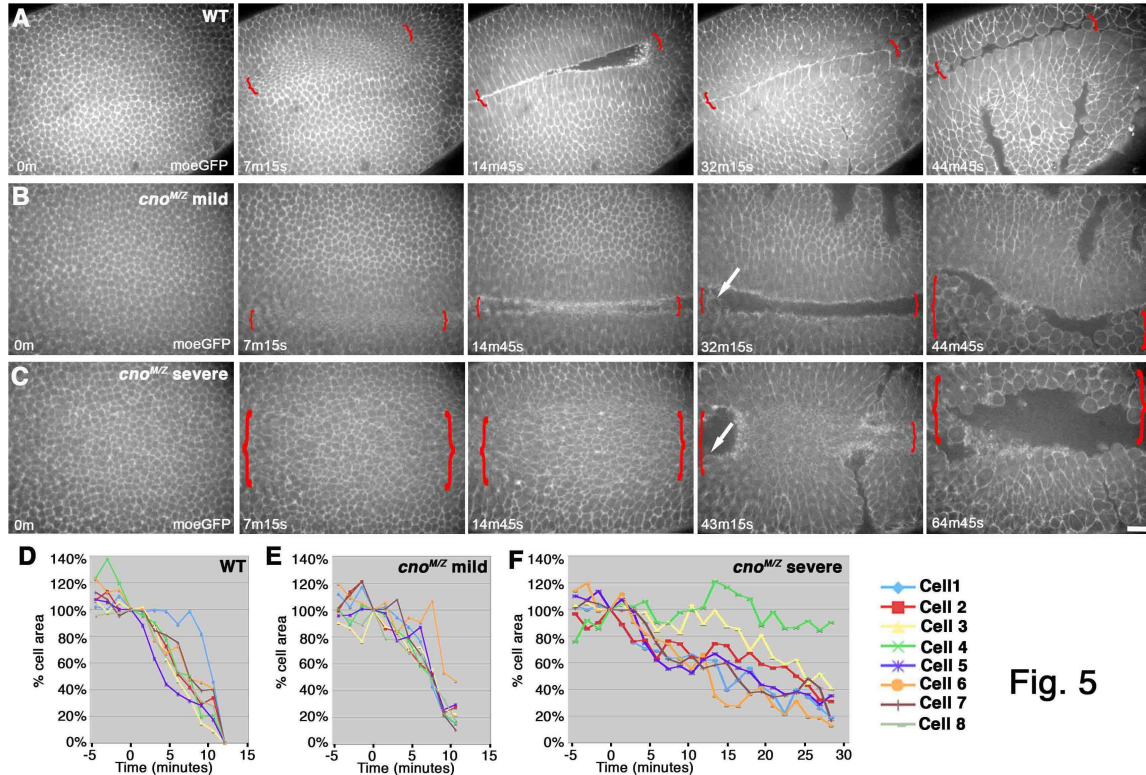
**Figure 2.5**. **Mesoderm invagination in *cno^MZ*.** (A-C) Embryos, ventral views, anterior left, genotypes indicated. MoeGFP reveals Factin. Brackets=ventral furrow. Arrows=mesoderm cells round up to divide and emerge from furrow. (A) Stills from Suppl. Video 1. (B) Stills from Suppl. Video 2 (C) Stills from Suppl. Video 3. (D-F) Graphs, cell cross sectional areas as ventral furrow invaginates. T=0 defined as 100%. Wildtype cells constrict to essentially zero before invaginating, while mutant cells disappear in furrow before fully constricting. Bar = 30µm.
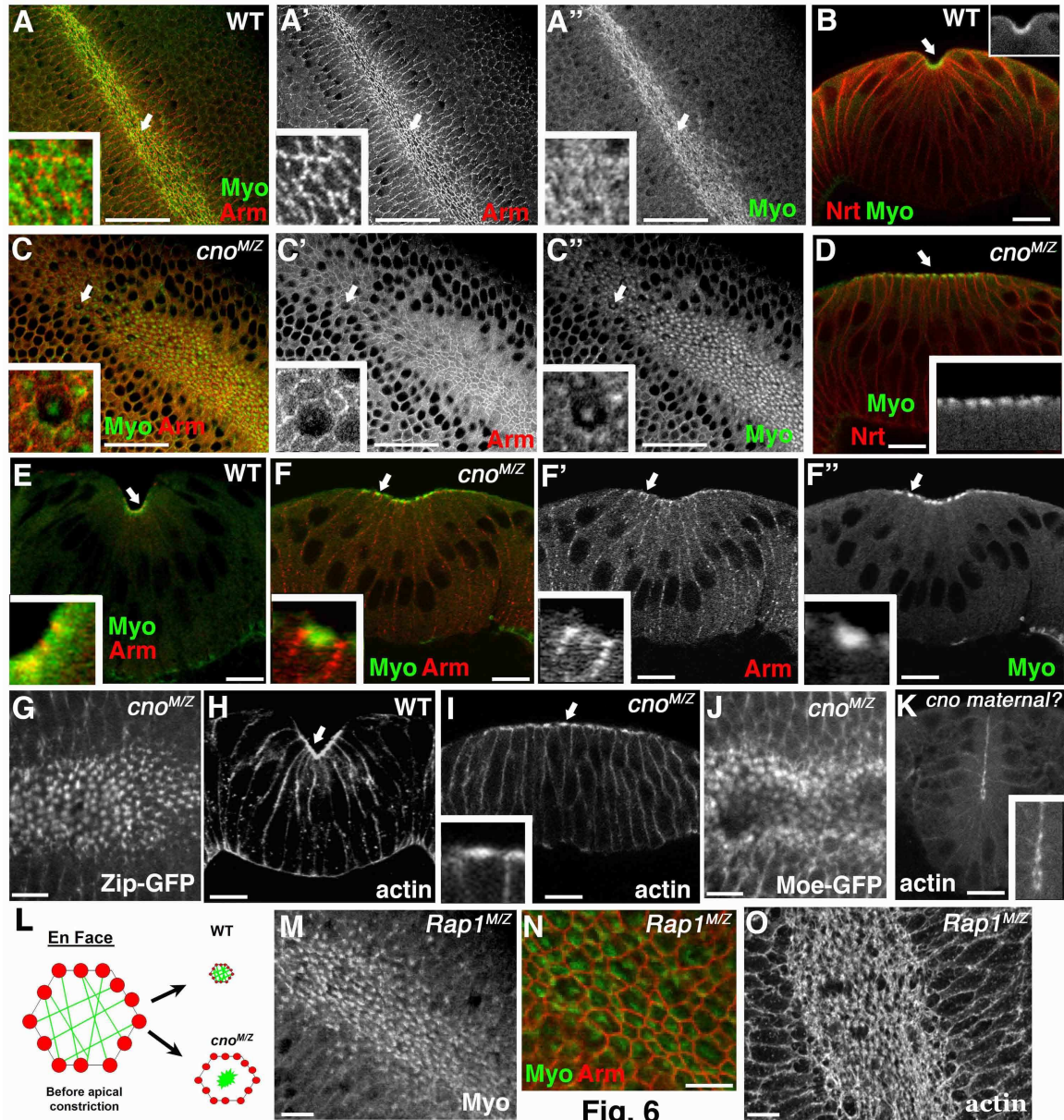
**Figure 2.6 Cno regulates coupling of AJs to contractile network.** Embryos, stage 6-8, antigens and genotypes indicated. (A-A',C-C',G,J,M-O) Ventral views. (B,D-F',H,I,K) Cross sections. (A-A",B,E) Wildtype ventral furrow. Myosin (Myo) covers cell apices (arrows and insets). Constriction coupled to actomyosin contraction. (C,D,F) $cno^{MZ}$. Myo condensed into balls that are not contiguous with AJs (white arrows and insets). Cell shape change is not completed. (G) $cno^{MZ}$. Myosin balls visualized live with Zipper-GFP. (H) WT. Actin accumulates evenly at apical surface (arrow). (I) $cno^{MZ}$. Actin condenses into balls that are not contiguous with actin at AJs. Constriction arrests (arrow, inset). (J) $cno^{MZ}$. Factin balls visualized live with MoeGFP. (K) Probable $cno$ maternal mutant. Balls of actin (inset) observed even in embryos initiating invagination. (L) Model of alterations in actin, myosin and constriction in $cno^{MZ}$. (M-O) $Rap1^{MZ}$. (M,N) Similar balls of Myo form and separate from AJs. (O) Balls of actin. Bars = 30µm (A,C), 10µm (B, D-O).
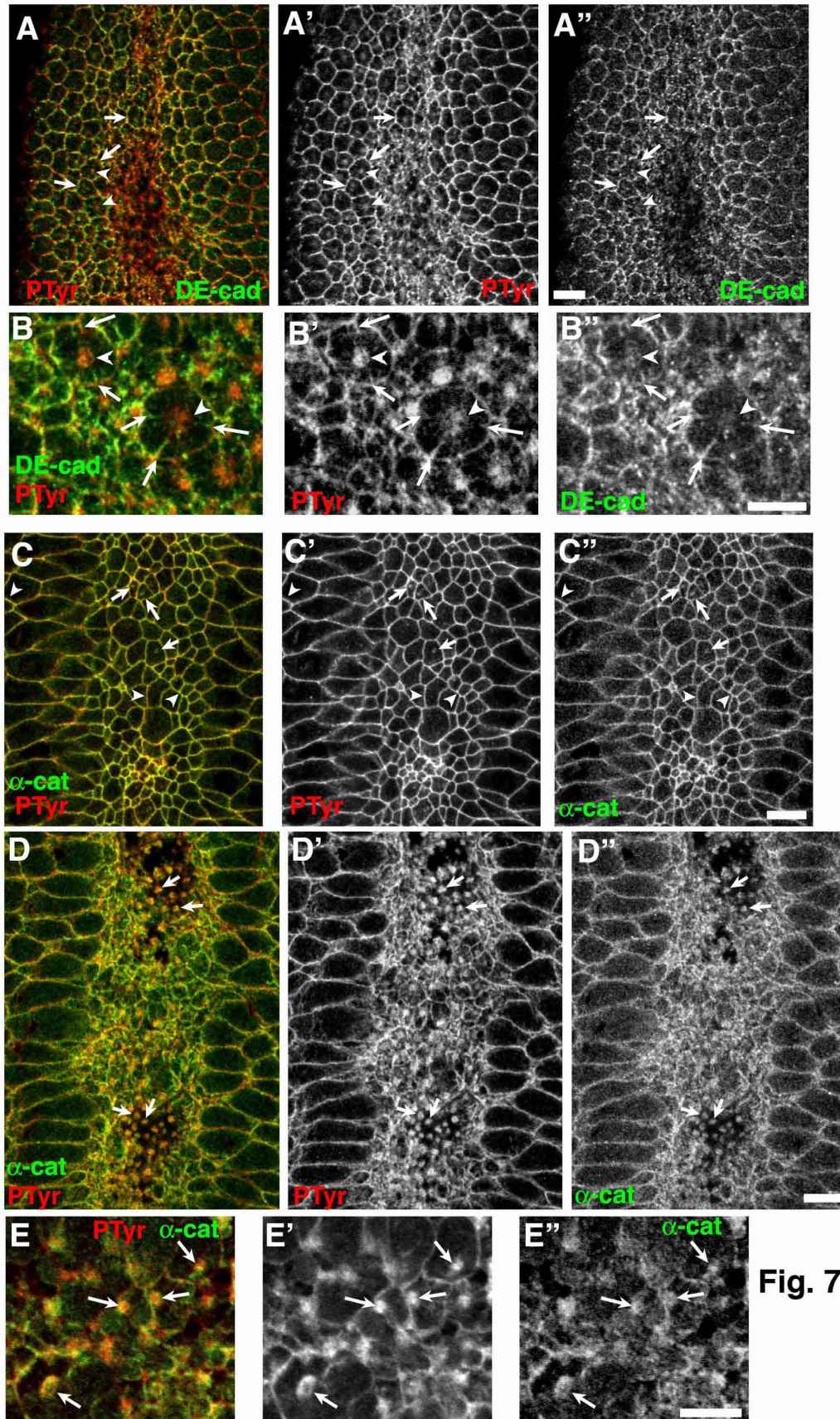
Fig. 7

**Figure 2.7. Pools of αcat at AJs and actomyosin balls.** Ventral views, gastrulating *cno*<sup>MZ</sup>, antigens indicated. (A-B") DEcad localizes to AJs (A-A", arrows) but is only very weakly found in actomyosin balls (arrowheads). Strands of DEcad connect AJs to balls (B-B", arrows). (C-E") Apical (C-C") and more basolateral (D-D") views of same embryo, E-E"=closeup. Pools of αcat at AJs (C-C", arrowheads) and actomyosin balls (C-C",E-E" arrows). Bars = 10µm.
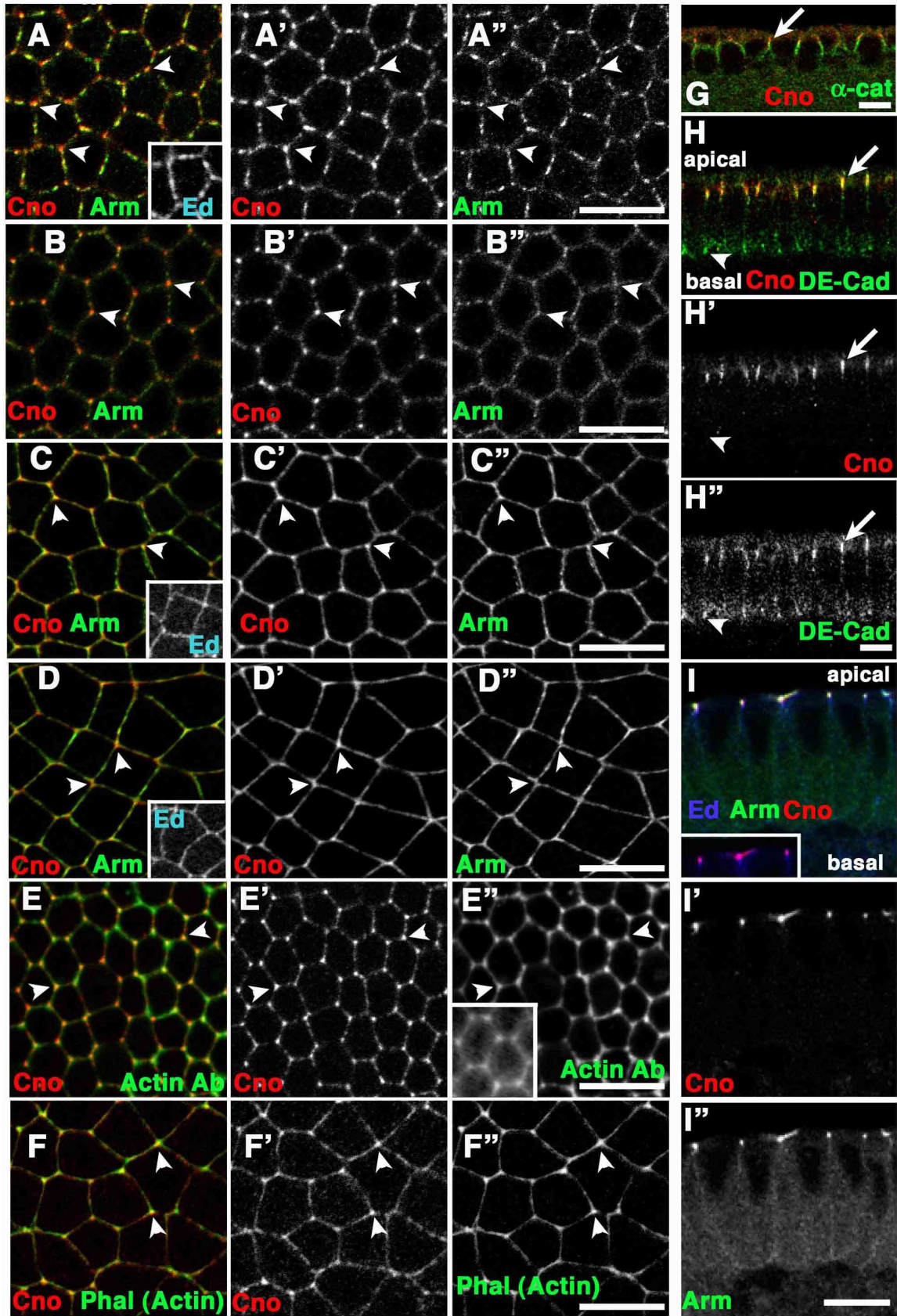
Fig. 8

68

**Figure 2.8. Cno is enriched at tricellular junctions with a subpool of actin.** Wildtype, antigens indicated. (A-F") Surface views. (G-I") Cross sections. (A-B") Cellularization. (A-A") Apically, Cno co-localizes with Arm and Ed (inset) in spot AJs, with enrichment at tricellular junctions (arrowheads). (B-B") 2µm more basal, Cno is strongly enriched at tricellular junctions relative to Arm (arrowheads). (C-D") Mid (C-C") to late (D-D") gastrulation. Cno, Arm, and Ed (inset) form belt AJs. Cno remains enriched at tricellular junctions (arrowheads). (E-F") Cno localizes with a subpool of actin at tricellular junctions (arrowheads) during cellularization (E-E") and gastrulation (F-F"). (E" inset) Actin visualized with Moesin-GFP. (G) Cno already apical in syncytial embryo (arrow). (H-H") Cno colocalizes with DEcad in apical AJs (arrow), but not basal junctions (arrowhead). (I-I") Gastrulation. Cno tightly localized at AJs with Arm and Ed. Inset = Cno and Ed channels alone. Bar = 10µm.

**Fig. 9**

A

B
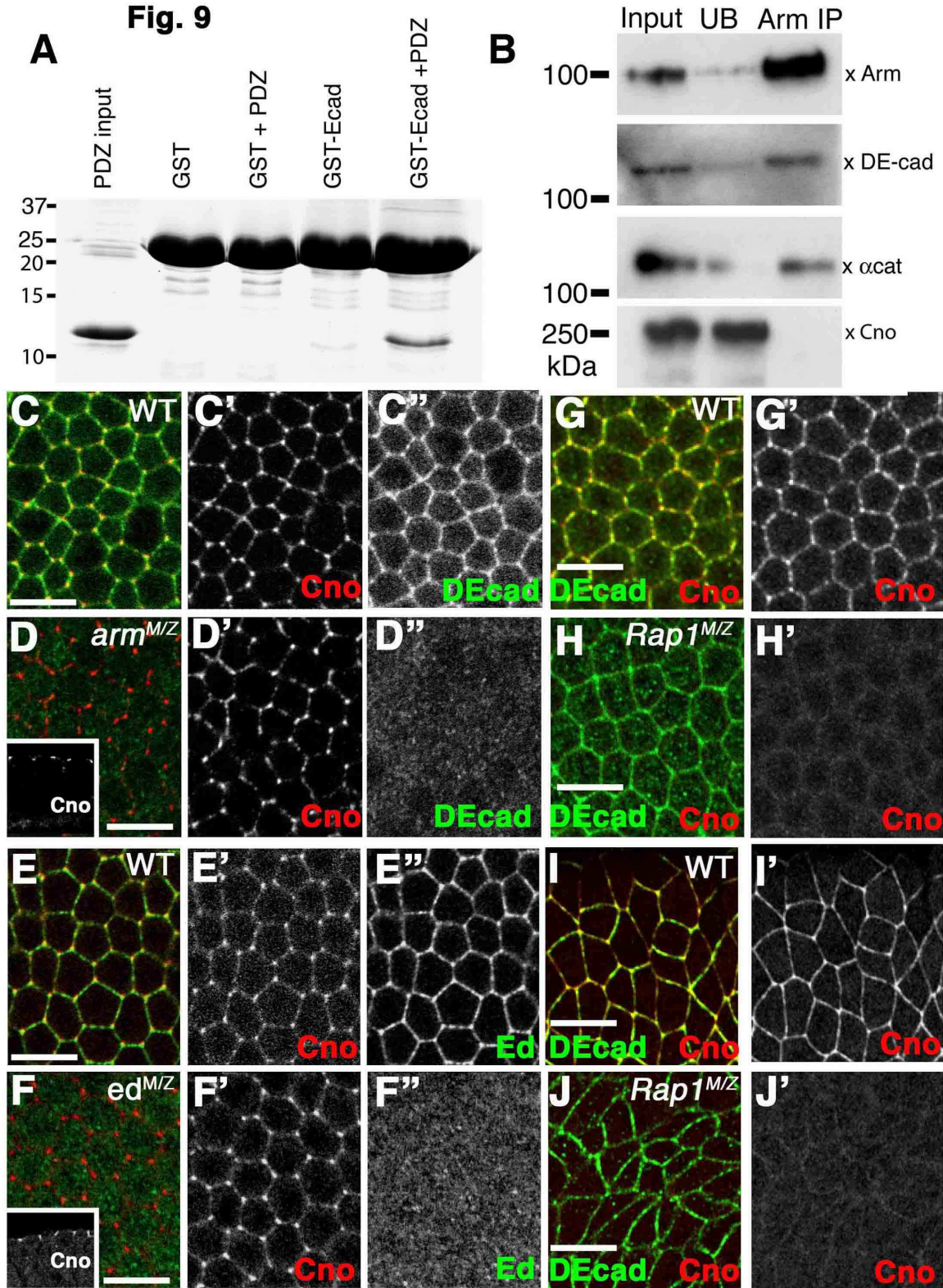
**Figure 2.9. Rap1 but not AJs or Ed are required for apical Cno recruitment.** (A) Purified Cno PDZ domain incubated with GST or GST fused to C-terminal 7 amino acids of DEcad. Input =1% of load, bound = 10% of bound fraction. (B) Embryonic extracts IPed with anti-Arm. Input, unbound and IP fractions immunoblotted with indicated antibodies. (C-J") Late cellularization or early gastrulation (I,J). Antigens and genotypes indicated. Apical surface, except D,F insets, which are cross sections. (C-F") Removing AJs (C-D"; $arm^{043A01}$) or Ed (E-F"; $ed^{F72}$) does not affect Cno localization. (G-J") Removing Rap1 reduces cortical Cno. Bars = 10μm.
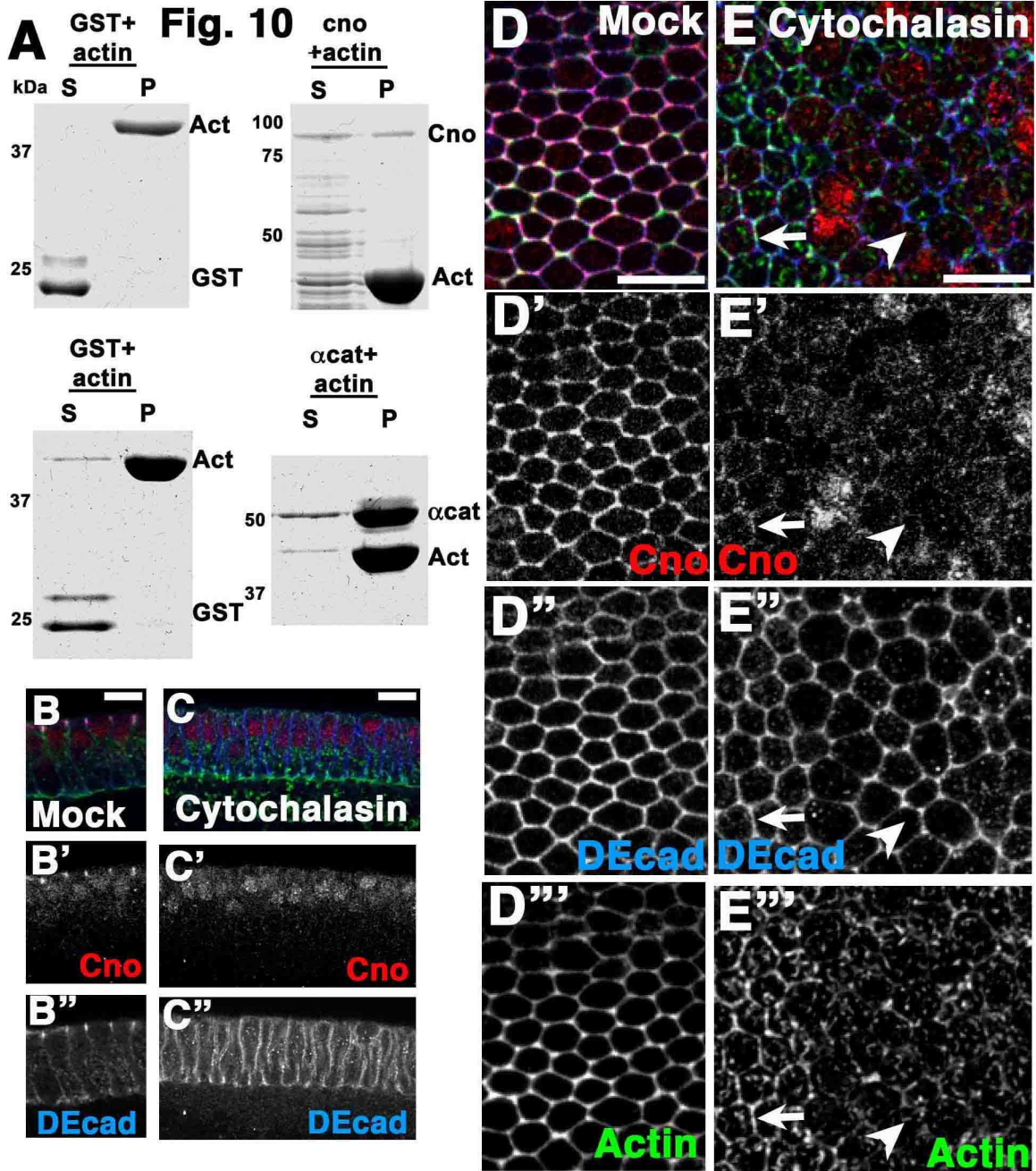
**Figure 2.10. Factin is required for Cno cortical localization**. (A) Actin co-sedimentation assays of GST-CnoCT, GST-αcat, and GST as a negative control. S=supernatant, P=high speed pellet. (B-B",D-D"') DMSO treated controls. (C-C",E-E"') Cytochalasin treated. (B-B") DEcad at apical and basal junctions. Cno only at apical junctions. (C-C") After depolymerization, DEcad all along lateral cortex. Cno cytoplasmic and nuclear. (D-D"') Normal DEcad, Cno and actin localization. (E-E"') Actin depolymerized; some residual cortical actin in cells at left (arrows). DEcad remains cortical. Cno lost from cortex (arrowhead) except where residual cortical actin remains (arrows). Bars = 10μm.

cellularization    Stage 7/8    Late stage 8

A WT    B WT    C WT    K DE-cad
Arm    Arm    Arm    zygotically rescued

D cno^{M/Z}    E cno^{M/Z}    F cno^{M/Z}    L cno M/Z
Arm    Arm    Arm    M cno M/Z

G WT    H cno^{M/Z}    I WT    J cno^{M/Z}
Ed    Ed    Pyd    Pyd

N1 moe-GFP    N2    N3    P WT stage 7-8    P'    P''
WT    Arm Myosin    Arm    Myosin

O1    O2    O3
cno M/Z

Q cno M/Z stage 7-8    Q'    Q''
Arm Myosin    Arm    Myosin

R WT late stage 8    S cno M/Z late st 8
    Arm
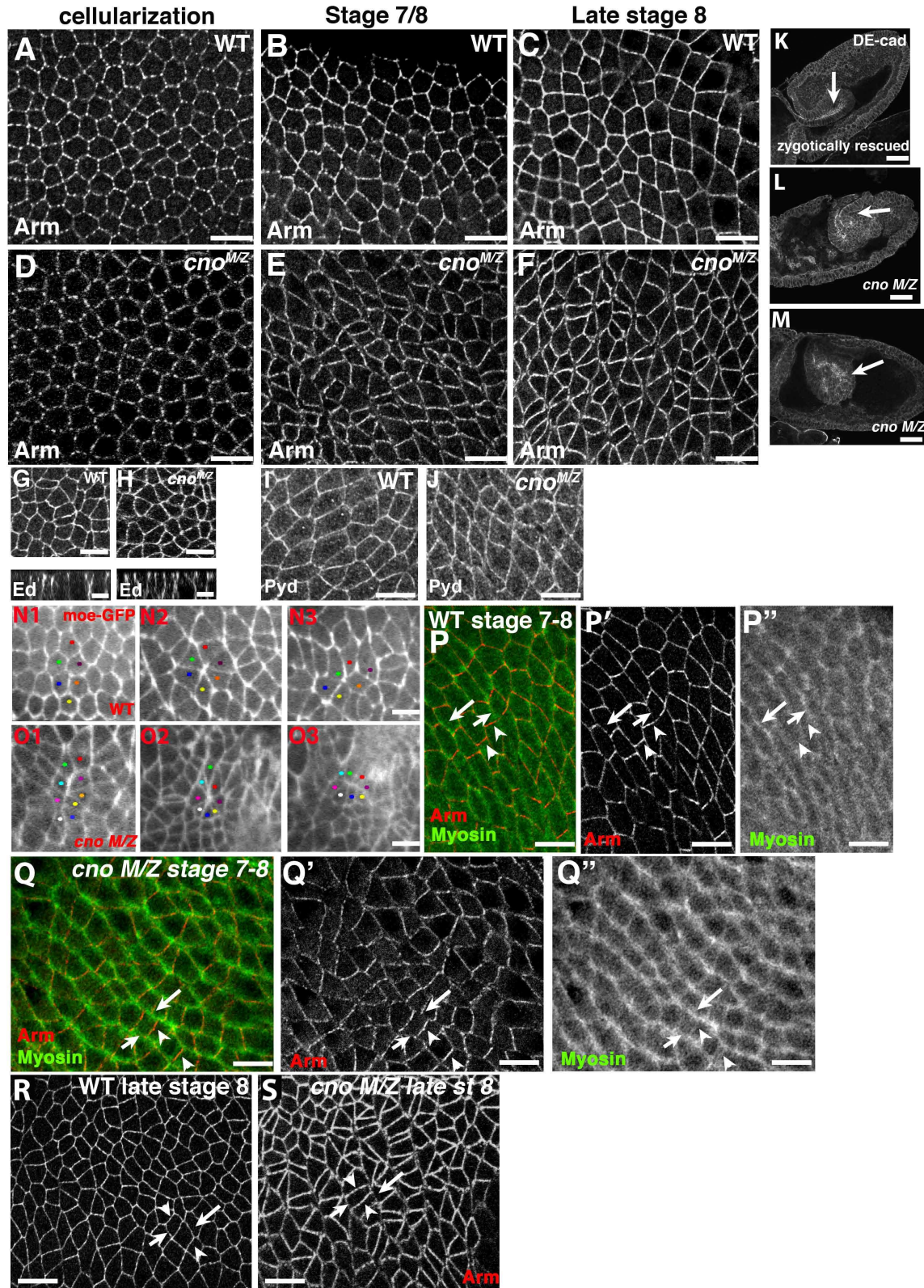
**Figure 2.S1. Cno is not required for the transition from spot to belt adherens junctions, posterior midgut invagination, and is not essential for intercalation but restrains planar polarity during germband extension.**  Embryos, antigens and genotypes indicated.  Apical surface sections except bottom panels of (G,H) which are cross sections. (A-F) Spot to belt AJ transition, stages indicated.  (G-J)  The Cno binding partners Ed (G-H) and Pyd (I,J) still localize to AJs in $cno^{MZ}$ mutants.  (K-M)  Embryos, cross-sections, stage 8-9,  DEcad, genotypes indicated. Arrows point to posterior midgut.  (K) Zygotically-rescued sibling with normal midgut invagination.  (L,M). $cno^{MZ}$ mutants.  Midgut invagination is initiated (L) but invaginated midgut appears disorganized (M).  (N-S)  Embryos, antigens and genotypes indicated. (N,O)  Each sequence shows successive stills from movies of live stage 8 wildtype (N) or $cno^{MZ}$ mutant embryos, visualizing MoeGFP to outline cells.  Intercalating cells are color-coded.  (P-Q"). Stage 7-8 wild type (P-P") or $cno^{MZ}$ mutant (Q-Q").  Normal planar polarity of Myosin (enriched at anterior/posterior boundaries; arrows) and Arm (enriched at dorsal/ventral boundaries; arrowheads) is accentuated in $cno^{MZ}$.  (R,S) Late stage 8 wild type (R) or $cno^{MZ}$ (S).  AJ planar polarity remains strong in $cno^{MZ}$.  Cells form rows. Bars =  (A-J, N-S) - 10µm. (K-M) - 30µm.
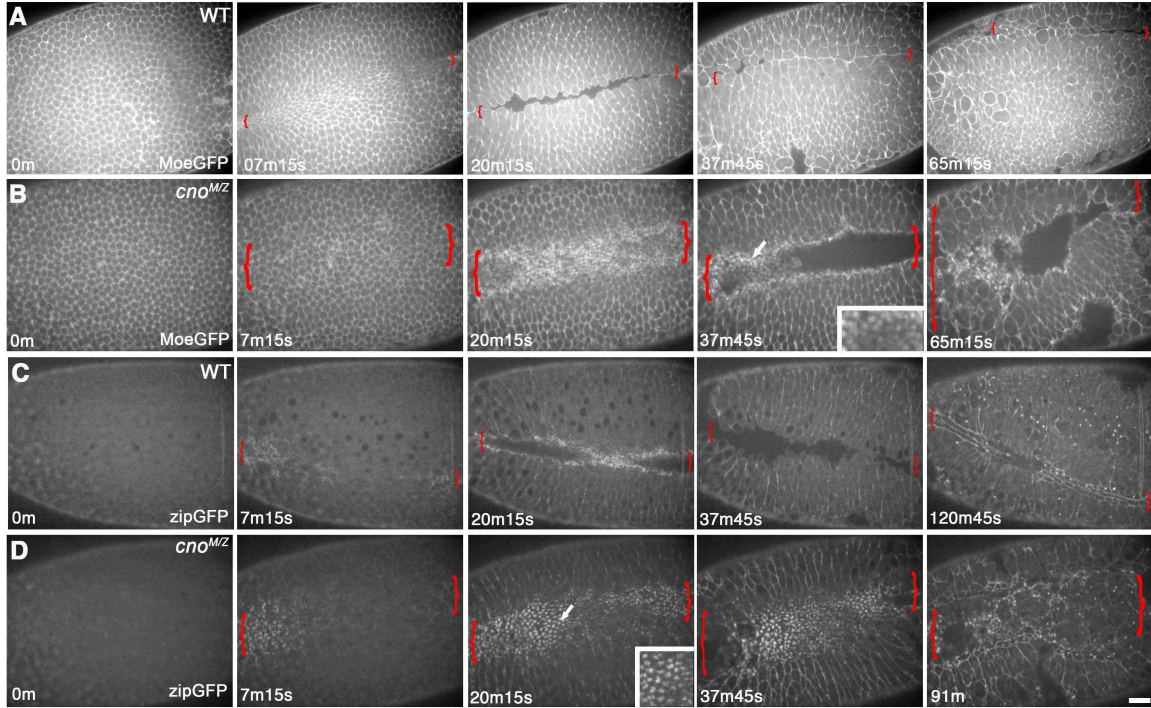
**Figure 2.S2. The actomyosin cystoskeleton becomes uncoupled from cell shape change in** *cno^MZ* **mutants.** Stills from live imaging of gastrulating embryos, ventral view, anterior to the left, genotypes indicated. Brackets mark ventral furrow as it progresses. Arrows and insets show "balls" of either actin (B) or myosin (D). (A) Stills from Suppl. Video 4. (B) Stills from Suppl. Video 5 (C) Stills from Suppl. Video 6. (D) Stills from Suppl. Video 7.Bar = 30µm.
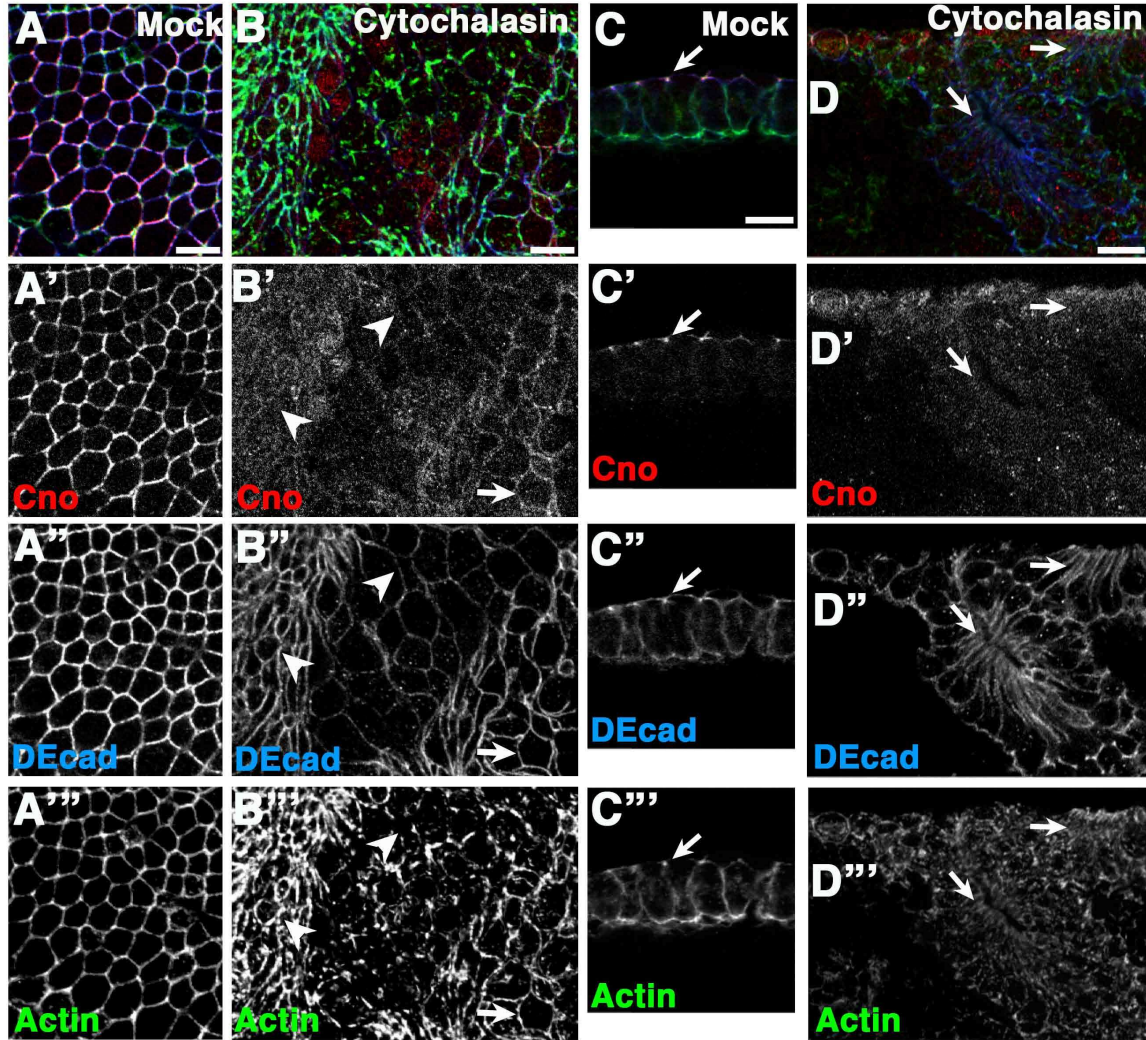
**Figure 2.S3. Actin is required to retain Cno at the cortex after gastrulation.** Stage 9 embryos, treatments and antigens indicated. (A-A'",C-C'") DMSO-treated control embryos. (B-B'",D-D'") Cytochalasin-treated embryos. (A-A'") Surface view. Normal DEcad, Cno and actin localization. (B-B'") Surface view after cytochalasin treatment. Some residual cortical actin is seen in columnar ectodermal cells (left arrowheads) and in amnioserosa (arrows). DEcad remains cortical. Cno is largely lost from the cortex (arrowheads), though some remains at cortex in amnioserosa (arrows). (C-C'") Cross-section. DEcad, Cno, and actin at AJs (arrows). (D-D'") Cross-section through furrow after cytochalasin treatment. DEcad is now all along lateral cortex and Cno becomes largely cytoplasmic (arrows). Bar = 10µm.
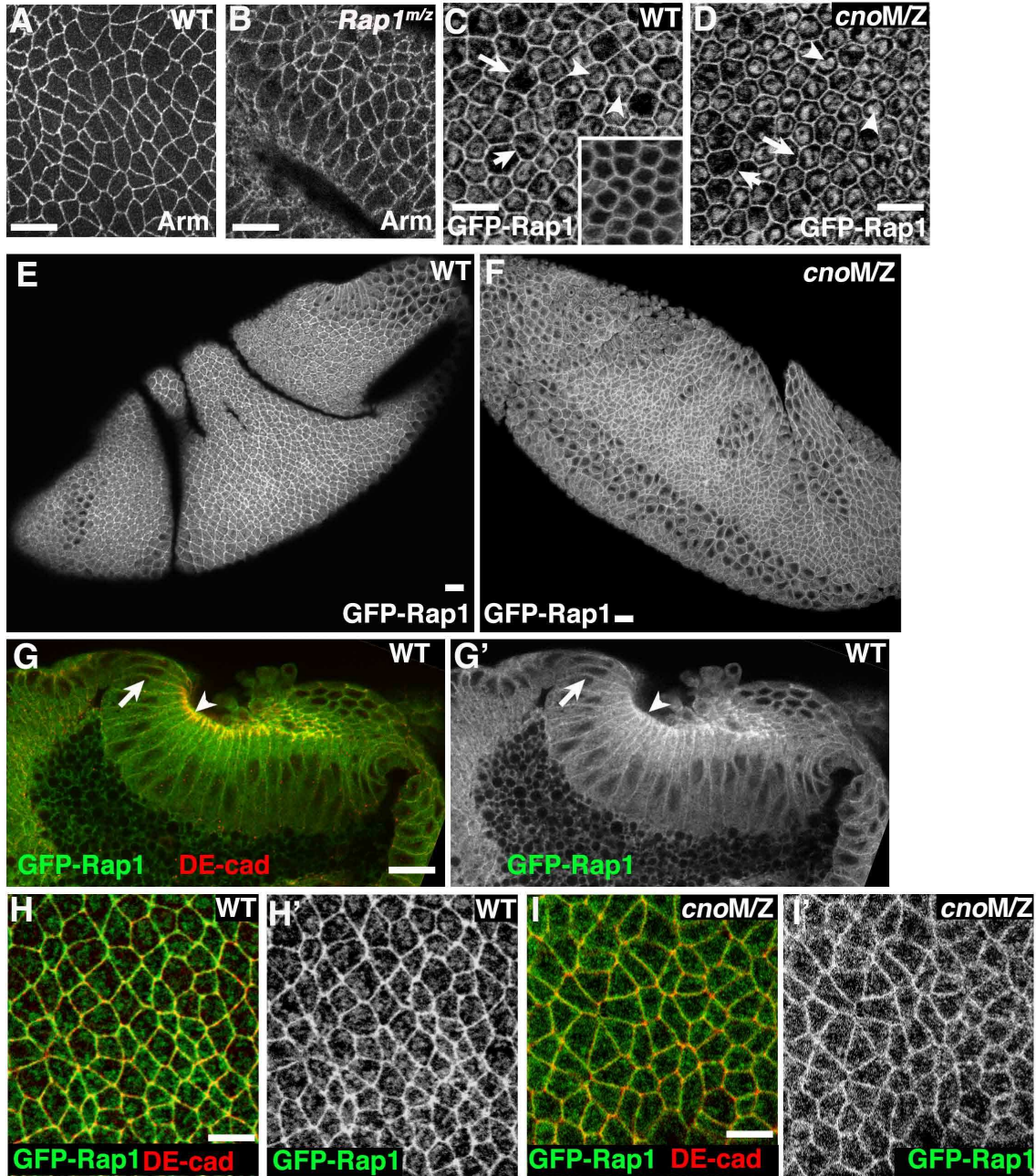
**Figure 2.S4. GFP-Rap1 localization overlaps AJs and does not require Cno function.** GFP-Rap1 localization in wild type (A,C,E,F,H-H') and *cno^{MZ}* mutants (B,D,G-G',I-I'). (A,B) Late cellularization. (C-G) Midgastrulation. (E) Cross section through posterior midgut. (C,D) Arrows = cortical GFP-Rap1, arrowheads = localization to apical punctate structure. (C inset) Basal section of cells shown in C. Bars = 10µm.
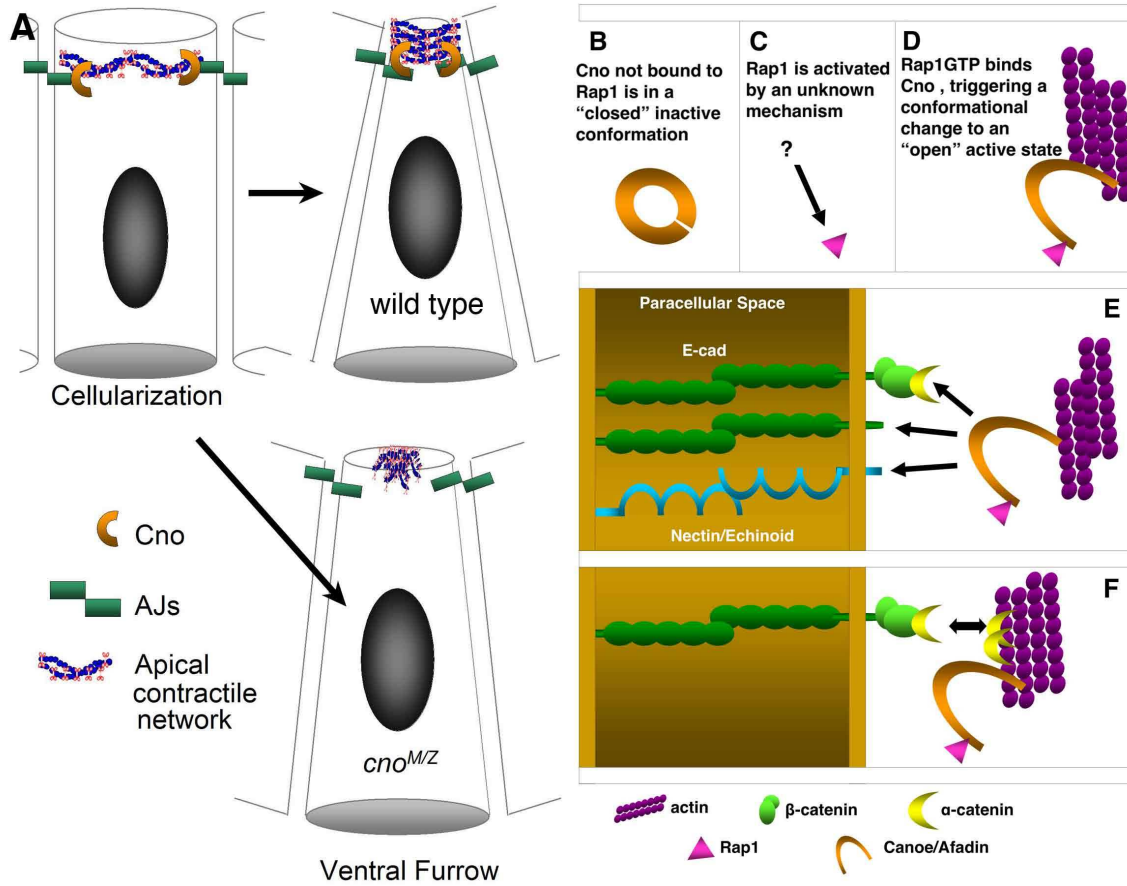
**Figure 2.S5. Models for Cno function.** (A) Apical constriction with and without Cno. (B) Potential molecular links between AJs and actin.

**Table 2.S1: Fly Stocks, Antibodies, and Probes**

| Fly stocks | Source |
|---|---|
| Moesin-GFP | D. Kierhart (Duke University, NC, USA) |
| Zip-GFP (trap #CC01626) | The Carnegie Protein Trap Library (Buszczak et al., 2007) |
| HisGFPIII | R. Saint, (University of Adelaide, South Australia, AUSTRALIA) |
| $arm^{043.A01}$FRT101/FM7 | E. Wieschaus (Princeton, NJ, USA) |
| $ed^{F72}$FRT40A/CyotwiGFP | L. Nilson (McGill University, Quebec, Canada) |

| Antibodies/Probes | Dilution | | Source |
|---|---|---|---|
| | *IF* | *Western* | |
| anti-DE-DCAD2 | 1:100 | | DSHB |
| anti-DE-CAD1 | | 1:200 | M. Takeichi (Kyoto University, Japan) |
| anti-ArmN27A1 | 1:100 | 1:50 | DSHB |
| anti-alpha-catenin | 1:100 | 1:200 | DSHB |
| Phopho-Tyrosine | 1:1000 | | Upstate Biotechnology |
| MAB150 1R (Actin) | 1:1000 | | Chemicon |
| anti-Cno | 1:1000 | 1:1000 | K. Takahashi (Waseda University, Japan) |
| anti-Twist | 1:2000 | | S. Roth (University of Köln, Germany) |
| anti-Zipper ((Myosin II heavy chain) | 1:1000 | | C. Field (Harvard, MA, USA) D. Kiehart (Duke University, NC, USA) |
| anti-Echinoid | 1:1000 | | L. Nilson (McGill University, Quebec, Canada) |
| anti-Polycheatoid | 1:1000 | 1:2000 | A. Fanning (UNC-CH, NC, USA) |
| Alexa-phalloidin | 1:500 | | Molecular Probes |
| anti-alpha-tubulin | | 1:2000 | Sigma |
| Secondary antibodies: Alexas 488, 568, and 647 | 1:500 | | Molecular Probes |
| HRP Secondary Antibodies: | | | Thermo Scientific |
| Mouse/Rat | | 1:10,000 | |
| Rabbit | | 1:100,000 | |

**CHAPTER 3**

A CONTRACTILE ACTOMYOSIN NETWORK LINKED TO ADHERENS
JUNCTIONS BY CANOE/AFADIN HELPS DRIVE CONVERGENT EXTENSION

Jessica K. Sawyer[1], Wangsun Choi[1]*, Kuo-Chen Jung[1]*, Li He[3]*, Nathan J. Harris[1], and

Mark Peifer[1,2]

*authors contributed equally

[1]Department of Biology, University of North Carolina at Chapel Hill, Chapel Hill, NC

27599, USA; [2]Lineberger Comprehesive Cancer Center, University of North Carolina at

Chapel Hill, NC 27599, USA; [3]Department of Biological Chemistry, Johns Hopkins

School of Medicine, Baltimore, MD 21205, USA

**Preface**

The following work further examined the role of Cno in strengthening the

connection between AJs and the actin cytoskeleton outside of the mesoderm. We

uncovered an apical actomyosin network within the lateral ectoderm. Watching this

network using real-time microscopy, we observed periodic contractions of the network

via the coalescence of myosin, correlating with changes in cell shape. The actions of this

contractile network appeared to help control the morphogenetic movement of germband

extension; therefore, we asked if Cno had a role here. Indeed, we found that loss of Cno

led to reduced germband extension in addition to exaggerated planar polarization of

polarity cues along dorsal/ventral cell boundaries. By examining myosin in *cno* mutants,

we observed that the actomyosin network was partially uncoupled, leading to a lack of

cell shape change. This appeared to result from detachment of myosin cables from the cell cortex reminiscent of the defects previously observed in the mesoderm. In addition, loss of Cno did not cause excessive planar polarization of actomyosin components. These two pieces of evidence suggest that excessive polarization of polarity cues was caused by reduced actomyosin contractile activity following the loss of the contractile network's attachment to the cell cortex. This paper and our previous work highlighted a conserved role of Cno in strengthening AJs to properly regulate cortical tension within a changing epithelium.

My part in this work was characterizing mutants of Rho signaling to observe whether planar polarity was altered in other mutants that also failed at mesoderm invagination. Looking at *fog* mutants, which fail to produce the ligand that induces actomyosin contraction in the mesoderm, we observed that planar polarity of Baz remained relatively unperturbed. In addition, myosin cables were still properly formed in these mutants and did not appear to separate from the cell cortex as was observed in cno mutants. Lastly, I provided support in developing the methods used to measure changes in cell shape.

**Summary**

Integrating individual cell movements to create tissue-level shape change is essential to build an animal. We explored mechanisms of adherens junction(AJ):cytoskeleton linkage and roles of the linkage regulator Canoe/Afadin during *Drosophila* germband extension(GBE), a convergent-extension process elongating the body axis. We found surprising parallels between GBE and a quite different morphogenetic movement, mesoderm apical constriction. Germband cells have an apical

actomyosin network undergoing cyclical contractions. These coincide with a novel cell shape change, cell extension along the anterior-posterior axis. In Canoe's absence, GBE is disrupted. The apical actomyosin network detaches from AJs at anterior-posterior cell borders, reducing coordination of actomyosin contractility and cell shape change. Normal GBE requires planar-polarization of AJs and the cytoskeleton. Canoe loss subtly enhances AJ planar-polarity, and dramatically increases planar-polarity of the apical polarity proteins Bazooka/Par3 and aPKC. Changes in Bazooka localization parallel retraction of the actomyosin network. Globally reducing AJ function doesn't mimic Canoe loss, but many effects are replicated by global actin disruption. Strong dose-sensitive genetic interactions between *canoe* and *bazooka* are consistent with them affecting a common process. We propose a model in which an actomyosin network linked at anterior-posterior AJs by Canoe and coupled to apical polarity proteins regulates convergent-extension.

**Introduction**

Morphogenesis is an amazing process that converts simple tissue shapes into complex structures. It begins at gastrulation, when a ball of cells converts itself into an outline of the body, with three germ layers and defined anterior-posterior and dorsal-ventral axes. We must learn how morphogenesis is regulated at all levels: from molecular mechanisms to cellular events to tissue-level integration. During morphogenesis, cells change shape, divide, and move, all while maintaining tissue integrity. This requires coordinating cell-cell adhesion and cell shape change, events driven by cadherin-based adherens-junctions (AJs) and the actomyosin cytoskeleton. Molecular mechanisms underlying this coordination remain largely mysterious. The

82

connection was initially thought to be simple and direct, with cadherins linking to actin via ß- and □-catenin, but biochemical evidence suggests otherwise (Drees *et al.*,2005; Yamada *et al.*,2005). Instead, recent work suggests distinct linkers act in different events (e.g. Abe and Takeichi, 2008; Cavey *et al.*,2008; Sawyer *et al.*,2009); among these is the actin-binding protein Canoe(Cno=mammalian afadin). Another important challenge is defining the roles and mechanisms of action of different linkers during distinct biological processes.

Apical cell constriction during *Drosophila* mesoderm internalization provides a model of cell shape change during morphogenesis. While the textbook model of apical constriction involved constriction of a circumferential belt of actin filaments underlying cell-cell AJs, recent work revealed that this is not always the case. Instead, in the fly mesoderm and amnioserosa, cell fate cues initiate a signaling pathway triggering assembly and constriction of an apical actomyosin network covering the surface of each cell (Harris *et al.*,2009). This network constricts in a cyclical fashion, with an unidentified molecular ratchet driving progressive cell shape change (Martin *et al.*,2009; Solon *et al.* 2009). Cell shape change requires that the contractile network is connected to AJs (Dawes-Hoang *et al.*,2005). AJs also join cells, transmitting forces from cell to cell across epithelial sheets. Tissue-level integration plays a key role in mesoderm invagination. Forces transduced via AJs across the tissue modify individual cell shape changes, as cells respond both to internally-generated contractile forces and those generated by the supracellular network (Martin *et al.*,2010).

While it was clear that linkage of the apical contractile network to AJs is crucial for mesoderm apical constriction, the molecular linkage initially remained unclear. We

previously explored the role of Cno in this process.  Cno interacts with nectins and other

AJ proteins, and was suggested to play important roles in mammalian cell adhesion

(Takai *et al.*,2008).  We found Cno isn't essential for *Drosophila* cell adhesion, but is

required for proper mesoderm invagination (Sawyer *et al.*,2009).  In Cno's absence, the

apical actomyosin network constricts and cells initiate shape change, but then the

network detaches from AJs, preventing effective mesoderm invagination.  These data

suggested that Cno mediates or regulates attachment between the actomyosin

cytoskeleton and cell-cell AJs during mesoderm apical constriction.

Here we explore coordination of the actomyosin cytoskeleton and AJs during a

very different cell behavior: convergent-extension, in which cells intercalate between one

another in the plane of the epithelium to elongate the body axis (Harris *et al.*,2009; Yin *et

al.*,2009).  This morphogenetic movement is also common to gastrulation in many

animals, but is thought to be cell biologically and mechanistically very different from

apical constriction, though myosin regulation is also critical.

In *Drosophila* this process is called germband extension (GBE; Fig. 1A,A';

Zallen and Blankenship,2008).  During GBE the embryo elongates two-fold along the

anterior-posterior (AP) axis, while narrowing along the dorsal-ventral (DV) axis.

Because embryos are constrained within the eggshell, this leads to the posterior end of

the embryo moving from the posterior end of the egg (Fig. 1A, red arrowhead) up around

the dorsal side to lie above the head (Fig. 1A', red arrowhead).  Elongation in the first

few minutes is driven at least in part by oriented cell division (da Silva and Vincent,2007)

and relaxation of DV cell elongation caused by mesoderm invagination (Butler *et

al.*,2009).  In our current view, extension during the rest of GBE is dominated by

intercalation of ectodermal cells (Fig. 1D; Irvine and Wieschaus,1994). As GBE

initiates, cells become planar-polarized, with AJ proteins and Bazooka (=Par3) enriched

along DV borders and actin and non-muscle myosin II (myosin) enriched along AP

borders (Fig.1D left; note they aren't lost from the other borders). Myosin enrichment

leads to formation of myosin cables extending across several cell diameters. Their

constriction shrinks AP borders, driving intercalation and elongating the ectoderm

(Fig.1D; Blankenship *et al.*,2006; Fernandez-Gonzalez *et al.*,2009; Rauzi *et al.*,2008;

Zallen and Wieschaus, 2004). Consistent with this, zygotic myosin is required for full

GBE (Bertet *et al.*,2004). Thus, cell shape changes and myosin arrangement during GBE

are thought to be quite distinct from those during apical constriction.

Given the important role of Cno in apical constriction during mesoderm

invagination, we explored whether it plays roles in subsequent morphogenetic events.

We found Cno is required for completion of GBE. In analyzing Cno's role, we

discovered surprising parallels between GBE and mesoderm apical constriction in wild-

type embryos. Ectodermal cells are covered by an oscillating apical network of actin and

myosin that drives periodic cell constriction. Further, this coincides with progressive

elongation of ectodermal cells along the anterior-posterior axis, contributing to body axis

elongation. In Cno's absence, the apical actomyosin network detaches from cell-cell

junctions in a planar-polarized way. This disrupts coordination of apical myosin

constriction and cell shape change, blunting elongation of cells along the AP axis. Loss

of Cno also leads to dramatic changes in localization of the apical polarity proteins Baz

and aPKC, which correlate with changes in myosin localization. We propose a model in

which a contractile apical actomyosin network plays an important role in driving body

axis elongation during convergent-extension, with Cno helping to maintain network:AJ connections in a planar-polarized fashion, and thus coordinate contractility and cell shape change.

**Results**

*Cno loss disrupts GBE*

For actomyosin contractility to be coupled to cell shape change, it is important that the cytoskeleton is anchored at cell-cell AJs. Given Cno's importance in linking AJs and the actomyosin cytoskeleton during mesoderm apical constriction (Sawyer *et al.*, 2009), we explored whether Cno loss affects GBE, comparing GBE speed and extent in wild-type (WT) and maternal/zygotic null *cno$^{R2}$* mutants (*cno$^{MZ}$*). We imaged live for 80min from cephalic furrow initiation to the end of WT GBE. During the first 10 min of GBE, WT and *cno$^{MZ}$* mutants extend at similar rates, but then *cno$^{MZ}$* mutants slow significantly and fail to complete GBE (Fig.1C). *cno$^{MZ}$* mutants only extend 74% as far as WT (Fig.1A-C). The midgut is still internalized in *cno$^{MZ}$* mutants (Sawyer *et al.*,2009), suggesting midgut invagination failure isn't what blocks elongation. These data demonstrate Cno plays an important role in GBE, with its loss disrupting GBE to a degree similar in extent to that seen in *baz* or *zipper* (myosin heavy chain) zygotic mutants (Zallen and Wieschaus, 2004; Bertet *et al.*, 2004).

*An apical contractile actomyosin network during germband extension*

During GBE, the ectoderm lengthens ~2-fold in the AP axis and narrows in the DV axis. In the current view, this is largely driven by cell intercalation (Fig. 1D; Irvine and Wieschaus, 1994), with important contributions from DV cell relaxation (Butler *et al.*,2009) and oriented cell division (da Silva and Vincent, 2007) during the first 10 min

(Fig. 1C).  Cytoskeletal and AJ proteins become reciprocally planar-polarized during

GBE (Bertet *et al.*,2004; Zallen and Wieschaus, 2004; Fig.1D), with actin and myosin

enriched on AP borders and AJ proteins enriched on DV borders.  Myosin planar-

polarization triggers formation of myosin cables, often extending several cell diameters

(Fig.2A arrowheads), constriction of which helps drive intercalation (Fig. 1D;

Blankenship *et al.*,2006; Fernandez-Gonzalez *et al.*,2009; Rauzi *et al.*,2008).

  We re-examined the dynamic localizations of myosin and AJs during WT GBE.

The planar-polarized myosin cables that others previously reported were easily observed

(Fig.2A), but we were surprised to find myosin wasn't confined to AJs.  Instead the

apical surface of each ectodermal cell was covered by a dynamic myosin network

(Fig.2B; Movie1) resembling that in apically-constricting mesoderm (Martin *et al.*,2009)

. Our live-imaging revealed that, as in mesoderm, myosin spots and filaments formed on

the apical surface, coalesced by constriction, and dissipated (Fig.2C,arrowheads).  Thus

despite major differences in cell shape changes during mesoderm invagination and GBE,

both share an apical contractile network.  While our manuscript was in preparation, Rauzi

*et al*., (2010) and Fernandez-Gonzalez and Zallen (in press) independently identified and

characterized this contractile apical actomyosin network.

  In fact, individual germband cells go through multiple rounds of myosin network

formation, constriction, and dissipation (Fig.2D=cell undergoing 6 rounds;

Movie1,asterisk).  Double-imaging with DEcadherinGFP (DEcadGFP) revealed pulses of

myosin constriction coincided with periodic decreases in apical cell area (Fig. 2D),

suggesting the network is coupled to AJs.  We used automated analysis of many cells (He

*et al.*,2010) to quantitate this.  This also revealed periodic pulses of apical myosin

accumulation and of cell shape change in individual cells (Fig. 3A); the amount of apical

myosin accumulation and the degree of change in cell area varied between pulses, as was

previously observed in the *Drosophila* mesoderm and amnioserosa (Martin *et al.*, 2009;

Solon *et al.*, 2009).  When we calculated the rate of change in these two parameters, the

peaks of apical myosin change and cell area change were more regular (Fig.3C).  Apical

myosin pulses peaked every 162±44s (Fig.3E).  This regularity was also revealed by

auto-correlation analysis of individual apical myosin peaks; in addition to the correlation

of a peak with itself, there were also clear peaks off-set by ~160s (Fig.3G,I arrows).

Finally, this analysis revealed a strong correlation between the timing of pulsatile

increases of apical myosin and timing of cell constriction (Fig.3J arrow,L,M).  Myosin

increase slightly preceded constriction (by ~6.5s; Fig.3J,L), consistent with the

hypothesis that myosin contractility drives cell constriction.  This hypothesis is reinforced

by instances where myosin cables bridging AJs at different cortical points appeared to

exert force and alter cell shape (Fig.2E, arrowheads; Movie2).  Together, these data

reveal a surprising parallel between cells undergoing convergent extension during GBE

and cells undergoing apical constriction:  both share a contractile apical actomyosin

network undergoing pulsatile constriction.

*A novel cell shape change--anterior-posterior cell elongation--coincides with cycles of*

*actomyosin contraction*

The cyclical pulses of myosin contractility in the mesoderm lead to progressive

apical constriction (Martin *et al.*, 2009).  We thus tested the hypothesis that cyclical

constriction of ectodermal cells also coincides with progressive cell shape change.  At

gastrulation onset, cells begin isometric and hexagonal (Zallen and Zallen, 2004), but

88

mesoderm invagination drives substantial elongation of ectoderm cells along the DV axis, especially near the ventral midline. During the first ten minutes of GBE, these cells then return to a more isometric shape (Butler *et al.*,2009).

We observed a second novel, spatially distinct cell shape change during the period of pulsatile contractions in germband cells. While cell areas increased after each round of myosin dissipation (Fig.2D), over multiple rounds cells underwent a progressive change in cell shape. This lengthened cells along the AP axis (Fig.2D, arrows; Movie1, asterisk; below we refer to this as AP cell elongation).

This change in individual cell length could contribute to the elongation of the entire tissue. To test this hypothesis and to determine the average amount of cell elongation during this process, we quantitated changes in cell shape and apical area in many cells between the end of cellularization and the middle of GBE. We compared lengths of AP and DV cell borders and assessed apical cell area (Suppl.Fig.1A,B). To remove bias, we measured all borders and used ImageJ to classify borders as AP or DV (Suppl.Fig.1 legend). Prior to mesoderm invagination, cells are isometric with equal AP and DV border lengths (mean AP:DV border=2.6:2.6µm; Suppl.Fig.2A, E left). As GBE and pulsatile ectodermal cell constriction begins, cells elongated ~2-fold along the AP axis (elongating DV cell borders). In contrast, cell length along the DV axis (and thus AP cell borders) remains constant (mean AP:DV border=2.5:4.3µm; Suppl. Fig. 2B, E right). As a result of cell elongation, the apical area of cells increases ~50% (Suppl.Fig.2C,D). These changes parallel those we observed in individual cells (Fig.2D,arrows). These data are consistent with the hypothesis that this novel cell shape change—AP cell elongation—helps elongate the tissue along the AP axis during GBE

(Suppl.Fig.3C). Perhaps the same planar-polarized myosin cables that help drive cell intercalation (Suppl.Fig.3A,B double-headed arrows) also constrain cell elongation along the DV axis and thus restrict it to the AP axis.

***During GBE myosin detaches from AJs in a planar-polarized way in cno^MZ mutants***

Since Cno is required for effective GBE (Fig. 1C), we next explored the cell biological effects of Cno loss. Based on its known roles, we tested two hypotheses. Cno might regulate linkage between the actomyosin cytoskeleton and AJs during GBE, or it could regulate cell-cell adhesion. Consistent with the first hypothesis, myosin localization was dramatically altered in the lateral ectoderm of *cno^MZ* mutants during GBE. As in WT, myosin became planar-polarized early in GBE, enriched along AP borders. In WT, a single myosin cable co-localized with AP AJs (Fig.4A, J arrows), suggesting cables in adjacent cells are very closely opposed. In contrast, in *cno^MZ* mutants, we saw two distinct myosin cables at AP cell borders that remained at the apical cortex but separated from one another (Fig.4B, between arrows; single myosin cables were seen at DV borders). This suggests the myosin networks in adjacent cells detached from AJs, retracting unto the apical surface. These separated myosin cables were also apparent in live imaging with myosin-mCherry (Fig.4C, between arrows; Movie3). F-actin exhibited similarly altered localization; WT cortical cables (Fig.4D, arrows) sometimes appeared detached in *cno^MZ*, forming parallel cables (Fig. 4E, between arrows). Detached myosin cables were seen throughout the germband during early GBE (Suppl.Fig.4A-B; unless noted, phenotypes were highly penetrant-quantitation is in Suppl.Table3). Myosin separation from AJs was also quite striking in rosettes, where multiple cell vertices meet. Normally, myosin localizes tightly to vertices (Fig.4L,

magenta arrow, insets).  In contrast, in $cno^{MZ}$ myosin instead formed rings around

vertices (Fig.4M, arrows).  Despite these dramatic changes, an apical myosin network

remained, in which myosin condensations formed and dissipated (Suppl.Fig.4E, arrows;

Movie3).  Together these data suggest that Cno plays a specific, planar-polarized role in

attaching the apical myosin network and junctional myosin cables to AP cell borders and

to cell vertices during GBE.

### *Myosin cable detachment is not due to cell separation*

The simplest hypothesis to explain these observations is that Cno regulates

linkage between the actomyosin cytoskeleton and AJs during GBE, as it does during

mesoderm apical constriction (Sawyer *et al.*, 2009).  However, we first needed to rule out

an alternate hypothesis: that in Cno's absence, cell adhesion is compromised, causing

cells to separate.  AJs assemble normally in $cno^{MZ}$ mutants, and in dorsal ectodermal cells

AJs are maintained through the end of morphogenesis, making this possibility less likely

(Sawyer *et al.,*2009).  To rule out more subtle changes in cell adhesion, we explored

whether cells separate using SEM.  Cells went from rounded during cellularization

(Suppl.Fig.5A,B) to more tightly adherent during early GBE (Suppl.Fig.5C,E vs D,F,G),

with no discernable differences between $cno^{MZ}$ and WT.  As GBE progresses, mitotic

domains in the lateral and ventral ectoderm begin mitosis, and those cells round up in WT

and mutants.  However, cells that hadn't yet divided remained similarly adherent in WT

and $cno^{MZ}$ (Suppl.Fig.5H vs I).  Thus substantial cell separation does not explain myosin

detachment in $cno^{MZ}$ mutants.

We also analyzed lateral and AJ markers.  In WT, the basolateral protein Nrt

directly underlies the single myosin cable (Fig.4F, arrows).  In $cno^{MZ}$ a single Nrt-stained

cell border (Fig.4G,between arrows) remained between the two myosin cables, supporting the idea that cells didn't substantially separate. We also examined the relationship between AJs and myosin cables. WT myosin cables co-localize with AJ proteins like DEcad (Fig.2E, 4J arrows). In contrast, in $cno^{MZ}$ mutants, myosin cables separated from AJs (Fig. 4H,K; as observed both in fixed embryos using Arm (fly ßcat) as an AJ marker, or via live imaging, using DEcad-GFP). Arm and DEcad remained as a single border at AJs between detached myosin cables (Fig.4H,K, between arrows; Movie3). Together, our data support the hypothesis that myosin cables detach primarily due to weakened AJ:actomyosin network linkages, not cell separation

We examined AJs and myosin further, exploring their relationship along the apical-basal axis. WT cortical myosin cables and AJs are in the same plane (Fig.2E,4J arrows). In contrast, detached myosin cables in $cno^{MZ}$ are more apical than the AJs from which they detached. In the apical plane where detached Myosin cables reside, gaps and discontinuities in Arm localization are sometimes observed (Suppl.Fig.4B, purple arrows). However, at the level of the AJs (1.5µm more basal), Arm was substantially more continuous (Suppl.Fig.4C, purple arrows). Other apparent apical discontinuities in Arm localization occur at cell vertices where multiple cells met (Suppl.Fig 4B,C, yellow asterisks and arrows; abnormal cell arrangements at vertices were also seen in SEM; Suppl.Fig 4D, arrows). Together, these data suggest Cno helps link the actomyosin network tightly to AP AJs and at multicellular junctions, and that in its absence the network detaches.

***Cno loss reduces coupling between the apical actomyosin network and cell shape change***

92

These dramatic changes in linkage of the apical actomyosin network in *cno^{MZ}*

mutants provide a possible mechanistic explanation of the defects seen in GBE—perhaps

tight linkage is critical for coupling apical actomyosin contractility and cell shape change.

To test this hypothesis, we analyzed the effects of Cno loss on periodic contractions of

the actomyosin network and on cell shape change, by automated analysis of many cells.

*cno^{MZ}* cells retained a contractile apical myosin network that underwent cycles of

appearance and dissipation (Fig.3B,D), suggesting that tight AP connections of the

network to AJs are not essential for maintaining this process.  However, pulses of apical

myosin became significantly less frequent and less regular in periodicity than in WT

(225±67s vs. 162±44s in WT; Fig.3C vs. D, E vs F,G vs H,I).  Further, the correlation

between pulses of apical myosin and periodic changes in cell shape was significantly

reduced (Fig.3J vs. K, L,M).  These data suggest that attachment of the actomyosin

network to AP cell boundaries mediated by Cno is important for the fidelity and coupling

of periodic pulses of apical actomyosin and periodic cell shape change.

Our data above suggest that the pulsatile changes in cell shape coincide with a

novel progressive cell shape change that contributes to GBE: cell elongation along the

AP body axis (Suppl.Fig.2E).  We hypothesized that disruption of the fidelity and

coupling of actomyosin contractility and shape change seen in *cno^{MZ}* mutants might

disrupt AP cell elongation.  We found that in *cno^{MZ}* mutants cell elongation along the AP

axis is significantly reduced (Suppl.Fig.2B; cell elongation along the AP axis elongates

DV cell borders), leading to reduced cell shape anisometry during early GBE (DV/AP

cell border ratio=1.41 vs. 1.70 in WT).  This fits well in with the reduction of GBE we

observed in *cno^{MZ}*.  Failure to fully extend cells along the AP axis also resulted in smaller

apical areas of *cno^MZ* cells (Suppl.Fig.2D). Thus, Cno loss reduces normal asymmetric cell elongation, supporting a mechanism in which anchoring of the actomyosin network along AP borders may help drive GBE.

We also examined the effects of Cno on the other shape change, which occurs during the first 10 minutes of GBE, in which ectodermal cells that were stretched along the DV body axis by mesoderm invagination relax to an isometric shape (Butler *et al.*,2009). In contrast to AP cell elongation, this cell shape change does <u>not</u> require Cno. *cno^MZ* mutants elongate as fast as WT during the first 10 minutes of GBE (Fig. 1C), when DV relaxation plays an important role (Butler *et al.*, 2009). Further, live-imaging confirmed that DV relaxation still occurs in *cno^MZ* mutants (Suppl.Fig.6Avs.B).

While Cno plays a clear role in AP cell elongation, the effects of Cno loss on tissue-level rearrangements are more complex. Mutant cells retain some ability to change shape, and detached myosin cables still appear able to drive cell rearrangements, shrinking AP boundaries (Suppl.Fig.3D-F, blue, red, yellow arrows, G vs. H), but there are clear delays in GBE (Fig. 1). In the future it will be important to explore in detail how Cno loss affects the entire suite of cell behaviors driving GBE.

***The apical myosin network in the ectoderm detaches from AJs in cno^MZ mutants but spot connections remain***

One puzzling feature of the detachment of myosin from AP AJs in *cno^MZ* mutants is that the detached myosin cables remain within a few microns of AJs. This contrasts with what we observed in the mesoderm, where the detached apical actomyosin network constricted to a ball (Sawyer *et al.,* 2009; Suppl.Fig.4F,G, arrows). We hypothesized that this might reflect residual, Cno-independent connections between AJs and the apical

actomyosin network in the ectoderm.  To test this, we looked compared progression of

detachment in the invaginating mesoderm and the germband.  Strikingly, live-imaging of

invaginating mesoderm revealed DEcad-containing membrane strands (Supp. Fig.4G,

arrowheads) extending between myosin balls (Suppl.Fig.4G, arrows), suggesting residual

network:AJ connections exist in this tissue.  These were also visible in SEM

(Suppl.Fig.4H; similar membrane strands were seen in cells with reduced AJ function;

Martin *et al.*,2010).  Thus, in mesoderm residual AJ:network connections exist, but are

not sufficient to resist constriction of the apical myosin network.

We then explored lateral ectoderm cells that participate in GBE.  In $cno^{MZ}$

mutants, during early GBE, the apical myosin network in ectodermal cells separated from

AJs, but didn't collapse into balls as it did in the mesoderm.  Instead, myosin initially

formed rings just inside AJs (e.g., Fig.5A, arrows; Movie4), consistent with remaining

connections between the network and AJs.  Strikingly, these myosin rings went through

cycles of formation, constriction, and dissipation (e.g., Fig.5B-cell 1 arrows; Movie4).

Cells also periodically changed shape (Fig.5B'-cells 1-3 constrict and then relax, while

cell 4 starts constricted and relaxes; Movie4), consistent with the possibility that some

connection remains between network and AJs.  A third observation also supported a

remaining connection.  Along the basolateral cell surface, cortical DEcad was smooth

(Fig.5C,D basal), as in WT.  However, in the apical-most plane where DEcad was visible

(1µm more apical), the cortex appeared very convoluted, with membrane strands less

dramatic but reminiscent of those in mesoderm (Fig.5C,D apical, arrows).  Strands were

often embedded in the apical myosin network, as if they remained attached to it

(Fig.5E,arrows).  These strands were also visible in SEM (Fig.5F vs. G).  Together, these

data suggest Cno helps maintain tight connections between the apical actomyosin network and AJs in the ectoderm, but that other proteins mediate residual spot connections.  Further, the effects of Cno loss in the GBE suggest that Cno has a planar-polarized role in maintaining AJ:network linkages in the GBE, whereas in the mesoderm its role is uniform around the cell.

### *Cno is planar-polarized with cytoskeletal rather than AJ proteins*

Given the striking planar-polarized defects in the actomyosin network during GBE in $cno^{MZ}$, we examined if Cno is planar-polarized in this process.  Cno largely colocalizes with AJs from gastrulation onset (Sawyer *et al.*, 2009), suggesting the hypothesis that during GBE it would become enriched on DV cell borders like the AJ proteins.  However, unlike DEcad, Cno is enriched at tricellular junctions with a subset of actin (Sawyer *et al.*,2009), and its affects on myosin attachment are most dramatic at AP cell borders where myosin and actin are enriched, consistent with the alternate hypothesis that it would co-localize with cytoskeletal proteins.  To determine if Cno is planar-polarized, we immunostained WT embryos, measured mean fluorescence intensity of Cno on all cell borders, and then compared borders aligned along AP or DV axes of the embryo (AP borders=0-29° vs. DV borders=60-90°; Suppl.Fig.1).  Interestingly, Cno is enhanced on AP borders with myosin and F-actin, rather than being enriched along DV borders with other AJ proteins (AP/DV=1.20; Fig.6B, arrows vs. arrowheads; Fig.6M; Table 1).  This is consistent with the planar-polarized myosin detachment we observed in $cno^{MZ}$, supporting the hypothesis that Cno plays a particularly important role in regulating linkage between AJs and apical actomyosin along AP borders.

*Cytoskeletal planar polarity is not altered in cno^MZ*

During GBE, myosin and actin become enriched on AP borders (Bertet *et al.*,2004; Blankenship *et al.*,2006; Zallen and Wieschaus, 2004). This is thought to help drive GBE. Given the dramatic, polarized disruption of the apical actomyosin network in *cno^MZ*, we initially hypothesized that Cno loss would alter cytoskeletal planar polarity, reducing asymmetric accumulation along AP cell borders. In our previous studies we noted in passing that Arm and myosin planar polarity might be altered in *cno^MZ* (Sawyer *et al.*,2009). To examine this in detail, we quantitated junctional and cytoskeletal planar polarity in WT and *cno^MZ* during early GBE, comparing protein ratios on AP/DV borders to remove variation between experiments due to differential staining. Surprisingly, Cno loss had no effect on planar-polarization of myosin or F-actin. They were similarly enriched on AP borders in *cno^MZ* and WT (Fig.6M; in contrast, Nrt isn't planar-polarized in WT or *cno^MZ*; Fig.6C,D,M; Table 1; Suppl.Table 1). Thus, detachment of the actomyosin network from anterior-posterior AJs doesn't affect myosin's ability to accumulate in a planar-polarized manner and Cno is not essential for myosin planar-polarization.

**Cno loss subtly enhances AJ planar polarity**

Cno and its mammalian homolog Afadin both localize to AJs, and Cno can bind to DE-cadherin in vitro (Sawyer *et al.*, 2009). One hypothesis is that Cno regulates localization of AJ proteins, perhaps specifically affecting AP cell borders where myosin detaches in its absence. In *cno^MZ* mutants AJ proteins remain at AP borders where myosin has detached (Fig. 4; Suppl.Fig. 4B,C), but this didn't rule out more subtle changes in their localization. We thus quantitated Arm and DEcad planar-polarization.

Previous studies revealed subtle Arm and DEcad planar-polarization in WT (Blankenship *et al.*,2006; Harris and Peifer, 2007). In our hands, Arm has a trend toward slight DV enrichment in WT (Fig.6E,N, red vs. yellow arrowheads; Suppl.Table 1), while we didn't detect DEcad planar-polarization in WT (Fig.6G,N; Suppl.Table 1), perhaps due to differences in fixation or measurement. In $cno^{MZ}$, in contrast, both Arm and DEcad were noticeably planar-polarized, with clear DV border enrichment (Fig.6F,H red vs. yellow arrowheads, 6N; Table 1; Suppl.Table 1). We also examined absolute levels of AJ proteins by immunostaining WT and mutant embryos together. Nrt was unchanged, while overall levels of DEcad and Arm were reduced about two-fold on both AP and DV borders (Suppl.Table2). However, this reduction is unlikely to disrupt cell adhesion, as heterozygous mutants for either gene are WT during GBE; in fact, no defects were observed in DEcad zygotic null mutants until after GBE (Tepass *et.al.,*1996). Thus Cno helps restrain planar-polarization of cadherin-catenin complexes; this could be direct, or indirect via effects on actin and myosin.

### Planar polarity of apical polarity proteins Baz and aPKC is dramatically enhanced in $cno^{MZ}$

Like myosin, the apical polarity protein Baz is an important player in GBE (Zallen and Wieschaus, 2004). The contractile apical actomyosin network we observed during GBE is reminiscent of that in one-cell *C. elegans* embryos (Munro *et al.*,2004). In *C. elegans,* this network plays a role in cell polarization; upon fertilization, the actomyosin network contracts anteriorward and "anterior Par" proteins including Par3 (fly Baz) and aPKC move anteriorly (Munro *et al.*,2004), suggesting the possibility the two may be coupled. Therefore, we tested the hypothesis that loss of Cno and the

98

dramatic changes in the apical actomyosin network would affect Baz and aPKC localization.

Baz initially colocalizes with DEcad in spot AJs (Harris and Peifer, 2005), and then becomes planar-polarized during GBE, with enrichment on DV borders with AJ proteins. Strikingly, Baz planar polarity is <u>very</u> strongly enhanced in $cno^{MZ}$, increasing from ~2-fold to ~9-fold (Fig.6I vs. J, red vs. yellow arrowheads, 5N; Table 1; Suppl.Table 1). We also measured absolute Baz levels at AP and DV borders in WT and $cno^{MZ}$, immunostaining them together and quantitating fluorescence. While Baz is only slightly reduced on DV borders in $cno^{MZ}$ relative to WT (13% less; Suppl.Table 2), it is substantially reduced on AP borders (60% less; Suppl.Table 2), suggesting enhanced planar polarity is primarily due to Baz loss from AP borders (Fig.6J). We cannot exclude the possibility that the techniques we used (immunofluorescence and SEM) missed slight cell separation apically, which might contribute to apparent Baz reduction, but we think this less likely as we measured multiple planes in the z-axis. Thus Cno function is required to retain Baz at AP borders, preventing its excess planar-polarization.

Along DV cell borders, we observed another dramatic change in Baz localization in $cno^{MZ}$ mutants. While Baz remained enriched at DV borders in $cno^{MZ}$, it was largely restricted to central regions and didn't extend to vertices where DV met AP borders (marked by Nrt; Fig.7A-A", arrows). In contrast with Baz, AJ proteins like Arm are not restricted to central DV borders and extend all the way to cell vertices (Fig.7B', arrows). Strikingly, Baz localization along DV borders did not extend past the myosin cables that were detached from AP border AJs (Fig.7C,D,arrows). This raises the possibility that Baz localization may be influenced by, or influence, myosin localization.

To determine whether these changes in localization were particular for Baz or affected other apical polarity proteins, we examined aPKC. aPKC localizes apically to Baz and AJs during early gastrulation (Harris and Peifer, 2005), but its planar-polarization during GBE had not been assessed. We found aPKC is enriched with Baz on DV borders in WT (Fig.6K red vs. yellow arrowheads, 6N). Strikingly, aPKC planar polarity is also strongly enhanced in $cno^{MZ}$ (Fig.6L, red vs. yellow arrowheads, 6N; Table 1; Suppl.Table 1); like Baz, aPKC appeared reduced on AP borders . Further like Baz and unlike AJ proteins, aPKC was restricted to central DV borders in $cno^{MZ}$ (Fig.7A''', arrows). Thus Cno is required for correct planar-polarization of both Baz and aPKC. These data raise the possibility that apical actomyosin may be coupled in some way to Baz and aPKC, as Cno loss affects their localization in parallel.

Mesoderm influences ectodermal cell shape change in the first ten minutes of GBE (Butler *et al.*,2009). While we had ruled out a role for Cno in this early cell shape change, to be certain that failure to fully invaginate mesoderm did not contribute to alterations in myosin and Baz localization in $cno^{MZ}$, we examined Myosin and Baz in *fog* mutants, which do not complete mesoderm invagination. Fog acts via a completely different mechanism than Cno, acting as the ligand in a signaling pathway that triggers apical myosin accumulation and apical constriction of the mesoderm (Harris *et al.,* 2009). In *fog* mutants we found that myosin cables don't detach from AP AJs, and Baz planar-polarization isn't dramatically altered (Suppl.Fig.6C-E), confirming that the changes we see in $cno^{MZ}$ (Suppl. Fig. 6F) aren't solely due to defective mesoderm invagination. Together, these data suggest that Cno is required to properly maintain Baz and aPKC at AP borders, and prevent their excessive planar-polarization.

*Globally reducing cell adhesion does not closely mimic Cno loss*

Our data suggest Cno helps maintain integrity of the apical actomyosin network and couple it to AJs, disrupting this network impairs cell shape change and GBE, and Cno also helps maintain normal Baz and aPKC localization and planar-polarization.  We next explored the mechanisms by which Cno regulates GBE, actomyosin, and planar polarity.  We tested three hypotheses.  First, Cno might be essential for cell adhesion, as suggested for mammalian afadin (Takai *et al.*,2008).  Second, Cno might affect actomyosin.  Third, Cno might cooperate with Baz in this process.

To test the hypothesis that reduced adhesion explains the effects of Cno loss, we examined embryos with globally reduced cell adhesion.  We used embryos maternally/zygotically mutant for the strong allele, $arm^{043A01}$, which have severely reduced Arm function ($arm^{MZ}$; null *arm* alleles disrupt oogenesis; Peifer *et al.*,1993).  In $arm^{MZ}$ mutants, epithelial integrity is lost during late GBE, as cells lose adhesion to neighbors (Fig.8A vs. C).  In contrast, $cno^{MZ}$ mutants maintain epithelial integrity (Fig.8A vs. B; Sawyer *et al.*, 2009), suggesting any role of Cno in adhesion is less critical than that of Arm.  However, one can examine $arm^{MZ}$ mutants during early to mid-GBE, before the ectodermal epithelium disintegrates (Dawes-Hoang *et al.*,2005; Martin *et al.*,2010).

We explored whether globally reducing AJ function mimics the effects of Cno loss during early GBE, before $arm^{MZ}$ mutants lose epithelial integrity.  First we examined myosin cables at AP cell borders.  In $arm^{MZ}$, myosin planar polarity isn't altered (Fig.8L, Table 1), and initially myosin cables remain tightly associated with AJs on AP borders (Fig.8D, arrows), thus resembling WT (Fig.8E, arrows).  This contrasts with widespread

cable detachment at AP cell borders in $cno^{MZ}$ (Fig.8F, arrows). Myosin localized

normally to puncta at the center of some rosettes in $arm^{MZ}$ (Fig.8G, arrow). However, as

GBE progressed, while some groups of cells retained normal myosin localization

(Fig.8H, yellow arrows), myosin was preferentially disrupted at AP boundaries (Fig.8H,

blue arrows), as epithelia began to disintegrate (Fig.8C). Thus, strongly reducing AJ

function doesn't affect apical actomyosin anchoring as rapidly as does as Cno loss, but

ultimately disrupts myosin cables anchored at AJs.

We next examined localization of Cno, Baz, and aPKC in $arm^{MZ}$ (Arm and DEcad

levels are strongly reduced in $arm^{MZ}$, preventing examination; Dawes-Hoang *et al.*,2005;

Sawyer *et al.*,2009). Cno planar polarity isn't affected in $arm^{MZ}$ (Fig.8L; Table 1).

Interestingly, Baz localization also wasn't substantially altered during early GBE in

$arm^{MZ}$—Baz planar polarity remained unchanged (Fig.8L;Table 1), Baz was retained on

AP borders (Fig.8J'vs I', yellow arrows), and on DV borders Baz extended to vertices

(Fig.8J'vs I', arrowheads). This is in strong contrast with $cno^{MZ}$, where Baz was strongly

reduced on AP borders (Fig.8K,arrows) and was restricted to central DV borders

(Fig.8K,arrowheads). aPKC planar polarity was enhanced in $arm^{MZ}$ (Fig.8L; Table 1),

but this enhancement was substantially weaker than in $cno^{MZ}$ (Fig.8L; Table 1). In

contrast to $cno^{MZ}$ (Fig.8K"), aPKC was not restricted to central DV borders in $arm^{MZ}$

(Fig.8J"vs. I"). Thus globally reducing adhesion doesn't have the striking effects on Baz

and aPKC localization we saw in $cno^{MZ}$.

Globally reducing cell adhesion also doesn't mimic effects of Cno loss on cell

shape. Unlike $cno^{MZ}$, in which cell elongation along the AP axis is impaired, in early

GBE $arm^{MZ}$ cells elongated as much along the AP axis as WT (Suppl. Fig. 2B), and

*arm^{MZ}* cells have normal apical areas (Suppl.Fig.2D).  Unlike both *cno^{MZ}* and WT, *arm^{MZ}*

cells also elongated along the DV axis (Suppl.Fig.2B), perhaps because cells round-up as

adhesion fails.  Consistent with this, *arm^{MZ}* cells also have larger apical areas than WT or

*cno^{MZ}* before GBE (Suppl.Fig 2C), perhaps due to reduced apical tension (Martin *et al.*,

2010).  Thus, globally reducing adhesion alone does not phenocopy the changes in cell

shape or protein localization observed in *cno^{MZ}* mutants.  However, it remains possible

that in *cno^{MZ}* adhesion is reduced in a planar-polarized way along AP borders, and this

asymmetric loss of adhesion accounts for phenotypes observed in *cno^{MZ}*.

### *Globally reducing F-actin partially mimics Cno loss*

We next tested the hypothesis that Cno's primary role is to regulate apical

actomyosin, by disrupting actin with the actin-depolymerizing drug cytochalasinD

(cytoD) during early GBE.  DEcad and Baz become planar-polarized prematurely in

cytoD-treated embryos (Harris and Peifer, 2005).  In this study we examined the effects

of actin depolymerization in more detail, quantitating planar-polarization.  CytoD

strongly reduced cortical actin, as expected (Suppl. Fig.7A,B).  This, in turn, strongly

reduced cortical myosin (Suppl. Fig.7C vs. D,arrows), preventing assessment of its planar

polarity.  Like Cno loss (Fig.6N), however, CytoD treatment subtly enhanced DEcad and

Arm planar polarity (Suppl. Fig.7E'-H' yellow vs red arrowheads, Suppl. Fig.7K,Table

1;data not shown).  Strikingly, actin depolymerization also had effects similar to Cno loss

on Baz and aPKC planar polarity, increasing both (Suppl. Fig.7G" vs. H", I" vs. J";

yellow vs red arrowheads; Suppl. Fig.7K; Table 1).  CytoD-treatment made Baz

localization less continuous on DV borders; however, the obvious retraction of Baz and

aPKC from vertices seen in *cno^{MZ}* is not apparent.

Effects of actin depolymerization or Cno loss on cell shape change were also roughly similar. Both reduced AP cell elongation during early GBE (Suppl.Fig.2B)—in fact actin depolymerization had even more dramatic effects, with AP and DV borders remaining almost the same length. In addition, both actin depolymerization and Cno loss reduced apical area during early GBE relative to WT or DMSO-treated controls (Suppl.Fig.2D). Taken together, these results suggest that disrupting the cytoskeleton more closely mimics Cno loss than does global reduction in cell adhesion. However, global cytoskeletal disruption didn't precisely phenocopy Cno loss, perhaps because Cno preferentially regulates AJ:cytoskeleton connections along AP cell borders.

### cno and baz exhibit strong, dose-sensitive genetic interactions

We then tested the hypothesis that Cno cooperates with Baz during GBE. One method of assessing whether two proteins work in a common cell biological process is to look for dose-sensitive genetic interactions, in which lowering levels of one protein enhances effects of reducing levels of another. While maternal/zygotic *baz* mutants lose cell adhesion at gastrulation (Harris and Peifer,2004), zygotic *baz* mutants, which retain maternal Baz, maintain epithelial integrity past GBE, and >90% have only modest defects in integrity of the epidermal epithelium later, as revealed by holes in the cuticle secreted by the epidermis (Shao *et al.*,2010; Fig.9A,B). This phenotype is enhanced by 50% reduction (maternal/zygotic heterozygosity) of known Baz binding partners like DEcad, aPKC and Crumbs (Shao *et al.*,2010), demonstrating that phenotypic enhancement can indicate cooperation with Baz. *cno* is recessive, and thus flies with 50% reduced Cno levels (maternal/zygotic heterozygotes) are adult viable with no noticeable defects. We thus tested the hypothesis that Cno cooperates with Baz during GBE, by assessing

104

whether reducing Cno levels by 50% (using *cno* heterozygous mothers), modifies effects

of reducing Baz.  To do so, we crossed females heterozygous for both genes to WT

males; all progeny thus had reduced maternal levels of both proteins, and because *baz* is

on the X chromosome, 25% were zygotically *baz* mutant, while none were *cno* zygotic

mutants.  Reducing Cno levels strongly enhanced *baz*'s phenotype.  The fraction of

embryos with severe cuticular integrity defects (Fig.9C-E) increased from 5% in *baz*

mutants alone to 59% in *baz* mutants with reduced Cno levels (Fig.9F).  Thus *cno* and

*baz* exhibit strong dose-sensitive genetic interactions.

In contrast, reducing Cno levels didn't enhance the phenotype of zygotic myosin

heavy chain mutants (=*zipper*); there was no change in severity of *zipper's* cuticle

phenotype (32% mild/68% severe defects versus 35% mild/65% severe defects).

However, absence of a dose-sensitive interaction is not evidence for or against a

functional relationship, as it depends on relative levels of maternal and zygotic gene

product.

To explore the cell biological mechanisms by which this *baz cno* genetic

interaction affects development, we compared morphogenesis in *baz* zygotic mutants

versus *baz* mutants with reduced Cno levels, generated using the cross outlined above.  In

*baz* mutants, epidermal AJs remain largely intact through the extended germband stage

(Shao *et al.*,2010; Fig.9G vs. L).  Reducing Cno levels promoted earlier disruption of

AJs; 21% of extended germband embryos had moderate to strong AJ disruption

(n=66;Fig.9H,I, arrowheads) vs. 8% of *baz* mutants (n=63).  Most strikingly, 47% of *baz*

mutants with reduced Cno levels had a partially open ventral furrow (Fig.9I-K; n=49),

suggesting a possible failure of apical constriction.  This phenotype was never observed

in *baz* mutants (n=27), but is characteristic of *cno^MZ* mutants (Sawyer *et al.,* 2009). Thus *baz* and *cno* exhibit strong, dose-sensitive genetic interactions from gastrulation onward, consistent with the two proteins cooperating in the same process.

**Discussion**

Coordinating adhesion and the cytoskeleton is essential for morphogenesis. Recent work on apical constriction provides a model of how cell shape change is coupled to actomyosin contractility. Our data suggest that coupling AJs to a contractile apical actomyosin cytoskeleton plays an important role in a very different cell movement: convergent-extension during *Drosophila* GBE. We identified a novel cell shape change, AP cell elongation, which contributes to WT GBE. Further, we found that Cno is required for maintaining attachment of the apical actomyosin network AJs in a planar-polarized way. Disrupting this connection results in failure of GBE and prevents coordination of apical myosin contractility and cell shape change. Our data are consistent with a model in which Cno tightly couples apical actomyosin to AP AJs and coordinates apical polarity proteins with the network, helping integrate individual cell shape changes across the tissue.

*A dynamic apical actomyosin network as a general feature of cell intercalation*

Previous studies illustrated how an apical contractile actomyosin network powers apical constriction (reviewed in Sawyer *et al.*,2010). In contrast, convergent-extension during *Drosophila* GBE was thought to involve planar-polarized enhancement of contractile actomyosin cables, driving cell intercalation and body elongation (Zallen and Blankenship, 2008). We were surprised to find that, in addition to junctional cables, germband cells also have an apical actomyosin network that undergoes cyclical

106

constriction and relaxation. This coincides with and may help drive cell shape change. The asymmetric cue of planar-polarized myosin is likely to impose asymmetry. Together, asymmetric cortical myosin and cyclical contractions may help extend cells in one-dimension, instead of shrinking them in all dimensions, thus contributing to tissue elongation. While our manuscript was being revised, Lecuit's and Zallen's labs independently discovered and described the apical network—the Lecuit lab data further suggest myosin condensations preferentially move toward AP borders, helping drive cell rearrangement (Rauzi *et al.*,2010; Fernandez-Gonzalez and Zallen, in press). Both our data on Cno and the Lecuit lab's data on α-catenin further suggest that different proteins linking this apical network to AJs are critical for the fidelity and coupling of apical myosin contraction to cell shape change.

We also identified a novel cell shape change that may help drive AP body axis extension—AP cell elongation. Cno and presumably linkage of the apical actomyosin network to AJs are important for this cell shape change. One speculative possibility is that an asymmetric ratchet acts in germband cells, selectively preventing elongation along the DV body axis while allowing cell elongation along the AP body axis. It is also possible that outside forces, such as shape changes of the first cells to divide, help reshape ectodermal cells, but we think this is less likely as we examined cell shapes during early GBE before germband mitotic domains divide. Ratchets have also been proposed during mesoderm invagination (Martin *et al.*,2009) and during dorsal closure, where amnioserosal cells apically constrict (Solon, *et al.*,2009). Prior to dorsal closure onset, amnioserosal cells have periodic apical actomyosin contractions, but cells only retain changes in shape after a junctional actomyosin purse string appears. Disrupting the

purse string disrupts dorsal closure, suggesting a junctional actomyosin cable can act as a ratchet.

Studies in *Xenopus* suggest that the role of a dynamic, planar-polarized apical actomyosin network in convergent-extension is conserved (Skoglund *et al.*,2008; Kim and Davidson,2011). Myosin organizes actin into dynamic foci that move within intercalating cells along their mediolateral axis. In myosin's absence, actin foci are lost and convergent-extension is disrupted. Thus dynamic actomyosin foci may play a conserved role in convergent-extension.

It will be interesting to identify regulators shaping contractile activity in different tissues. Jak/Stat signaling restricts apical constriction to the mesoderm (Bertet *et al.*,2009); in its absence apical myosin accumulates in the ectoderm and those cells inappropriately apically constrict. Thus although both mesoderm and ectoderm share an apical contractile network, its regulation is tuned differently. Further, different actin regulators regulate apical and junctional myosin, with Wasp regulating the apical pool.

### Cno: one of several important players linking AJs to actin during gastrulation

Linking AJs to actin is key in diverse processes from adhesion itself to morphogenetic movements as different as apical constriction and collective cell migration (Gates and Peifer, 2005). Cno regulates linkage during mesoderm apical constriction, but isn't required for cell adhesion (Sawyer *et al.*,2009). Other AJ-actin linkers act in other contexts (e.g., Abe and Takeichi,2008; Cavey *et al.*,2008), suggesting cells use distinct linkers in circumstances with different force regimes. Our data suggest that during GBE, Cno regulates AJ:actomyosin network connections, acting specifically along AP borders. Core AJ proteins are more reduced on AP borders in $cno^{MZ}$ mutants than in WT. In WT,

108

slightly reducing AJ proteins on AP borders may facilitate shrinkage of these borders during GBE. It is tempting to speculate that Cno enhancement along AP borders provides extra support when DEcad/Arm are reduced, strengthening AJ-actomyosin linkages along AP borders, yet still allowing cell shape change. In this model, when Cno is absent, AJ-actomyosin linkage is weakened at AP borders, leading to inefficient cell shape change, impairing GBE, and accentuating reduction of AJ proteins.

Our data further suggest Cno isn't the only AJ:actomyosin linker during GBE. While the actomyosin network detaches from AJs in $cno^{MZ}$, it doesn't collapse into a ball; instead cables remain 0.2-0.5μm distant from AJs. A second connection is also supported by the appearance of apical strands of DEcad stretching from the cortex to detached myosin in $cno^{MZ}$. It will be interesting to determine what proteins compose these other AJ:actomyosin links. α-catenin regulates actin:AJ linkage just prior to this stage (Cavey *et al.*,2008), and also plays a role in GBE (Rauzi *et al.*, 2010), although how α-catenin mediates linkage remains mysterious.

### *Coordinating actomyosin and apical polarity proteins: a conserved contractility modulator?*

Both myosin and Baz/Par3 are important GBE regulators (Bertet *et al.*,2004; Zallen and Wieschaus, 2004). One of the most surprising consequences of Cno loss was dramatic change in Baz and aPKC localization. Their strong reduction along AP borders and restricted localization along DV borders correlates well with altered localization of apical actomyosin, which detached from AP AJs and retracted along DV borders from vertices. These data suggest coordination of the actomyosin network and Baz/aPKC facilitates efficient cell shape change. Consistent with this, an interesting recent paper

demonstrated that Baz is required for reciprocal planar-polarized distribution of myosin and AJs. Baz localization, in turn, is restricted by the cytoskeletal regulator Rho-kinase (Rok), leaving Baz enriched at DV borders (Simoes Sde *et al.*,2010). This suggests a complex network of interactions.

In *C. elegans* a contractile actomyosin cytoskeleton positions apical-polarity proteins (PAR3/PAR6/aPKC) anteriorly in one-cell embryos, and this complex then alters the actomyosin network, promoting asymmetric cortical flow to maintain anterior and posterior domains (Munro *et al.*, 2004). It is tempting to speculate that the germband contractile actomyosin network plays a similar role. In this model, planar-polarization of the network would create a symmetry break (Bertet *et al.*,2004; Blankenship *et al.*,2006; Simoes Sde *et al.*,2010), helping trigger Baz/aPKC planar-polarization. They, in turn may feedback to modulate actomyosin contractility, driving GBE. Strengthening AJ-actomyosin linkages via Cno could help ensure efficient cell shape changes that are integrated across the tissue.

Several mechanistic hypotheses are consistent with our data, which aren't mutually exclusive. First, Cno may directly affect Baz/aPKC localization during assembly or maintenance, working in parallel or in series with Rok (Simoes Sde *et al.*,2010), with actomyosin positioning and contractility then modulated by Baz/aPKC. Consistent with this, previous work revealed that Baz remains apical in the absence of AJs; residual epithelial cells retain polarized actin but have hyperconstricted apical ends (Harris and Peifer,2004). Further, PAR proteins regulate actomyosin contractility during DC (David *et al.*, 2010). Second, Cno could alter the actomyosin network, which in turn may affect proper Baz/aPKC localization. Baz apical positioning requires the actin

cytoskeleton (Harris and Peifer,2005). We found actin disruption and Cno loss alter Baz localization similarly, consistent with this hypothesis. Finally, Baz/aPKC may mediate Cno apical positioning, as Baz does for AJs (Harris and Peifer,2004). Of course, more complex interplay with feedback between actomyosin and Baz/aPKC seems likely, creating a network of interactions rather than a linear pathway. Teasing out the complex coordination of AJs, apical polarity protein, and the actomyosin network during morphogenesis is an exciting challenge.

**Acknowledgements**

**Materials and Methods**

*Flies*

Mutations/fly stocks are described at flybase.bio.indiana.edu and Suppl.Table 4. WT=yellow white. Experiments done at 25°C unless noted. cno germline clones were made by heat-shocking 48-72h hsFLP[1]; FRT82Bcno[R2]/FRT82Bovo[D1-18] larvae 3h at 37°C. arm[043A01] germline clones were generated similarly.

*Microscopy*

Antibodies are in Suppl.Table 4. Embryo fixation, preparation, and drug treatments as in Sawyer et al.,(2009). For SEM, embryos were dechorionated with 50%bleach, fixed 5 min in 37%formaldehyde, hand-devitillinized, post-fixed in

2.5%gluteraldehyde:0.1M Cacodylate, specimens prepared by UNC's Microscopy

Services Laboratory, and imaged on a Zeiss Supra25FieldEmissions Scope. Fixed

samples were imaged with a LSM510, a Zeiss 40X-Plan-Neofluar-NA1.3 oil immersion

objective, and LSM software. Live imaging was performed with a Perkin-

ElmerUltraVIEW spinning disc confocal, ORCA-ER camera, Nikon-60X-PlanApo-

NA1.4 or 100X-PlanApoVC-NA1.4 objectives, and Metamorph. 4-D DIC imaging used

a Diagnostic Instruments SPOT2 camera and NikonEclipse800 microscope with a 20X-

Nikon Plan-Fluor-DICM-infinite-NA0.5 objective. 11μm optical sections were acquired

every 2 min for 5h and analyzed with Metamorph. In Adobe PhotoshopCS2 we adjusted

input levels so the main range of signals spanned the entire output grayscale and adjusted

brightness and contrast.

*Quantification of planar polarity and cell shape change*

Stacks from Stage7-early stage8 embryos were acquired with a Zeiss40X-Plan-

Neofluar-NA1.3 oil immersion objective, zoom 2. Mean fluorescence intensities of all

borders (zoom 300%) were measured with ImageJ's line tool (line width=3). To ensure

the entire border was measured, stacks of 4 planes, 0.5μm apart were used, and

measurements were averaged to obtain border value, with background (measured

similarly, but in the cytoplasm) subtracted to obtain the final value. Borders were sorted

by angles (relative to embryo DV axis). AP borders=0-29°. DV=60-90°. Ratios from 5

embryos from ≥2 experiments were averaged. Cell border lengths and areas were

similarly measured.

*Automated analysis of apical myosin accumulation and cell area*

To obtain the data analyzed in Fig. 3, time-lapse images of DEcad-GFP were first processed using NIH-ImageJ software in the following steps: 1) image background was first subtracted by the rolling ball algorithm function with a radius of 50. 2) remaining background noise and irrelevant dim particles were further subtracted by direct subtraction. 3) the resulting images were filtered by a Gaussian blur filter with radius of 3-4 pixels and segmented by watershed segmentation plug-in. 4) segmented images were corrected manually based on the original images. The segmented images were analyzed by MATLAB (MathWork) to track each cells, measure cell area and calculate average Sqh-mCherry intensity within the area. To analyze changes over time, time series data of cell area and average Sqh-mCherry intensity were first smoothed by a Gaussian filter with a width of 5 data points in MATLAB software, and intervals between neighboring peaks were calculated. For area reduction, because we were interested in cell constriction, the inverse of the changes was used. The correlation coefficient was calculated with time offsets from -200 to +200 sec as previously described (He et.al., 2010). The heat-map was constructed by correlations of different individual cells with coefficients coded in rainbow color. Two-side t-test with unequal variance was conducted in Microsoft Excel. All error bars are standard deviation of the mean (s.d.m.).

# References

Abe, K. and Takeichi, M. (2008). EPLIN mediates linkage of the cadherin catenin complex to F-actin and stabilizes the circumferential actin belt. Proc Natl Acad Sci U S A 105, 13-9.

Bertet, C., Rauzi, M. and Lecuit, T. (2009). Repression of Wasp by JAK/STAT signalling inhibits medial actomyosin network assembly and apical cell constriction in intercalating epithelial cells. Development 136, 4199-212.

Bertet, C., Sulak, L. and Lecuit, T. (2004). Myosin-dependent junction remodelling controls planar cell intercalation and axis elongation. Nature 429, 667-71.

Blankenship, J. T., Backovic, S. T., Sanny, J. S., Weitz, O. and Zallen, J. A. (2006). Multicellular rosette formation links planar cell polarity to tissue morphogenesis. Dev Cell 11, 459-70.

Butler, L. C., Blanchard, G. B., Kabla, A. J., Lawrence, N. J., Welchman, D. P., Mahadevan, L., Adams, R. J. and Sanson, B. (2009). Cell shape changes indicate a role for extrinsic tensile forces in Drosophila germ-band extension. Nat Cell Biol 11, 859-64.

Cavey, M., Rauzi, M., Lenne, P. F. and Lecuit, T. (2008). A two-tiered mechanism for stabilization and immobilization of E-cadherin. Nature 453, 751-6.

da Silva, S. M. and Vincent, J. P. (2007). Oriented cell divisions in the extending germband of Drosophila. Development 134, 3049-54.

David, D. J., Tishkina, A. and Harris, T. J. (2010). The PAR complex regulates pulsed actomyosin contractions during amnioserosa apical constriction in Drosophila. Development 137, 1645-55.

Dawes-Hoang, R. E., Parmar, K. M., Christiansen, A. E., Phelps, C. B., Brand, A. H. and Wieschaus, E. F. (2005). folded gastrulation, cell shape change and the control of myosin localization. Development 132, 4165-78.

Drees, F., Pokutta, S., Yamada, S., Nelson, W. J. and Weis, W. I. (2005). α-Catenin is a Molecular Switch that Binds E-cadherin/ß-Catenin and Regulates Actin-Filament Assembly. Cell 123, 903-915.

Fernandez-Gonzalez, R., Simoes Sde, M., Roper, J. C., Eaton, S. and Zallen, J. A. (2009). Myosin II dynamics are regulated by tension in intercalating cells. Dev Cell 17, 736-43.

Fernandez-Gonzalez, R. and Zallen, J. A. (2011). Oscillatory behaviors and hierarchical assembly of contractile structures in intercalating cells. Physical Biology, in press.

Gates, J. and Peifer, M. (2005). Can 1000 reviews be wrong? Actin, alpha-Catenin, and adherens junctions. Cell 123, 769-72.

Harris, T. J. and Peifer, M. (2004). Adherens junction-dependent and -independent steps in the establishment of epithelial cell polarity in Drosophila. J Cell Biol 167, 135-47.

Harris, T. J. and Peifer, M. (2005). The positioning and segregation of apical cues during epithelial polarity establishment in Drosophila. J Cell Biol 170, 813-23.

Harris, T. J. and Peifer, M. (2007). aPKC controls microtubule organization to balance adherens junction symmetry and planar polarity during development. Dev Cell 12, 727-38.

Harris, T. J., Sawyer, J. K. and Peifer, M. (2009). How the cytoskeleton helps build the embryonic body plan: models of morphogenesis from Drosophila. Curr Top Dev Biol 89, 55-85.

He, L., Wang, X., Tang, H.L., and Montell, D.J. (2010). Tissue elongation requires oscillating contractions of a basal actomyosin network. Nat Cell Biol 12, 1133-1142.

Irvine, K. D. and Wieschaus, E. (1994). Cell intercalation during Drosophila germband extension and its regulation by pair-rule segmentation genes. Development 120, 827-41.

Kim, H. Y. and Davidson, L. A. (2011). Punctuated actin contractions during convergent extension and their permissive regulation by the non-canonical Wnt-signaling pathway. J Cell Sci 124, 635-46.

Martin, A. C., Gelbart, M., Fernandez-Gonzalez, R., Kaschube, M. and Wieschaus, E. F. (2010). Integration of contractile forces during tissue invagination. J Cell Biol 188, 735-49.

Martin, A. C., Kaschube, M. and Wieschaus, E. F. (2009). Pulsed contractions of an actin-myosin network drive apical constriction. Nature 457, 495-9.

Munro, E., Nance, J. and Priess, J. R. (2004). Cortical flows powered by asymmetrical contraction transport PAR proteins to establish and maintain anterior-posterior polarity in the early C. elegans embryo. Dev Cell 7, 413-24.

Peifer, M., Orsulic, S., Sweeton, D. and Wieschaus, E. (1993). A role for the *Drosophila* segment polarity gene *armadillo* in cell adhesion and cytoskeletal integrity during oogenesis. Development 118, 1191-1207.

Rauzi, M., Lenne, P. F. and Lecuit, T. (2010). Planar polarized actomyosin contractile flows control epithelial junction remodelling. Nature 468, 1110-4.

Rauzi, M., Verant, P., Lecuit, T. and Lenne, P. F. (2008). Nature and anisotropy of cortical forces orienting Drosophila tissue morphogenesis. Nat Cell Biol 10, 1401-10.

Sawyer, J. K., Harris, N. J., Slep, K. C., Gaul, U. and Peifer, M. (2009). The Drosophila afadin homologue Canoe regulates linkage of the actin cytoskeleton to adherens junctions during apical constriction. J Cell Biol 186, 57-73.

Sawyer, J. M., Harrell, J. R., Shemer, G., Sullivan-Brown, J., Roh-Johnson, M. and Goldstein, B. (2010). Apical constriction: a cell shape change that can drive morphogenesis. Dev Biol 341, 5-19.

Shao, W., Wu, J., Chen, J., Lee, D. M., Tishkina, A. and Harris, T. J. (2010). A modifier screen for Bazooka/PAR-3 interacting genes in the Drosophila embryo epithelium. PLoS One 5, e9938.

Simoes Sde, M., Blankenship, J. T., Weitz, O., Farrell, D. L., Tamada, M., Fernandez-Gonzalez, R. and Zallen, J. A. (2010). Rho-kinase directs Bazooka/Par-3 planar polarity during Drosophila axis elongation. Dev Cell 19, 377-88.

Skoglund, P., Rolo, A., Chen, X., Gumbiner, B. M. and Keller, R. (2008). Convergence and extension at gastrulation require a myosin IIB-dependent cortical actin network. Development 135, 2435-44.

Solon, J., Kaya-Copur, A., Colombelli, J. and Brunner, D. (2009). Pulsed forces timed by a ratchet-like mechanism drive directed tissue movement during dorsal closure. Cell 137, 1331-42.

Takai, Y., Ikeda, W., Ogita, H. and Rikitake, Y. (2008). The immunoglobulin-like cell adhesion molecule nectin and its associated protein afadin. Annu Rev Cell Dev Biol 24, 309-42.

Tepass, U., Gruszynski-DeFeo, E., Haag, T. A., Omatyar, L., Török, T. and Hartenstein, V. (1996). *shotgun* encodes *Drosophila* E-cadherin and is preferentially required during cell rearrangement in the neurectoderm and other morphogenetically active epithelia. Genes Dev 10, 672-685.

Yamada, S., Pokutta, S., Drees, F., Weis, W. I. and Nelson, W. J. (2005). Deconstructing the Cadherin–Catenin–Actin Complex. Cell 123, 889-901.

Yin, C., Ciruna, B. and Solnica-Krezel, L. (2009). Convergence and extension movements during vertebrate gastrulation. Curr Top Dev Biol 89, 163-92.

Zallen, J. A. and Blankenship, J. T. (2008). Multicellular dynamics during epithelial elongation. Semin Cell Dev Biol 19, 263-70.

Zallen, J. A. and Wieschaus, E. (2004). Patterned gene expression directs bipolar planar polarity in Drosophila. Dev Cell 6, 343-55.

Zallen, J. A. and Zallen, R. (2004). Cell-pattern disordering during convergent extension in *Drosophila*. J Phys: Condes Matter 16, S5073-S5080.
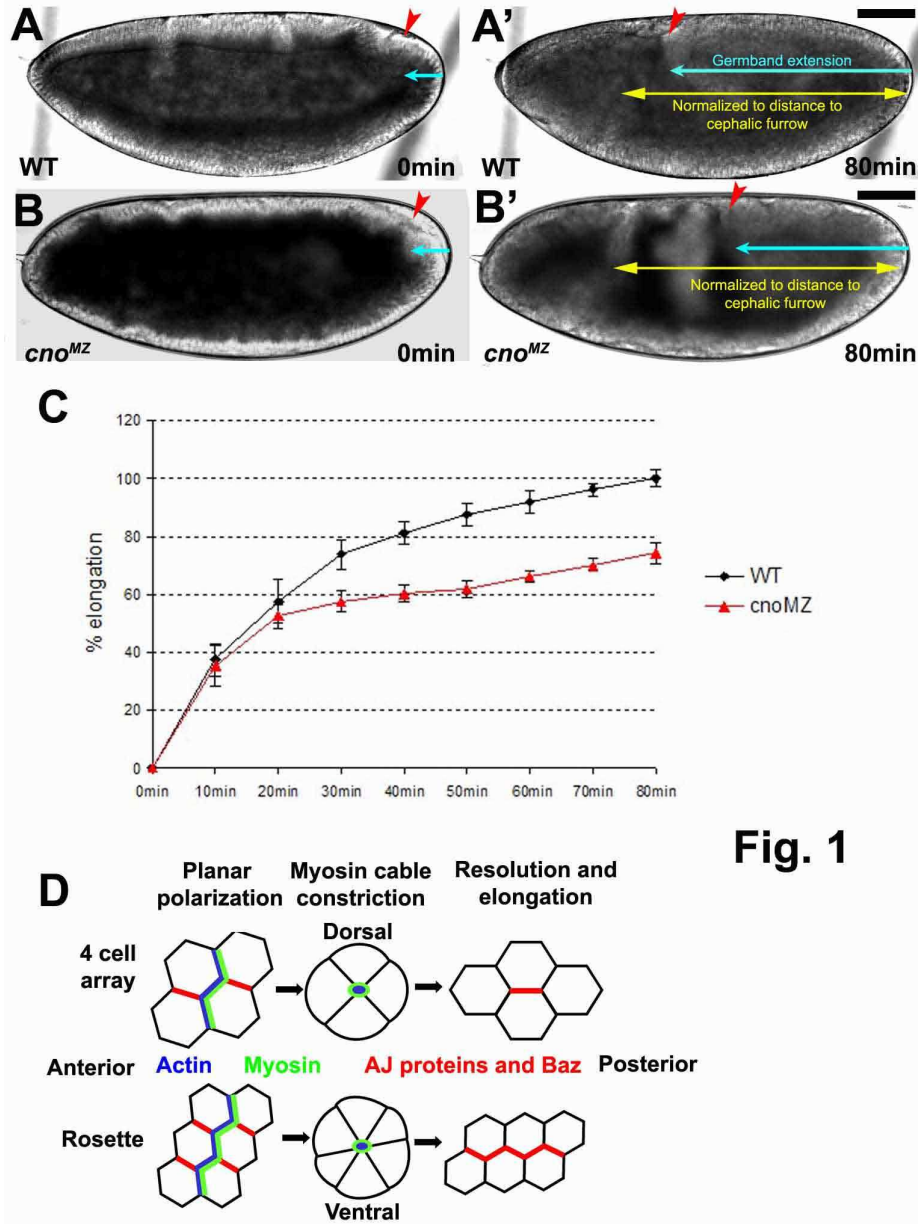
**Figure 3.1. Cno loss disrupts GBE.** A,B. Embryos, anterior left. A,A' Stills from a movie of WT. embryo. A. t=0. The onset of GBE, as marked by appearance of the cephalic furrow. A'. t=80min, GBE is complete. Red arrow=end of germband. Yellow line=total length from cephalic furrow to posterior. Blue line=elongated germband. Note that in 80 min the end of germband extends from the posterior end of the egg up around the dorsal surface to a position above and just behind the head. B. $cno^{MZ}$, onset of GBE. B'. $cno^{MZ}$, 80min. GBE does not go to completion--note position of end of germband (red arrow). C. GBE slows and does not go to completion in $cno^{MZ}$ mutants. Degree of extension was normalized to embryo size using the ratio of the length of the posterior portion of the germband to the total distance from cephalic furrow to posterior end; WT extends 84% of this distance. In this chart, full WT GBE was thus set at 100%. WT, N=8. $cno^{MZ}$, N=6. Error bars=s.d. Bars=20μm. D. Diagram illustrating planar-polarization and cell intercalation in WT. Actin and myosin are enriched at AP borders and AJ proteins and Baz enriched at DV borders. Contraction of myosin cables is thought to drive cell intercalation.

118
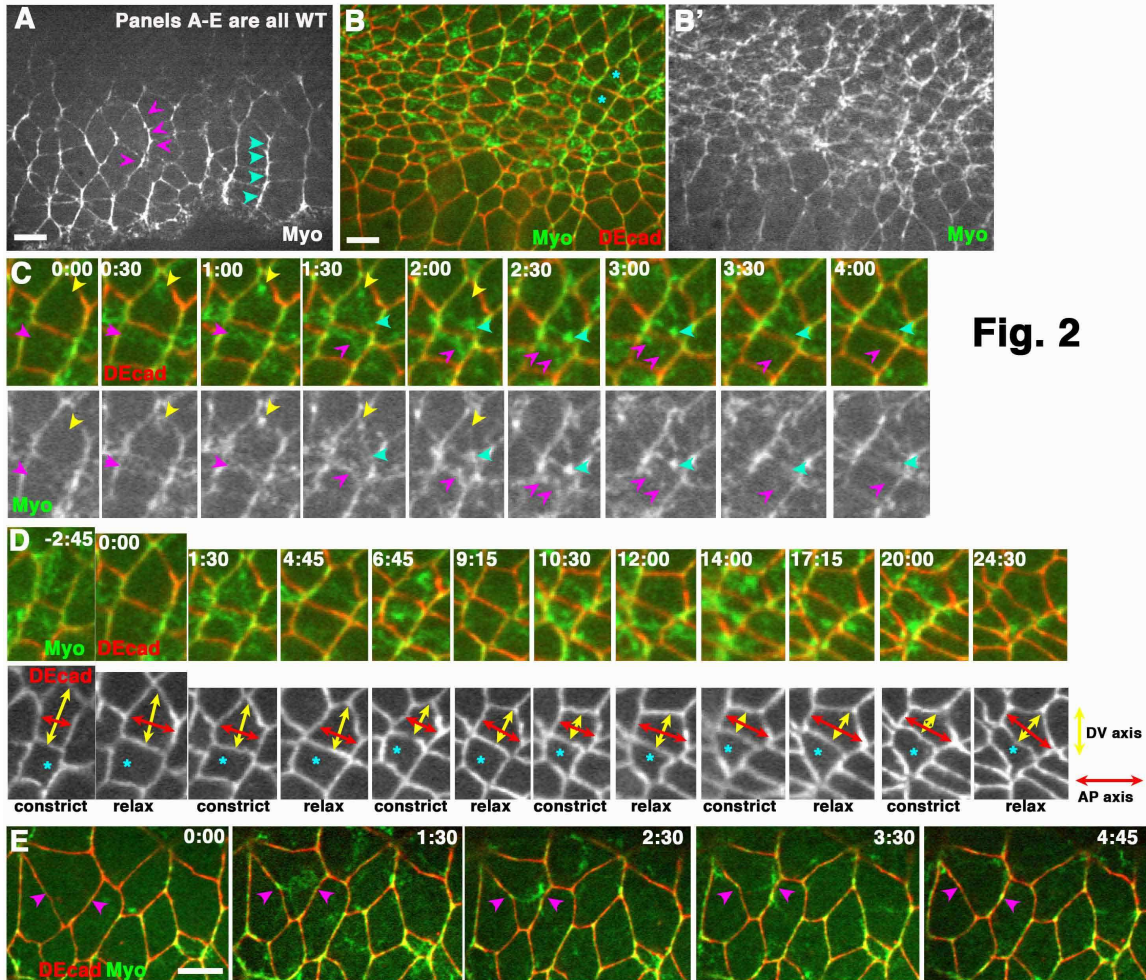
**Figure 3.2. An apical contractile actomyosin network and cell shape change during GBE.**
WT embryos expressing DEcad-GFP and myosin light chain-mCherry(=Spaghetti-squash (sqh)), stage 7 . In all Figures, unless noted embryos are anterior left, dorsal up, antigens and genotypes indicated. A. Arrowheads=myosin cables at AJs. B. Apical view, contractile actomyosin network (asterisks=cells in C,D). C-E. Movie stills, time=Minutes:seconds. C,D. Single pair of cells. C. Arrowheads=myosin condensations forming and dissipating. D. Multiple cycles of contraction and relaxation coincide with progressive elongation of cells along the AP body axis (red arrows). E. Myosin cable forms and constricts cell (arrowheads). Bars=5μm.
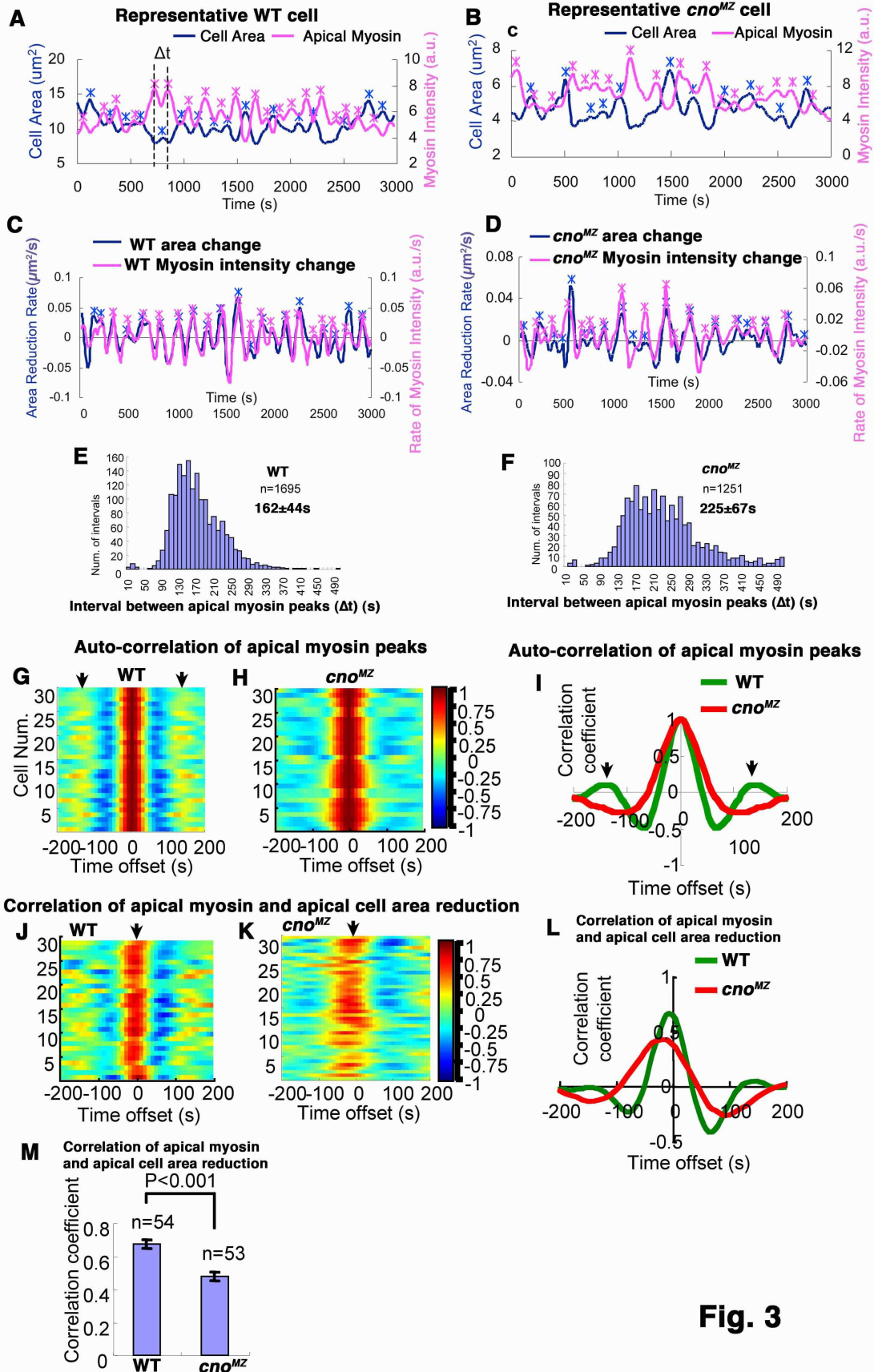
**Fig. 3**

**Figure 3.3. Automated analysis reveals correlated apical myosin accumulation and cell constriction in WT, and a reduced correlation in *cno^{MZ}* mutants.** A,B. Cells undergo periodic changes in apical myosin accumulation and cell area. Cell surface area (blue line) and apical myosin intensity (Sqh-mCherry intensity; pink line) of one representative WT (A) or *cno^{MZ}* (B) cell over time. Asterisks=positions of peaks recognized by MATLAB. Δt=time interval between neighboring peaks. C,D. Rate of change of apical cell area (blue line) and apical myosin intensity (pink line). These are the same cells analyzed in panels A and B. E,F. Histograms, time intervals between neighboring apical myosin peaks in WT(E) and *cno^{MZ}*(F). In *cno^{MZ}* the time between peaks lengthens and the regularity of peaks diminishes. G,H. Auto-correlation coefficient of the rate of apical myosin intensity changes in WT (G) and *cno^{MZ}* mutant (H). Each row shows the correlation from a different cell as a function of time offsets from -200s to 200s. The correlation coefficient from -1 to 1 was color-coded according to the scale on the left color bar. I. Averaged auto-correlation coefficients of apical myosin intensity from 54 WT cells (green line) and 53 *cno^{MZ}* mutant cells (red line) plotted with different time offsets. The curve of WT cells showed clear peaks around +/- 150s (arrows) which were lost in *cno^{MZ}*. This result suggests periodic activity in WT is more regular than in *cno^{MZ}* mutants, which is consistent with the broader distribution of Δt in *cno^{MZ}*. J,K. Correlation coefficients between cell surface area reduction and the rate of apical myosin intensity change in WT (J) and *cno^{MZ}* (K). Each row shows the correlation from a different cell as a function of various time offsets. I. Averaged correlation coefficients between cell area reduction and apical myosin intensity change from 54 WT cells (green line) and 53 *cno^{MZ}* cells (red line). Both showed a negative shift (-6.5s for WT and -17.5s for *cno^{MZ}*), suggesting that in both situations myosin changes preceded the cell area activity. The increased time shift between myosin and cell area in *cno^{MZ}* might be a consequence of weakened mechanical linkage. J. The average maximum correlation coefficients between area reduction and apical myosin intensity change of WT and *cno^{MZ}* plotted in a bar graph for comparison. p-value was calculated by Student's t-test. Reduction of the maximum correlation coefficient suggested Cno loss weakened linkage between cell area dynamics and myosin activity.
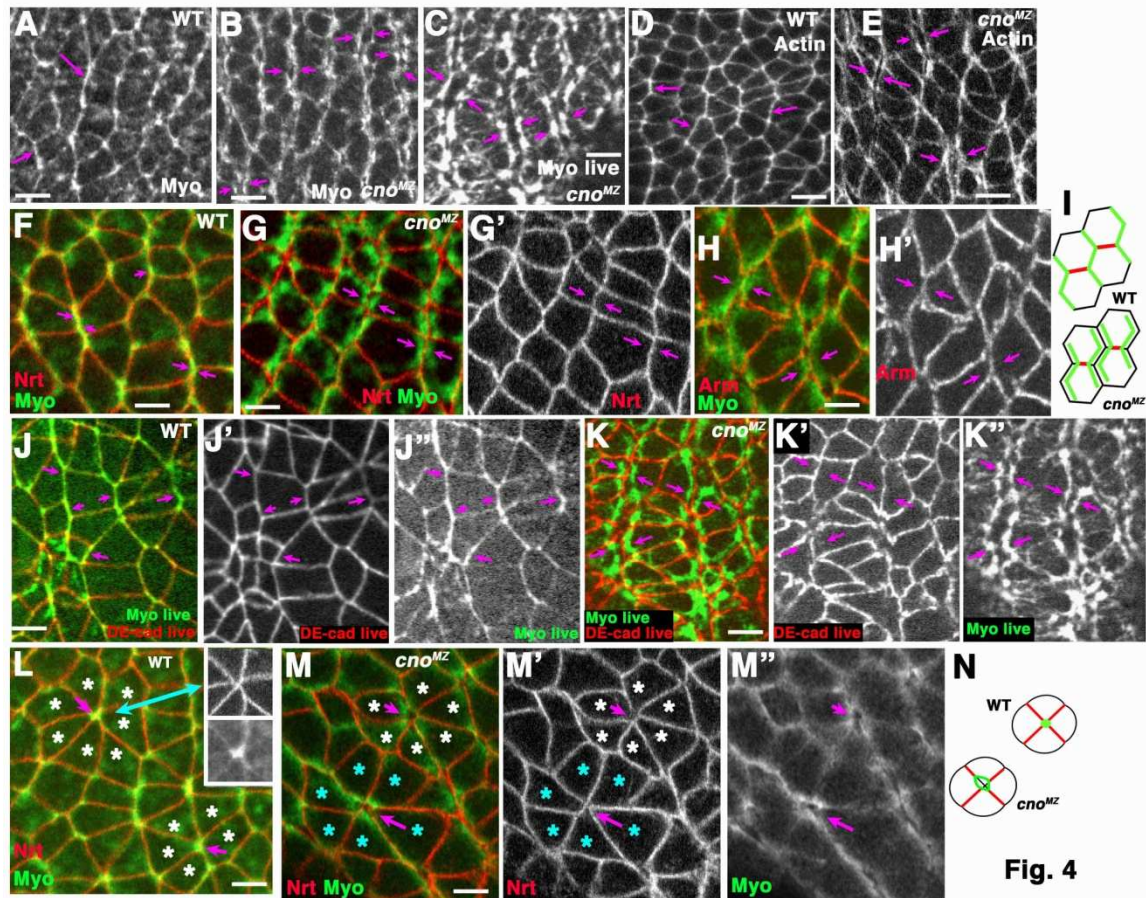
**Figure 3.4. Cno loss leads to planar-polarized detachment of the apical actomyosin network.** Embryos, stage7. A-C. Fixed(A,B) or live(C) embryos. Contrast the single myosin cable on AP borders in WT (A,arrows) with the detached cables on AP borders in *cno^MZ* (B,C,arrows). D,E. Cortical actin (D,arrows) is also detached at some AP borders in *cno^MZ* (E,arrows). F-K. WT myosin cables co-localize with Nrt (F,arrows) and DEcad (J) at cell borders. In *cno^MZ* Nrt (G,arrows), Arm (H,arrows), and DEcad (K,arrows) localize between detached myosin cables. L-N. In WT, myosin localizes to rosette vertices (L, arrows=vertices, asterisks=cells in rosettes), while in *cno^MZ* myosin localizes in rings around vertices (M,arrows). I and N illustrate these changes diagrammatically. Bars=5μm.

122
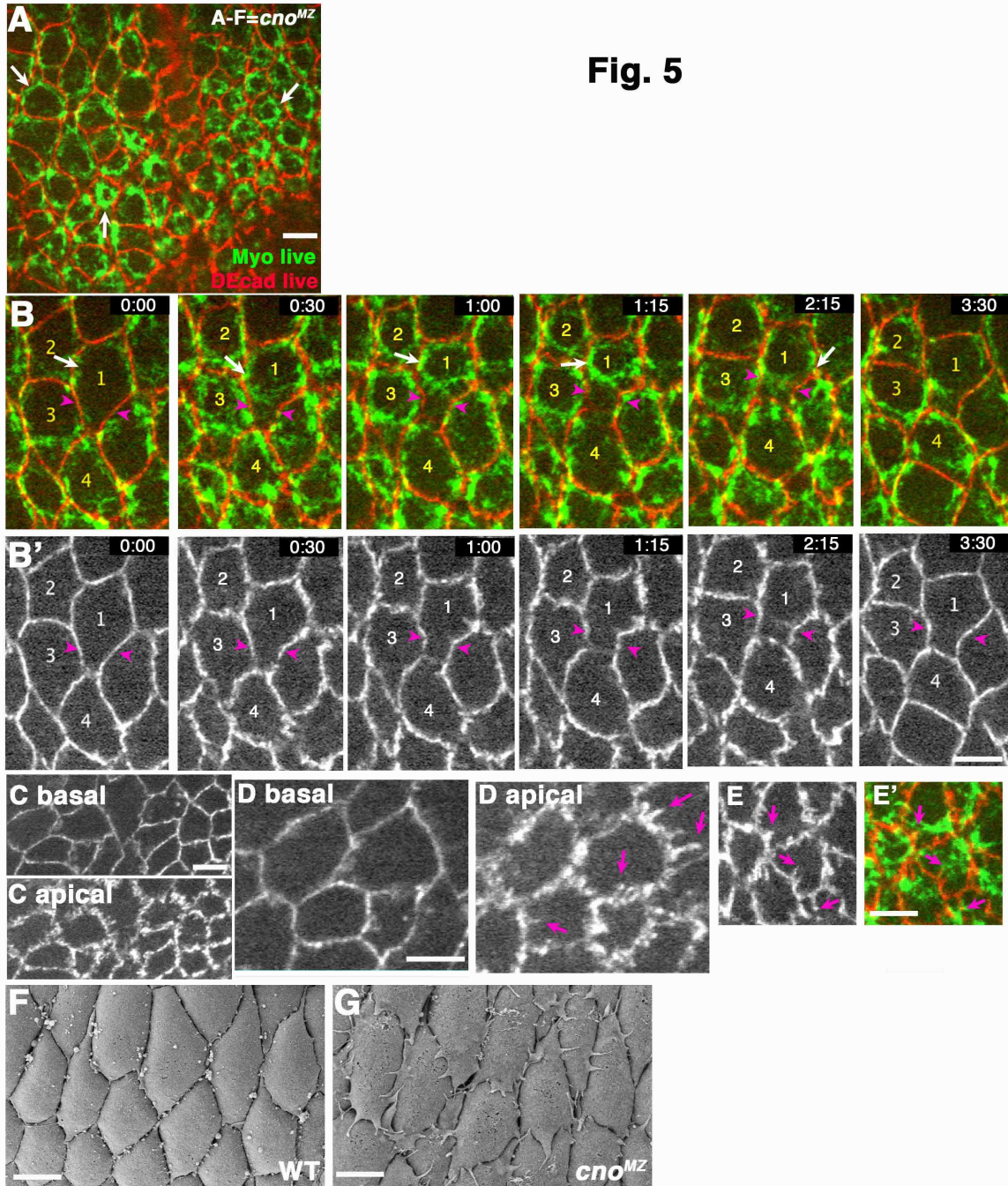
**Figure 3.5. After Cno loss, apical actomyosin retains connections with AJs in the ectoderm.**
A-E. *cno^MZ*, DEcad-GFP and Myosin(Sqh)-mCherry. Lateral ectoderm soon after mesoderm invagination. A. Myosin rings detach from AJs but do not constrict to balls (arrows), in contrast to the mesoderm. B. Movie stills from movie 4—time=minutes:seconds. Myosin rings appear and disappear (B, afrrows). Cells 1-3 constrict and then relax (e.g. B', arrowheads) while cell 4 relaxes. C,D. Apical and more basolateral sections of lateral ectoderm in *cno^MZ* mutants Apically DEcad-containing membrane is stretched into strands (D, arrows), while 1µm basally it is more continuous. E. Strands are often embedded in myosin rings (arrows). F,G. SEM also reveals membrane-strands in *cno^MZ* (G) which are not observed in WT (F). Bars=5µm.

123
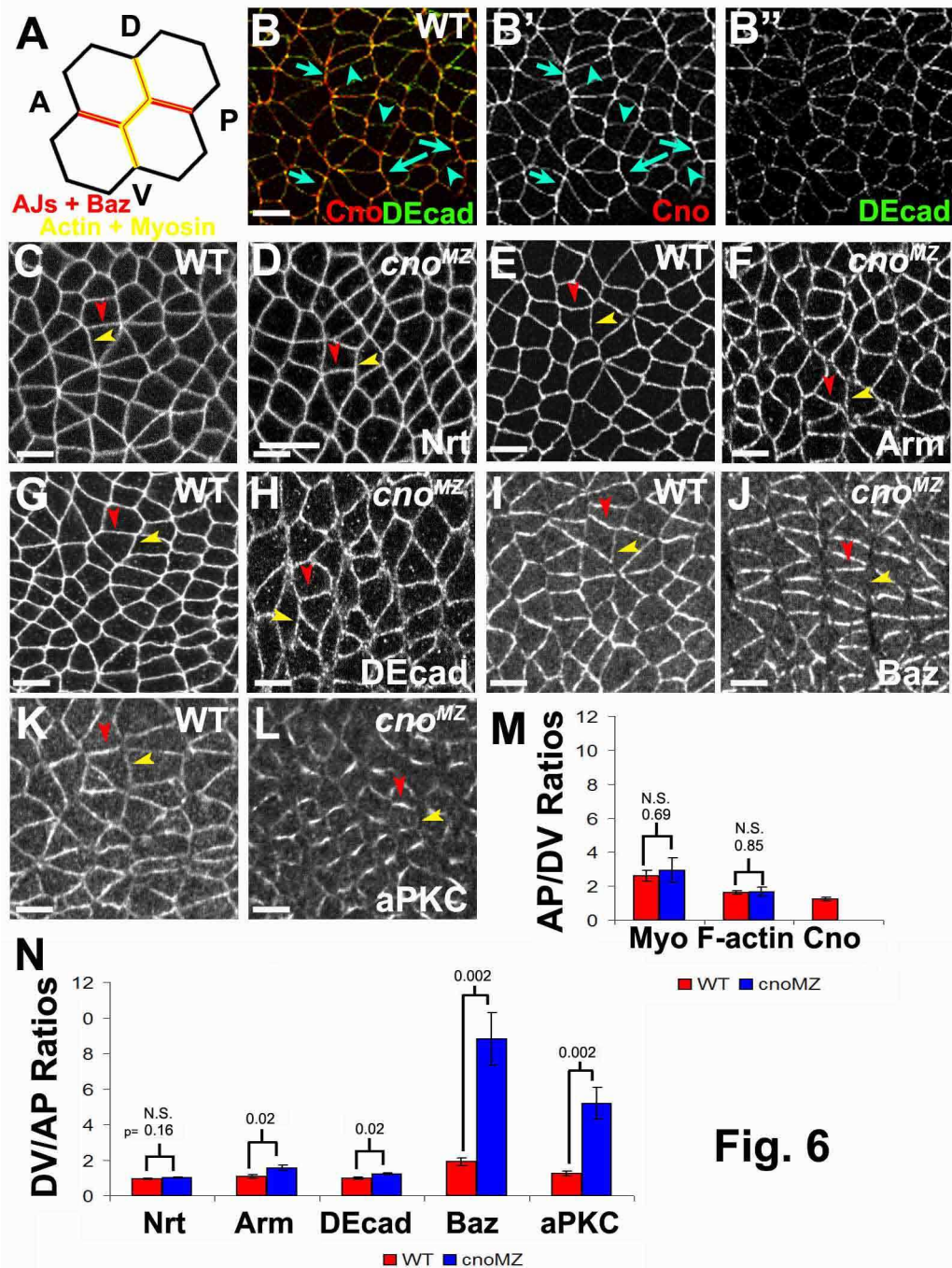
**Figure 3.6. Cno loss doesn't affect cytoskeletal planar polarity but enhances planar polarity of AJ and apical polarity proteins.** A. Diagram, actin/myosin are enriched on AP borders (yellow) and junctional proteins are enriched on DV borders (red). B-L. Stage7. B. Cno is enriched on AP (arrows) relative to DV borders (arrowheads). C-L. Planar polarity, WT versus *cno^{MZ}*. Red arrowheads=DV borders. Yellow arrowheads=AP borders. C,D. Nrt isn't planar-polarized in either genotype. E-H. Cno loss subtly enhances Arm and DEcad planar polarity. I-L. Cno loss dramatically accentuates Baz and aPKC planar polarity. Bars=5μm. M,N. Quantitation of planar polarity in *cno^{MZ}* mutants versus WT.

124
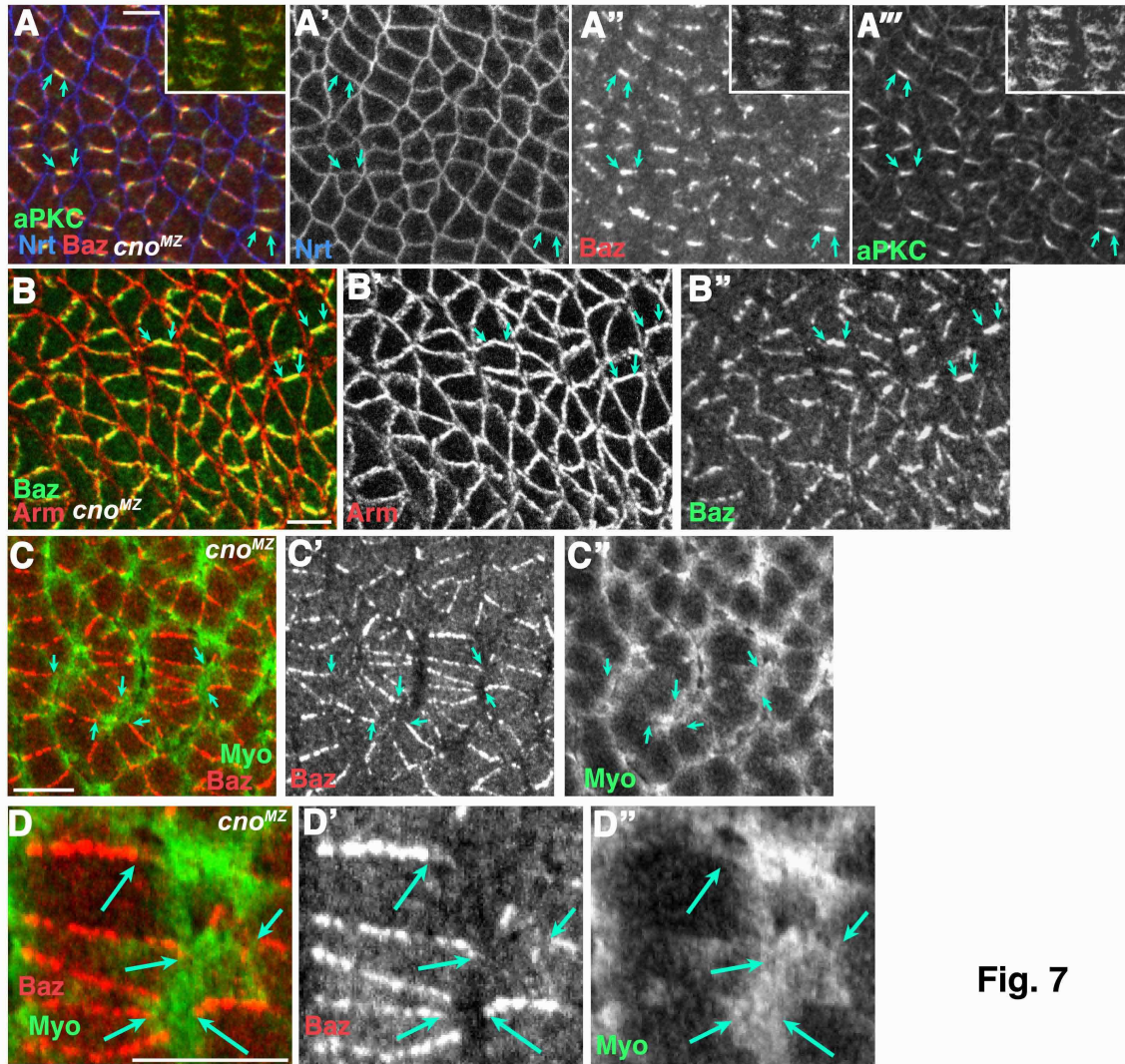
**Figure 3.7. Changes in Baz and aPKC localization in *cno^MZ* mutants parallel actomyosin retraction.** Stage7 *cno^MZ* mutants, antigens indicated. A. Baz and aPKC often localize only to central DV borders (arrows), not reaching vertices with AP borders. B. Arm (B', arrows) isn't similarly restricted, but extends all the way to vertices. C,D. (D=close-up). Baz along DV borders often only reaches edge of detached myosin cables (arrows). Bars=5μm.
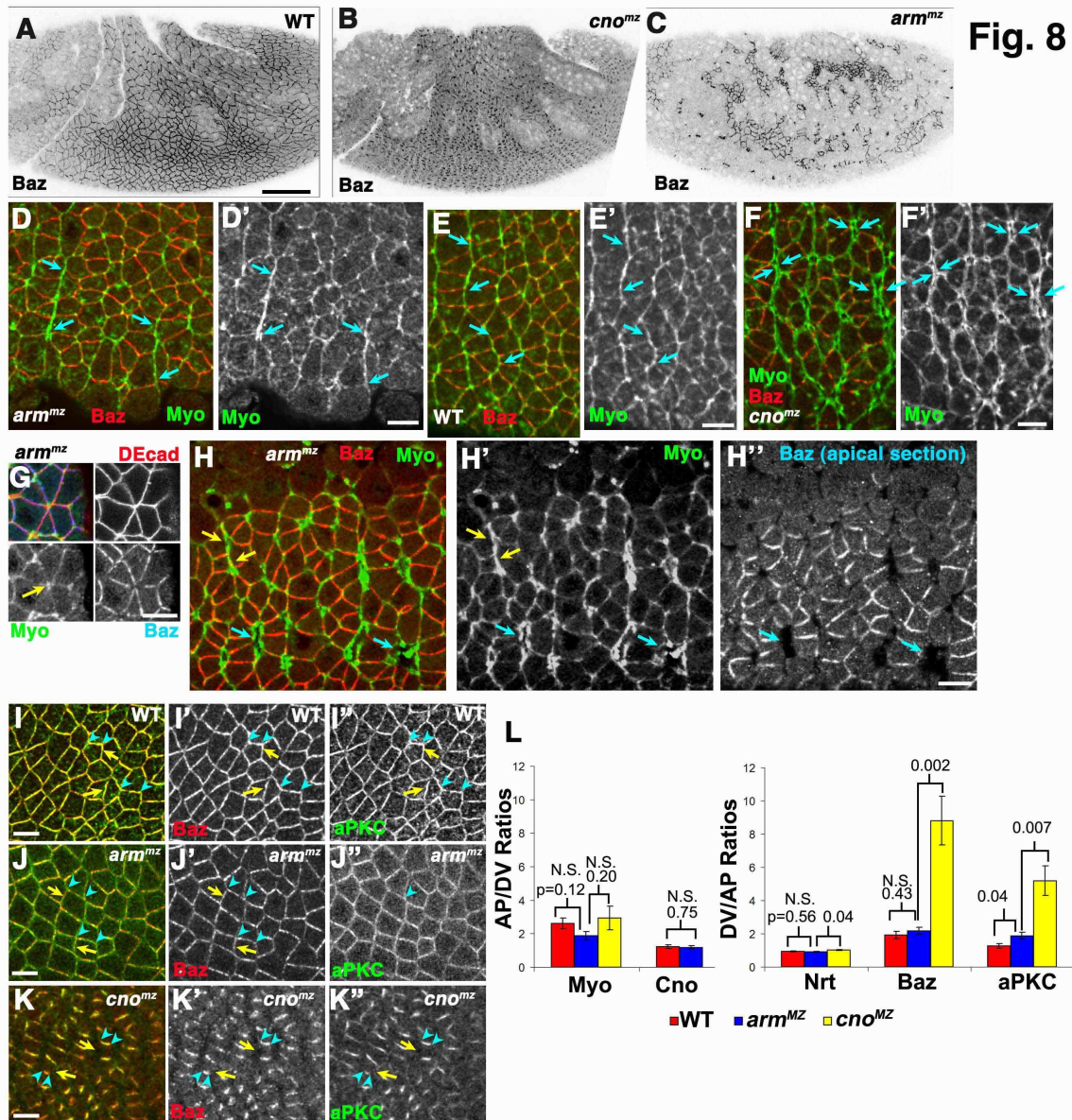
**Figure 3.8. Globally reducing cell adhesion doesn't mimic Cno loss.** A-C. Stage8. D-K. Stage7. A-C. Arm reduction (C) but not Cno loss (B) leads to widespread disruption of cell adhesion and epithelial integrity during early stage8. D-F. In $arm^{MZ}$ myosin initially remains in attached cortical cables (D,arrows), as in WT (E,arrows), but in contrast to $cno^{MZ}$ (F, arrows). G. In $arm^{MZ}$, some rosettes retain tight myosin localization to the vertex (arrow). H. As GBE continues, $arm^{MZ}$ cells begin to separate, and many myosin cables detach (blue arrows). However, some cables remain tightly cortical (yellow arrows). I-K. Baz and aPKC are retained on AP borders in $arm^{MZ}$ (J, yellow arrows) and extend all along DV borders (J, blue arrowheads), more resembling WT (I) than $cno^{MZ}$(K). L. Planar polarity quantitation. Bars A-C=20μm, D-L=5μm.

126
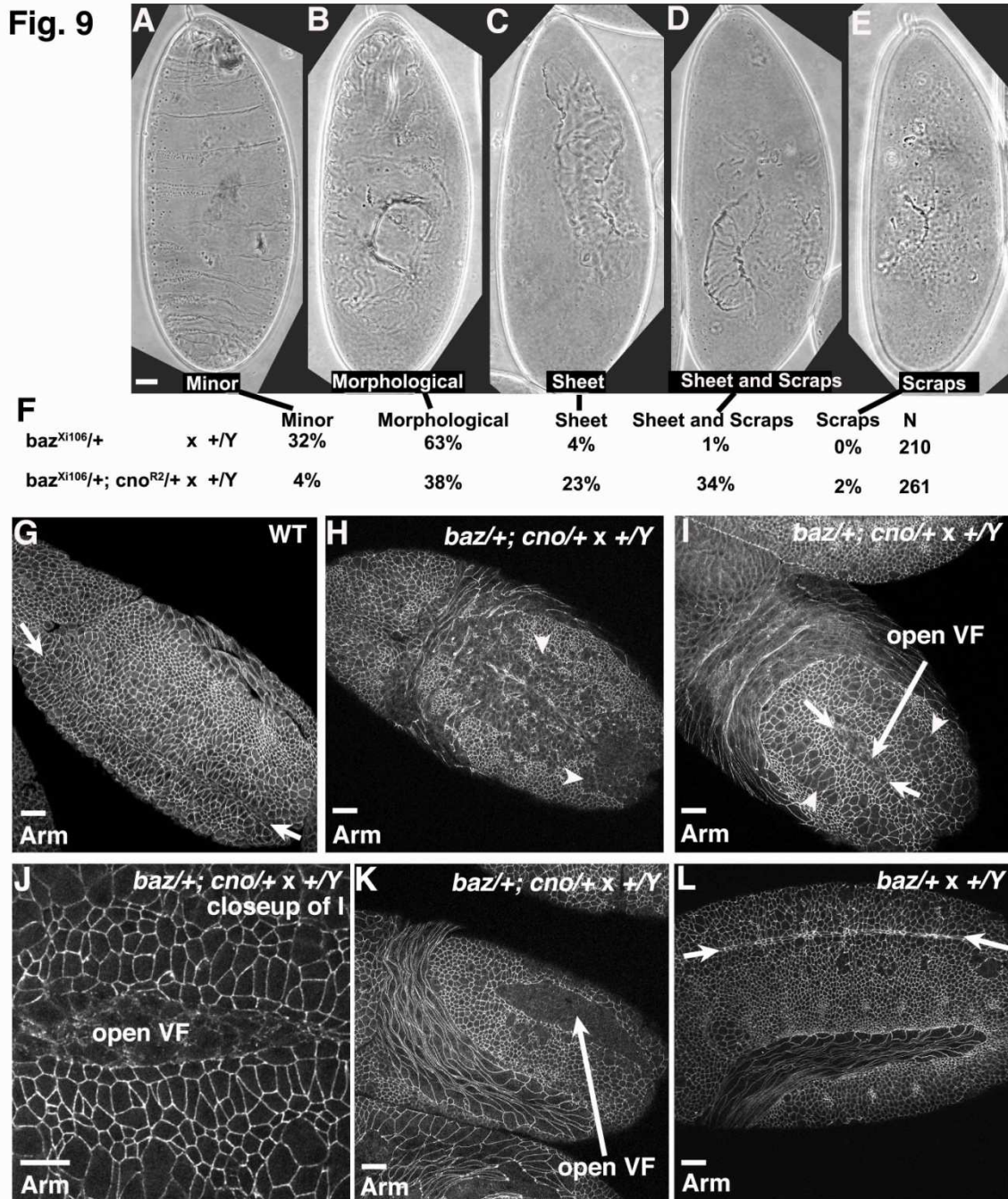
**Figure 3.9. Reducing Cno levels enhances the phenotype of zygotic *baz* mutants.** A-E. Cuticle preparations illustrating different phenotypes seen in progeny. F. Reducing Cno enhances the *baz* phenotype. In both cases, we analyzed *baz* zygotic mutant progeny. In the top cross, embryos had wild-type levels of maternal and zygotic Cno. In the bottom cross, levels of maternal Cno were reduced by 50% (note—no embryos in this cross are homozygous mutant for *cno*). G-L. Stage 9-11 embryos of the indicated genotypes. Reducing Cno leads to earlier defects in epithelial integrity in *baz* mutants (arrowheads=epithelial disruption), and also leads to failure of mesoderm invagination in many embryos. Arrows=closed (G,L) or open (I,K) ventral furrows. Bars=20μm.

127
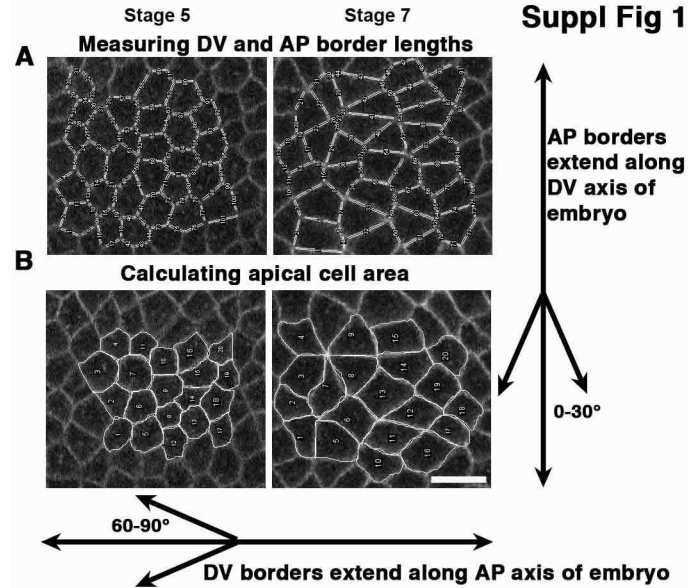
**Figure 3.S1. Quantitating cell shape, apical cell area and Fluorescence intensity.** All images used for measurements were acquired with a Zeiss 40X-Plan-Neofluar- NA1.3 oil immersion objective with zoom 2. A. Measuring AP and DV borders and Fluorescence Intensity Measurements. Border lengths and Fluorescence Intensity were measured using ImageJ's line tool. Border lengths were measured for stage5/6 (left panel) and stage7 (right panel). Measurements were subsequently sorted by angles (relative to the embryo DV axis). AP borders=angles 0-29° and DV borders=angles 60-90°. Only borders fitting these definitions were used to calculate DV and AP border lengths. 5 embryos were measured for each stage. Fluorescence Intensity was determined using ImageJ's line tool with a line width of 3, and obtaining the Mean Gray Value for each line. Stacks of 4 planes, 0.5μm apart, were used to ensure the entire border was measured. These four measurements were averaged to obtain a mean fluorescence intensity border value. From this, the background (measured the same way, but in the cytoplasm) was subtracted to obtain the final value. For markers that showed separation in apical planes, a neutral marker (i.e. Nrt) was used to direct measurements. The line width used often overlapped separated borders. Only stage7 (right panel) and early stage8 embryos (not depicted) were measured. Measurements were sorted by angles relative to the embryo AP axis as described above. Ratios from 5 embryos from at least two different experiments were averaged. B. Area Measurements. Cell areas of 20 cells for stage5/6 (left panel) and stage7 (right panel) were measured using ImageJ's free hand selection tool and then measuring the area of that selection. 5 embryos were measured for each stage.

**A** Cell Border Lengths at end of cellularization (stage 5)

border lengths (μm)

WT: 2.6, 2.6 | cno^MZ: 2.5, 2.6 | arm^MZ: 2.9, 3.0 | DMSO: 2.4, 2.3 | cytoD: 2.3, 2.8

☐ AP borders = Cell length along DV axis    ■ DV borders = Cell length along AP axis

**B** Cell Border Lengths during early GBE (stage 7)

border lengths (μm)

WT: 2.5, 4.3 | cno^MZ: 2.4, 3.4 | arm^MZ: 3.5, 4.5 | DMSO: 2.1, 4.0 | cytoD: 2.4, 2.7

☐ AP borders = Cell length along DV axis    ■ DV borders = Cell length along AP axis

**C** Apical Areas at end of cellularization

apical areas (μm²)

WT: 22.9 | cno^MZ: 22.9 | arm^MZ: 30.0 | DMSO: 21.8 | cytoD: 20.3

**D** Apical Areas during early GBE

apical areas (μm²)

WT: 32.5 | cno^MZ: 18.0 | arm^MZ: 32.1 | DMSO: 32.4 | cytoD: 19.4

Suppl. Fig. 2

**E** Dorsal, Anterior, Posterior, Ventral

**Diagrammatic representation of change in cell shape**

**Figure 3.S2. Cell shape and apical cell area in WT and mutants.** A-D. See Suppl. Fig 1 and legend for Methods. E. Diagrammatic representation of AP cell elongation from stage 5 (left) to stage 7 (right).

129
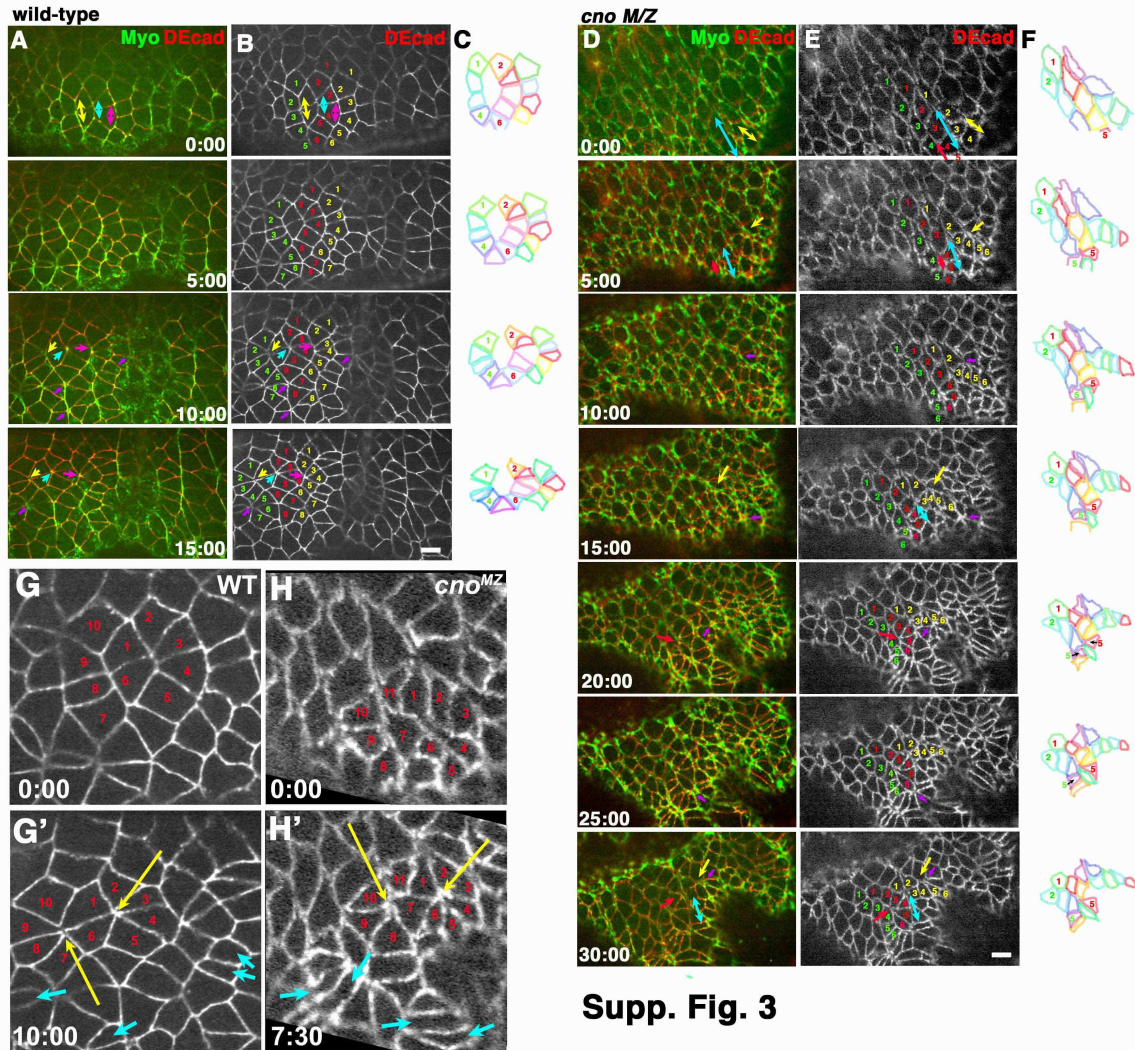
**Figure 3.S3. Cell rearrangements in WT versus *cno^MZ*.** Movie stills, stage6-7 WT (A,B) and *cno^MZ* (D,E), expressing DEcad-GFP and myosin(sqh)-mCherry; times=minutes:seconds. WT and *cno^MZ* cells begin roughly isometric in shape (0:00). Numbered cells=three cell columns in each genotype. Double-headed and single headed yellow, blue and red arrows=shrinking cell boundaries, presumably due to myosin cable constriction. Purple arrows=other rosettes forming during movie. C,F. Subset of the illustrated cell columns. Cell shape changes and rearrangements re-shape the tissue, narrowing it in the DV axis and elongating it in the AP. G-H. Close-ups of two timepoints in the WT (G) or *cno^MZ* (H) movies illustrating the formation of two cell rosettes in each genotype (yellow arrows), as well as a cells in each genotype that have changed shape (blue arrows). Scale bars=5μm.

**A** Stage 7 *cno^MZ* — Myo (green) Arm (red)

**B** Stage 7 *cno^MZ* Apical — Myo Arm

**B'** Arm

**C** 1.5µm more basal — Myo Arm

**C'** Arm

**D** Stage 7 *cno^MZ* — 3 µm

**E** *cno^MZ* 0:00 — Myo live DE-cad live

**E'** 0:40

**E''** 1:20

**F** *cno^MZ* mesoderm

**G** *cno^MZ*

**H** *cno^MZ*

Suppl.
Fig. 4

131
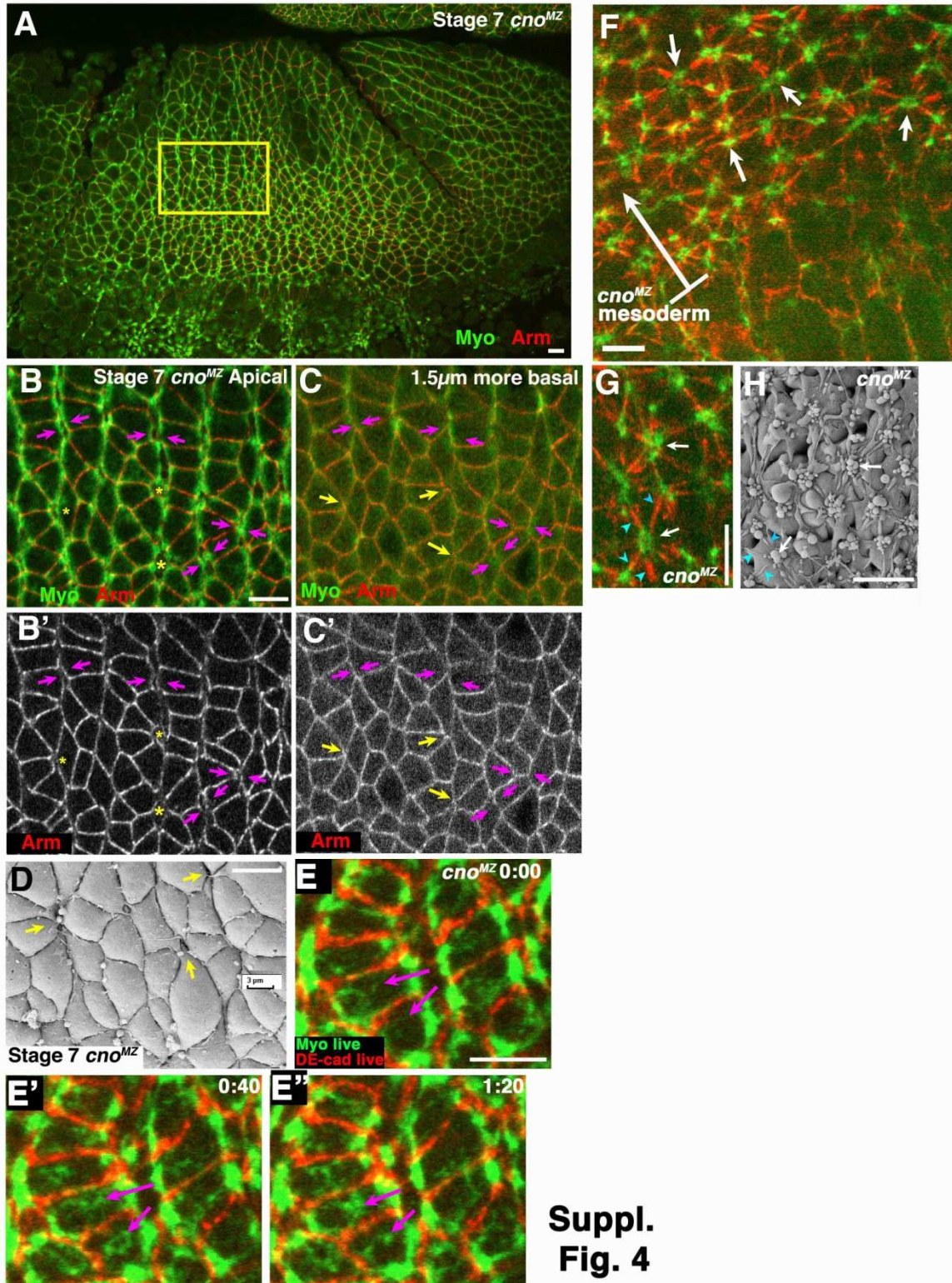
**Figure 3.S4. Myosin detachment from adherens junctions in *cno^MZ*.**  A. Late stage7 *cno^MZ* embryo, illustrating widespread detachment of myosin cables from AP borders. B,C.  Apical and more basal views of the region boxed in panel A.  Detached myosin cables are very apical.  Purple arrows illustrate that most regions of maximal myosin detachment apically have largely intact AJs more basally.  Asterisks and yellow arrows are regions of apparent apical "cell separation" that correspond to vertices of cell rosettes with largely intact AJs  more basally.  D.  SEM of similar stage *cno^MZ* mutant.  Yellow arrows are presumptive rosettes. E. Stills from Movie 3 illustrating that *cno^MZ* cells retain cyclical actomyosin appearance and disappearance  (arrows).  F,G.  Mesoderm in *cno^MZ*. Myosin balls (arrows) are connected to DEcad-containing membrane strands (arrowheads).  H.  SEM, same stage *cno^MZ* mutant, with apparent balls (arrows) and strands (arrowheads).  Scale bars=5μm.

**Suppl. Fig. 5**

**Figure 3.S5. Cell-cell adhesion is not substantially reduced in *cno^{MZ}*.** SEMs of WT or *cno^{MZ}* embryos of the indicated stages. Scale bars=5μm.
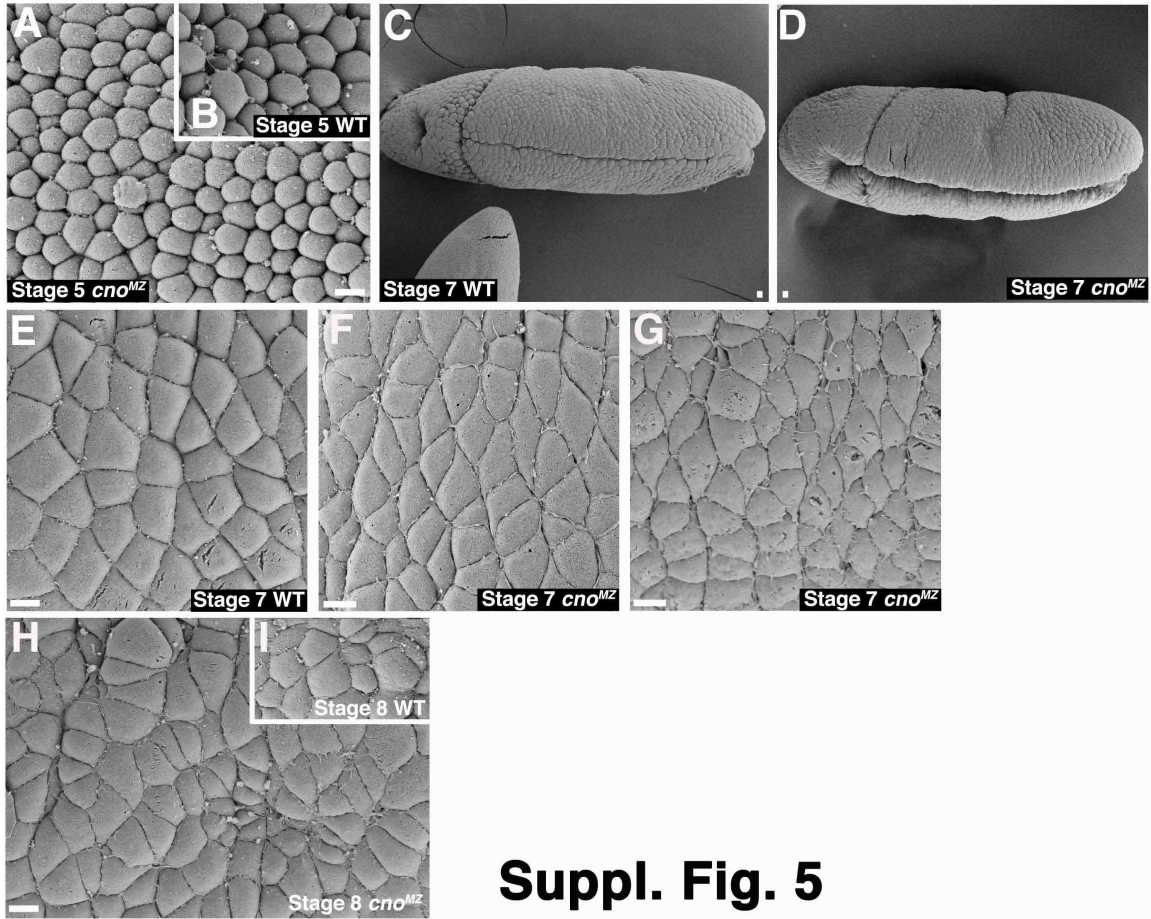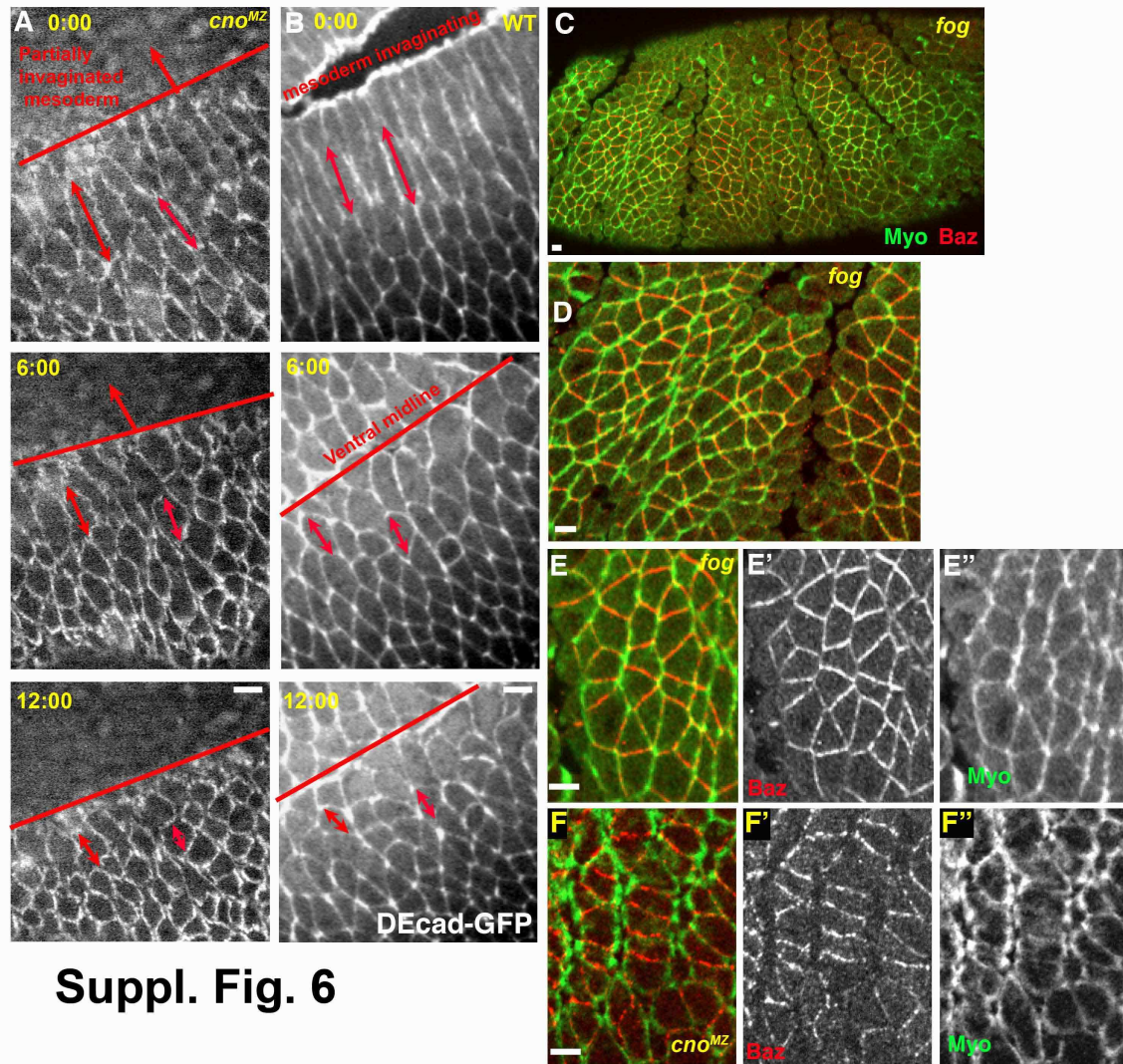
**Figure 3.S6. *cno^MZ* undergo some cell shape changes of GBE correctly, and failure to fully invaginate mesoderm is not the sole cause of *cno^MZ* myosin or Baz defects.** A,B. Stills from DEcad-GFP movies of ventral ectoderm undergoing dorsal-ventral relaxation to isometric shapes in WT and *cno^MZ*. Double-headed arrows indicate individual cells undergoing this cell shape change. C-F. Stage 7 *fog* (C-E) or *cno^MZ* mutant (F) embryos, stained for myosin and Baz. Neither myosin detachment nor enhanced Baz planar polarity is seen in *fog* mutants. Scale bars=5μm.

**Figure 3.S7. Actin depolymerization partially mimics effects of Cno loss.** Stage7. A,B. Cortical actin is strongly reduced by cytoD (DMSO=control). C,D. Cortical myosin (C,arrows) is also strongly reduced by cytoD (D,arrows). E-J. Yellow arrowheads=AP borders, Red arrowheads=DV. DEcad (F,H,J), Baz (F,H), and aPKC(J) planar polarity are all enhanced by actin depolymerization relative to the DMSO control (E,G,I) K. Planar polarity quantitation. Bars=5µm.

**Table 3.1: Comparing degree of planar-polarization between different genotypes and conditions**

### WT vs. *cno*$^{MZ}$

| Protein | *WT DV/AP Ratio*^ | *cno*$^{MZ}$ DV/AP Ratio^ | p values  Differences in degree of planar polarity[1]: WT vs. *cno*$^{MZ}$ |
|---|---|---|---|
| Nrt | 0.94±0.03 | 0.96±0.03 | 0.157 |
| Arm | 1.08±0.09 | 1.56±0.14 | 0.021 |
| DEcad | 0.98±0.06 | 1.23±0.05 | 0.015 |
| aPKC | 1.26±0.14 | 5.19±0.89 | 0.002 |
| Baz | 1.91±0.22 | 8.81±1.48 | 0.002 |
| | *WT AP/DV Ratio*^ | *cno*$^{MZ}$ AP/DV Ratio^ | **p**[1] |
| Myo | 2.61±0.33 | 2.93±0.71 | 0.688 |
| F-actin | 1.61±0.10 | 1.67±0.26 | 0.852 |
| Cno | 1.22±0.10 | --- | --- |

### WT vs. *arm*$^{MZ}$ and *cno*$^{MZ}$ vs. *arm*$^{MZ}$

| Protein | *WT DV/AP Ratio*^ | *arm*$^{MZ}$ DV/AP Ratio^ | p values Differences in degree of planar polarity[1]: WT vs *arm*$^{MZ}$ | p values Differences in degree of planar polarity[1]: *arm*$^{MZ}$ vs *cno*$^{MZ}$ |
|---|---|---|---|---|
| Nrt | 0.94±0.03 | 0.91±0.03 | 0.561 | 0.040 |
| aPKC | 1.26±0.14 | 1.87±0.21 | 0.038 | 0.007 |
| Baz | 1.91±0.22 | 2.17±0.22 | 0.434 | 0.002 |
| | *WT AP/DV Ratio*^ | *arm*$^{MZ}$ AP/DV Ratio^ | | |
| Myo | 2.61±0.33 | 1.88±0.24 | 0.107 | 0.196 |
| Cno | 1.22±0.10 | 1.17±0.10 | 0.746 | --- |

### DMSO vs. cytoD

| Protein | *DMSO DV/AP Ratio*^ | *CytoD DV/AP Ratio*^ | p values  Differences in degree of planar polarity[1]: DMSO vs *cytoD* |
|---|---|---|---|
| Nrt | 0.93±0.01 | 0.83±0.02 | 0.004[2] |
| Arm | 1.28±0.04 | 1.47±0.09 | 0.073 |
| DEcad | 1.10±0.05 | 1.48±0.08 | 0.003 |
| aPKC | 1.19±0.08 | 1.61±0.10 | 0.010 |
| Baz | 1.60±0.08 | 3.21±0.15 | p<0.0001 |

\*\*N = 5 embryos, from at least 2 different experiments
^ ± s.e.m
[1] p values of comparisons of degree of planar polarity between different genotypes or conditions, as determined by student T-test
[2] The planar-polarization of Nrt in *arm*$^{MZ}$ and after CytoD treatment may reflect partial failure of the restriction of Nrt to the basolateral domain (see Harris and Peifer, 2004), perhaps in a planar-polarized way.

**Table 3.S1: Assessment of planar polarity of junctional and cytoskeleton proteins in different genotypes and conditions**

| Protein | WT | |
|---|---|---|
| | **DV/AP Ratio± s.e.m** | **p value of DV/AP difference** |
| Nrt | 0.94±0.03 | 0.068 |
| Arm | 1.08±0.09 | 0.39 |
| DEcad | 0.98±0.06 | 0.59 |
| aPKC | 1.26±0.14 | 0.025 |
| Baz | 1.91±0.22 | p<0.0001 |
| | **AP/DV Ratio± s.e.m** | **p value** |
| Myo | 2.61±0.33 | p<0.0001 |
| F-actin | 1.61±0.10 | p<0.0001 |
| Cno | 1.22±0.10 | 0.030 |
| **Protein** | ***cno*** $^{MZ}$ | |
| | **DV/AP Ratio± s.e.m** | **p value** |
| Nrt | 0.96±0.03 | 0.86 |
| Arm | 1.56±0.14 | 0.0004 |
| DEcad | 1.23±0.05 | 0.0004 |
| aPKC | 5.19±0.89 | p<0.0001 |
| Baz | 8.81±1.48 | p<0.0001 |
| | **AP/DV Ratio± s.e.m** | |
| Myo | 2.93±0.71 | p<0.0001 |
| F-actin | 1.67±0.26 | 0.002 |
| **Protein** | ***arm*** $^{MZ}$ | |
| | **DV/AP Ratio± s.e.m** | **p value** |
| Nrt | 0.91±0.03 | 0.0009 |
| aPKC | 1.87±0.21 | 0.0002 |
| Baz | 2.17±0.22 | p<0.0001 |
| | **AP/DV Ratio± s.e.m** | **p value** |
| Myo | 1.88±0.24 | 0.0002 |
| Cno | 1.17±0.10 | 0.035 |
| **Protein** | **DMSO** | |
| | **DV/AP Ratio± s.e.m** | **p value** |
| Nrt | 0.93±0.01 | 0.011 |
| Arm | 1.28±0.04 | p<0.0001 |
| DEcad | 1.10±0.05 | 0.022 |
| aPKC | 1.19±0.08 | 0.007 |
| Baz | 1.60±0.08 | p<0.0001 |
| **Protein** | **CytoD** | |
| | **DV/AP Ratio± s.e.m** | **p value** |
| Nrt | 0.83±0.02 | p<0.0001 |
| Arm | 1.47±0.09 | p<0.0001 |
| DEcad | 1.48±0.08 | p<0.0001 |
| aPKC | 1.61±0.10 | p<0.0001 |
| Baz | 3.21±0.15 | p<0.0001 |

N= 5 embryos, p-values determined by student t-test
AP borders and DV borders were normalized using the average fluorescence of all borders measured in an embryo

**Table 3.S2: Absolute Values – Nrt, Baz, DEcad, Arm**

### NRT

| Protein | $AP\pm s.d.$ | $DV\pm s.d.$ |
|---|---|---|
| WT $cno^{MZ}$ | 45.89±13.54 47.58±13.82 | 42.28±16.11 41.22±15.72 |
| | **WT vs. $cno^{MZ}$ AP borders p[1]** | **WT vs. $cno^{MZ}$ DV borders p[1]** |
| | 0.9 | 0.9 |
| | 4% more Nrt on $cno^{MZ}$ AP borders | 3% less Nrt on $cno^{MZ}$ DV borders |

### BAZ

| Protein | $AP\pm s.d.$ | $DV\pm s.d.$ |
|---|---|---|
| WT $cno^{MZ}$ | 42.84±21.75 17.05±9.13 | 78.42±29.64 67.91±16.95 |
| | **WT vs. $cno^{MZ}$ AP borders p[1]** | **WT vs. $cno^{MZ}$ DV borders p[1]** |
| | 0.04 | 0.5 |
| | 60% less Baz on $cno^{MZ}$ AP borders | 13% less Baz on $cno^{MZ}$ DV borders |

### DECAD

| Protein | $AP\pm s.d.$ | $DV\pm s.d.$ |
|---|---|---|
| WT $cno^{MZ}$ | 60.63±13.01 23.16±2.64 | 64.26±10.82 25.72±1.55 |
| | **WT vs. $cno^{MZ}$ AP borders p[1]** | **WT vs. $cno^{MZ}$ DV borders p[1]** |
| | 0.0002 | P<0.0001 |
| | 62% less DEcad on $cno^{MZ}$ AP borders | 60% less DEcad on $cno^{MZ}$ DV borders |

### ARM

| Protein | $AP\pm s.d.$ | $DV\pm s.d.$ |
|---|---|---|
| WT $cno^{MZ}$ | 90.05±37.55 43.75±17.47 | 99.52±36.77 61.55±24.27 |
| | **WT vs. $cno^{MZ}$ AP borders p[1]** | **WT vs. $cno^{MZ}$ DV borders p[1]** |
| | 0.04 | 0.09 |
| | 51% less Arm on $cno^{MZ}$ AP borders | 38% less Arm on $cno^{MZ}$ DV borders |

\*\*N = 5 embryos for each condition, WT and $cno^{MZ}$ from the same experiment, imaged on the same slide
[1] p values determined by student T-test, using n= 5 embryos

## Table 3.S3: Penetrance of major phenotypes

| $cno^{MZ}$ Phenotype | Penetrance in stage6-8 embryos |
|---|---|
| Widespread myosin detachment from AP boundaries (fixed embryos) | 15/15 embryos scored |
| Arm planar-polarization enhanced (fixed embryos) | 23/23 embryos scored |
| Baz retracted from tricellular junctions (fixed embryos) | 20/20 embryos scored |
| aPKC retracted from tricellular junctions (fixed embryos) | 23/25 embryos scored |
| Myosin detached from AP borders (live with sqh-mCherry) | 8/12 embryos scored* |
| DEcad planar-polarization enhanced (live with DEcad-GFP) | 8/12 embryos scored* |
| Myosin Rings in stage6/7 | 7/9 embryos scored* |

| $arm^{MZ}$ Phenotype | Penetrance in stage6-8 embryos |
|---|---|
| Widespread myosin detachment from AP boundaries (fixed embryos-st 6/7 before ectoderm fragments) | 9/29 embryos scored |
| Myosin detachment primarily at vertices and AP borders but some borders OK | 8/29 scored |
| Myosin detachment primarily at vertices and many borders OK | 7/29 embryos scored |
| Myosin largely unaffected | 5/29 embryos scored |
| Baz retracted from tricellular junctions (fixed embryos) | 0/53 embryos scored |
| aPKC retracted from tricellular junctions (fixed embryos) | 0/29 embryos |

Fixed embryos were evaluated visually for major phenotypes not otherwise quantitated. Embryos were staged by examining pattern of divisions in mitotic domains, and $cno^{MZ}$ mutant embryos were identified by severity of defects in mesoderm invagination.
* For living embryos, because filming sometimes started before gastrulation, some paternally rescued mutants are included, thus reducing apparent penetrance.

**Table 3.S4: Fly stocks, antibodies, and probes**

| Fly stocks | Source |
| --- | --- |
| yw | Bloomington Stock Center (IN, USA) |
| ubiecadGFP,sqhCherII | J. Zallen (Sloan-Kettering, NY, USA) |
| tubCnoGFP | Marek Mlodzik (Mount Sinai Medical Center, NY, USA) |
| $cno^{R2}$/TM3twiGFP | |
| $arm^{043A01}$FRT101/FM7 | E. Wieschaus (Princeton, NJ, USA) |

| Antibodies/Probes | Dilution | Source |
| --- | --- | --- |
| anti-DE-DCAD2 | 1:100 | Developmental Studies Hybridoma Bank |
| anti-ArmN27A1 | 1:100 | Developmental Studies Hybridoma Bank |
| Anti-Nrt | 1:100 | Developmental Studies Hybridoma Bank |
| anti-Cno | 1:1000 | J. Sawyer and N. Harris (UNC-CH, NC, USA) |
| anti-Baz | 1:1000 | J. Zallen (Sloan-Kettering, NY, USA) |
| anti-aPKC | 1:1000 | Santa Cruz Biotechnology |
| anti-Zip (myosin II heavy chain) | 1:1000 | C. Field (Harvard, MA, USA) |
| | | D. Kiehart (Duke University, NC, USA) |
| MAB150 1R (actin) | 1:1000 | Millipore |
| Alexa-phalloidin | 1:500 | Molecular Probes |
| Secondary antibodies: Alexas 488, 568, and 647 | 1:500 | Molecular Probes |

# CHAPTER 4

## RAP1 AND CANOE/AFADIN ARE ESSENTIAL FOR ESTABLISHMENT OF APICAL-BASAL POLARITY IN THE DROSOPHILA

Nathan J. Harris*, Wangsun Choi*, Kaelyn D. Sumigray, and Mark Peifer

*authors contributed equally

**Preface**

In this chapter, I have included mine and others work toward understanding the role of Rap1 signaling in regulating both the establishment and maturation of polarity during *Drosophila* embryogenesis. Included is work done in parallel by my lab colleague Wangsun Choi examining the role of Cno in this process. In my previous work (described in Chapter 2), we learned that Rap1 mutants exhibited multiple defects in morphogenesis during gastrulation. This suggested that we had yet to uncover the primary defects caused by loss of Rap1 that ultimately lead to these observed defects. As a result, I examined events prior to gastrulation to better understand Rap1's role in building a polarized epithelia competent for effective morphogenesis. In working with Rap1, it quickly became apparent that we also needed to further our understanding of how polarity is primarily established and its role in regulating the localization of Rap1's binding partner Cno. Therefore, I also examined the effects on Cno localization caused by disrupting apical polarity. We have prepared a manuscript covering this work for publication.

**Abstract**

The establishment and maintenance of apical-basal cell polarity is critical for assembling epithelial tissues and maintaining proper organ architecture. The *Drosophila* embryo provides a superb model for this process. In our current model, apically positioned Bazooka/Par3 protein is the initial polarity cue as cells form during cellularization. Bazooka then helps position both adherens junctions and aPKC. While we know that a polarized cytoskeleton is critical for apical positioning of Bazooka, the proteins mediating this process remained unknown. Here, we report that the small GTPase Rap1 and the actin-junctional linker protein Canoe/afadin are essential for the initial establishment of polarity, as both adherens junctions and Bazooka are mis-positioned in their absence. This does not simply involve a role for Rap1 or Canoe in organizing the actin or microtubule cytoskeletons, as these become properly polarized in their absence. We found that Rap1 and Canoe play continuing roles in proper polarization of Bazooka during gastrulation, with consequences for epithelial integrity. However, after gastrulation other polarity cues come into play and partially restore apical Baz localization in the absence of Rap1 or Canoe. We next tested whether the current linear model for establishment of apical polarity is too simple. We found that both Baz and aPKC play roles in initial Canoe localization, despite being "downstream" of Canoe. Further, Rap1, Bazooka and aPKC, but not Canoe, play roles in establishing columnar cell shape. These data re-shape our model for polarity establishment, suggesting it is regulated by a network of proteins rather than a linear pathway.

**Introduction**

Polarity is a fundamental property of all cells, from polarized cell divisions in bacteria or fungi to the elaborate polarity of neurons. Among the most intensely studied

142

forms of polarity in animal cells is epithelial apical-basal polarity (Goldstein and Macara, 2007). Polarity of epithelial sheets is key to their function as barriers between body compartments, and is also critical in collective cell migration and cell shape change during morphogenesis, as cytoskeletal and apical-basal polarity often go hand in hand. Loss of apical-basal polarity is a hallmark of metastasis (Wodarz and Nathke, 2007). We have made significant advances in defining the machinery required for cell polarity in many settings, but fundamental questions remain unanswered.

Cadherin-catenin complexes, which assemble into adherens junctions (AJs) near the apical end of the lateral cell interface, are critical polarity landmarks that define the boundary between apical and basolateral domains (Gumbiner *et al.*, 1988). Studies in *C.elegans* and *Drosophila* identified and characterized other key regulators of apical-basal polarity (Goldstein and Macara, 2007; Lynch and Hardin, 2009; Harris and Tepass, 2010; Laprise and Tepass, 2011). In the textbook view, the apical domain is defined by the Par3/Par6/aPKC and Crumbs/Stardust(Pals1)/PATJ complexes (Assemat *et al.*, 2008), while Scribble, Dlg, Lgl, and Par1 define the basolateral membrane. Complex cross-regulatory interactions between apical and basolateral proteins maintain these mutually exclusive membrane territories (Bilder *et al.*, 2003; Tanentzapf and Tepass, 2003; Laprise *et al.*, 2009). These proteins also play roles in other types of polarity during morphogenesis (St Johnston and Sanson, 2011); e.g. fly Par3 (Bazooka; Baz), aPKC, and AJ proteins are planar-polarized along the anterior-posterior axis during *Drosophila* convergent extension, thus regulating polarized cell movements (Zallen, 2007).

Polarized cytoskeletal networks also play key roles in establishing and maintaining apical-basal and planar polarity. These networks are thought to be physically linked to apical junctional complexes. The earlier model suggesting that cadherin-catenin complexes link directly to actin via α-catenin is now viewed as over-simplified (Drees *et al.*, 2005; Yamada *et al.*, 2005). Instead, different proteins are thought to mediate this connection in different tissues and times (e.g., Abe and Takeichi, 2008; Cavey *et al.*, 2008; Sawyer *et al.*, 2009).

Among the linkers is Canoe (Cno)/Afadin, an actin-binding protein that binds transmembrane nectins via its PDZ domain (Mandai *et al.*, 1997). While originally hypothesized to be essential for cell adhesion, subsequent work support a model in which afadin modulates adhesive and cytoskeletal machinery during cell migration in vitro (Lorger and Moelling, 2006; Miyata *et al.*, 2009; Fournier *et al.*, 2011) and the complex events of mouse gastrulation (Ikeda *et al.*, 1999; Zhadanov *et al.*, 1999). Afadin has two N-terminal Ras association domains for which the small GTPase Rap1 is the major binding partner (Linnemann et al., 1999), and Afadin and Rap1 are functionally linked in both flies and mice (Boettner *et al.*, 2003; Hoshino *et al.*, 2005). Rap1, Cno, and the Rap1 GEF Dizzy/PDZGEF are all essential for maintaining effective linkage between AJs and the apical actomyosin cytoskeleton during apical constriction of *Drosophila* mesodermal cells during fly gastrulation (Sawyer *et al.*, 2009; Spahn *et al,* 2012). Rap1 regulates Cno loclaization to the membrane (Sawyer *et al.*, 2009). Cno plays a related role during convergent extension, though its role is planar polarized during this process (Sawyer *et al.*, 2011). Cno also regulates collective cell migration, signaling, and oriented asymmetric divisions (e.g. Boettner *et al.*, 2003; Carmena *et al.*, 2006; Carmena *et al.*,

144

2011; Wee *et al.*, 2011). The Rap1/Cno regulatory module is also important in disease, as Afadin or Rap1 are implicated in congenital disorders of the cardiovascular system (Glading *et al.*, 2007) and cancer metastasis (Fournier *et al.*, 2011). It remains unclear whether these diverse roles all involve junction-cytoskeletal linkage or whether some are independent functions.

The small GTPase Rap1 plays diverse cellular roles. Mammalian Rap1 isoforms are perhaps best known for regulating integrin–based cell matrix adhesion (Bos, 2005; Kim *et al.*, 2011), but Rap1 also regulates cell-cell AJs in both *Drosophila* and mice (Kooistra *et al.*, 2007; Boettner and Van Aelst, 2009). In murine endothelial cells, for example, Rap1, its effector Krit1, and VE-cadherin form a complex that regulates endothelial cell junctions and stabilizes apical-basal polarity (Glading *et al.*, 2007; Lampugnani *et al.*, 2010; Liu *et al.*, 2011). In *Drosophila* imaginal disc cells, Rap1 regulates the symmetric distribution of DE-cadherin (DEcad) around the apical circumference of each cell (Knox and Brown, 2002). Rap1 carries out these functions via a diverse set of effector proteins, including Krit1, TIAM, RIAM, and Cno/Afadin (Kooistra *et al.*, 2007; Boettner and Van Aelst, 2009). Thus Rap1 and its effectors are candidate proteins for regulating interactions between AJs, polarity proteins and the cytoskeleton during polarity establishment and maintenance.

The early *Drosophila* embryo provides among the best models for establishing and maintaining apical-basal polarity (Harris, 2012). Flies start embryogenesis as a syncytium, with 13 rounds of nuclear division without cytokinesis. Membranes then simultaneously invaginate around each nucleus, forming ~6000 cells in a process known as cellularization (Fig. 1A, right). Prior to cellularization, the egg membrane is a polarity

cue for underlying nuclei.  This ultimately becomes the apical end of the new cells.

Apical-basal polarity is initiated during cellularization (Harris, 2012).  In the absence of

cadherin-catenin complexes, cells form normally but then lose adhesion and polarity as

gastrulation begins (Cox *et al.*, 1996).  These data and earlier work from cell culture

(Gumbiner *et al.*, 1988) suggested AJs are the initial apical cue.  However, we found that

Bazooka (Baz)/Par3 acts upstream of AJs in this process (Harris and Peifer, 2004).

Strikingly, Baz and DEcad co-localize apically from the onset of cellularization in spot

AJs (Fig. 1A right; cadherin-catenin complexes are also enriched in "basal junctions" just

above the invaginating actomyosin front; Hunter and Wieschaus, 2000).  In the absence

of Baz, DEcad loses its apical enrichment and redistributes all along the lateral

membrane, while in the absence of AJ proteins, Baz remains apically localized, and a

subset of cells retain residual apical-basal polarity, although cell shapes are highly

abnormal (Harris and Peifer, 2004).  Cadherin-catenin and Baz complexes form

independently before cellularization, and Baz then helps position DEcad) in the

apicolateral position where spot AJs will form (McGill *et al.*, 2009).

This placed Baz atop of the polarization network (Fig. 1A, left), raising the

question of how it is positioned apically.  Two cytoskeletal networks play important roles

in initial Baz positioning (Harris and Peifer, 2005).  Disrupting dynein led to Baz

spreading along the lateral membrane, suggesting polarized transport along microtubules

(MTs) plays a role.  Depolymerizing actin also destabilized apical Baz, as did

significantly overexpressing Baz, suggesting an actin-based scaffold with a saturable

number of binding sites anchors Baz apically.  While both actin and MTs are required for

initial Baz polarization, they are not the only cues.  Mis-localized Baz is re-recruited or

re-stabilized apically at gastrulation onset if either initial cue is disrupted, suggesting a third cue (Harris and Peifer, 2005) perhaps involving aPKC/Par6 (Hutterer *et al.*, 2004). Thus the current model for initial establishment of apical-basal polarity involves a relatively simple pathway in which Baz is positioned apically, and then positions other apical polarity players (Fig. 1A, left). However, once initial polarity is established, events become more complex, with a network of mutually reinforcing and inhibitory interactions between apical and basolateral polarity complexes leading to polarity elaboration and maintenance.

These were significant advances, but the proteins directing apical accumulation of Baz remained unknown. Work on apical constriction in the fly mesoderm (Dawes-Hoang *et al.*, 2005; Martin *et al.*, 2010), convergent extension during gastrulation (Bertet *et al.*, 2004; Zallen and Wieschaus, 2004), establishment of anterior-posterior polarity in one cell *C. elegans* embryos (Munro *et al.*, 2004), and on apically constricting *Drosophila* amnioserosal cells (David *et al.*, 2010), suggested that a complex network of interactions link AJs, the apical polarity proteins Baz and aPKC, and the actomyosin cytoskeleton. Our recent work on Canoe and Rap1's roles in mesoderm apical constriction (Sawyer *et al.*, 2009) and convergent elongation (Sawyer *et al.*, 2011) suggested they also fit into this network. These data led us to explore whether Rap1 and Cno play roles in initial apical positioning of AJs and Baz and thus in the establishment and early maintenance of polarity.

**Results**

*Rap1 is required for initial apical positioning of AJs*

In our current model for apical-basal polarity establishment, apical Baz directs

apical positioning of AJs and aPKC, while a polarized cytoskeleton is important for Baz apical localization and/or retention (Harris and Peifer, 2004, 2005). However, the proteins directing Baz apical positioning remained unknown. Based on Rap1's roles in regulating cell-cell and cell matrix adhesion (Kooistra *et al.*, 2007; Kim *et al.*, 2011) and AJ:actin linkage during apical constriction (Sawyer *et al.*, 2009), and its presence at the plasma membrane during cellularization (Sawyer *et al.*, 2009), we hypothesized that Rap1 might be part of the mechanism regulating initial apical positioning of AJs and Baz. To test this hypothesis, we used the FRT/DFS approach (Chou *et al.*, 1993) to generate embryos completely lacking maternal Rap1, using the null allele *Rap1$^{B1}$* (called *Rap1* below) and crossed them to *Rap1/ +* fathers. We cannot distinguish maternal/zygotic mutants (*Rap1$^{MZ}$*) from embryos receiving paternal wild-type *Rap1* (*Rap1$^{M}$*) until mid-late gastrulation.

Cadherin-catenin complexes are already at the membrane in wild-type syncytial embryos (Grevengoed *et al.*, 2003). As cellularization begins, they form puncta in the egg membrane that are recruited into apicolateral spot AJs as membranes invaginate (Fig. 1A; Harris and Peifer, 2004; McGill *et al.*, 2009; Fig. 1D bracket=Armadillo (Arm)=ß-catenin;). AJ proteins also accumulate in basal junctions (Fig. 1A, D arrowhead; Hunter and Wieschaus, 2000) just behind the actomyosin rings at the front. Lower levels of DEcad and Arm are also found all along the newly formed lateral membrane. The twin apical and basolateral enrichment of cadherin-catenin complexes is readily apparent in maximum intensity projections of many cross sections (Fig. 1F), which overlay the forming AJs of many nascent cells.

We tested the hypothesis that Rap1 helps regulate initial apical positioning of AJs.

148

*Rap1^{MZ}* mutants end embryogenesis with a fragmented cuticle (Suppl. Fig. 1A vs B; Sawyer *et al.*, 2009), suggesting epithelial integrity is disrupted, but this could due to early effects on polarity establishment or much later effects on polarity maintenance. When we examined initial apical positioning of spot AJs during cellularization, it was significantly disrupted in *Rap1* mutants. While AJ proteins still accumulated in basal junctions (Fig. 1E,H arrowheads, I vs. J), the apical enrichment of AJ complexes was substantially reduced during late cellularization (as seen in individual cross sections; Fig. 1D vs. E, brackets). The difference was accentuated in projected cross-sections (Fig. 1F), overlaying AJs of many cells (Fig. 1G vs. H, brackets). In *Rap1* mutants, AJ puncta localized all along the lateral cell interface. Differences began as early as mid-cellularization (Fig. 1K vs. L, brackets). To quantitate alterations in AJ positioning and to compare multiple embryos, we used Plot Profile in ImageJ to measure average image intensity in projected cross sections from four embryos at late cellularization—these are displayed as heat maps (Fig. 2A, left; intensity is color coded), or graphically (Fig. 2A, right) from apical (top) to basal (bottom). While there is some variability between embryos, the dual peaks of Arm at forming AJs and basal junctions are readily apparent in wild-type (Fig. 2A). In contrast, in *Rap1* mutants, the apical peak of Arm at assembling spot AJs is essentially gone, though the basal junction peak remains in 3 of 4 embryos. Some apical spot AJs were seen in *Rap1* embryos at gastrulation onset (Fig. 1B vs C; stage 6), suggesting that the initial defect in their positioning may be partially rescued later—we explore this below. Together, these data suggest that Rap1 is required for initial apical positioning of AJs.

***Cno is also required for initial apical positioning of AJs***

Rap1 has many effectors mediating its diverse functions (Kooistra *et al.*, 2007), including Cno/afadin. Cno regulates AJ:actin interactions during gastrulation (Sawyer *et al.*, 2009; 2011). Furthermore, Cno is positioned to affect early polarization, as like Baz (Suppl. Fig 2H) and AJ proteins (McCartney *et al.*, 2001), Cno already localizes to the egg plasma membrane in syncytial embryos (Suppl. Fig. 2A), and to developing apical junctions during cellularization (Suppl. Fig. 2B,C; (Sawyer *et al.*, 2009). Finally, Rap1 is required for effective localization of Cno during cellularization and early gastrulation (Sawyer et al., 2009). Given their parallel roles in many events, we tested the hypothesis that Cno is the Rap1 effector regulating initial apical AJ positioning.

To do so, we examined $cno^{R2}$ maternally null mutant embryos (hereafter *cno;* as with *Rap1* we can only definitively identify the 50% zygotically rescued embryos until late in gastrulation). Strikingly, while wild-type cellularizing embryos exhibit enrichment of cadherin-catenin complexes in both spot AJs and basal junctions (Fig. 1P), *cno* mutants lost apical AJ protein enrichment (Fig. 1P vs. Q, brackets, R vs. S brackets, U vs. V). In contrast, basal junctions appeared normal (Fig. 1P vs. Q, arrowheads, R vs. S arrowheads, W vs. X). We quantitated these changes in multiple embryos, as we had with *Rap1* mutants. Once again, in wild-type peaks of Arm were readily apparent both in assembling apical AJs and in basal junctions (Fig. 2C), while in *cno* mutants the apical peak was blunted or lost (Fig. 2D). Apical spot AJs are seen later in gastrulating *cno* embryos (Sawyer *et al.*, 2009), even those in which mesoderm invagination had stalled (Fig. 1M, N vs O), suggesting that this initial defect may be partially rescued later. Together, these data suggest that both Rap1 and its effector Cno regulate the initial positioning of AJs during establishment of apical-basal polarity.

*Rap1 and baz exhibit strong dose-sensitive genetic interactions in epithelial integrity*

These data are consistent with the possibility that Rap1 and Cno directly regulate AJ positioning or that they act on the upstream regulator of AJ positioning, Baz/Par3. One way to assess whether two proteins work together in a cell biological process is to look for dose-sensitive genetic interactions, such that reducing levels of one protein enhances the effect of lowering levels of the other. We adopted an approach used by Harris' lab to screen for proteins working with Baz in epithelial development (Shao *et al.*, 2010), using zygotic mutants to reduce rather than eliminate gene function. Embryos retaining maternal Baz but lacking zygotic Baz slowly run out of Baz protein. While they establish apical-basal polarity correctly (unlike *baz^{MZ}* mutants), a subset of embryos lose full epithelial integrity later, and end with holes in the cuticle (explaining the name *bazooka*) ranging from minor (27%) to significant (71%), but almost all retain large portions of intact cuticle (Fig. 3A,B). This genotype is sensitized for alterations in apical-basal polarity regulators, and is significantly enhanced by heterozygosity for known regulators including Crumbs, aPKC and DEcad (Shao *et al.*, 2010).

We thus hypothesized that if Rap1 is an important player in apical-basal polarity, it would also enhance *baz*. *Rap1* heterozygotes are viable and fertile, and even *Rap1* zygotic mutants survive embryogenesis normally on maternally supplied Rap1, dying as late larvae/pupae. We thus assessed whether reducing Rap1 enhanced the effect of reducing Baz levels. Strikingly, even the small reduction in Rap1 levels in embryos maternally and zygotically <u>heterozygous</u> for *Rap1* enhanced the defects of *baz* zygotic mutants, leading to stronger disruption of cuticle integrity (Fig. 3B, top versus middle genotype). Further reducing Rap1 levels by removing zygotic Rap1 caused an even

151

stronger enhancement (Fig. 3B, top versus bottom genotype). To confirm this was due to

effects on AJ integrity, we visualized Arm at stage 10, focusing on the amnioserosa as it

is especially sensitive to reduced Baz levels (Shao *et al.*, 2010). While only 12% of *baz*

zygotic mutants had defects in amnioserosal AJ integrity, this increased to 64% when

Rap1 was reduced maternally and zygotically (Fig. 3C vs D, E). Together, these data are

consistent with the hypothesis that Rap1 and Baz cooperate in maintaining epithelial

integrity; similar dose-sensitive genetic interactions exist between *cno* and *baz* (Sawyer *et*

*al.*, 2011).

### *Rap1 and Cno act upstream of Baz/Par3, regulating its apical positioning*

These genetic data are consistent with the hypothesis that Rap1 and Cno act

together with Baz to maintain epithelial integrity. During wild-type cellularization, Baz

helps recruit AJ proteins into apicolateral complexes, the spot AJs (McGill *et al.*, 2009).

Baz remains in this apical position throughout cellularization (Fig. 1A); unlike AJ

proteins, however, Baz does not assemble into basal junctions (Harris and Peifer, 2004;

McGill *et al.*, 2009). While it is clear that cytoskeletal interactions help position Baz

apically (Harris and Peifer, 2005), proteins mediating this remained unknown. We

considered two mechanisms by which Rap1 and Cno might mediate the initial apical

positioning of AJs. First, as Baz is required for apical AJ positioning (Harris and Peifer,

2005), Rap1 and Cno may be the missing players acting upstream of Baz. Alternatively,

Rap1 and Cno might not affect Baz localization but instead might directly position AJ

proteins. To distinguish between these mechanisms, we examined the initial apical

positioning of Baz in *Rap1* and *cno* mutants.

When we examined Baz localization in *Rap1* mutants, we found the normal

exclusively apical localization of Baz during cellularization was substantially disrupted. In wild-type, Baz is restricted to apical complexes (Fig. 4A,A',C). In contrast, in *Rap1*mutants, while Baz still formed membrane-associated puncta, its restricted apical localization was lost and Baz was redistributed all along the lateral membrane, both at the end of cellularization (Fig. 4B, B', D), and even earlier during mid-cellularization (Fig. 4E vs. F). Baz was found basal to its normal position in spot AJs (Fig. 4I3 vs J3, arrows) and also more apical (Fig. 4I1 vs J1, arrows). Consistent with the partial zygotic phenotypic rescue seen in later embryos (see below), while all embryos had defects in Baz localization, the degree of disruption of Baz localization fell into two overlapping classes, which we hypothesize represent *Rap1* maternal mutants that receive a wild-type paternal copy of *Rap1,* and *Rap1* maternal/zygotic mutants (*Rap1$^{MZ}$*)—these are present at a 1:1 ratio in the progeny. In the most severe class, which we suspect are the *Rap1$^{MZ}$*mutants, Baz apical localization is almost completely lost. Strikingly, we saw a very similar disruption in apical enrichment of Baz in *cno* mutants (Fig. 4G vs H; I vs K). We quantitated the effects of both mutants on Baz localization, once again measuring relative intensity of Baz from the apical to the basal ends of the cells in multiple embryos. Wild-type embryos uniformly displayed a sharp apical peak of Baz at the position of the forming spot AJs (Fig 4L). In contrast, in *Rap1* mutants this sharp apical peak was lost. *Rap1* mutants fell into two phenotypic categories of equal frequency and different severity, likely representing *Rap1$^{MZ}$* mutants (Fig. 4M) and zygotically rescued embryos (Fig. 4N). However, in both classes exclusive apical Baz enrichment was lost—this is particularly apparent when the levels in all the embryos in each phenotypic category were averaged (Fig. 4Q). In *cno* mutants, Baz also becomes distributed all along the apical-

153

basal axis (Fig. 4O vs P).  There was no obvious zygotic rescue of this phenotype, as the embryos did not fall into two clear classes, and averaging the distribution in the entire set of embryos emphasized the loss of apical enrichment (Fig. 4R).  Thus both Cno and Rap1 are essential for the initial apical positioning of Baz, putting them atop the current hierarchy of factors mediating the establishment of apical-basal polarity.

*Rap1 and Cno are not essential for basic cytoskeletal organization during cellularization*

These data suggest Rap1 and Cno act upstream of Baz to regulate its apical positioning.  One mechanism by which this could occur is by regulating cytoskeletal polarity, which is established prior to cellularization. As cellularization begins, the centrosomes in each cell are positioned above the nuclei, and nucleate a basket of MTs with their plus ends deeper in the cytoplasm (Fig. 1A).  Meanwhile, actin rearranges from a cap above each nucleus into a network of actin and myosin at the embryo cortex, which begins contracting, pulling in membrane around each cell as the cellularization front moves inward (Fig 1A, actomyosin front).  A pool of actin also remains at nascent apical AJs (Fig. 1A, actin scaffold).  Baz positioning requires both the apical actin scaffold and Dynein-directed MT transport toward what will become the apical domain (Harris and Peifer, 2005).  We thus tested the hypothesis that Cno and Rap1 regulate Baz via roles in organizing actin or MTs.

To test this mechanism, we examined the organization of the actin and MT cytoskeletons in *Rap1* and *cno* mutants during cellularization (at this early stage we cannot determine which embryos are paternally rescued).  We first examined MT and centrosomal polarity.  In wild-type, centrosomes are apical to each nucleus (Fig. 5A,

154

arrowheads) and baskets of MTs extend basally (Fig. 5A, arrows)—these baskets are also

visible as rings of bundled MTs in cross sections of forming cells (Fig. 5C). In *Rap1*

mutants we saw no obvious defects in either apical centrosomal positioning (Fig. 5B,

arrowheads) or in MT baskets projecting basally (Fig. 5B, arrows, Fig.5D). As we

explore in detail below, defects in apical cell shape begin to appear during cellularization

in *Rap1* mutants, but centrosomes were positioned apically above nuclei even in

misshapen cells (Fig 5B; Fig. 5E vs. F). Similarly, we saw no apparent defects in apical

centrosome positioning or formation of MT baskets in *cno* mutants (Fig. 5G vs H, C vs

I). Thus the MT cytoskeleton becomes correctly organized in the absence of Rap1 or

Cno, suggesting their effects on Baz localization do not result from indirect effects on

MTs.

We also examined actin and myosin during cellularization. The fact that mutant

embryos cellularize correctly already suggested that there were not major defects.

Myosin accumulated correctly at the cellularization front in both *Rap1* (Fig. 5J vs K,

arrowheads) and *cno* mutants (Fig. 5R vs S, arrowheads), and to the closing myosin rings

(Fig. 5L vs M). Actin accumulated at the cellularization front in both *Rap1* (Fig. 5N vs

O, arrowheads; P vs Q) and *cno* (Fig 5T vs U). Actin also accumulated normally at

nascent apical AJs (Fig. 5N vs O, brackets). Consistent with this, myosin is correctly

recruited apically in the mesoderm of both *Rap1* and *cno* mutants at gastrulation onset,

and initiates constriction (Sawyer *et al.*, 2009). Together these data suggest that there

are not substantial disruptions of the actomyosin or MT cytoskeletons in either *Rap1* or

*cno* mutants, making it less likely this indirect mechanism explains their effects on

apical-basal polarization. We discuss alternate mechanisms in the Discussion.

*Rap1 and Cno play roles in polarity maintenance but other cues partially restore apical*

*Baz during gastrulation*

The data above suggest Rap1 and Cno regulate the initial establishment of apical-basal polarity by helping position Baz and AJs. However, loss of Cno (Sawyer *et al.*, 2009) does not cause the same early, dramatic disruption of the ectodermal epithelium seen when either Baz or AJ proteins are lost (Cox *et al.*, 1996; Tepass *et al.*, 1996). Two mechanisms could be at play: 1) While the presence of Baz is clearly required for epithelial polarity, perhaps its apical restriction is not essential or 2) alternately, other cues might restore more normal Baz localization, when additional polarity cues like the aPKC/Par6 module come into play at gastrulation onset to reinforce and elaborate initial polarity (Hutterer *et al.*, 2004; Harris and Peifer, 2005).

To test these alternate hypotheses, we examined Baz localization in *Rap1* and *cno* mutants at gastrulation onset (stage 6) and as germband extension began (stage 7). In both mutants, 50% of embryos receive a wild-type paternal copy of the relevant gene, and thus are potentially zygotically rescued. As gastrulation begins in wild-type, AJs and Baz continue to co-localize (Harris and Peifer, 2004, 2005). Apical junctional complexes tighten along the apical-basal axis, and during stage 7 they move to the apical end of the lateral cell interface (Fig 6A,G). We found above that *Rap1* mutants lost apical enrichment of Baz during cellularization. As gastrulation commenced (stage 6; Fig. 6B,C) and germband extension began (stage 7; Fig. 6H,I), Baz continued to be mis-localized in *Rap1* mutants, with many Baz puncta remaining basal to the apical junctions. However, there was clearly some restoration of apical Baz, both in presumptive *Rap1^{MZ}* (Fig. 6B,H) and presumptive zygotically-rescued embryos (Fig. 6C,I; we divided

embryos into classes based on phenotypic severity; 7/14 stage 6 and 6/12 stage 7 embryos

had the less severe phenotype).  There was similar partial rescue of apical Baz

enrichment in $cno^{MZ}$ mutants, with subtle restoration of apical Baz enrichment at stage 6

(Fig. 6D vs E), and significant restoration of apical Baz, albeit with remaining mis-

localized Baz, at stage 7 (Fig. 6J vs K).   Presumptive zygotically rescued embryos had

slightly less severe phenotypes, with more complete restoration of apical Baz (Fig. 6F,L;

9/17 stage 6 and 8/15 stage 7 embryos had the less severe phenotype).  We once again

quantitated Baz localization in multiple embryos, confirming our qualitative

observations.  The wild-type profiles show the sharpening of the apical Baz peak during

gastrulation from stage 6 (Fig. 6M,S) to stage 7 (Fig. 6P,V).  In *Rap1* mutants, an apical

Baz peak begins to reappear at gastrulation onset (stage 6; Fig. 6N,O), even in

presumptive $Rap1^{MZ}$ mutants (Fig. 6O), but some Baz remains mis-localized, broadening

and lowering the peak.  By stage 7, most Baz is apical (Fig. 6Q,R), but even in the least

severe mutants the apical peak does not sharpen as it does in wild-type (Fig 6R).  In *cno*

mutants the situation is similar--an apical Baz peak begins to reappear by stage 6 (Fig.

6T,U) and strengthens at stage 7 (Fig. 6W,X).  Averaging the individual embryos

revealed that the overall the degree of rescue was somewhat more complete in *cno* than in

*Rap1* mutants (Suppl. Fig. 3A vs C, B vs D).   Thus, Rap1 and Cno play continuing roles

in the maintenance of apical Baz, but additional cues that come into play at gastrulation

onset partially restore apical Baz enrichment.

***Rap1 and Cno are required for proper organization of Baz into planar polarized***

***junctional belts***

In the XY-plane, junctional protein localization is more complex.  As the

germband extends (Fig. 7A), spot AJs and associated Baz smooth into less punctate, more continuous belt AJs (Tepass and Hartenstein, 1994), and both Baz and AJ proteins become planar polarized, with enrichment along dorsal/ventral (Fig. 7D' arrowheads, D' closeup) vs. anterior/posterior cell borders (Fig. 7D', arrows; Bertet *et al.*, 2004; Zallen and Wieschaus, 2004). In $cno^{MZ}$ mutants, Baz planar polarization is significantly accentuated, with near loss of Baz on anterior-posterior borders (Sawyer *et al.*, 2011). We found that in *Rap1* mutants, Baz localization was similarly altered, with the most severe embryos (likely $Rap1^{MZ}$, based on strength of mesoderm invagination defects) having cortical Baz significantly reduced overall, and virtually lost on anterior-posterior borders (Fig. 7B,E,E' closeup). This coincided with separation of myosin from the anterior and posterior cortex (Fig. 7G), as occurs in $cno^{MZ}$ mutants (Sawyer *et al.*, 2011). In less affected *Rap1* mutants (presumptive zygotically rescued embryos), Baz cortical localization was less reduced, but Baz remained more punctate along the cortex than in wild-type (Fig. 7D' vs F'). Thus both Cno and Rap1 are required for proper maintenance of Baz localization during gastrulation, regulating both its apical-basal and planar polarity.

*Loss of Rap1 or Cno leads to disruption of epithelial integrity by the end of gastrulation*

We next tested whether this junctional disruption affected epithelial integrity, or whether the partial rescue of Baz localization coincided with restored epithelial architecture. As germband extension continues in stage 8, ectodermal cells undergo patterned mitosis, rounding up, reducing cortical AJ proteins (Suppl. Fig 1C) and Baz (Suppl. Fig 1E,H) during division, and then rebuilding apical junctions and resuming a

158

columnar shape.  While cells assemble and maintain AJs in in some tissues in Cno's

absence (e.g. the dorsal epidermis), other tissues, like the ventral epidermis, ultimately

lose epithelial integrity, disrupting the ventral cuticle (Sawyer *et al.*, 2009).  *Rap1^MZ*

mutants had similar or more severe cuticle defects; in many even the dorsal epidermis

was reduced to fragments (Suppl. Fig. 1B).  To determine when loss of Rap1 affected

epithelial architecture, we examined later *Rap1^MZ* mutants.  In wild-type stage 8 embryos,

non-dividing cells have strong apical Baz localization, and even dividing cells have

continuous but lower level junctional Baz (Suppl. Fig. 1E,H arrows).  In contrast,

junctional Baz was substantially less continuous in *Rap1* mutants.  In *Rap1^MZ* mutants

(Suppl. Fig. 1G; 10/21 stage 8-9 mutants had this strong phenotype), junctional Baz was

weak in the dorsal ectoderm (Suppl. Fig. 1H' vs J' arrows), and in the ventrolateral

ectoderm Baz localized only to junctional fragments (Suppl. Fig. 1H' vs J', arrowheads).

Zygotically-rescued embryos (Suppl. Fig. 1F; 11/21 stage 8-9 mutants had the weaker

phenotype) had similar but less severe defects (Suppl. Fig. 1I' arrows, arrowheads).

Thus, the partial rescue of apical Baz localization in *Rap1^MZ* mutants is not sufficient to

allow ventral ectodermal cells to maintain junctional integrity during gastrulation,

consistent with the fragmented cuticle.  These data suggest that Cno and Rap1 are

important to maintain epithelial integrity in morphogenetically active tissues.

***Baz and aPKC are not essential for apical Cno enrichment but play roles in Cno***

***positioning***

        The data above support the hypothesis that Rap1 and Cno act upstream of Baz,

ensuring its restriction to nascent spot AJs.  In this view, Rap1 and Cno fill the missing

place in a linear model of polarity establishment, with Baz then acting upstream of both

AJs and aPKC to ensure their apical positioning (Fig. 1A; Harris and Peifer, 2004, 2005). In this linear model, neither Baz nor aPKC should be essential for positioning Cno, as both are "downstream" of it. However, later junctional maintenance/elaboration does not involve a linear pathway, but instead relies on an interlocking network of positive and negative interactions (e.g. (Bilder *et al.*, 2003; Tanentzapf and Tepass, 2003). To test the alternate hypotheses that polarity establishment behaves in a linear fashion, or that Baz and Cno fit into an interlocked network with feedback loops, we examined Cno positioning in embryos lacking Baz or aPKC.

We generated embryos with severely reduced levels of Baz using the new Valium RNAi lines (Ni *et al.*, 2009), expressing shRNAs targeting *baz* in the germline using maternal GAL4 drivers. We confirmed that this led to the expected lethality and disrupted cuticle integrity (data not shown), consistent with very strong loss of function, and further confirmed this treatment reduced Baz protein to background levels in situ (Suppl Fig. 4A' vs B'). To confirm that Baz reduction affected AJ assembly, we examined Arm localization. As we previously observed in $baz^{MZ}$ mutants (Harris and Peifer, 2004), *baz* RNAi disrupted apical Arm enrichment in nascent spot AJs (Suppl Fig. 4" vs. B", brackets), leading to accumulation all along the basolateral axis, but without disrupting Arm enrichment in basal junctions (Suppl Fig. 4A" vs. B", arrows).

We used *baz* RNAi to determine whether Baz helps regulate Cno localization. In wild-type embryos, Cno is enriched in nascent apical junctions from the onset of cellularization, and by mid- to late-cellularization Cno is enriched apically in spot AJs (Fig, 8A), with strong enrichment at tricellular junctions (Fig. 8G; Sawyer *et al.*, 2009). The Cno at tricellular junctions extends deeper into the cell, creating apical-basal

"cables" of Cno at each tricellular junction, which are apparent in cross-sections (Fig. 8A', maximum intensity projection). At gastrulation onset, Cno moves further apically, but the cables remain prominent (Fig. 8E'). Baz knockdown affected both cell shape and Cno localization. As documented below, in Baz-depleted embryos apical cell shape was already altered during cellularization, with the apicalmost region of the cells expanded or reduced in area. In Baz-depleted embryos, Cno was still largely restricted to membrane-associated puncta in the apical third of the cell (Fig. 8B', brackets), and still accumulated in spot AJs (Fig. 8D2). However, Cno was not as tightly focused where spot AJs normally form, instead spreading along the basolateral membrane (Fig. 8A' vs B', brackets). Further, the cables of Cno were essentially eliminated (Fig. 8A' vs B'). Finally, Cno was not properly restricted from the apical domain (Fig. 8C1 vs. D1). All of these changes in Cno localization in Baz-depleted embryos were further accentuated as gastrulation began (Fig 8E vs F). Thus while Baz is not essential for apical Cno enrichment, Baz depletion altered the precise positioning of Cno at tricellular junctions during cellularization, and prevented the apical exclusion of Cno as gastrulation began. These data suggest that a strictly linear model with Cno "upstream" of Baz is oversimplified.

We next extended this analysis to aPKC, which regulates polarity maintenance during gastrulation (Hutterer *et al.*, 2004). In aPKC's absence, AJs and Baz assemble into spot AJs during cellularization (Harris and Peifer, 2005); Fig. 9A vs. B,E-H Arm), but at gastrulation onset AJs and Baz abnormally coalesce on dorsal and ventral cell borders (Harris and Peifer, 2007), in an exaggerated version of their normal planar polarity. Cells then lose polarity, with Baz and AJs forming non-polarized aggregates

161

(Hutterer *et al.*, 2004; Harris and Peifer, 2007). To determine whether initial Cno apical localization is independent of aPKC, as predicted by the linear model, we generated embryos maternally and zygotically mutant for the strong *aPKC* allele *aPKC^K06403^* (*aPKC* below; 50% of embryos receive paternal wild-type *aPKC*, and cannot be distinguished prior to gastrulation).

We were surprised to find that loss of aPKC affected Cno localization during cellularization. In wild-type cellularization, there is a modest pool of Cno in the apicalmost region of the cell early (Fig. 9A, arrow), both diffuse and in puncta that maybe similar to the apical puncta of DEcad and Baz seen at this time (McGill *et al.*, 2009). By late cellularization, most apical Cno disappeared (Fig., 9I', arrow, L'), as Cno assembled into cables at tricellular junctions (Fig. 9I' bracket, I' Maximum intensity projection). Loss of aPKC did not prevent Cno from localizing to nascent spot AJs in roughly the appropriate apical-basal position (Fig 9B,J, brackets) where Arm and Cno co-localize AJs (Fig 9B, E,G,K' vs, F,H.L). However, loss of aPKC had two more subtle effects on Cno localization. First, the cables of Cno that normally assemble at tricellular junctions were disrupted (Fig. 9I' vs J', maximum intensity projections), mimicking the disruption in Baz-depleted embryos. Second, Cno was not lost from the apical region, as it normally is by late cellularization (Fig. 9I' vs. J' arrow, K vs L). These data suggest that aPKC plays an unexpected early role in precisely positioning Cno during cellularization.

We were surprised that aPKC had such an early role, since our earlier work (Harris and Peifer, 2005) suggested it did not localize to the membrane until late cellularization and did not affect AJs until gastrulation. We thus re-examined when

162

cortical aPKC appears. We previously used used heat fixation (Harris and Peifer, 2005), a relatively harsh fixation that enhances junctional staining of AJ proteins by allowing removal of the cytoplasmic pool. We thus explored whether there was a membrane-associated pool of aPKC we missed in our previous work. Cno (Suppl. Fig. 2A), AJ proteins (Suppl. Fig 2A; McCartney *et al.*, 2001), and Baz (Suppl. Fig. 2H) are all present at the membrane in metaphase furrows of syncytial embryos. When we examined embryos fixed with formaldehyde, we detected a pool of aPKC we previously missed in heat-fixed embryos. We saw membrane-localized aPKC as early as syncytial stages, where it localized to metaphase furrows (Suppl. Fig. 2L). Cortical aPKC remained during cellularization (Suppl. Fig. 2M-O; we confirmed the specificity of this membrane pool by determining that it is lost in *aPKC* mutants; data not shown), when Cno, Arm and Baz enter nascent spot AJs (Suppl. Fig. 2B-G, J). aPKC was not enriched in spot AJs during cellularization (Suppl. Fig 2N) but instead localized all along the lateral membrane (Suppl. Fig. 2O)—the apical aPKC visualized after heat-fixation during late cellularization (Harris and Peifer, 2005) may be a more stable, perhaps cytoskeletally associated pool. Thus aPKC is positioned to regulate Cno localization during cellularization.

During gastrulation and after, aPKC helps maintain the apical domain by mediating exclusion of basolateral and junctional proteins. Consistent with this, the elevated apical accumulation of Cno in *aPKC* mutants became even more accentuated at gastrulation onset (Suppl. Fig. 5A vs B, arrows). As gastrulation proceeded, Cno became even more highly elevated in the apical membrane of *aPKC* mutants (Suppl. Fig. 5E vs. F), and Cno also localized with Arm in the mis-localized spot AJs at the dorsal and

ventral cell boundaries (Suppl. Fig. 5H, arrowheads). As we observed with Baz depletion, this change in apical restriction of Cno in *aPKC* mutants coincided with alterations in apical cell shape, with the apical most regions of the cells expanded or reduced in area (see below). Thus aPKC restricts Cno from localizing to the apical domain from cellularization onward, once again inconsistent with a simple linear hierarchy. Together, these data suggest that initial junctional assembly is not a simple linear pathway, but rather proteins are localized through a network of regulatory interactions, with, for example, Cno regulating Baz localization and Baz also regulating Cno positioning.

### *Rap1 plays a role in regulating cell shape that is Cno-independent*

Our data suggest Rap1 and Cno both regulate polarity establishment and maintenance. However, Rap1 has other effectors in addition to Cno/afadin, suggesting that it might have Cno-independent mechanisms of regulating junctions and the cytoskeleton. In stage 5 *Rap1* mutants, we noted a defect in cell shape that was not apparent in *cno* mutants. During wild-type cellularization, as the actomyosin network constricts to draw membranes around each nucleus, the resulting cells are columnar in architecture, with relatively uniform cell areas from apical to basal, and with each cell similar in this regard to its neighbors (Fig. 10A-A"; cells are slightly more variable apically). In contrast, the cell areas of *Rap1* mutants were quite a bit more variable, with some cells enlarged or reduced apically and others enlarged or reduced basally (Fig. 10C-C", arrows; cell areas in *Rap1$^{MZ}$* mutants were also on average overall larger, likely due to an elevated frequency of nuclear loss during syncytial stages (data not shown). To quantitate these differences in columnar cell shape, we stained cellularizing embryos for

the membrane protein neurotactin, and took slices at three apical-basal positions—near the apical surface (0.9µm deep; Fig 10A-E), at spot AJs (3.0µm deep; Fig. 10A'-E') and at the level of the nuclei (6.9µm deep; Fig. 10A"-E"). We then analyzed cell areas using ImageJ, measuring areas of hundreds of cells and comparing the largely uniform columnar cell area of wild-type (Fig. 10A) with that of cells in *Rap1* mutants (Fig. 10C). We then calculated the coefficient of variance (CV), which quantitates the degree of variability in cell area, and assessed the significance of CV differences using Tukey's HSD test to correct for multiple comparisons. This confirmed our visual impressions: *Rap1* mutant cell areas are more variable than those of wildtype (Fig. 10F). The difference was statistically significant at the level of the nuclei (Fig. 10A",C",H CV 0.20 versus 0.09 in wild-type) and there was a trend toward more variability apically (CVs 0.29 vs 0.23 and 0.15 vs. 0.20; Fig 10F,G). Thus Rap1 plays a role in initial establishment of columnar cell shape.

We next examined whether Rap1 is required to maintain columnar cell shape, or whether this effect was rescued at gastrulation onset. While gastrulation results in significant changes in cell shape, most wild-type lateral ectodermal cells retain quite uniform apical areas during stages 6 and 7 (Fig. 11A,F-H; 12AF-H). In contrast, cells in *Rap1* mutants continue to be significantly more variable in apical (Fig. 11C,F; 12C,F) and more basal cell areas (Fig. 11C",G; 12C',G) at gastrulation onset (Fig.11) and during germband extension (Fig. 12). Thus Rap1 plays an important role in both establishment and maintenance of columnar cell shape.

Since Rap1 has other effectors, we examined whether Cno shares Rap1's role in establishing or maintaining columnar cell shape. Visual inspection suggested that *cno*

165

mutants had relatively uniform cell areas during cellularization, resembling wild-type (Fig. 10A-A" vs B-B"). To verify this, we quantitated cell shape in *cno* mutants. Apical cell areas in *cno* were less variable than in *Rap1* mutants, and were not statistically distinguishable from wild-type (e.g., basal cell area CV 0.12 for *cno* vs. 0.09 for wild-type and 0.20 for *Rap1*; Fig. 10F). These data suggest Cno does not play a key role in initially establishing columnar cell shape. We also examined maintenance of columnar cell shape in *cno* mutants during gastrulation. As we saw during cellularization, at gastrulation onset *cno* mutants retained more uniform apical cells areas than did *Rap1*mutants (Fig. 11A-A" vs B-B")—the variation is cell area in *cno* mutants was not statistically distinguishable from wild-type (Fig. 12F-H). During germband extension, while cell areas were more variable in *cno* mutants than in wild-type (Fig. 12A-A" vs B-B"), these differences did not reach statistical significance (Fig. 12F-H), unlike those in in *Rap1*mutants. Overall, these data are consistent with the possibility that Rap1 has a Cno-independent role in establishing and maintaining columnar cell shape.

### Baz and aPKC also play early roles in cell shape regulation

Baz, aPKC and AJ proteins are all required for <u>maintaining</u> columnar cell shape—embryos lacking them ultimately round up as they lose adhesion. However, complete loss of cell adhesion and epithelial architecture occurs at different times in these different genotypes—most cells in embryos lacking Baz or AJs round up and fall apart at gastrulation onset (Cox *et al.*, 1996; Harris and Peifer, 2004) while *aPKC$^{MZ}$* mutants proceed farther, only fully losing epithelial architecture at the end of germband extension (Hutterer *et al.*, 2004; Harris and Peifer, 2007). Given the data above suggesting that Rap1 may have a Cno-independent role in cell shape maintenance, and the data

suggesting that both Baz and aPKC are at the apical cortex before cellularization, we

examined whether either Baz or aPKC also regulate the establishment of columnar cell

shape.

Using the approach above, we quantitated apical cell area during cellularization in

*baz* RNAi and *aPKC* mutants. Strikingly, loss of Baz or aPKC affected initial

establishment of columnar cell shape at stage 5, increasing variability in apical cell area

(Fig. 10A vs. E,F). Apical cell areas in *baz* RNAi or *aPKC* mutants were significantly

more variable than in wild-type (Fig. 10F). However, unlike *Rap1* (Fig. 10C'), there was

less variability in cell area in more basal sections of *baz* RNAi or *aPKC* mutants ((Fig.

10D',E',E",F",G,H). These data suggest that both Baz and aPKC are important for

initially establishing columnar cell shape, in particular regulating the apicalmost region of

the nascent cells. Consistent with their known roles in maintaining epithelial

architecture, both *baz* RNAi and *aPKC* mutants also had defects in cell shape after

gastrulation onset (Fig. 11D-F,12D-F)—once again their most striking and significant

effects were on apical cell area. Together, these data demonstrate that both Baz and

aPKC act early in the process of cell shape establishment, further supporting the idea that

a network of regulatory interactions are already in place during cellularization.

**Discussion**

*Rap1 and Cno are critical for positioning Baz/Par3 and AJs during polarity*
*establishment*

*Drosophila* embryogenesis provides a superb model for apical-basal polarity

establishment and maintenance in vivo. The simultaneous formation of thousands of

cells during cellularization allows one to view the process from start to finish with high

resolution. Previous work suggested a hierarchy with Baz/Par3 protein at the top, with

Baz positioned by cytoskeletal cues and then directing apical positioning of both AJs and

the aPKC/Par6 complex (Harris and Peifer, 2004, 2005; Suppl. Fig. 6A). However,

proteins regulating Baz apical positioning remained unknown. Our data provide new

mechanistic insights into this process. They demonstrate that the small GTPase Rap1 and

the actin-binding protein Cno are essential for polarity establishment, regulating initial

apical positioning of both Baz and AJs (Suppl. Fig 6B).

In regulating polarity establishment, Rap1 and Cno could act by several possible

mechanisms. Their role in AJ positioning may be solely due to their effects on Baz

localization, or alternatively Rap1 and Cno may independently affect the localization of

both Baz and AJs. In the latter case, Cno may directly link AJs to the apical actin

scaffold, as we suggested it acts in apical constriction (Sawyer *et al.*, 2009). Rap1 and

Cno also clearly regulate Baz positioning. Since Baz apical positioning requires an apical

actin scaffold and dynein-based MT transport (Harris and Peifer, 2005), we examined

whether Rap1 and Cno act indirectly, by regulating cytoskeletal organization. However,

our data suggest this is not the case: both the MT and actomyosin cytoskeletons appear

normal in mutants. We thus think the most likely model is that Rap1 and Cno are

required for anchoring Baz apically. This could occur directly, by, for example Cno

binding Baz, or indirectly, via as yet known intermediaries. Of course, it remains

possible that Cno and Rap1 regulate Baz positioning through effects on MT transport or,

given Cno's apical localization, unloading at an apical docking site. It will be important

to test these possibilities. As we discuss in more detail below, it will also be important to

define the Cno- and Rap1-independent mechanisms that partially restore apical Baz

localization after gastrulation onset.

Since Rap1 is uniformly distributed along the apical basal axis (Sawyer *et al.*, 2009), the most likely hypothesis is that it is locally activated apically by a GEF (Suppl. Fig. 6B). A number of Rap1GEFs exist, many of which are conserved between mammals and flies. Recent work from the Reuter lab demonstrated that, like Cno and Rap1 (Sawyer *et al.*, 2009), the Rap1 GEF Dizzy (PDZ-GEF) plays an important role in coordinated mesodermal apical constriction (Spahn *et al.*, 2012), suggesting it is the GEF acting upstream of Cno and Rap1 in that process. They also suggest that Rap1 and Dizzy help regulate establishment of AJs (Spahn *et al.*, 2012). While similar in outline, their analysis of AJs differs from ours in detail, as they see strong effects on DEcad localization without similar effects on Arm localization. This is surprising, since these two components of the cadherin-catenin complex generally localize very similarly at the cortex. However, these differences aside, their data are consistent with Dizzy acting with Cno and Rap1 in AJ establishment—it will be important to examine the effects of Dizzy on Baz localization.

***Establishing columnar cell shape—a Cno-independent role for Rap1?***

In addition to the parallel roles of Rap1 and Cno in regulating initial apical-basal polarization, we identified a second role for Rap1 in establishing and maintaining columnar cell shape (Suppl. Fig. 6B). Our data suggest that this is partially or completely Cno-independent, and thus one of the many other Rap1 effectors may play a role in this process. It will be exciting to examine embryos mutant for other Rap1 effectors (Kooistra *et al.*, 2007), such as Krit1/Billi, TIAM/Stilllife, RIAM/Pico, or RhoL to see if they are required for establishing columnar cell shape. *baz* and *aPKC* mutants also had

defects in establishing columnar cell architecture (Suppl. Fig. 6B). It is possible that each

protein provides an independent mechanistic input into this process. This is consistent

with the observed differences in the details of how columnar cell shape is disrupted, with

Baz and aPKC primarily regulating apical cell area, while Rap1 affects cell shape at

multiple apical-basal positions. A more speculative but perhaps less likely possibility is

that Rap1 uses Baz and aPKC as effectors in establishing columnar cell shape. Fly Rap1

can form a complex with aPKC and Par6 (Carmena *et al.*, 2011), and Rap1 acts upstream

of cdc42/Par3/ aPKC in regulating polarity of cultured neurons (Schwamborn and

Puschel, 2004).

Having identified Rap1's direct effector(s) in regulating cell shape, we will need

to move downstream. Based on analogies with other epithelial tissues in fly

development, we hypothesize establishing columnar cell shape involves regulating apical

tension. Other small GTPases play key roles in this; e.g., Rho and cdc42 have striking

and opposing roles in apical tension regulation during fly eye development (Warner and

Longmore, 2009a,b). In that context, Rho acts via separate effectors to maintain AJs and

apical tension—it regulates tension via Rok, Diaphanous, and ultimately myosin

contractility. It will be interesting to determine whether the defects in apical cell shape in

the absence of Rap1, Baz, or aPKC also reflect unbalanced contractility in different

nascent cells, and which contractility regulators are involved. However, for now, this is

speculative.

### *Cell polarity establishment—a network model*

In our previous work, we had suggested a linear hierarchy regulating polarity

establishment, with Baz at the top, positioning AJs and aPKC (Suppl. Fig 6A; Harris and

Peifer, 2004, 2005). Our current work extends this hierarchy, positioning Rap1 and Cno upstream of Baz in this process. However, our data further suggest that viewing polarity establishment as a linear process is significantly over-simplified (Suppl. Fig. 6B).

We now know that all of the relevant players—including the AJ proteins, Baz, Cno and aPKC—are at the cortex in syncytial embryos, prior to cellularization and the initiation of apical-basal polarity. This places them in position to cross-regulate one another. Consistent with this, our data suggest that viewing relationships with an "upstream-downstream" point of view misses important reciprocal interactions that occur as polarity is established. Two examples point this out most clearly. First, our earlier work suggested that localization of aPKC occurs "downstream" of Baz, as apical positioning of aPKC at gastrulation onset requires Baz function (Harris and Peifer, 2005). Our new data reveal that Rap1 and Cno are, in turn, "upstream" of Baz, and thus, if things work in a strictly linear fashion, Rap1 and Cno should be "upstream" of aPKC. However, in contrast to this simple view, we found that precise positioning of Cno during cellularization requires aPKC—in its absence, Cno is not cleared from the apical region, and the apical-basal cables of Cno at tricellular junctions are not properly assembled. In a similar fashion, Baz, which in a linear model is "downstream' of Cno, also regulates precise positioning of Cno during cellularization. aPKC and Baz also play important roles in Cno localization during the early polarity maintenance phase beginning at gastrulation onset. Together, these data suggest that initially positioning of proteins along the apical-basal axis involves a network of protein interactions, similar to that previously suggested to regulate polarity elaboration during the extended germband phase and beyond, as cells develop the full suite of epithelial junctions (Bilder *et al.*, 2003;

171

Tanentzapf and Tepass, 2003; Laprise *et al.*, 2009). It will now be important to define mechanisms by which aPKC and Baz act to precisely position Cno—two broad possibilities are that they act on Cno directly, or that they modulate the fine scale architecture of the actin cytoskeleton, with indirect effects on Cno. It will also be exciting to determine if other polarity determinants, like the basolateral proteins Dlg, Scribble or Lgl, or the basolateral kinase Par1 also play roles in polarity establishment, as they do in polarity maintenance. Finally, it will be interesting to identify the cues that come into play at gastrulation onset, which partially restore apical Baz localization, as part of the increasingly complex network of partially redundant regulatory cues that give polarity its robustness.

**Acknowledgements**

**Materials and Methods**

*Fly Stocks*

Mutations are described at flybase.bio.indiana.edu. Wild type was *yellow white*. All experiments were done at 25°C unless otherwise noted. Stocks to make *Rap1*, *cno, or aPKC* germline clones were from the Bloomington Stock Center. *Rap1* germline clones were made by heat shocking 48-72h old $hsFLP^1$/+; FRT3L$^{2A}$$Rap1^{rv(R)B1}$/FRT3L$^{2A}$$ovo^{D1-18}$ larvae for 3hrs at 37°C. $aPKC^{k06403}$ and $cno^{R2}$

germline clones were generated similarly. Knockdown of *baz* was carried out by crossing maternal GAL4-VP16 to UAS-*baz*shRNAi (VALIUM 20) (Ni *et al.*, 2011) allowing overexpression of a baz-targeted siRNA during oogenesis.

### Immunofluorescence

The following fixations were used: Baz/Arm/Cno/Myosin/Nrt, heat-methanol (Müller and Wieschaus, 1996); phalloidin, 12min, 10% formaldehyde or 5min, 37% formaldehyde. aPKC/$\alpha$-tubulin/$\delta$-tubulin/Nrt were fixed in 4% formaldehyde for 20min. Embryos were methanol-devitillinized, or hand-devitillinized for phalloidin. All embryos were blocked/stained in PBS/1% goat serum/0.1% Triton X-100 and mounted in Aqua-Polymount (Polysciences).

### Image acquisition

Fixed samples were imaged with either the Zeiss LSM 510 (Zeiss 40X NA 1.3 Plan-Neofluar or Zeiss 63X NA 1.4 Plan-Apochromat oil immersion objectives) or Zeiss LSM710 confocal microscopes (Zeiss 40X NA 1.3 Plan-Neofluar oil immersion objective), and LSM or ZEN software. Adobe Photoshop CS4 was used to adjust input levels so the main range of signals spanned the entire output grayscale and to adjust brightness and contrast.

### Quantification of cell area variation

Embryos were heat-fixed and stained with Nrt to mark cell membranes for measurement. Images were acquired as z-stacks with a 0.3 or 0.5 micron step using a LSM 510 (Zeiss 63X NA 1.4 Plan-Apochromat oil objective) or LSM 710 (Zeiss 40X NA 1.3 Plan-Neofluar oil objective) respectively with a digital zoom of 2. Slices at the three depths (0.3, 3.0, 6.9 µm below the apical surface) were exported using LSM

173

software. Background was subtracted from these slices in ImageJ using a Gaussian filter, before treatment with a "Watershed" algorithm to trace cell boundaries from Nrt staining. The "Analyze Particles" feature in ImageJ was used to measure cell areas of all outlined cells within the slice, but edges were excluded. CV values (standard deviation of cell areas/mean of cell areas) were generated for each depth per embryo within Microsoft Excel. CV values between genotypes were compared at each depth using JMP Statistical Software. Values for each genotype underwent a logarithmic transformation, making a more symmetrical distribution that could be analyzed using a generalized linear model that corrected for the comparison of multiple genotypes. Significance was then assessed using a Tukey's test to correct for multiple comparisons. "Beeswarm" plots of cell areas were generated in GraphPad.

*Analysis of apical-basal positioning*

Images from fixed embryos were acquired as z-stacks with a 0.3 or 0.5 micron step using a LSM 510 (Zeiss 63X NA 1.4 Plan-Apochromat oil objective) or LSM 710 (Zeiss 40X NA 1.3 Plan-Neofluar oil objective) respectively with a digital zoom of 2. Using ZEN software, stacks were cropped down to a 708.8 micron area on the xy-axis and the blocks of x-y-z images were used to create maximum intensity projects through the y-axis using ZEN software (Figure 1XX). With ImageJ software (NIH, Bethesda, MD), projections were rotated 90 degrees counterclockwise and analyzed using the "Plot Profile" function to generate values of average fluorescence intensity along the apical-basal axis. Values were exported to Microsoft Excel to calculate averages and standard deviations. Graphs and heatmap images were generated using Microsoft Excel.

# References

Abe, K, Takeichi, M. (2008). EPLIN mediates linkage of the cadherin catenin complex to F-actin and stabilizes the circumferential actin belt. Proc Natl Acad Sci USA 105, 13-19.

Assemat, E, Bazellieres, E, Pallesi-Pocachard, E, Le Bivic, A, Massey-Harroche, D. (2008). Polarity complex proteins. Biochim Biophys Acta 1778, 614-630.

Bertet, C, Sulak, L, Lecuit, T. (2004). Myosin-dependent junction remodelling controls planar cell intercalation and axis elongation. Nature 429, 667-671.

Bilder, D, Schober, M, Perrimon, N. (2003). Integrated activity of PDZ protein complexes regulates epithelial polarity. Nat Cell Biol 5, 53-58.

Boettner, B, Harjes, P, Ishimaru, S, Heke, M, Fan, HQ, Qin, Y, Van Aelst, L, Gaul, U. (2003). The AF-6 homolog canoe acts as a Rap1 effector during dorsal closure of the Drosophila embryo. Genetics 165, 159-169.

Boettner, B, Van Aelst, L. (2009). Control of cell adhesion dynamics by Rap1 signaling. Curr Opin Cell Biol 21, 684-693.

Bos, JL. (2005). Linking Rap to cell adhesion. Curr Opin Cell Biol 17, 123-128.

Carmena, A, Makarova, A, Speicher, S. (2011). The Rap1-Rgl-Ral signaling network regulates neuroblast cortical polarity and spindle orientation. J Cell Biol 195, 553-562.

Carmena, A, Speicher, S, Baylies, M. (2006). The PDZ protein Canoe/AF-6 links Ras-MAPK, Notch and Wingless/Wnt signaling pathways by directly interacting with Ras, Notch and Dishevelled. PLoS ONE 1, e66.

Cavey, M, Rauzi, M, Lenne, PF, Lecuit, T. (2008). A two-tiered mechanism for stabilization and immobilization of E-cadherin. Nature 453, 751-756.

Chou, T-B, Noll, E, Perrimon, N. (1993). Autosomal P[ovo[D1]] dominant female-sterile insertions in *Drosophila* and their use in generating female germ-line chimeras. Development 119, 1359-1369.

Cox, RT, Kirkpatrick, C, Peifer, M. (1996). Armadillo is required for adherens junction assembly, cell polarity, and morphogenesis during *Drosophila* embryogenesis. J Cell Biol 134, 133-148.

David, DJ, Tishkina, A, Harris, TJ. (2010). The PAR complex regulates pulsed actomyosin contractions during amnioserosa apical constriction in Drosophila. Development 137, 1645-1655.

Dawes-Hoang, RE, Parmar, KM, Christiansen, AE, Phelps, CB, Brand, AH, Wieschaus, EF. (2005). folded gastrulation, cell shape change and the control of myosin localization. Development 132, 4165-4178.

Drees, F, Pokutta, S, Yamada, S, Nelson, WJ, Weis, WI. (2005). α-Catenin is a Molecular Switch that Binds E-cadherin/β-Catenin and Regulates Actin-Filament Assembly. Cell 123, 903-915.

Fournier, G, Cabaud, O, Josselin, E, Chaix, A, Adelaide, J, Isnardon, D, Restouin, A, Castellano, R, Dubreuil, P, Chaffanet, M, Birnbaum, D, Lopez, M. (2011). Loss of AF6/afadin, a marker of poor outcome in breast cancer, induces cell migration, invasiveness and tumor growth. Oncogene 30 3862-74.

Glading, A, Han, J, Stockton, RA, Ginsberg, MH. (2007). KRIT-1/CCM1 is a Rap1 effector that regulates endothelial cell-cell junctions. J Cell Biol 179, 247-254.

Goldstein, B, Macara, IG. (2007). The PAR proteins: fundamental players in animal cell polarization. Dev Cell 13, 609-622.

Grevengoed, EE, Fox, DT, Gates, J, Peifer, M. (2003). Balancing different types of actin polymerization at distinct sites: roles for Abelson kinase and Enabled. J Cell Biol 163, 1267-1279.

Gumbiner, B, Stevenson, B, Grimaldi, A. (1988). The role of the cell adhesion molecule uvomorulin in the formation and maintenance of the epithelial junction complex. J Cell Biol 107, 1575-1587.

Harris, TJ, Peifer, M. (2004). Adherens junction-dependent and -independent steps in the establishment of epithelial cell polarity in Drosophila. J Cell Biol 167, 135-147.

Harris, TJ, Peifer, M. (2005). The positioning and segregation of apical cues during epithelial polarity establishment in Drosophila. J Cell Biol 170, 813-823.

Harris, TJ, Peifer, M. (2007). aPKC controls microtubule organization to balance adherens junction symmetry and planar polarity during development. Dev Cell 12, 727-738.

Harris, TJ, Tepass, U. (2010). Adherens junctions: from molecules to morphogenesis. Nat Rev Mol Cell Biol 11, 502-514.

Harris, TJC. (2012). Adherens Junction Assembly and Function in the Drosophila Embryo. Int Rev Cell Mol Biol, 293, 45-83.

Hoshino, T, Sakisaka, T, Baba, T, Yamada, T, Kimura, T, Takai, Y. (2005). Regulation of E-cadherin endocytosis by nectin through afadin, Rap1, and p120ctn. J Biol Chem 280, 24095-24103.

Hunter, C, Wieschaus, E. (2000). Regulated expression of nullo is required for the formation of distinct apical and basal adherens junctions in the Drosophila blastoderm. J Cell Biol 150, 391-401.

Hutterer, A, Betschinger, J, Petronczki, M, Knoblich, JA. (2004). Sequential roles of Cdc42, Par-6, aPKC, and Lgl in the establishment of epithelial polarity during Drosophila embryogenesis. Dev Cell 6, 845-854.

Ikeda, W, Nakanishi, H, Miyoshi, J, Mandai, K, Ishizaki, H, Tanaka, M, Togawa, A, Takahashi, K, Nishioka, H, Yoshida, H, Mizoguchi, A, Nishikawa, S, Takai, Y. (1999). Afadin: A key molecule essential for structural organization of cell-cell junctions of polarized epithelia during embryogenesis. J Cell Biol 146, 1117-1132.

Kim, C, Ye, F, Ginsberg, MH. (2011). Regulation of integrin activation. Annu Rev Cell Dev Biol 27, 321-345.

Knox, AL, Brown, NH. (2002). Rap1 GTPase regulation of adherens junction positioning and cell adhesion. Science 295, 1285-1288.

Kooistra, MR, Dube, N, Bos, JL. (2007). Rap1: a key regulator in cell-cell junction formation. J Cell Sci 120, 17-22.

Lampugnani, MG, Orsenigo, F, Rudini, N, Maddaluno, L, Boulday, G, Chapon, F, Dejana, E. (2010). CCM1 regulates vascular-lumen organization by inducing endothelial polarity. J Cell Sci 123, 1073-1080.

Laprise, P, Lau, KM, Harris, KP, Silva-Gagliardi, NF, Paul, SM, Beronja, S, Beitel, GJ, McGlade, CJ, Tepass, U. (2009). Yurt, Coracle, Neurexin IV and the Na(+),K(+)-ATPase form a novel group of epithelial polarity proteins. Nature 459, 1141-1145.

Laprise, P, Tepass, U. (2011). Novel insights into epithelial polarity proteins in Drosophila. Trends Cell Biol 21, 401-408.

Liu, JJ, Stockton, RA, Gingras, AR, Ablooglu, AJ, Han, J, Bobkov, AA, Ginsberg, MH. (2011). A mechanism of Rap1-induced stabilization of endothelial cell-cell junctions. Mol Biol Cell 22, 2509-2519.

Lorger, M, Moelling, K. (2006). Regulation of epithelial wound closure and intercellular adhesion by interaction of AF6 with actin cytoskeleton. J Cell Sci 119, 3385-3398.

Lynch, AM, Hardin, J. (2009). The assembly and maintenance of epithelial junctions in C. elegans. Front Biosci 14, 1414-1432.

Mandai, K, Nakanishi, H, Satoh, A, Obaishi, H, Wada, M, Nishioka, H, Itoh, M, Mizoguchi, A, Aoki, T, Fujimoto, T, Matsuda, Y, Tsukita, S, Takai, Y. (1997). Afadin: A novel actin filament-binding protein with one PDZ domain localized at cadherin-based cell-to-cell adherens junction. J Cell Biol 139, 517-528.

Martin, AC, Gelbart, M, Fernandez-Gonzalez, R, Kaschube, M, Wieschaus, EF. (2010). Integration of contractile forces during tissue invagination. J Cell Biol 188, 735-749.

McCartney, BM, McEwen, DG, Grevengoed, E, Maddox, P, Bejsovec, A, Peifer, M. (2001). *Drosophila* APC2 and Armadillo participate in tethering mitotic spindles to cortical actin. Nat Cell Biol 3, 933-938.

McGill, MA, McKinley, RF, Harris, TJ. (2009). Independent cadherin-catenin and Bazooka clusters interact to assemble adherens junctions. J Cell Biol 185, 787-796.

Miyata, M, Ogita, H, Komura, H, Nakata, S, Okamoto, R, Ozaki, M, Majima, T, Matsuzawa, N, Kawano, S, Minami, A, Waseda, M, Fujita, N, Mizutani, K, Rikitake, Y, Takai, Y. (2009). Localization of nectin-free afadin at the leading edge and its involvement in directional cell movement induced by platelet-derived growth factor. J Cell Sci 122, 4319-4329.

Müller, H-AJ, Wieschaus, E. (1996). *armadillo*, *bazooka*, and *stardust* are critical for formation of the zonula adherens and maintenance of the polarized blastoderm epithelium in *Drosophila*. J Cell Biol 134, 149-165.

Munro, E, Nance, J, Priess, JR. (2004). Cortical flows powered by asymmetrical contraction transport PAR proteins to establish and maintain anterior-posterior polarity in the early C. elegans embryo. Dev Cell 7, 413-424.

Ni, JQ, Liu, LP, Binari, R, Hardy, R, Shim, HS, Cavallaro, A, Booker, M, Pfeiffer, BD, Markstein, M, Wang, H, Villalta, C, Laverty, TR, Perkins, LA, Perrimon, N. (2009). A Drosophila resource of transgenic RNAi lines for neurogenetics. Genetics 182, 1089-1100.

Ni, JQ, Zhou, R, Czech, B, Liu, LP, Holderbaum, L, Yang-Zhou, D, Shim, HS, Tao, R, Handler, D, Karpowicz, P, Binari, R, Booker, M, Brennecke, J, Perkins, LA, Hannon, GJ, Perrimon, N. (2011). A genome-scale shRNA resource for transgenic RNAi in Drosophila. Nat Methods 8, 405-407.

Sawyer, JK, Choi, W, Jung, KC, He, L, Harris, NJ, Peifer, M. (2011). A contractile actomyosin network linked to adherens junctions by Canoe/afadin helps drive convergent extension. Mol Biol Cell. 22, 2491-2508.

Sawyer, JK, Harris, NJ, Slep, KC, Gaul, U, Peifer, M. (2009). The Drosophila afadin homologue Canoe regulates linkage of the actin cytoskeleton to adherens junctions during apical constriction. J Cell Biol 186, 57-73.

Schwamborn, JC, Puschel, AW. (2004). The sequential activity of the GTPases Rap1B and Cdc42 determines neuronal polarity. Nat Neurosci 7, 923-929.

Shao, W, Wu, J, Chen, J, Lee, DM, Tishkina, A, Harris, TJ. (2010). A modifier screen for Bazooka/PAR-3 interacting genes in the Drosophila embryo epithelium. PLoS One 5, e9938.

Spahn, P, Ott, A, Reuter, R. (2012). The PDZ-GEF Dizzy regulates the establishment of adherens junctions required for ventral furrow formation in Drosophila. J Cell Sci., in press.

St Johnston, D, Sanson, B. (2011). Epithelial polarity and morphogenesis. Curr Opin Cell Biol 23, 540-546.

Tanentzapf, G, Tepass, U. (2003). Interactions between the crumbs, lethal giant larvae and bazooka pathways in epithelial polarization. Nat Cell Biol 5, 46-52.

Tepass, U, Gruszynski-DeFeo, E, Haag, TA, Omatyar, L, Török, T, Hartenstein, V. (1996). *shotgun* encodes *Drosophila* E-cadherin and is preferentially required during cell rearrangement in the neurectoderm and other morphogenetically active epithelia. Genes Dev 10, 672-685.

Tepass, U, Hartenstein, V. (1994). The development of cellular junctions in the *Drosophila* embryo. Dev Biol 161, 563-596.

Warner, SJ, Longmore, GD. (2009a). Cdc42 antagonizes Rho1 activity at adherens junctions to limit epithelial tension. J Cell Biol 187, 119-133.

Warner, SJ, Longmore, GD. (2009b). Distinct functions for Rho1 in maintaining adherens junctions and apical tension in remodeling epithelia. J Cell Biol 185, 1111-1125.

Wee, B, Johnston, CA, Prehoda, KE, Doe, CQ. (2011). Canoe binds RanGTP to promote Pins(TPR)/Mud-mediated spindle orientation. J Cell Biol 195, 369-376.

Wodarz, A, Nathke, I. (2007). Cell polarity in development and cancer. Nat Cell Biol 9, 1016-1024.

Yamada, S, Pokutta, S, Drees, F, Weis, WI, Nelson, WJ. (2005). Deconstructing the Cadherin–Catenin–Actin Complex. Cell 123, 889-901.

Zallen, JA. (2007). Planar polarity and tissue morphogenesis. Cell 129, 1051-1063.

Zallen, JA, Wieschaus, E. (2004). Patterned gene expression directs bipolar planar polarity in Drosophila. Dev Cell 6, 343-355.

Zhadanov, AB, Provance, DW, Jr., Speer, CA, Coffin, JD, Goss, D, Blixt, JA, Reichert, CM, Mercer, JA. (1999). Absence of the tight junctional protein AF-6 disrupts epithelial cell-cell junctions and cell polarity during mouse development. Curr Biol 9, 880-888.
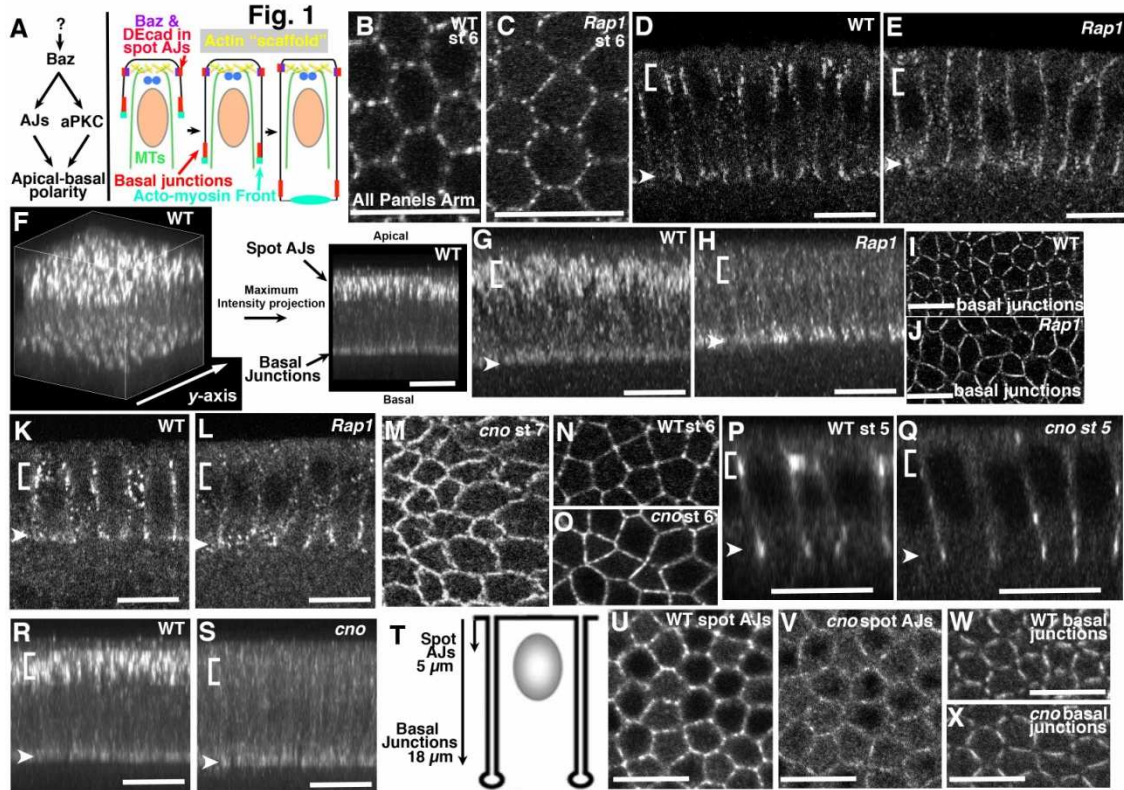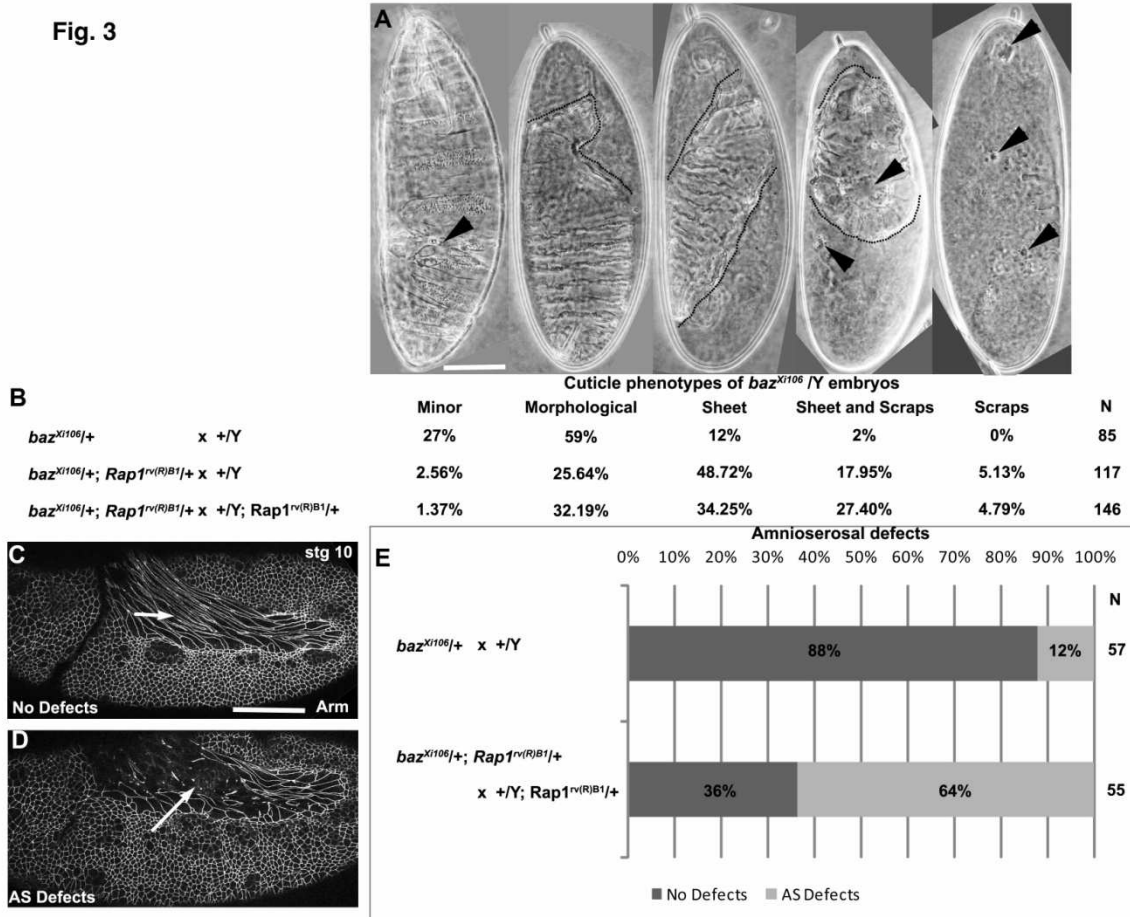
**Figure 4.1. Rap1 and Cno are required for initial assembly of apical adherens junctions.** A. Diagram of current model of polarity establishment (left) and of initial apical-basal polarization during cellularization (right). A-X. AJ protein Arm. B,C. Apical views, stage 6 (gastrulation onset). Spot AJs are present in both WT (B) and *Rap1* mutants (C). D-J Late cellularization. D,E. Apical-basal cross-sections. In WT (D) Arm is enriched at nascent apical spot AJs (bracket) and in basal junctions (arrowhead). In contrast, in *Rap1* mutants, apical spot AJ enrichment is reduced or lost (bracket). F. Approach for creating projections of cross sections. Image stacks were collected and maximum intensity projections created along the y-axis. This makes enrichment at forming apical junctions and basal junctions more readily apparent. G,H. Projections highlight loss of apical Arm enrichment in *Rap1* (H, bracket) versus WT (G, bracket), while basal junction enrichment remains (arrowheads). I, J. Basal junctions remain essentially unchanged in *Rap1* mutants (I vs J). K,L. Reduced apical enrichment in *Rap1* mutants (L, brackets) is already present at mid-cellularization. M-O. AJs are present in stage 7 *cno* mutants (M), and apical spot AJs are visible in stage 6 *cno* mutants (O) and WT (N). P-X. Late cellularization. P,Q. Single apical-basal cross sections. R,S. Projections of apical-basal cross sections (as in F). Arm is enriched in both spot AJs and basal junctions in WT (P,R brackets), while Arm enrichment in spot AJs is lost in *cno* mutants (Q,S bracket), although basal junction enrichment remains (arrowhead). Apical Arm enrichment is lost in in *cno* mutants (S), as compared to WT (R). T. Planes of surface views in U-X. U,V. The uniform enrichment of spot AJs in WT (U) is reduced in *cno* mutants (V), while basal junctions remain relatively unaltered (W vs. X). Scale bars=10µm.

181
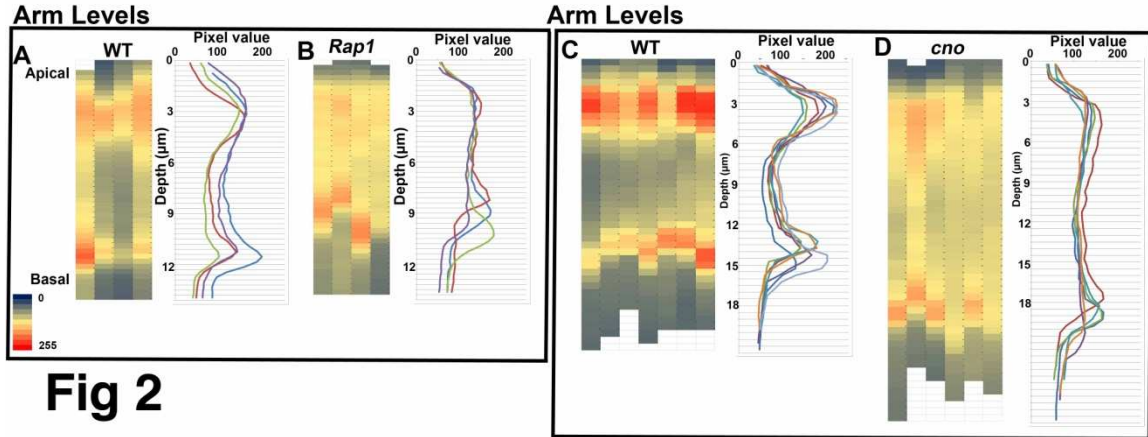
**Figure 4.2. Rap1 and Cno regulate apical positioning of Arm in forming apical junctions.**
A-D. The Plot Profile option in ImageJ was used to measure average image intensity in projected cross sections, and data was either displayed as heat maps illustrating intensity with different colors (left side—apical is on top; each column is a different embryo) or graphically, displaying pixel intensity versus depth from the apical surface (right side; each line is a different embryo). Note that since we utilized embryos from more than one experiment, these quantitative measures are useful for comparing signal intensity along the apical-basal axis within an embryo but absolute intensities between embryos vary due to variations in staining and imaging.

**Fig. 3**

**A**

**Cuticle phenotypes of *baz^{Xi106}*/Y embryos**

**B**

| | | Minor | Morphological | Sheet | Sheet and Scraps | Scraps | N |
|---|---|---|---|---|---|---|---|
| *baz^{Xi106}*/+ | x +/Y | 27% | 59% | 12% | 2% | 0% | 85 |
| *baz^{Xi106}*/+; *Rap1^{rv(R)B1}*/+ | x +/Y | 2.56% | 25.64% | 48.72% | 17.95% | 5.13% | 117 |
| *baz^{Xi106}*/+; *Rap1^{rv(R)B1}*/+ | x +/Y; Rap1^{rv(R)B1}/+ | 1.37% | 32.19% | 34.25% | 27.40% | 4.79% | 146 |

**C** — stg 10 — No Defects

**D** — AS Defects — Arm

**E**

**Amnioserosal defects**

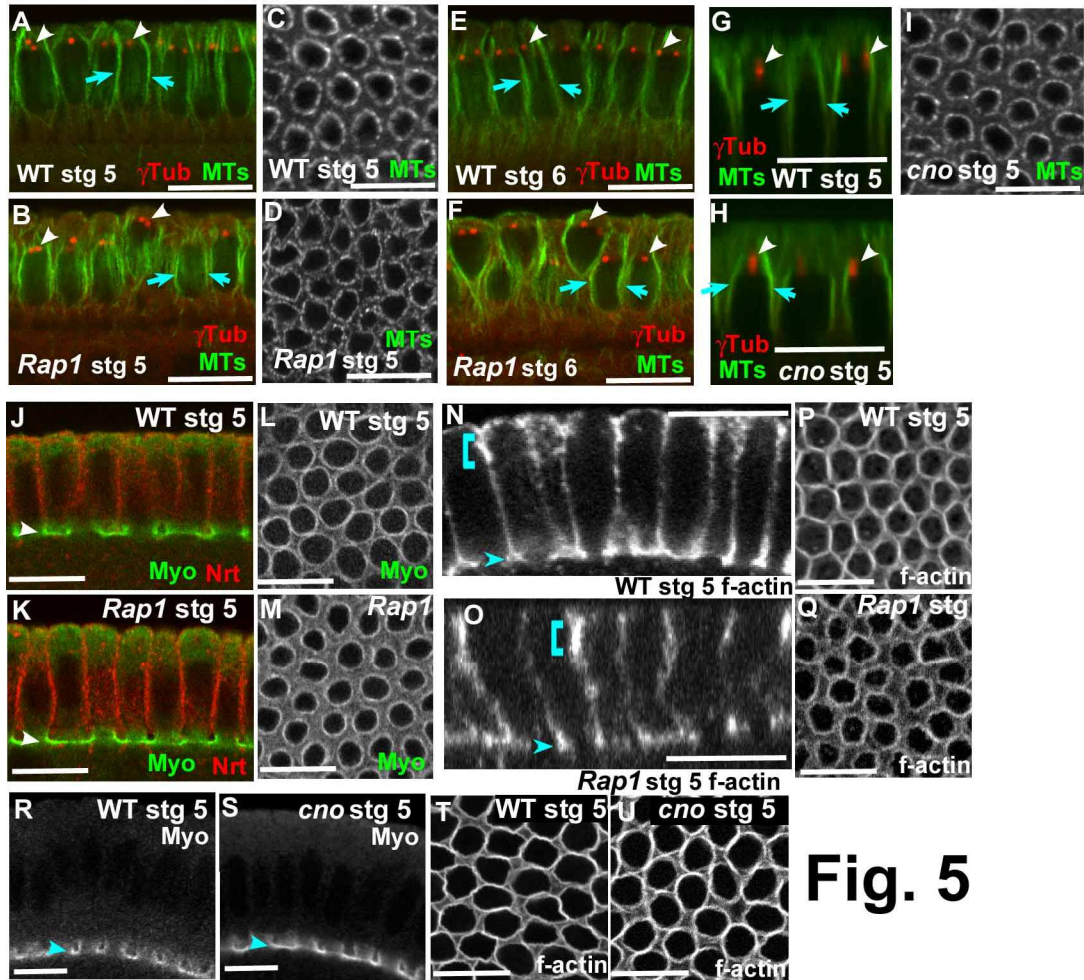| | No Defects | AS Defects | N |
|---|---|---|---|
| *baz^{Xi106}*/+  x +/Y | 88% | 12% | 57 |
| *baz^{Xi106}*/+; *Rap1^{rv(R)B1}*/+  x +/Y; Rap1^{rv(R)B1}/+ | 36% | 64% | 55 |

■ No Defects  ■ AS Defects

**Figure 4.3. Reducing Rap1 levels enhances the effects of reducing Baz function on epithelial integrity.** A. Cuticle preparations illustrating the range of defects in epithelial integrity seen in embryos with reduced Baz levels (zygotic *baz* mutants; embryos were left inside the vitelline eggshell). These range from nearly wild-type, with only minor cuticle holes (Minor, arrow), to strong defects in the head (Morphological), to half the cuticle remaining (Sheet), to smaller sheets of intact cuticle (Sheet and Scraps), to only fragments of cuticle remaining (Scraps). B. All embryos have reduced maternal Baz (mothers are heterozygous). We assessed the phenotype of the ~25% of embryos that die because they are *baz* zygotic mutant. Most *baz* zygotic mutants (top row) have only mild to moderate cuticle defects. Reducing maternal Rap1 levels by 50% (middle row) significantly enhances the epithelial defects of *baz* zygotic mutants. Further reducing Rap1 levels (heterozygous mothers; 25% of progeny are zygotic *Rap1* mutant) further enhances the epithelial defects of *baz* zygotic mutants. C-E. Analysis of amnioserosal AJ integrity (Arm) in progeny of crosses in B. In the cross generating zygotic *baz* mutants (E, top) 12% of embryos display defects in Arm localization within the amnioserosa as Baz levels run down (C arrow vs. D arrow; E). Reducing maternal and zygotic Rap1 substantially enhances the frequency of these defects, with 64% of embryos with amnioserosa defects (E, bottom). Scale bars=75µm
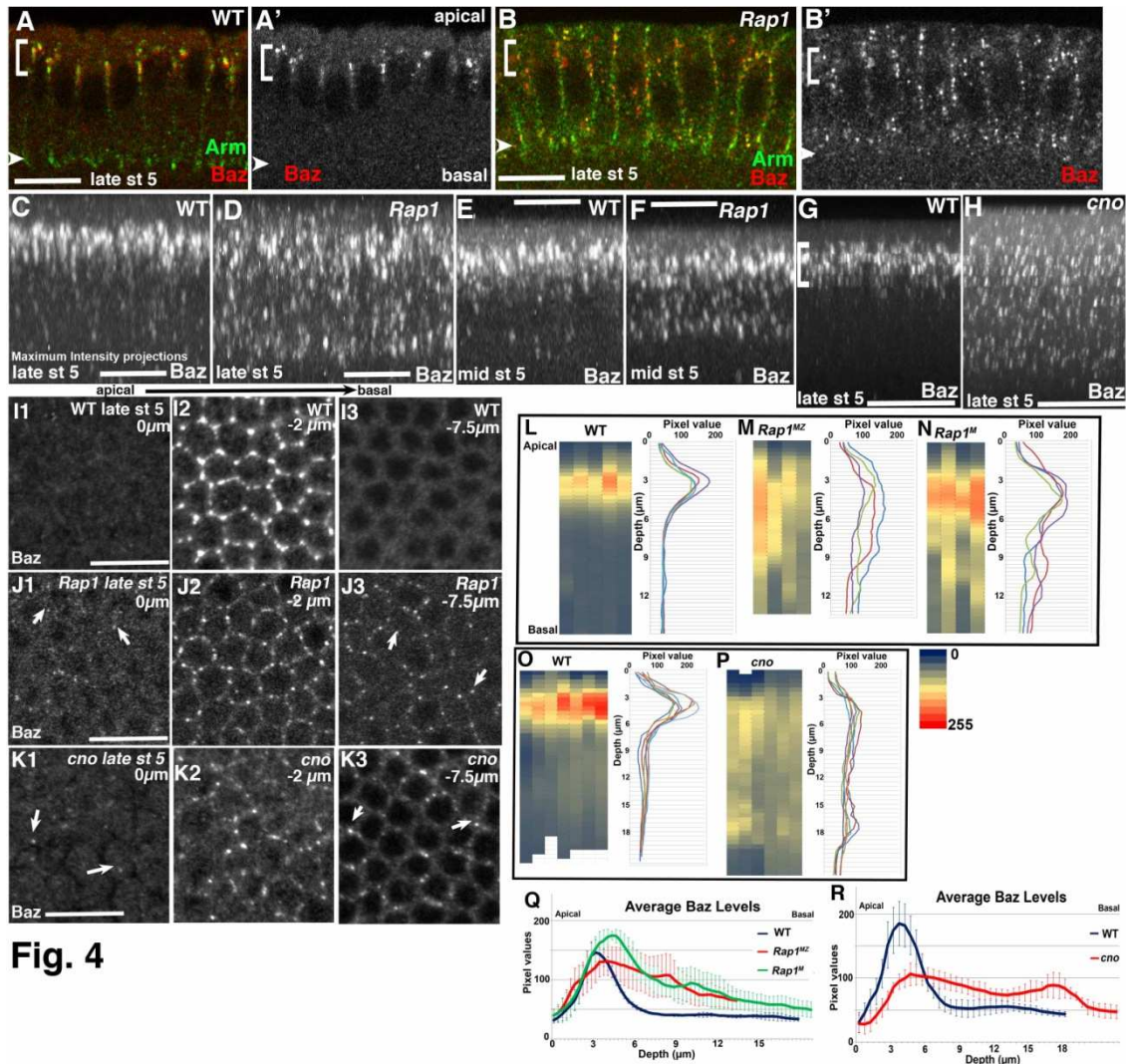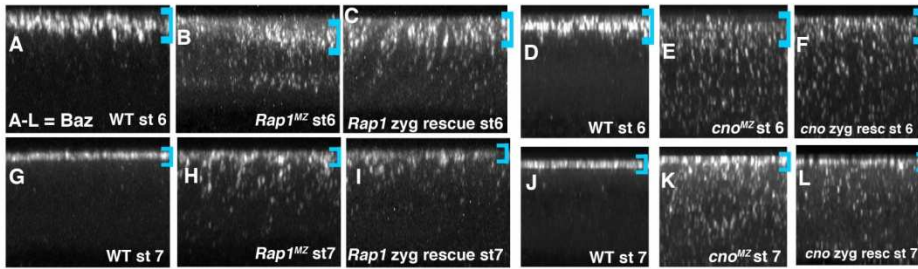
**Figure 4.4. Rap1 and Cno are required for initial apical enrichment of Baz.** A,B. Late cellularization. In WT Baz is restricted to forming apical junctions (A, bracket) while in *Rap1* mutants apical enrichment is lost and Baz puncta are all along the lateral border down to the basal junctions (arrowheads). C-H. Maximum intensity projections along the y-axis of cross sections. In late cellularization (C,G) this highlights exclusively apical Baz enrichment in WT (D) and reduced apical restriction in *Rap1* (E) and *cno* mutants (H). E,F. Reduced apical restriction of Baz in *Rap1* mutants begins to become apparent by mid-cellularization. I-K. Surface sections at different apical-basal depths, as indicated. Note that while Baz puncta are relatively tightly localized to apical junctions in WT (I), they are found both apical and basal to this position in *Rap* (J) or *cno* mutants (K). Scale bars=10µm. L-P. Quantitative analysis of changes in Baz localization along the apical-basal axis, as in Figure 2. We measured average image intensity in projected cross sections of multiple embryos, and data was displayed as heat maps illustrating intensity with different colors (left side—apical is on top; each column is a different embryo) or graphically, displaying pixel intensity versus depth from the apical surface (right side; each line is a different embryo). Q,R. Plots displaying the average Baz image intensity in embryos of different genotypes (apical is to the left).
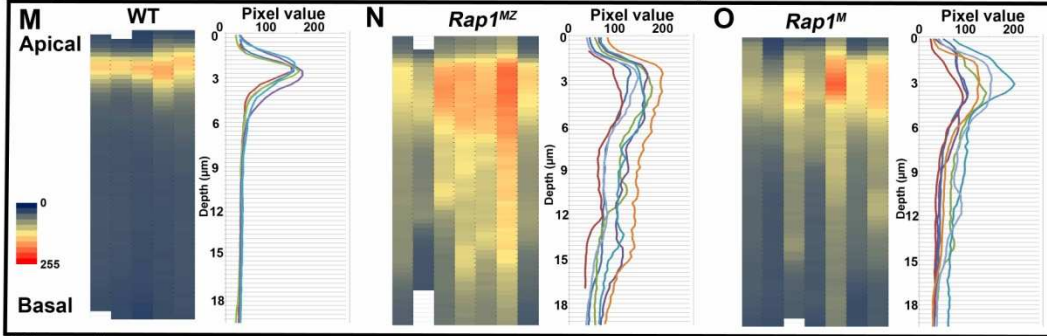
**Figure 4.5. Neither *Rap1* nor *cno* mutants have apparent defects in organization of the microtubule or actin cytoskeletons during cellularization.** Genotypes, antigens, and embryonic stages indicated—stage 5 = cellularization, stage 6=gastrulation onset. F-actin was detected with phalloidin. A-I. MTs and centrosomes visualized in apical-basal sections (apical up, A,B E,F,G,H) or in cross sections of nascent cells at level of nuclei (C,D,I) . Wild-type (WT), *Rap1* , and *cno* mutants all generate similarly polarized MT cytoskeletons during cellularization, with apical centrosomes (A,B,G,H arrowheads) and bundled MTs forming baskets projecting basally along the lateral surface (A,B,G,H arrows, C,D,I, in cross section). Even after *Rap1* mutants begin to lose columnar cell shape and some cells have enlarged (B, right arrowhead) or reduced apical ends, the MT cytoskeleton remains polarized. E,F. At gastrulation onset (stage 6) *Rap1* mutants retain a MT cytoskeleton with apical centrosomes (arrowheads) and MT baskets (arrows) even as they further lose columnar cell shape. J-M,R,S. Wild-type (WT), *Rap1*, and *cno* mutants all exhibited Myosin enrichment at the cellularization front (J,K,R,S, arrowheads) and form myosin rings (L,M). N-Q,T,U. Actin is similarly localized in wild-type (WT), *Rap1* , and *cno* mutants. Actin accumulates both in rings at the cellularization front (N,O arrowheads, P,Q,T,U in cross section) and at nascent apical junctions (N,O brackets). Scale bars=10μm.

185



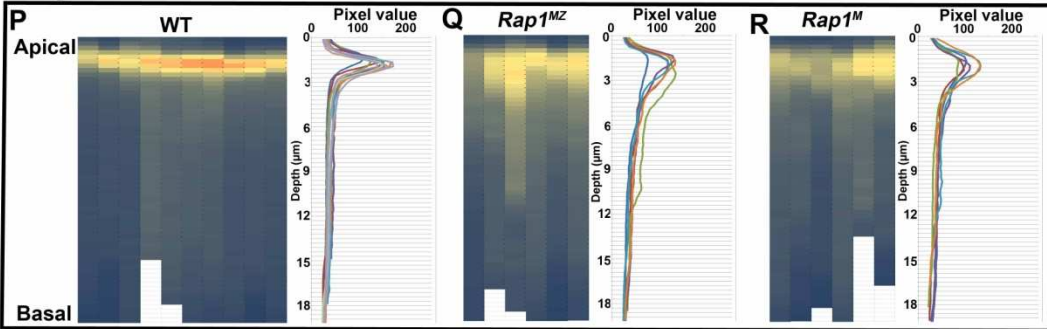
Fig. 6

Stage 6
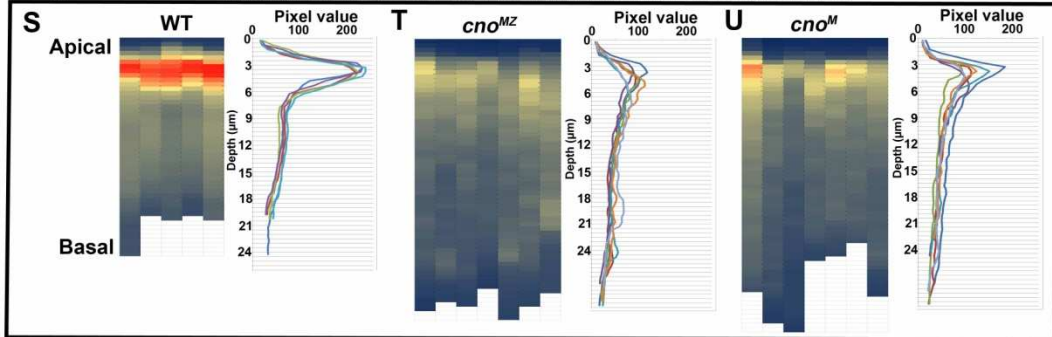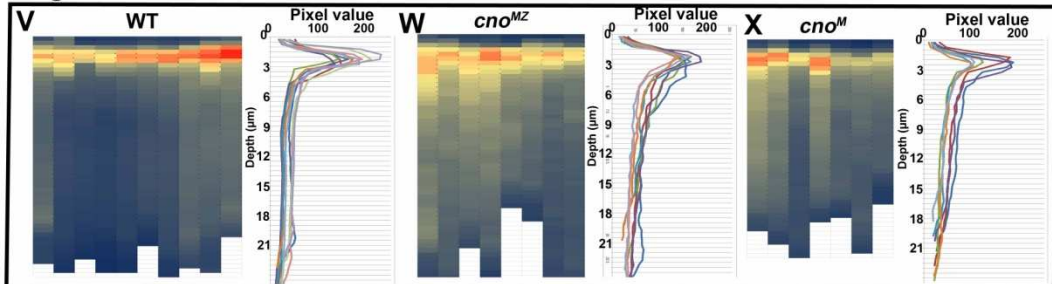**Maintenance of Baz localization in *Rap1* mutants**

Stage 7

Stage 6
**Maintenance of Baz localization in *cno* mutants**

Stage 7

186

**Figure 4.6. Rap1 and Cno regulate polarity maintenance but other cues partially restore apical Baz.** Genotypes and antigens indicated. A-L. Baz localization in apical-basal sections through embryos of indicated stages. We cannot distinguish maternal/zygotic and zygotically rescued mutants at this stage—we thus divided embryos into two classes based on phenotypic severity and show representative examples of each class). A,G,D,J. In wild-type (WT), Baz is apically localized at gastrulation onset (stage 6; A,D) and tighten up and moves to the extreme apical end of the cell during germband extension (stage 7; G,J). B,H.E,K. In presumptive $Rap1^{MZ}$ (B,H) and $cno^{MZ}$ mutants (E,K), Baz slowly becomes enriched apically but significant mis-localized Baz remains. C,I,F,L. In maternally mutant but zygotically rescued $Rap1^M$ (C,I) and $cno^M$ (F,L) embryos, restoration of apical Baz proceeds more completely than in maternal/zygotic mutants, but rescue remains incomplete. Scale bars=10µm. M-X. Average image intensity along the apical-basal axis in projected cross sections was assessed as in Fig 2, and data was either displayed as heat maps illustrating intensity with different colors (left side—apical is on top; each column is a different embryo) or graphically, displaying pixel intensity versus depth from the apical surface (right side; each line is a different embryo). Genotypes and stages are indicated. Since this analysis did not allow us to definitively distinguish zygotically rescued embryos, we binned the embryos into the most severe and least severe (they should be present in a 1:1 ratio), and labeled these as presumptive maternal/zygotic or zygotically rescued embryos.
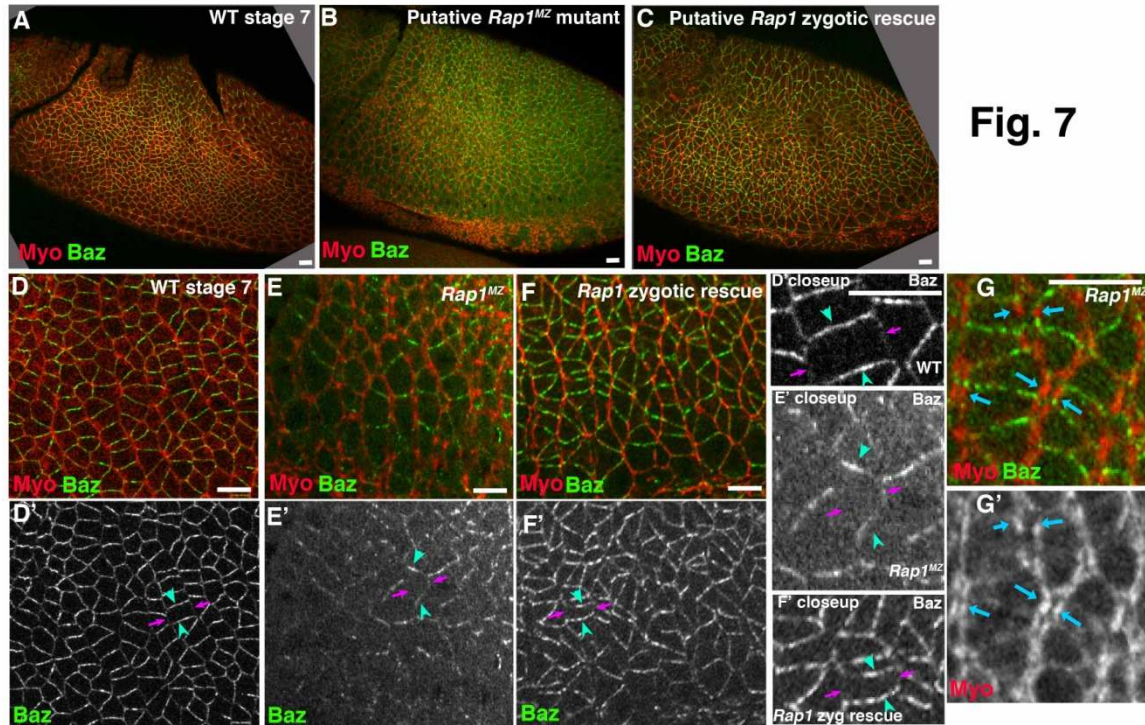
**Figure 4.7. Rap1 and Cno are important for maintaining Baz localization in planar polarized apical junctions during gastrulation** A-G. Surface views of stage 7 embryos. A-C. Lateral views. D-F. Closeups of lateral epidermis. D',E',F' further closeups. Baz becomes planar polarized in wild-type, with stronger accumulation on dorsal ventral boundaries (arrowheads) and weaker on anterior-posterior borders (arrows). E. Presumptive *Rap1^MZ* mutant (determined as in Fig. 6 legend). Overall accumulation of Baz at cortex is reduced, Baz is lost from anterior-posterior borders (arrows) and the remaining staining is discontinuous. F. Presumptive zygotically rescued *Rap1* mutant. Cortical Baz is more prominent but still less continuous than in wild-type. G. Myosin cables detach from anterior posterior boundaries in *Rap1* mutants (arrows), as we previously observed in *cno^MZ* mutants. Scale bars=10µm.
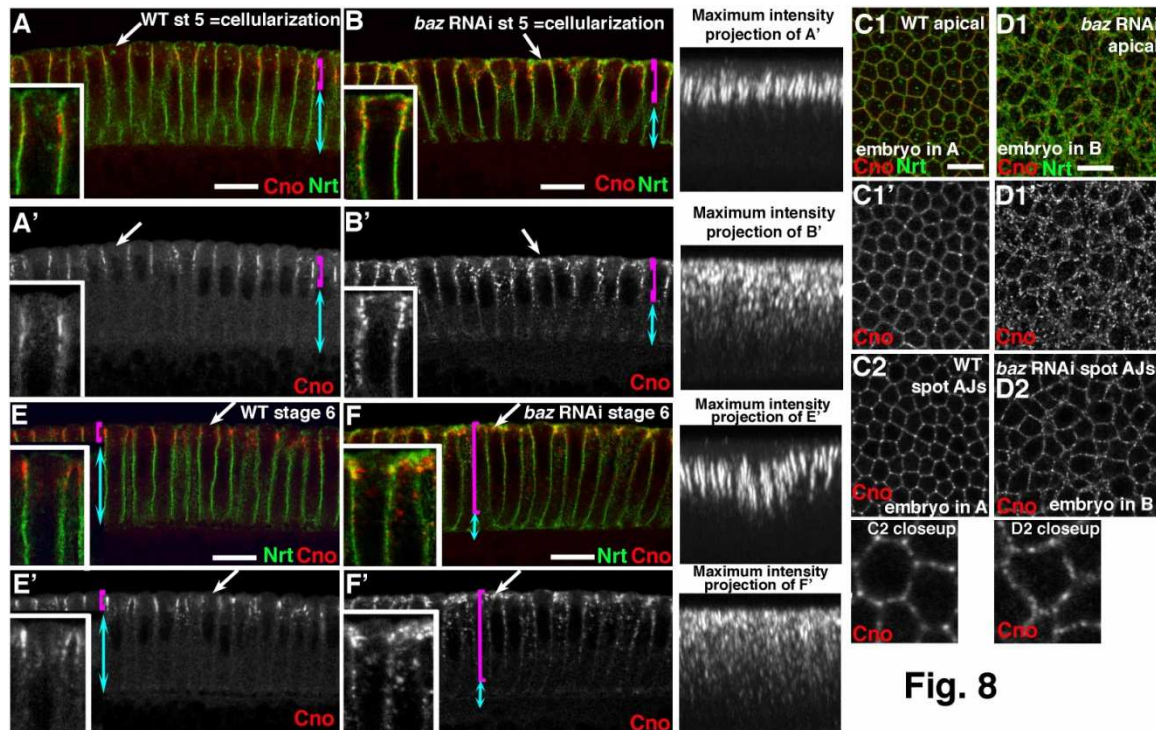
**Fig. 8**

**Figure 4.8. Baz is not required for Cno assembly into spot AJs, but does regulate precise Cno localization during polarity establishment.** A-D. Late Cellularization. A,B Apical-basal cross sections. C1,D1. Apical surface sections of embryo in A,B. C2,D2. Surface sections at level of normal spot AJs. In WT (A,C), Cno localizes along the apical end of the lateral membrane (A' bracket) to spot AJs (C2). In maximum intensity projections of multiple apical-basal sections (A'), cables of Cno that localize to tricellular junctions are apparent. Cno is also largely removed from the apical surface at this stage (A, arrow; E'). Reducing Baz by RNAi (B, F,H) leads to Cno spreading more basally (B' bracket vs. A' bracket), to loss of organized Cno cables as seen in maximum intensity projections (B'), and to failure to exclude Cno puncta from the apical membrane (B', arrow, C1' vs. D1'), but Cno still continues to assemble into spot AJs (D2). E,F. Gastrulation Onset (stage 6). In WT, Cno remains in spot AJs (E' bracket), and the apical-basal cables at tricellular junctions become even more prominent (E', projections). *baz* RNAi leads to spread of Cno basally (F'), perturbs assembly of Cno cables at tricellular junctions (F' maximum intensity projection) and allows Cno puncta to accumulate at the apical surface.(F' arrow and inset). Scale bars=10μm.

189
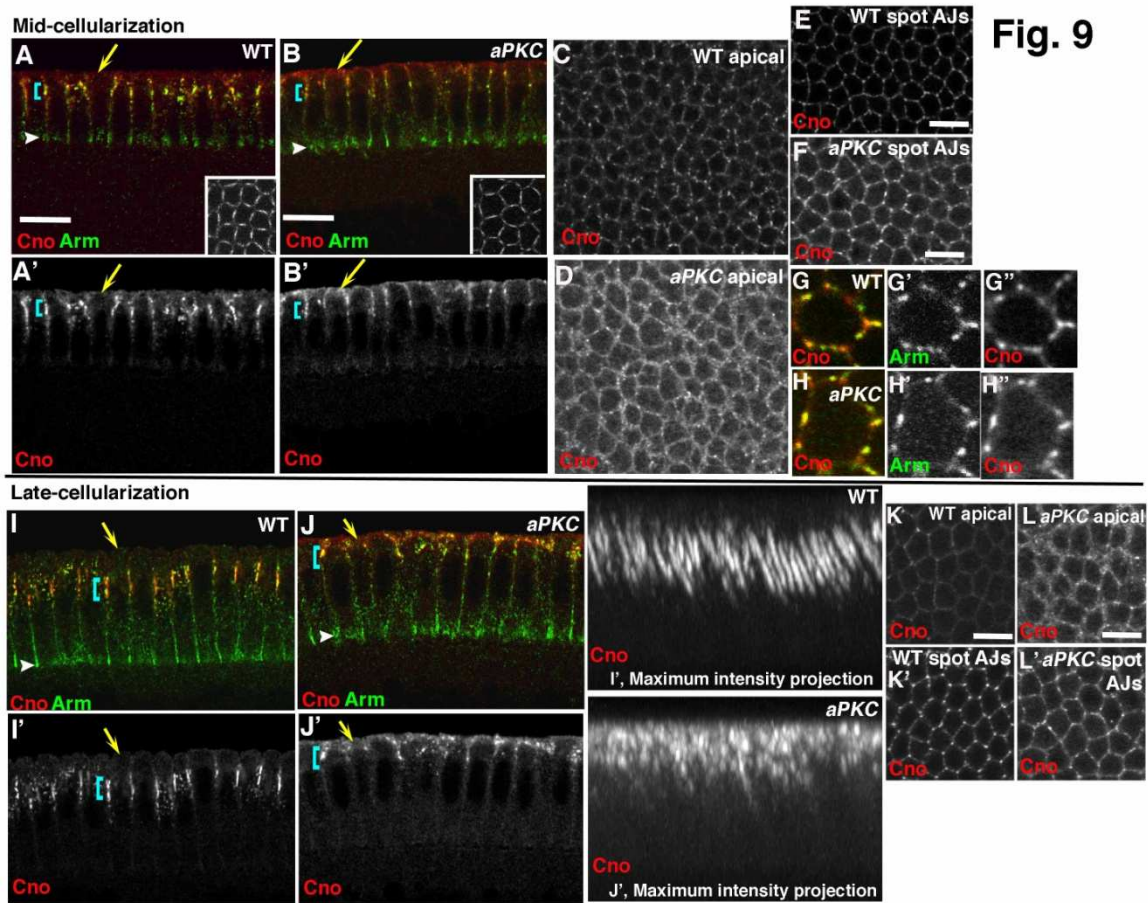
**Figure 4.9. *aPKC* mutants fail to exclude Cno from the apical domain.** A,B,I,J. Apical-basal sections. C-H,K,L. en face views. A-G . Mid-cellularization. Cno accumulates along the apicolateral membrane (A,B brackets) and in the apical region of the cell (A,B arrows) in both WT (A') and *aPKC* mutants (B'). Elevated Apical accumulation of Cno in *aPKC* mutants is already apparent in en face views (C vs. D), but Cno continues to accumulate in spot AJs (E,G vs F,H), and Arm accumulation in basal junctions is not perturbed (A,B arrowheads). I-L. Late cellularization, While in WT Cno is removed from the apical region (I' arrow, K), Cno remains there in *aPKC* mutants (J' arrow, L). Scale bars=10µm.
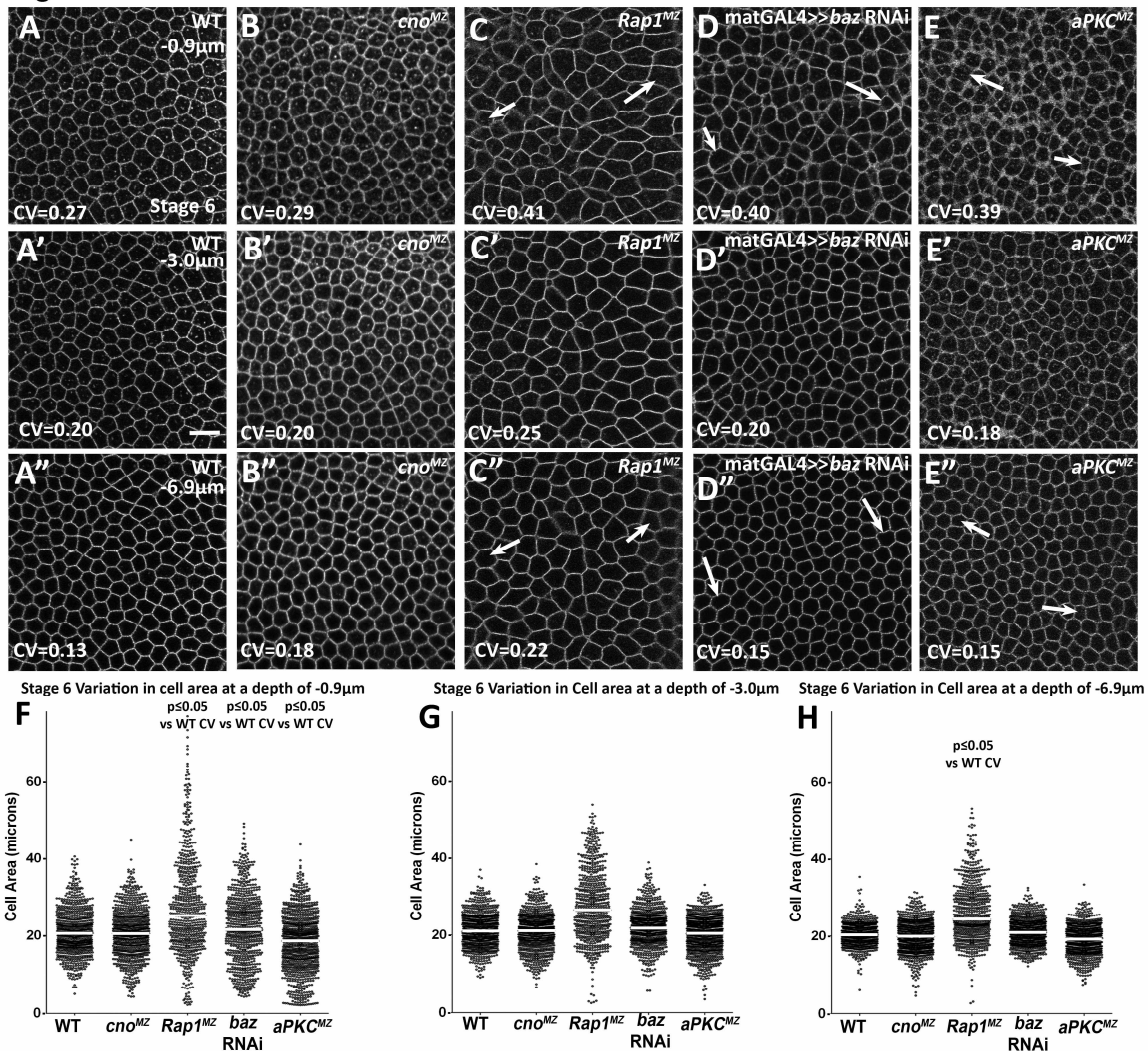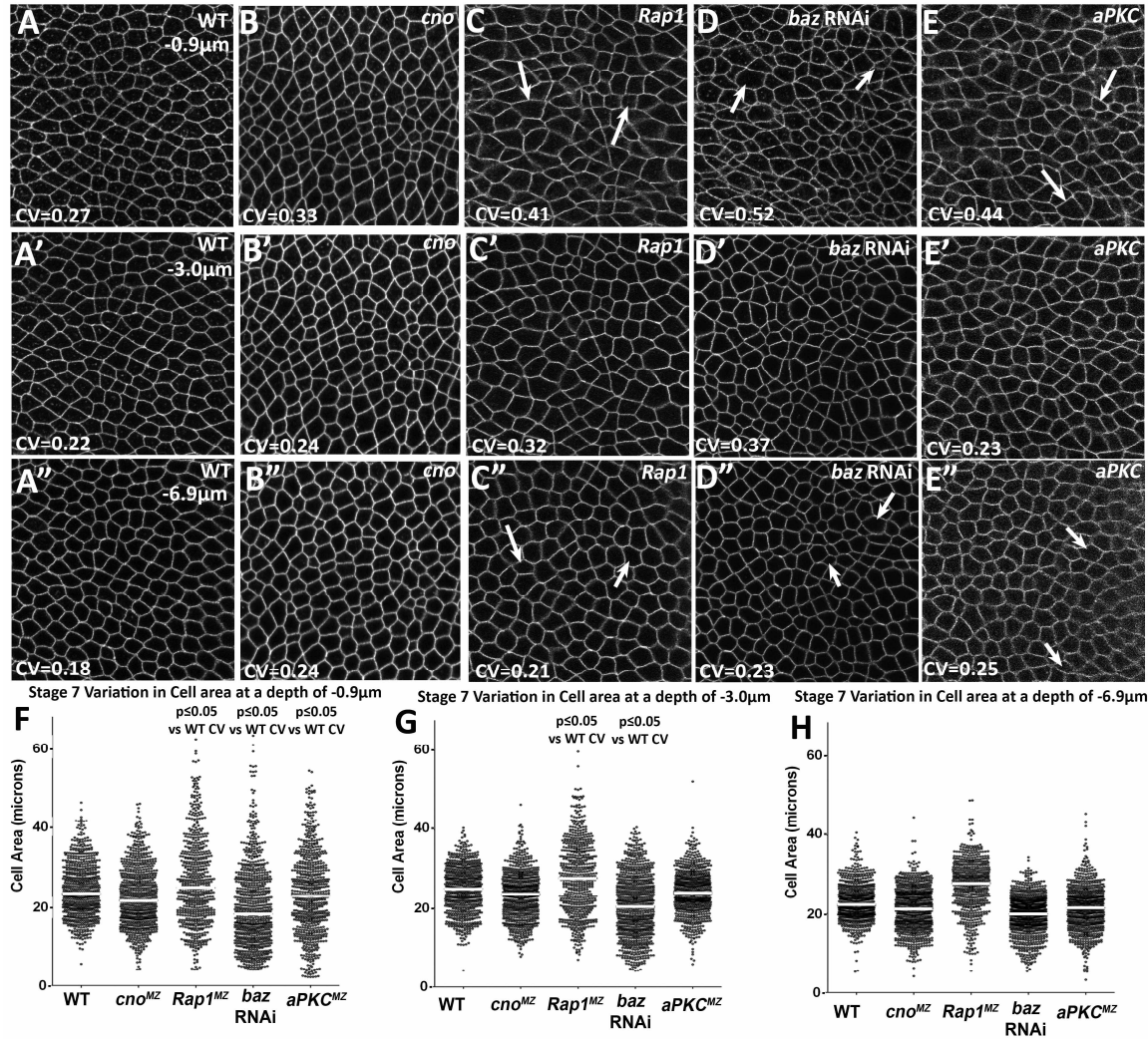
Fig. 10
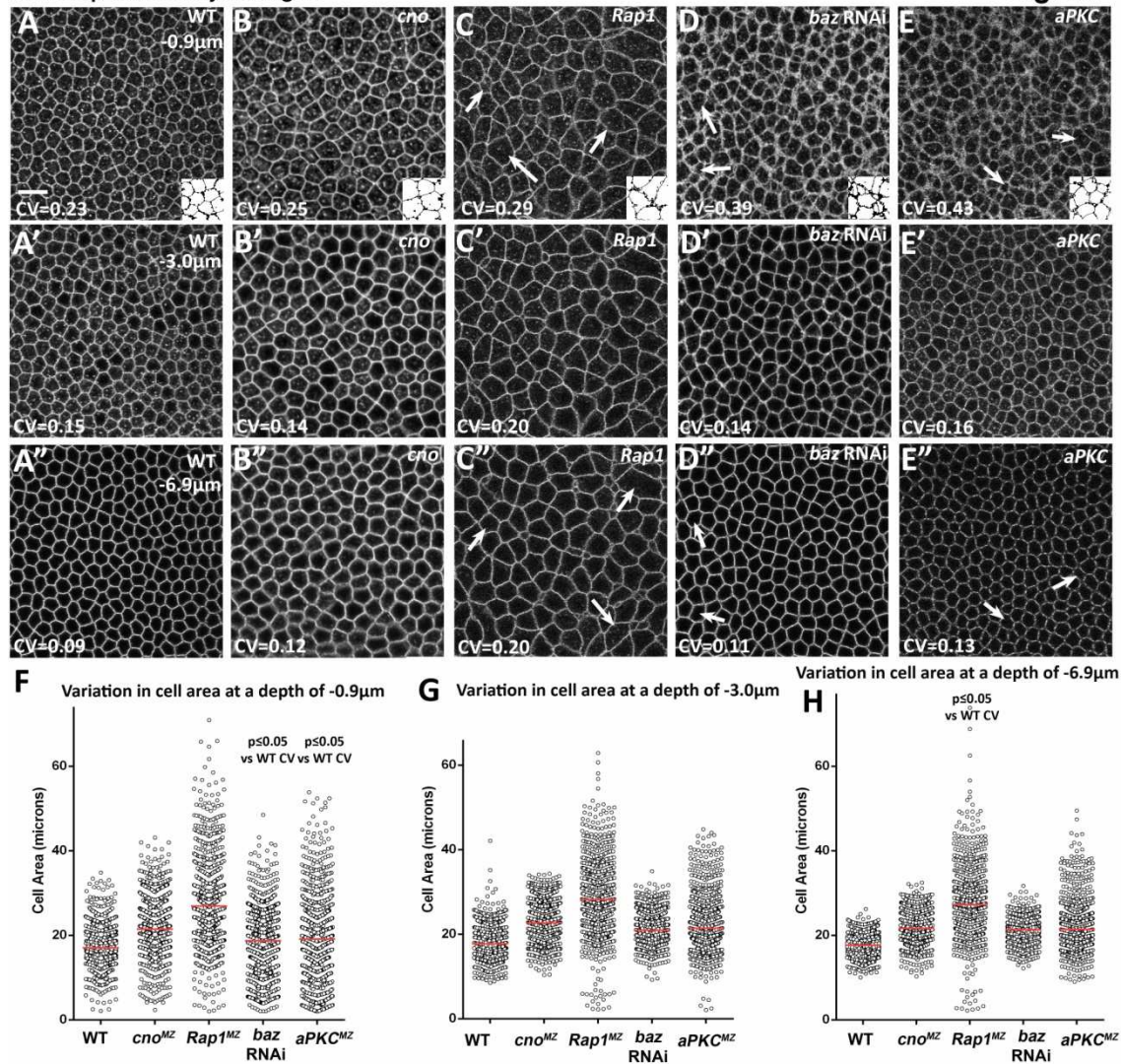


**Figure 4.10. Rap1, Baz and aPKC play roles in establishing columnar cell shape during cellularization.** A-E. Cell shapes during late cellularization at three different apical-basal depths (0.9, 3.0, and 6.9 µm below the apical surface). Cells were stained with antibody to the membrane protein Nrt, background was removed, images were processed with a "watershed" algorithm and thresholded (insets) to allow ImageJ to measure cell area. Representative embryos are shown. The degree of variation in cell shape is expressed by the coefficient of variation (CV). Arrows indicate examples of variable cell areas. F-H. Bee-swarm scatter plots of cell areas for all genotypes examined at the indicated depths. Significance of the degree of cell area variability (CV) was assessed by Tukey's HSD test, to correct for multiple comparisons. Red lines indicate the median value. Wild-type cells are essentially columnar (A-A''), and exhibit relatively little variation in cell area from cell to cell--what variation does exist is most prominent in the apical most slice. *cno* mutants (B-B'') also exhibit relatively uniform cell shapes. *Rap1* mutants (C-C'') are more variable in cell area than wild-type, and this difference reaches significance in the basal section. *baz* RNAi (D-D'') and *aPKC^{MZ}* mutants (E-E'') are significantly more variable in cell area than wild-type in the apical most region. Scale bar=10µm.

191

**Fig. 11**



**Figure 4.11. Rap1, Baz and aPKC play distinctive roles in maintaining columnar cell shape at gastrulation onset**. Cell areas were measured at three different apical-basal depths during stage 6 as in Fig. 10, and CV calculated for each genotype. A-E Representative embryos, with mean CV values for each genotype and section. Arrows indicate examples of cell area variation. F-H. Bee-swarm scatter plots of cell areas. *Rap1, baz* RNAi, and *aPKC* all affect variability of apical cell area, while only *Rap1* significantly affects cell area variability in the most basal section. White lines=median value. Scale bar=10µm.

**Figure 4.12. Rap1, Baz and aPKC are all required to maintain columnar cell shape during germband extension**. Cell areas were measured during stage 7, and CV calculated as in Fig. 10. A-E  Representative embryos, with mean CV values for each genotype and section.   Arrows indicate examples of variable cell areas.  F-H. Bee-swarm scatter plots of cell areas.  *Rap1, baz* RNAi, and *aPKC* all significantly affect variability of apical cell area.   Scale bar=10μm.
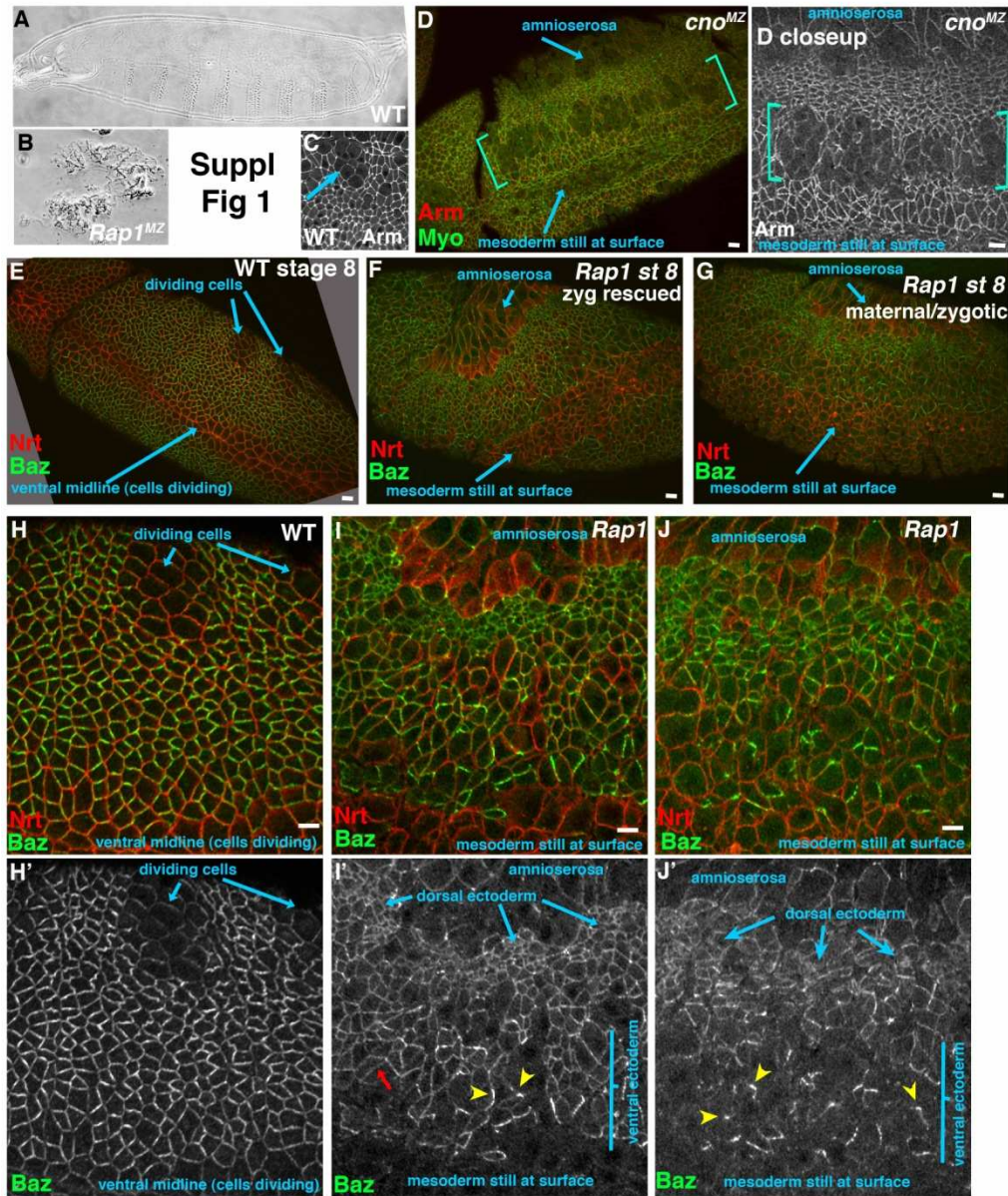
**Figure 4.S1.** *Rap1$^{MZ}$* mutants begin to lose epithelial integrity as development proceeds. A,B. Cuticle preparations of wild-type and *Rap1$^{MZ}$* mutant. C-J. Late germband extension (stage 8) embryos. Groups of cells in the epidermis round up and undergo synchronous divisions—cortical levels of AJ proteins (C) and Baz (H) are reduced in these cells. D. In *cno$^{MZ}$* mutants we previously found that once cells round up, they have difficulty regaining columnar cell shape, and thus rounded up cells accumulate (D,D close-up, brackets). E,H, In wild-type, while Baz is planar-polarized in the ectoderm, it still forms continuous junctions all around the cell, even in cells undergoing division (H, arrows). F,I. In presumptive zygotically rescued *Rap1$^{M}$* mutants, while Baz continues to surround cells of the dorsal ectoderm, in the lateral ectoderm Baz at junctions becomes weak (red arrow) or fragmented (arrowheads). G,J. Even more severe defects are seen in presumptive *Rap1$^{MZ}$* mutants, where Baz accumulation becomes highly fragmented in the lateral ectoderm (arrowheads). Scale bars=10µm.
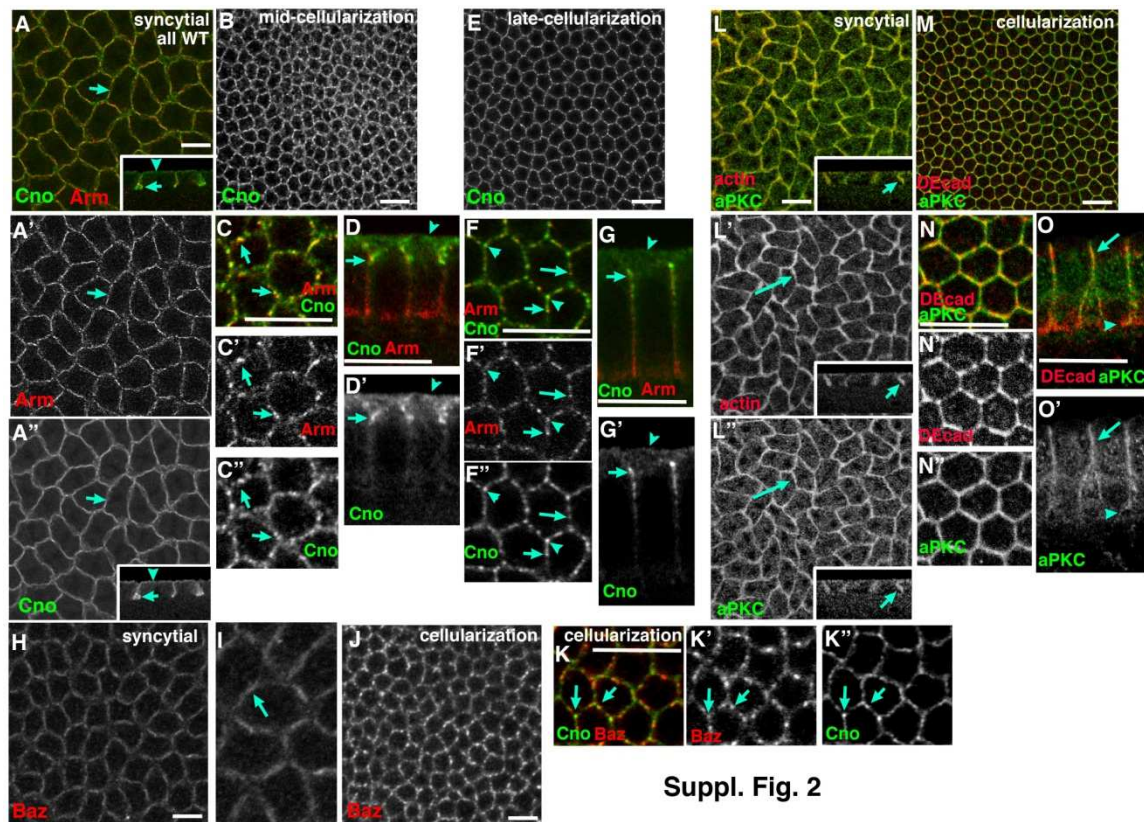
**Figure 4.S2. Cno, Baz, Arm, and aPKC localized to the membrane as early as syncytial divisions.** A, H, L. Syncytial Divisions (cycle 12/13). (A) Cno shows robust localization to pseudocleavage furrows during syncytial division. Baz (H) and Arm (A') also localize to psuedocleavage furrows at lower levels. aPKC (L) also displays membrane localization , when processed by formaldehyde fixation.  B-G, J-K, M-O. Mid (B-D, J-K) or late (F,G) Cellularization.  Cno , Arm, and Baz localize to spot AJs (C,D,K, arrows), Arm also localizes to basal junctions (O, arrowhead) and Cno also accumulates apically early (D, arrowhead).  aPKC remains membrane associated but localizes uniformly all along the lateral membrane (O).  Scale bars=10µm.
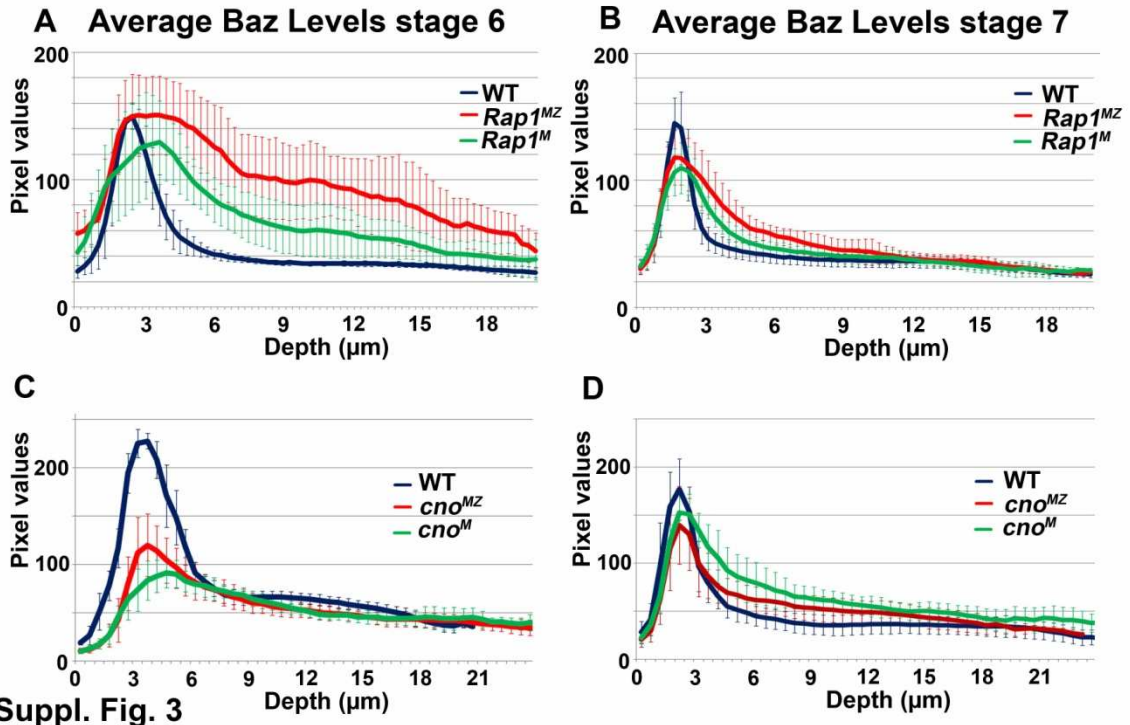
**Figure 4.S3. Rap1 and Cno play roles in maintenance of Baz localization but other cues partially restore apical Baz in their absence.** A-D. Plots displaying the average Baz image intensity in embryos of different genotypes (apical is to the left) at the indicated stages.

Suppl. Fig. 4
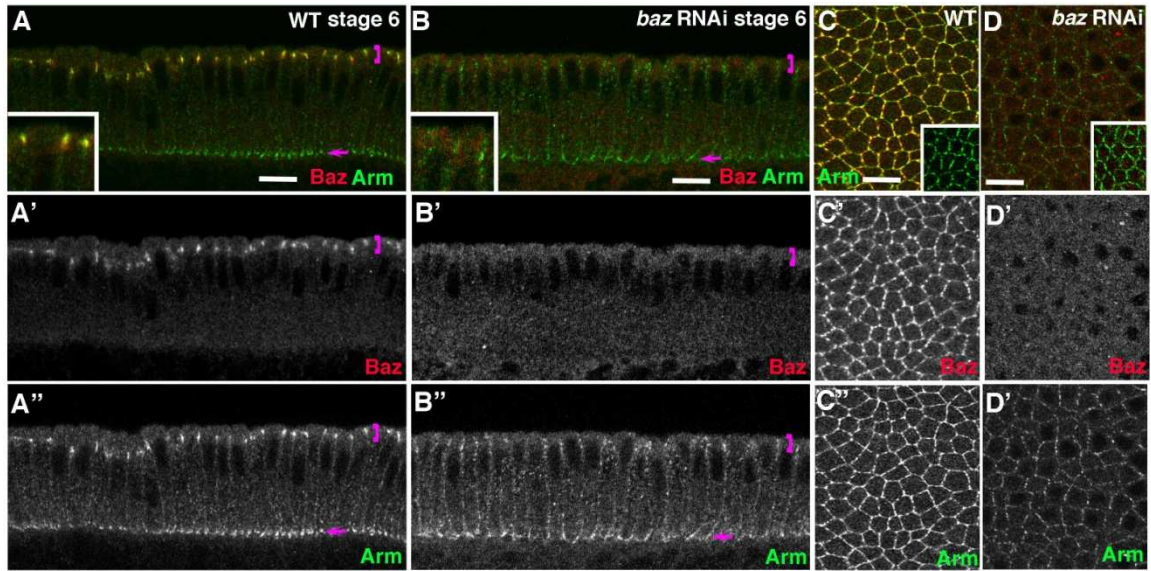
**Figure 4.S4. Baz RNAi reduces Baz levels and mimics the effect of baz maternal and zygotic mutants.** A-D. Maternal GAL4 driven *baz* RNAi effectively knocks down Baz, as assessed at gastrulation onset. In WT, Baz (A',C') is apically enriched and co-localizes with AJs (A,A'' brackets, C, C''). Unlike Baz, AJs are also basally enriched (A, A'' arrows, C inset). *baz* RNAi reduces Baz staining to background levels (B' vs. A'; D' vs. C') and disrupts apical accumulation of AJs (B'' bracket vs. A'' bracket).
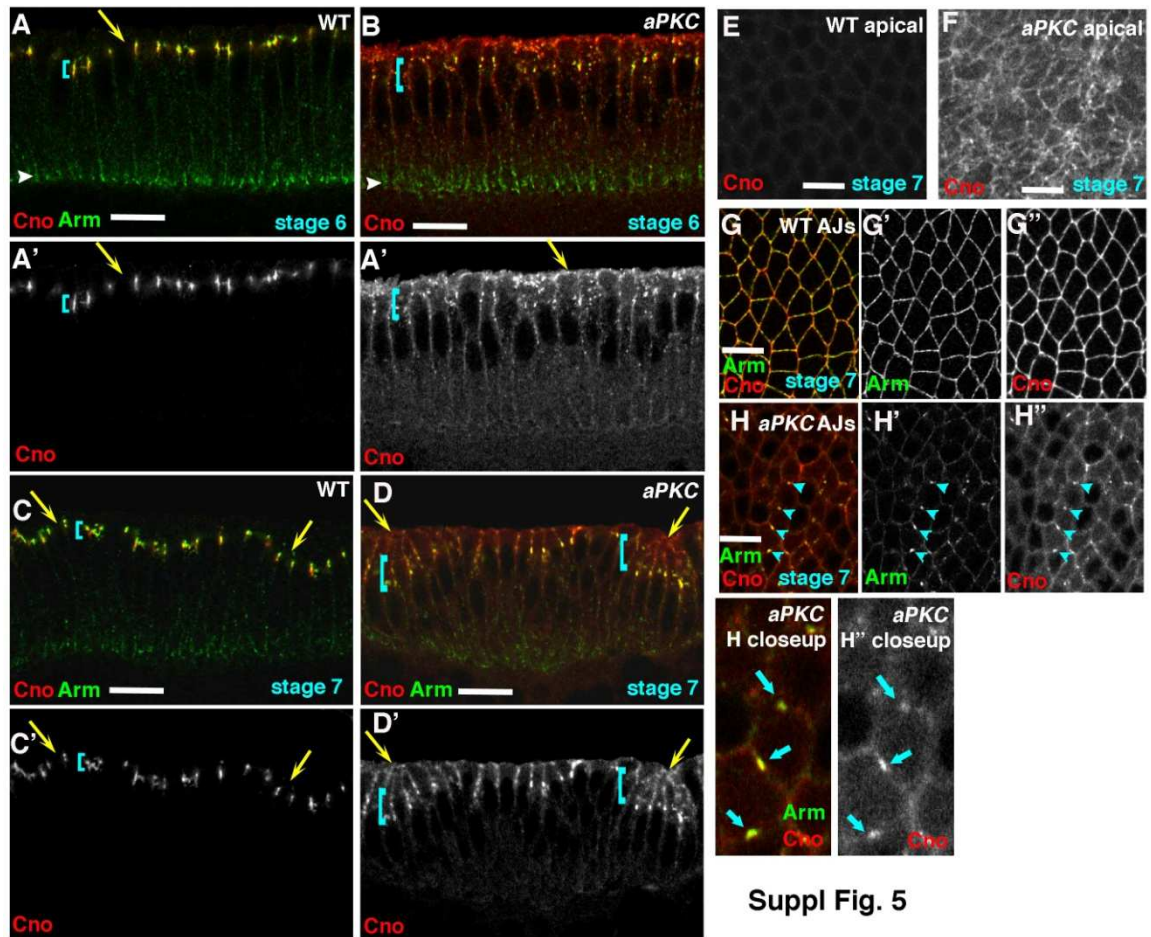
**Figure 4.S5. In the absence of aPKC, Cno is not removed from the apical domain during gastrulation.** A,B. Gastrulation Onset (stage 6). C-H, Germband extension (stage 7) . A-D. Loss of aPKC (B, D) leads to failure to exclude Cno apically (compare arrows), and reduced Cno coalescence along the apical-basal axis (compare brackets). During germband extension (stage 7). apical accumulation of Cno in *aPKC^MZ* mutants becomes more accentuated (E vs F). G,H. In *aPKC^MZ* mutants the belt AJs seen in WT (G) do not form—instead AJ proteins accumulate in puncta at the dorsal and ventral borders of cells (H' arrows). While the majority of Cno is located on the apical membrane in *aPKC^MZ* mutants (F), a portion co-localizes with these dorsal and ventral AJ puncta (H", arrows).
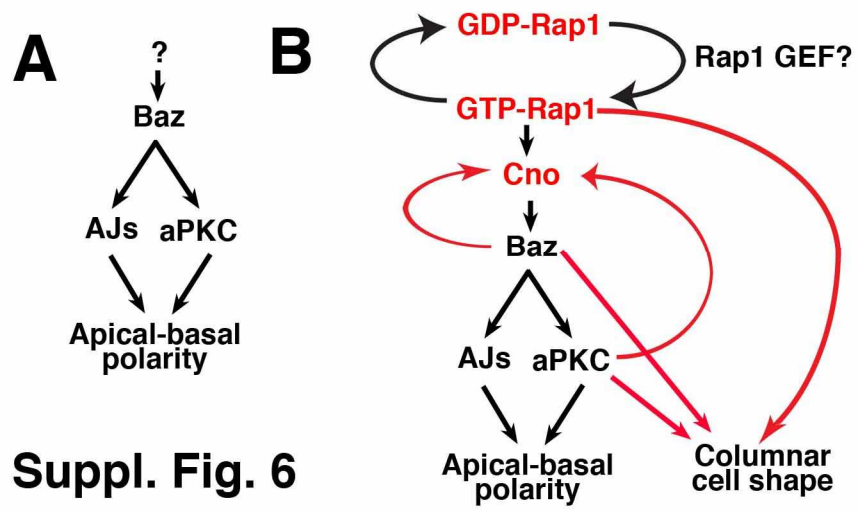
**Figure 4.S6. Old and new models of polarity establishment.**

**Table 4.1: Fly stocks, antibodies, and probes**

| Fly stocks | Source |
|---|---|
| *Rap1*$^{rv(R)B1}$FRT3L$^{2A}$/TM3*twi*GFP | I. Hariharan (UC-Berkeley) |
| FRT82B *cno*$^{R2}$/TM3*twi*GFP | U. Gaul (LMU, Munich, Germany) |
| *aPKC*$^{k06403}$FRT2R/CyO | C. Doe (Univ. of Oregon) |
| UAS*baz*RNAi | Bloomington Drosophila Stock Center |

| Antibodies/Probes (Species) | *Dilution* *IF* | Source |
|---|---|---|
| anti-ArmN27A1 (M-IgG2a) | 1:50 | DSHB# |
| anti-Nrt (M-IgG2a) | 1:100 (HF*)/ 1:25 (4%$^{+}$) | DHSB |
| anti-Cno (Rabbit (Rb)) | 1:1000 | J. Sawyer and N. Harris (UNC-CH, USA) |
| anti-Baz (Rb or Guinea Pig) | 1:500 | J. Zallen (Sloan-Kettering, USA) |
| anti-aPKC (Rb) | 1:1000 | Santa Cruz Biotechnology |
| anti-α-tubulin (clone YL1/2) (Rat) | 1:250 | Millipore |
| anti-γ-tubulin (clone GTU-88) (M-IgG1) | 1:500 | Sigma |
| anti-Zipper (Myosin II heavy chain) (Rb) | 1:1000 | C. Field (Harvard, MA, USA) or D. Kiehart (Duke University, NC, USA) |
| Alexa-phalloidin | 1:500 | Life Technologies |
| Secondary antibodies: Alexas 488, 568, and 647 | 1:500 | Life Technologies |

# DSHB=Developmental Studies Hybridoma Bank, *HF= heat-fixation, +4%=4% formaldehyde fixation

# CHAPTER 5

## DISCUSSION

Effective creation and maintenance of intact epithelial sheets requires a number of cell mechanisms so all the member cells are on the same page. At the core of these mechanisms is the establishment and regulation of cell polarity. Previous work introduced Rap1 has as a strong regulator of cell adhesion and migration (discussed in Chapters 1-3). My research has identified a novel role for the small GTPase Rap1 as a regulator during the establishment of polarity as formation of a naïve epithelial monolayer is completed. Our results suggest that Rap1 and its downstream effector Cno potentially work upstream of Baz to delineate a zone of early apical polarity (Chapter 4). In addition, these results suggest a potential role for aPKC feedback into Rap1 signalling to modify Cno localization as polarity matures.

### *Baz localization still brings everyone together*

Previous work has positioned Baz at the top of a cascade of protein interactions that is responsible for recruiting a variety of polarity cues to the apical side of the cell as nuclei surround themselves with cell membranes during cellularization (Harris and Peifer, 2004, 2005). Additionally, this work has shown the importance of both the actin and microtubule cytoskeletons in positioning Baz initially (Harris and Peifer, 2005). However, other players responsible for this initial positioning have proven to be elusive in the past. Here, we suggest that Rap1 signaling is a bona fide upstream regulator of initial Baz localization.

Figure 1 represents an updated model of apical polarity during its establishment at cellularization. This model adds both Rap1 and its downstream effector Cno above Baz. It also maintains the position of Baz as an important landmark for the proper recruitment of other polarity cues and AJs since loss of Rap1 did not alter localization of these other components in a way that we could differentiate from disruptions caused when Baz is reduced or lost. However, beyond this stage of embryogenesis, this and previous work highlights that Rap1 primarily acts as a strong modulator of polarity since its overall effects on maintaining epithelia integrity are less severe in comparison to core members of apical polarity like Baz or aPKC (Sawyer et al., 2009; Wodarz et al., 2000).

Due to Rap1's novel role during cellularization, numerous new questions arise while others have been answered. Here, we present additional evidence of Rap1's role in regulating the localization of Cno, suggesting that loss of appropriate Cno localization leads to an inability to apically enrich Baz apically as polarity is established.  Yet, how Rap1 and Cno interact with Baz to form this relationship is unclear. Our evidence supports a model where Baz localization occurs downstream of Rap1's control of Cno localization since reducing Baz or introducing mislocalized Baz via overexpression does not dramatically disrupt Cno localization along the apicobasal axis (Fig 1A) (Chapter 4). In this model, we might expect a direct interaction between Cno and Baz, allowing Cno to apically recruit Baz, especially since both proteins contain PDZ domains (Fig 1A) (McKinley et al., 2012; Sawyer et al., 2009). These domains have been shown to strongly interact with the PDZ domains of other proteins supporting this possibility (Wei et al., 2005). We can begin to test this model in vivo by overexpressing Cno and examining Baz localization. As shown with Baz overexpression, we would expect mislocalized puncta of

Cno that co-localized with Baz. Future work will have to focus on defining whether this relation between Cno and Baz is indirect or direct, potentially via additional biochemical and cell culture study.

### *Cno and Baz: an indirect relationship*

While our comparisons between *cno* and *baz* mutants thus far do not definitely explain the nature of the relationship between the two proteins as polarity is established, closer examination of wild-type and aPKC mutants provide hints of an indirect relationship between the two proteins bridged by additional polarity modulators. The first hints of this come from previous observations of Baz and Cno localization during germband extension where we found opposing localization. Cno showed a subtle preference for anterior/posterior cell boundaries while Baz was enriched on dorsal/ventral cell boundaries (Sawyer et al., 2011). In our current work, we looked at WT localization of both proteins before this morphogenetic event. We also observed potential opposing localization of Cno and Baz during cellularization as Cno puncta seem to have a closer affinity for tricellular junctions while Baz puncta predominantly inhabit the cortex of two cell boundaries (Sawyer et al., 2009) (Chapter 4). Nonetheless, both proteins are present in either site; however, each appears reduced where the other is enriched. The role of Cno's enrichment at this tricellular site is currently unclear, but previous analysis of Cno's function suggest it reinforces the connection between the actin cytoskeleton and cell adhesion, raising the possibility that Cno provides increased cell structure as cell adhesion is assembled by events after polarity is first established (Sawyer et al., 2011; Sawyer et al., 2009). Examination of AJ proteins shows a lack of preference for either site, suggesting that Cno and Baz may work independently to ensure even distribution of

junctional proteins to allow appropriate assembly of cell junctions in the events beyond cellularization (Fig 1C). Indeed, analysis of Rap1 mutant cells generated during larval stages in Drosophila showed an inability to maintain AJs around the cell cortex in newly formed daughter cells post-mitosis (Knox and Brown, 2002). Work with the mammalian homolog of Cno, AF-6, also shows a role in stabilizing cell junctions, by inhibiting cadherin endocytosis in the presence of active Rap1 (Hoshino et al., 2005). Our own previous work reinforces this relationship, as we demonstrated a direct interaction between Cno and E-cad in vitro (Sawyer et al., 2009). Alongside this, multiple pieces of direct and indirect evidence have been presented showing a close interaction between Baz and AJs as polarity is established and cell adhesion is established in *Drosophila* (Harris and Peifer, 2005; McGill et al., 2009). Further work would aim to determine whether Cno and Baz interact with AJs independently of one another. If so, it would raise the possibility that these two proteins are actively localized in an opposing fashion within the plane of an epithelial sheet. Discovering how this occurs would become vital to understanding downstream effects to cell adhesion and polarity maintenance.

Independent regulation of Cno and Baz localization is further suggested in our analysis of both in aPKC mutants. Previously, it was demonstrated that loss of aPKC failed to alter initial localization of either Baz or AJs during cellularization (Harris and Peifer, 2005). Building on this work, we show that Cno localization is not either (Chapter 4). However, as gastrulation proceeds, loss of aPKC causes unique differences between the localization of Baz and Cno. Here, Baz collapses into a large singular puncta on dorsal/ventral boundaries, while Cno is not properly excluded from the apical cell cortex (Harris and Peifer, 2007) (Chapter 4). While a portion of Cno does co-localize with the

Baz and AJs puncta, this is consistent with previous observations in WT puncta where lower levels of Cno co-localized with Baz-rich puncta during cellularization. Nonetheless, these separate effects on Baz and Cno localization suggest the presence of independent modulation of the two proteins, rather than direct modulation of one another. Additionally, this evidence suggests that Baz localization is not solely dependent on proper Cno localization, indicating that a simple model of polarity establishment and maintenance, where Cno recruits and maintains Baz apically (Fig 1A), is unlikely to be accurate. As a result, we need to look further upstream to develop a model that agrees with these observations.

As an alternative model to Cno directly positioning Baz, perhaps Cno maintains an active Rap1 signal at the appropriate place to promote apical enrichment of Baz via other Rap1 effectors. Indeed, previous work shows that levels of active Rap1 drop when AF-6 levels are reduced via RNAi in mammalian systems, supporting a model where maintaining an active Rap1 signal requires Cno (Zhang et al., 2005). Our analysis of cell shape during the early stages of embryogenesis potentially supports this divergence between Rap1 and Cno regulation of apical polarity. We found loss of Rap1, but not Cno, mimics the reduction of baz and loss of aPKC on cell shape regulation indicating Cno-independent roles for Rap1 signaling (Chapter 4). Due to these pieces of evidence, we propose a model where Cno localization aids in anchoring and maintaining an active, apical Rap1 signal that flags Baz into the correct position to recruit additional polarity cues and AJs (Fig 1B). Once recruited by Baz, aPKC then provides a feedback mechanism, excluding Cno from the superapical cell cortex as development proceeds (Fig 1B). This feedback could be delivered via phosphorylation of Cno or other Cno

binding partners by aPKC, analogous to the way phosphorylation of Baz causes

separation of aPKC/Par6 and Baz/AJs into different zones as polarity is elaborated

(Krahn et al., 2010; Morais-de-Sa et al., 2010). Recent evidence of Rap1 in complex with

aPKC and Par6 further support a relationship where aPKC alters Rap1 control of Cno

localization, as loss of Rap1 activity disrupts Cno's ability to localize at the cell cortex

(Carmena et al., 2011; Sawyer et al., 2009). Further work to strengthen this model hinges

on examination of Cno and Baz localization within two situations: after overexpression of

both wild-type and constitutively active forms of Rap1 during these stages, and after

blocking aPKC phosphoylation of Baz.

       If active Rap1 signal is solely responsible for Baz recruitment, we should observe

mislocalization of Baz along the apicobasal axis when constitutively active Rap1 is

placed all along the cell membrane due to Rap1's CAAX domain. In respect to our

model, we would not necessarily expect mislocalization of Cno if Rap1 works

independently to localize Cno and Baz. If Cno is not mislocalized, it would highlight

Rap1-independent mechanisms for localizing Cno, which we known already exist due our

previous observation that disruption of the actin cytoskeleton will disrupt Cno

localization (Sawyer et al., 2009). Whether similar effects will be seen to a lesser extent

when we overexpress wild-type Rap1 will depend on the relationship between Rap1 and

Cno. If Cno does work to propagate or maintain an active Rap1 signal, then there is

potential for more active Rap1 to exist in the system, and hence alter Baz localization;

however, this would also depend on the stoichiochemistry between Rap1 and Cno as

wild-type Cno may already be saturated with endogenous active Rap1. We could then

attempt to examine the effects of simultaneous overexpression of Rap1 and Cno on

polarity. Our current data suggests that proper Cno localization is somewhat impervious to the introduction of ectopic Cno, unlike Baz, however. Further work will need to be completed to examine the activity of Cno to determine to the effects of Cno overexpression; it is possible that ectopic Cno replaces stores of endogeneous Cno or is rapidly degraded to maintain Cno levels during development.

In addition to understanding how Rap1's activation state can alter polarity, we must also address questions regarding this relationship by altering the phosphorylation state of Baz and examining its effects on Cno localization. Previous work had identified a key serine within Baz that is phosphorylated by aPKC during development (Krahn et al., 2010; Morais-de-Sa et al., 2010). This phosphorylation event is important for proper separation of polarity cues into different zones as polarity is elaborated, and defects in polarity rapidly appear as when an unphosphorylatable form of Baz (S980A) is expressed during gastrulation (Krahn et al., 2010; Morais-de-Sa et al., 2010). On the other hand, expression of Baz that mimics phosphorylation of this residue (S980E) is well tolerated during these stages as no obvious defects in polarity or morphogenesis are observed (Morais-de-Sa et al., 2010). In our proposed model, we would expect that Cno localization would remain unchanged in the presence of either form of Baz. This would provide additional evidence that disruption of Cno localization in aPKC mutants is independent of Baz function, and not a consequence of aPKC failing to phosphorylate Baz.

### Cno under Surveillance

Like when Baz was placed a top of the polarity hierarchy, Rap1 and Cno's regulation of Baz, and therefore, control of polarity make questions regarding control of

Cno localization important in our understanding of polarity establishment and maintenance. Already, tools are in place to help us answer this question. Previous work showed that both the actin and microtubule cytoskeletons are important for localization of Baz (Harris and Peifer, 2005). While we have shown that disrupting the actin cytoskeleton alters Cno localization, we have yet to test whether the microtubule cytoskeleton plays a role in regulating Cno (Sawyer et al., 2009). If disruption of the microtubule cytoskeleton alters Cno localization then it would open up an additional field of questions in regard to how Cno interacts directly or indirectly with microtubules.

In addition, methods for real-time microscopy have improved significantly providing another method for examining Cno localization. These improvements in real-time microscopy have already yielded data that allowed us to observe an apical contractile network of actin and myosin that was previously uncharacterized (Fernandez-Gonzalez and Zallen, 2011; Sawyer et al., 2011). In additional, real-time analysis has provided insight into the dynamics of Baz and AJs through live visualization during early embryogenesis (McGill et al., 2009). We could complete similar work on Cno both alone and in combination with Baz to better understand localization and relative stability of their respective puncta and the transition of those puncta into belts during gastrulation. Lastly, with the advent of new techniques to reduce components of polarity and AJs in the early embryo, we can more easily observe Cno dynamics in situations where polarity is altered to test and build on our current model (Ni et al., 2011).

### *Polarity: A web of life*

One thing that has become clear from investigations into cellular polarity is that its creation and subsequent maintenance are not simply a linear chain of events with one

change leading to the next until all the switches are flipped, allowing a ball of cells to develop into a properly formed organism. Instead, we have seen multiple cases where core members of polarity and their regulatory network cause pleiotrophic effects within the same temporal space, triggering a cascade of changes to allow for effective formation and maintenance of epithelial sheets. These data suggest that the protein interactions that control polarity resemble a web. Indeed, my work with Rap1 and aPKC highlights multiple functions of these proteins, via the use or alteration of multiple downstream effectors. Since these proteins exercise influence on multiple effectors, it becomes important to continue studies of polarity, and to develop new tools to tease apart these functions to properly place new strands of understanding upon our current view of the web of life.
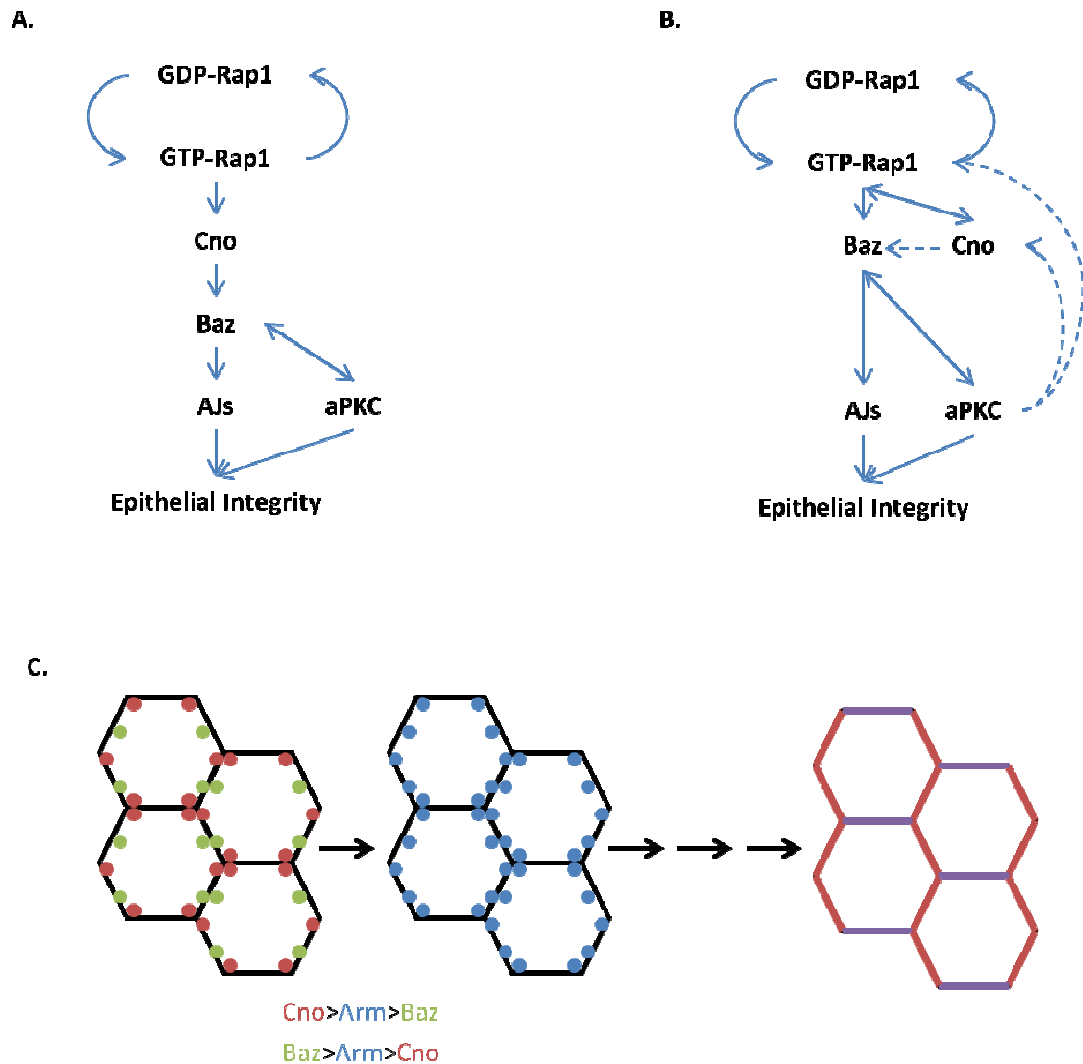
**Figure 5.1. Defining the Apical Domain.**
(A) Initial examination of *Rap1* and *cno* mutants suggests they are at the top of a functional hierarchy that defines apical polarity due to mislocalization of Baz.
(B) Examination of independent effects on Baz and Cno localization in *aPKC* mutants suggests that a simple model of polarity is inaccurate with Rap1 potentially controlling Baz localization independent of Cno localization (dashed arrow line). Cno localization may be controlled by direct interaction with aPKC or indirectly through aPKC's interaction with Rap1 (dashed curved arrows).
(C) Opposing localization of Cno and Baz puncta during polarity establishment suggests indirect interactions between the two. Equivalent levels of AJs (Arm) in all puncta indicate a potential mechanism for ensuring equal distribution of spot AJs around cell cortex. Opposing localization of Cno and Baz persists as spot AJs transform into belt AJs.

# References

Carmena, A., Makarova, A., Speicher, S., 2011. The Rap1-Rgl-Ral signaling network regulates neuroblast cortical polarity and spindle orientation. The Journal of cell biology 195, 553-562.

Fernandez-Gonzalez, R., Zallen, J.A., 2011. Oscillatory behaviors and hierarchical assembly of contractile structures in intercalating cells. Physical biology 8, 045005.

Harris, T.J., Peifer, M., 2004. Adherens junction-dependent and -independent steps in the establishment of epithelial cell polarity in Drosophila. The Journal of cell biology 167, 135-147.

Harris, T.J., Peifer, M., 2005. The positioning and segregation of apical cues during epithelial polarity establishment in Drosophila. The Journal of cell biology 170, 813-823.

Harris, T.J., Peifer, M., 2007. aPKC controls microtubule organization to balance adherens junction symmetry and planar polarity during development. Developmental cell 12, 727-738.

Hoshino, T., Sakisaka, T., Baba, T., Yamada, T., Kimura, T., Takai, Y., 2005. Regulation of E-cadherin endocytosis by nectin through afadin, Rap1, and p120ctn. The Journal of biological chemistry 280, 24095-24103.

Knox, A.L., Brown, N.H., 2002. Rap1 GTPase regulation of adherens junction positioning and cell adhesion. Science 295, 1285-1288.

Krahn, M.P., Buckers, J., Kastrup, L., Wodarz, A., 2010. Formation of a Bazooka-Stardust complex is essential for plasma membrane polarity in epithelia. The Journal of cell biology 190, 751-760.

McGill, M.A., McKinley, R.F., Harris, T.J., 2009. Independent cadherin-catenin and Bazooka clusters interact to assemble adherens junctions. The Journal of cell biology 185, 787-796.

McKinley, R.F., Yu, C.G., Harris, T.J., 2012. Assembly of Bazooka polarity landmarks through a multifaceted membrane-association mechanism. Journal of cell science 125, 1177-1190.

Morais-de-Sa, E., Mirouse, V., St Johnston, D., 2010. aPKC phosphorylation of Bazooka defines the apical/lateral border in Drosophila epithelial cells. Cell 141, 509-523.

Ni, J.Q., Zhou, R., Czech, B., Liu, L.P., Holderbaum, L., Yang-Zhou, D., Shim, H.S., Tao, R., Handler, D., Karpowicz, P., Binari, R., Booker, M., Brennecke, J.,

Perkins, L.A., Hannon, G.J., Perrimon, N., 2011. A genome-scale shRNA resource for transgenic RNAi in Drosophila. Nature methods 8, 405-407.

Sawyer, J.K., Choi, W., Jung, K.C., He, L., Harris, N.J., Peifer, M., 2011. A contractile actomyosin network linked to adherens junctions by Canoe/afadin helps drive convergent extension. Molecular biology of the cell 22, 2491-2508.

Sawyer, J.K., Harris, N.J., Slep, K.C., Gaul, U., Peifer, M., 2009. The Drosophila afadin homologue Canoe regulates linkage of the actin cytoskeleton to adherens junctions during apical constriction. The Journal of cell biology 186, 57-73.

Wei, S.Y., Escudero, L.M., Yu, F., Chang, L.H., Chen, L.Y., Ho, Y.H., Lin, C.M., Chou, C.S., Chia, W., Modolell, J., Hsu, J.C., 2005. Echinoid is a component of adherens junctions that cooperates with DE-Cadherin to mediate cell adhesion. Developmental cell 8, 493-504.

Wodarz, A., Ramrath, A., Grimm, A., Knust, E., 2000. Drosophila atypical protein kinase C associates with Bazooka and controls polarity of epithelia and neuroblasts. The Journal of cell biology 150, 1361-1374.

Zhang, Z., Rehmann, H., Price, L.S., Riedl, J., Bos, J.L., 2005. AF6 negatively regulates Rap1-induced cell adhesion. The Journal of biological chemistry 280, 33200-33205.